# Epigenetic regulation of *Epichloë festucae* secondary metabolite biosynthesis and symbiotic interaction with *Lolium perenne*

---

A thesis presented in partial fulfilment of the requirements for the degree of

Doctor of Philosophy

in

Genetics

at Massey University, Palmerston North

New Zealand

**Yonathan Lukito**

**2017**

## Abstract

Histone methylation is one of several epigenetic layers for transcriptional regulation. Most studies on the importance of this histone modification in regulating fungal secondary metabolite gene expression and pathogenicity have focussed on the role of histone methyltransferases, while few studies have focussed on the role of histone demethylases that catalyse the reversal of the modification. *Epichloë festucae* (Ascomycota) is an endophyte that forms a mutualistic interaction with perennial ryegrass. The fungus contributes to the symbiosis by the production of several classes of secondary metabolites, these have anti-insect and/or anti-mammalian activity. The *EAS* and *LTM* clusters in *E. festucae* are located subtelomerically and contain the biosynthetic genes for two of these important metabolites which are only synthesised *in planta*. Thus, in the host plant these genes are highly expressed, but they are tightly silenced in culture conditions. Previous study has shown that histone H3K9 and H3K27 methylation and their corresponding histone methyltransferases are important for this process. In this study, the role of histone lysine demethylases (KDMs) in regulating these genes and the symbiotic interaction is described.

Eight candidate histone demethylases (Jmj1-Jmj8) were identified in *E. festucae*, among these proteins are homologues of mammalian KDM4, KDM5, KDM8, JMDJ7, and *N. crassa* Dmm-1. The genes for the proteins were overexpressed in *E. festucae* and histone methylation levels were determined in the strains. Overexpression of the genes was not observed to cause any change to the culture and symbiotic phenotypes of the fungus. Western blot analysis subsequently identified one of the proteins, KdmB, as the histone H3K4me3 demethylase. Further analysis by ChIP- and RT-qPCR showed that demethylation of H3K4me3 by KdmB at the *eas*/*ltm* genes is crucial for the activation of these genes *in planta*. The full expression of several other telomeric genes was similarly found to require KdmB. On the other hand, the COMPASS H3K4 methyltransferase complex subunit CclA that is required for H3K4 trimethylation in *E. festucae* represses the *eas*/*ltm* genes in culture conditions by maintaining H3K4me3 levels at the loci. Thus, these findings suggest a repressive role for H3K4me3 at these subtelomeric secondary metabolite loci and are consistent with the role of H3K4me3 in yeast telomeric silencing. Disruption of *kdmB* did not affect the symbiotic interaction of *E. festucae* with the host grass but severely reduced the levels of lolitrem B, an animal neurotoxin. At the same time, the levels of ergovaline, another animal toxin, and peramine, an insect feeding deterrent, were not affected. Therefore, disruption or inhibition of KdmB may also serve as a promising approach for future endophyte improvement programmes.

The *E. festucae* homologue of KDM8 (an H3K36me2 demethylase), Jmj4, was further investigated in this study but no H3K6 demethylase activity was found for the protein. Both disruption and overexpression of the gene encoding Jmj4 similarly had no effect on the culture and symbiotic phenotypes of *E. festucae*. However, deletion of *setB*, encoding the homologue of yeast Set2 (H3K36 methyltransferase) specifically reduced histone H3K36me3 levels in *E. festucae*. This contrasts with deletion of Set2 in other fungi which affected H3K36 mono-, di- and trimethylation. The Δ*setB* mutant was severely impeded in development, and was unable to establish infection of the host plant. Introduction of the wild-type *setB* gene reversed these phenotypes.

This study shows that H3K4 trimethylation controlled by CclA and KdmB is an important regulator of subtelomeric secondary metabolite genes in *E. festucae* but not for the symbiotic interaction of the fungus with perennial ryegrass. On the other hand, the histone H3K36 methyltransferase SetB specifically

controls H3K36 trimethylation in *E. festucae* and is required for normal vegetative growth and ability of the fungus to infect the host plant.

## Acknowledgements

My sincerest gratitude to my MSc and PhD supervisor Professor Barry Scott who has kindly given me the opportunity to undergo my scientific training in his lab. Thank you for your incredible support throughout my studies, for the guidance but also the freedom to develop my ideas. I appreciate the generous support given towards attending conferences, the opportunity to be involved in side projects and am grateful for your enthusiasm in training us all to be good scientists.

A big thank you to my co-supervisors; Dr Tetsuya Chujo for his advice and technical training especially during my MSc years, to Dr Linda Johnson for the constant support and helpful directions for my research project, and to Dr Tracy Hale for the helpful discussions, technical training, and also for kindly allowing me to conduct the mammalian experiments in her lab. The *cclA* mutants used in this study were also generated by Dr Chujo.

To all the wonderful people in Scottbase, past and present, thank you for the support, discussions and ideas. Thanks also to Dr Pranav Chettri for the many helpful discussions and advice, to Dr Sarah Bond for spending considerable time with training on cell culture and immunofluorescence, to Dr Jeong Park for helpful discussions with ChIP and to Prof Derek White for valuable advice on the plant biology aspects. Thanks to Dr Pierre-Yves Dupont and Dr David Winter for helpful discussions and assistance on the statistics and bioinformatics. And thanks also to Wade Mace (AgResearch) for the alkaloid analysis. Finally, to Dr Mac Campbell for the invaluable discussions on… trout, and the awesome times on the river – this should be higher up!

I would also like to acknowledge the financial support provided by the AgResearch PhD scholarship. All imaging experiments in this study were performed at the Manawatu Microscopy and Imaging Centre (MMIC).

Finally, thanks to Monica, Chelsea and my parents for the love, support and encouragement.

## Table of Contents

## List of Figures

## List of Tables

# Chapter 1: Introduction

*1.1 The Epichloë group of ryegrass endophytes*

The terms 'endophyte' and 'epiphyte' are given to microorganisms that grow in association with a host plant - the former grows within the plant, while the latter grows on the surface of a plant. The Epichloë endophytes (Ascomycota, Clavicipitaceae) form a stable symbiosis with cool season grasses of the subfamily Pooideae, which includes perennial ryegrass *Lolium perenne*, a globally important and the most commonly sown pasture grass in New Zealand (Johnson *et al.*, 2013a).

*Epichloë festucae* grows within the host apoplastic (intercellular) spaces with hyphae aligned parallel to the leaf axes. The hyphae colonise aerial tissues of the host including the leaf blade, sheath and pseudostem tissues, except the root tissues. Unlike many biotrophic fungi, *E. festucae* does not form specialised feeding structures such as haustoria. Instead, it obtains its nutrients directly from the apoplastic fluid of the host and possesses complete sets of genes for the biosynthesis and assimilation of these nutrients (Scott *et al.*, 2012). As a sexual species, *E. festucae* is capable of both vertical and horizontal transmission. In the vertical (asexual) life cycle, the endophyte maintains a restrictive mode of growth within the plant, eventually colonising the host seeds to facilitate its dispersion. But in the horizontal or sexual life cycle, the fungus switches from a restrictive mode of growth to a proliferative one, eventually resulting in a diseased host condition known as 'choke'. This culminates in the formation of stroma, a fungal reproductive structure over the host flag leaf, preventing the emergence of the host inflorescence (Kirby, 1961). *Botanophila* flies visit these stromata to feed and lay eggs and in the process transfer conidia from stroma of one mating type to another of the opposite mating type to initiate the fungal sexual cycle (Bultman & Leuchtmann, 2008). To date, there has been no report of chokes in the mutualistic association between *E. festucae* and *L. perenne* (Scott *et al.*, 2012).

In the Epichloë-ryegrass symbiosis, the host grass benefits from the production of *E. festucae* secondary metabolites which possess anti-insect and anti-mammalian activities (Schardl *et al.*, 2004, Johnson *et al.*, 2013a). Studies have also shown that presence of Epichloë endophytes enhances nutrient (e.g. phosphorous) acquisition and drought and disease resistance (Malinowski & Belesky, 1999). The grass in return provides nutrients, protection, and a means of dissemination for the fungus.

*1.2 Epichloë secondary metabolites*

Fungal secondary metabolites (SMs) are a group of small molecular-weight compounds produced by members of the phylum Ascomycota, many of these compounds are biologically active. As opposed to primary metabolites, which are essential for survival of the fungus, SMs are produced during the secondary metabolic phase of a fungus, typically the late exponential phase of growth, and are nonessential for growth. Some clinically important fungal SMs include the antibiotic penicillin (produced by *Penicillium chrysogenum*), the cholesterol-lowering agent lovastatin (*Aspergillus terreus*), and the potent carcinogen aflatoxin (*Aspergillus flavus*). The four main classes of Epichloë SMs characterised to date are peramines, lolines, ergot alkaloids and indole-diterpenes (Schardl *et al.*, 2012). These metabolites

are only synthesised when the endophyte is in the host plant, while in axenic culture the biosynthetic genes are very weakly expressed with almost undetectable levels of the corresponding metabolites.

The first benefit reported in an endophyte-grass association was resistance of the endophyte-infected ryegrass to the Argentine stem weevil (*Listronotus bonariensis*) (Prestige, 1982). The responsible molecule, peramine, was later identified in the endophyte *Acremonium loliae* and subsequently found to also be produced by *E. festucae* (Rowan, 1993, Lane *et al.*, 1997). A major ryegrass pest, the Argentine stem weevil would have caused catastrophic damages to the New Zealand ryegrass pastures were it not for the protection conferred by the endophytes. The second group, loline alkaloids, possess broad-spectrum anti-insect activity, particularly against the aphid *Schizapus graminis* (Wilkinson *et al.*, 2000). At higher concentrations, these compounds additionally exhibit anti-nematode activities (Bacetty *et al.*, 2009). The third group, the ergot alkaloids, all contain cyclic ring structures and are toxic to both vertebrates and invertebrates (Schardl *et al*., 2004). These alkaloids were initially described in Claviceps, a genus of pathogenic fungi which have been notoriously recognised since the Middle Ages as contaminants of grain harvests (Tudzynski & Scheffer, 2004). In humans, long-term ingestions of these alkaloids can lead to ergotoxicosis; a neurological disorder that is accompanied by fever and dry gangrene, in some cases leading to death (Van Dongen & de Groot, 1995). Livestock feeding on endophyte-infected fescues containing high levels of these alkaloids develop similar symptoms such as hyperthermia, convulsions and dry gangrene (Bacon, 1995). One of the ergot alkaloids, ergovaline, possesses activity against the black beetle (*Heteronychus arator*), another major ryegrass pest in New Zealand (Popay & Baltus, 2001). The last group of compounds, the indole-diterpenes, are potent agonists of calcium-gated potassium channels, the most notorious of which is lolitrem B, a neurotoxin that causes tremors and ataxia (a loss of muscular coordination) in farm animals that graze on endophyte-infected ryegrass (Fletcher & Harvey, 1981).

The biosynthetic pathways of fungal SMs typically involve several genes. These genes tend to be organised in clusters in the genome and are often found near the telomeres (Keller *et al.*, 2005). Apart from peramine, which is synthesised by a single large non-ribosomal peptide synthetase, the genes for the other three secondary metabolite pathways in Epichloë are organised as clusters in the genome (Schardl *et al.*, 2012, Tanaka *et al.*, 2012). In *E. festucae* Fl1, the strain used in this study, the 11 genes of *EAS* and *LTM* clusters for ergovaline and lolitrem B biosynthesis are found in subtelomeric clusters near the ends of chromosomes I and III, respectively (Fig. 1.1). The enzymes encoded by these genes are predicted to participate in complex biochemical pathways that are still in the process of being fully elucidated. The ergovaline pathway begins with the synthesis of dimethylallyltryptophan from L-tryptophan and dimethylallyl diphosphate (DMAPP) that is catalysed by the enzyme dimethylallyltryptophan synthase encoded by the *dmaW* gene (Schardl *et al.*, 2012) (Fig. 1.2). The *lpsA* gene encodes a nonribosomal peptide synthetase (NRPS) that is involved in conversion of lysergic acid to the ergopeptine lactam and the final synthesis of ergovaline. The biosynthetic pathway for lolitrem B is not as linear but contains several routes for the synthesis of the final product, lolitrem B (Schardl *et al.*, 2012) (Fig. 1.3). Some intermediate or shunt products of the pathway, such as paxilline, also possess anti-insect activities, but lolitrem B represents the most abundant indole-diterpene of the fungus. The pathway can also lead to the production of other decorated indole-diterpenes in some Epichloë strains, such as the epoxy-janthitrems in *E. festucae* strain AR37 that also have insect deterrent activity (Johnson *et al.*, 2013a).

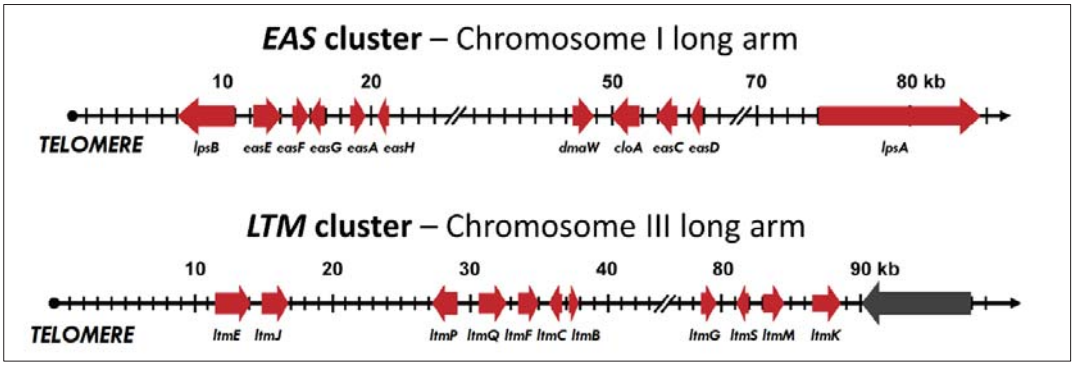


**Figure 1. 1. The *EAS* and *LTM* clusters of *E. festucae*.** Recent genome assembly and chromosome analyses have shown that the clusters are located at the subtelomeric ends of chromosomes I and III of *E. festucae* (Winter *et al.*, unpublished). Figure is modified from Chujo & Scott, 2014 and is drawn to scale.

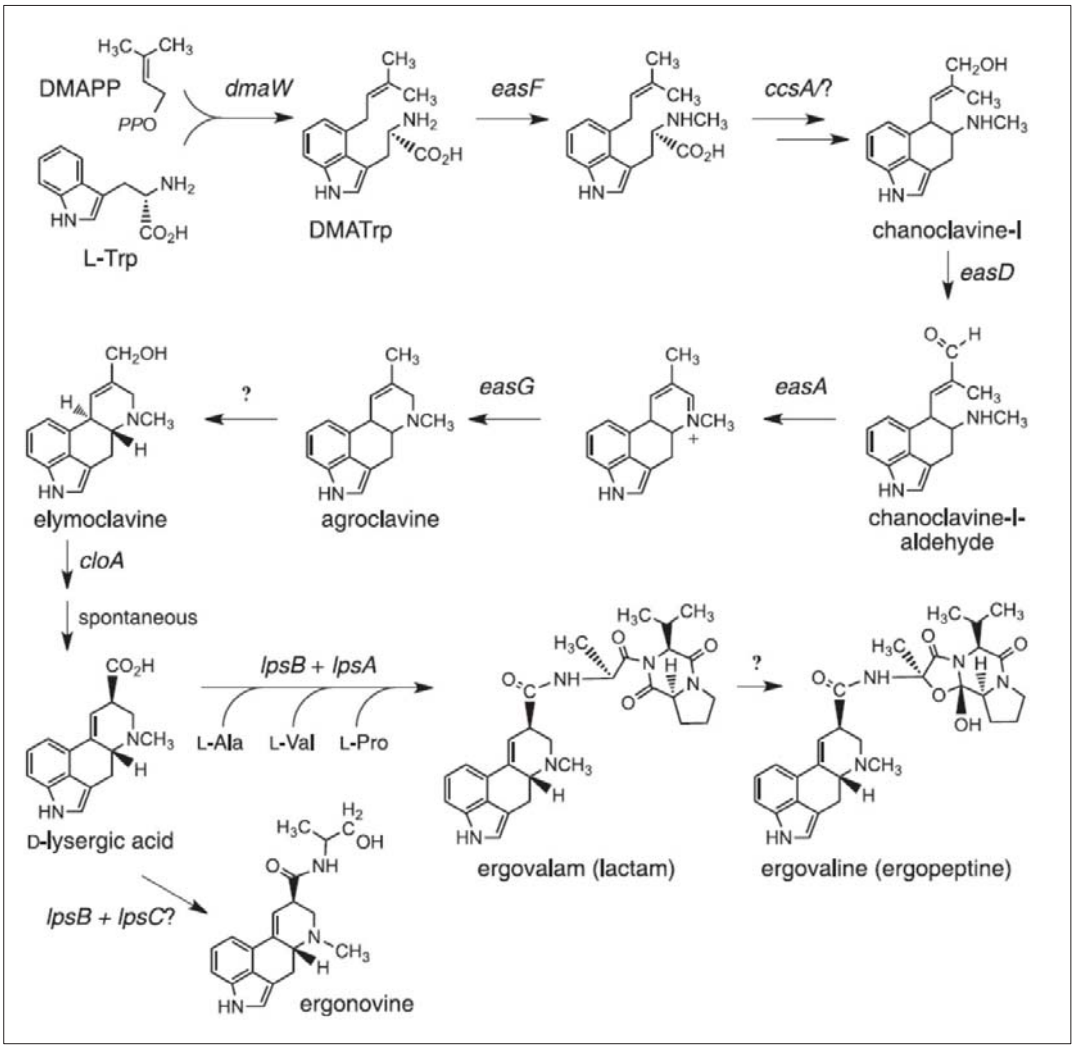


**Figure 1. 2. The proposed pathway for ergovaline biosynthesis.** DMAPP**:** dimethylallyl diphosphate, L-Trp: L-tryptophan, DMATrp: dimethylallyltryptophan. Figure is taken from Schardl *et al*. (2012).

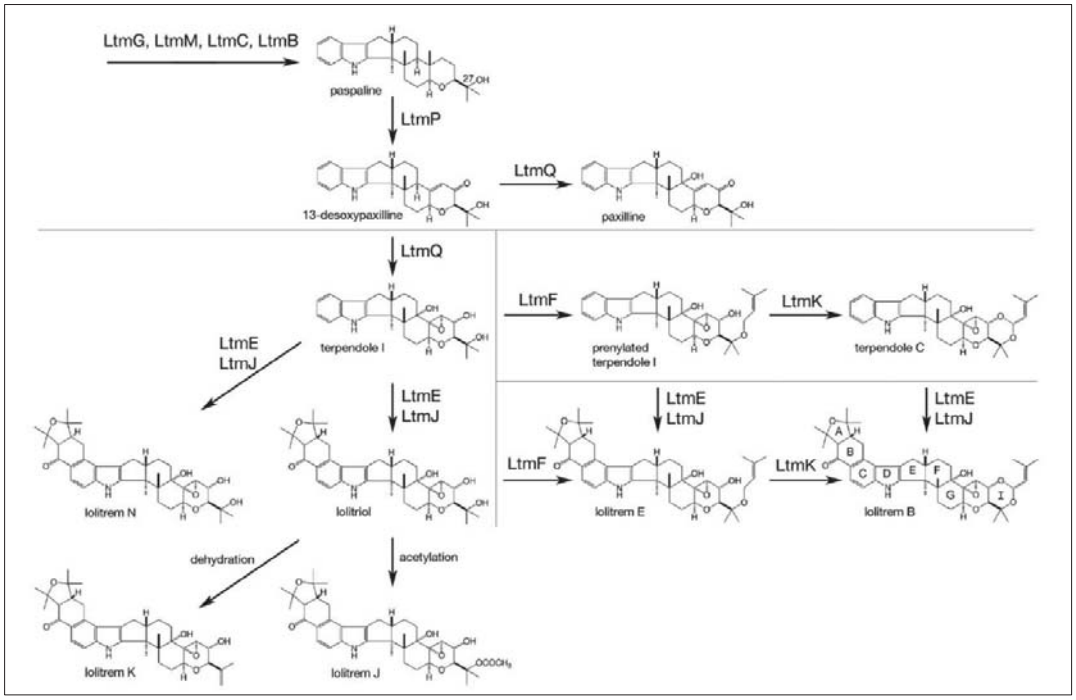


**Figure 1. 3. The proposed pathway for lolitrem B biosynthesis.** Figure is modified from Young *et al*. (2009).

*1.3 Molecular regulators of the symbiosis*

The interaction between the Epichloë and perennial ryegrass is a highly specialised and regulated interaction. The restrictive mode of growth of *E. festucae* in the grass suggests there is communication between the host and endophyte that serves to maintain the mutualistic relationship, and single gene mutations in the fungus are sufficient to cause a breakdown in the interaction due to a change in the interaction from mutualistic to antagonistic.

The first attempt to look into the molecular regulators of the interaction in *E. festucae* employed a forward genetic screen in order to identify mutants with a disrupted symbiotic phenotype (Tanaka *et al.*, 2006). The study found that disruption of *noxA* in *E. festucae*, encoding the catalytic subunit of an NADPH oxidase (Nox) enzyme complex (a homologue of the mammalian gp91phox) led to a breakdown in the symbiotic interaction. Growth of the mutant endophyte in the plant was unrestricted and extended aberrantly into the host vascular bundles. Development of the host plant was in turn severely affected with stunting and premature senescence of the plants. Later, deletion of two other genes encoding the NoxR and RacA subunits of the Nox enzyme complex was shown to result in similar disruptions in the interaction (Takemoto *et al*., 2006; Tanaka *et al*., 2008). NoxR and RacA are homologues of the mammalian p67phox and Rac2, respectively, which are required for the activation of gp91phox (NoxA) (Diebold & Bokoch, 2001). Thus, these studies demonstrate that the Nox complex and subsequent generation of reactive oxygen species (ROS), such as $O2^{-}$, are essential signalling components of the interaction. Several studies have since revealed other important molecular regulators of the interaction in *E. festucae*. These include SakA, a stress-activated mitogen-activated protein kinase (MAPK) in the fungus (Eaton *et al.*, 2010), Soft, a yet uncharacterised protein important in regulating hyphal anastomosis (Charlton *et al.*, 2012), ProA, a

zinc-finger transcription factor (Tanaka *et al*., 2012) and SidN, a siderophore synthetase involved iron homeostasis (Johnson *et al.*, 2013b).

### *1.4 Histones and chromatin*

The average human skin cell is 30 micron in diameter; but contains about 6 billion basepairs (bp) of DNA stretching over 2 metres in length (Annunziato, 2008). This requires the remarkable organisation of DNA into chromatin, the basic unit of which is the nucleosome, comprising 146 bp of negatively-charged DNA wrapped around an octamer of positively-charged core histones. The octamer itself contains two dimers of H2A and H2B, and a tetramer of H3 and H4. The linker histone H1 is important for stabilising the nucleosome and binds to the outside of the nucleosome at the exit/entry point of DNA, and protects another 20 bp of DNA (Li *et al.*, 2007).

Chromatin exists in different forms of compaction. Actively transcribed genes are found in euchromatin, where DNA is less compacted which allows for transcription to take place. On the other extreme end, DNA is tightly compacted into heterochromatin, where silenced genomic regions such as telomeres and centromeres can be found. The chromatin is not static; temporary dissociations of DNA from the histones are necessary for the separation of the DNA strands in order to allow replication and transcription machinery access to the DNA (Wang *et al.*, 2016).

The N-terminal tails of the core histones, containing about 40 amino acids protrude out of the nucleosome and are post-translationally modified (Fig. 1.4). Some of the most well studied modifications of the histone residues are acetylation, methylation, and phosphorylation, but the list of histone modifications also includes ubiquitylation, sumoylation and ADP-ribosylation. These covalent modifications are thought to bring about changes to the overall chromatin structure in three distinct ways; intrinsic, extrinsic and effector-mediated (Campos & Reinberg, 2009). Intrinsic effects include modifications that result in intranucleosomal variations, such as changes in histone protein conformation and affinity to DNA, while extrinsic effects refer to changes in internucleosomal interactions, such as histone to histone interactions. Finally, effector-mediated effects refer to changes within the chromatin structure brought about by interaction of the post-translationally modified tail residues with non-histone proteins (Campos & Reinberg, 2009).

### *1.5 Histone modifications*

The acetylation of histones takes place only on lysine residues and the acetylated histones are generally associated with transcriptionally active chromatin. Histone acetylation is catalysed by histone acetyltransferases (HATs) and the reverse process is catalysed by histone deacetylases (HDACs). Both of these enzymes represent the first classes of histone-modifying enzymes to be discovered (Brownell *et al.*, 1996, Taunton *et al.*, 1996) . The addition of the negatively charged acetyl group is thought to have a direct effect on the overall charge of a histone protein, particularly when many of the lysine residues on a single tail are acetylated (hyperacetylation). This process results in decreased affinity of histone for DNA and subsequent relaxation of the chromatin, facilitating gene transcription. The acetyl-lysine residues on

the histones can be recognised by proteins such as the SWI/SNF complex that can subsequently bring about decondensation of chromatin (Hassan *et al*., 2002). Phosphorylation can also take place on serine, threonine or tyrosine residues of the histones. Like acetyl groups, the phosphate group is similarly thought to impart a substantial negative charge to the histone protein, leading to chromatin relaxation (Ajiro, 2000, Bannister & Kouzarides, 2011).


**Figure 1. 4. Modified amino acid residues of the histone H3 and H4 N-terminal tails.** Modified residues are shown in enlarged fonts and modifications that have been characterised in filamentous fungi are indicated by asterisks. A: Acetylation, M: Methylation and P: Phosphorylation. Figure adapted from Lewis & Selker (2010).

ADP-ribosylation is another reversible histone modification where one or more adenosine diphosphate ribose moieties are covalently attached to glutamate or arginine residues of the histones. This modification is thought to influence the extent of chromatin condensation and can be observed when cells are challenged by mutagenic stress, such as by the presence of reactive oxygen species (Hassa *et al.*, 2006). In contrast, both ubiquitylation (9 kDa) and sumoylation (11 kDa) represent substantially larger covalent modifications of histone residues. The attachment of ubiquitin to histone lysine residues is a reversible histone modification that can occur singly or in tandem. In human cells, monoubiquitination of lysine 119 of histone H2A by the Polycomb-group proteins is linked to a silent chromatin state (Wang *et al.*, 2004). Similarly, the attachment of small ubiquitin-related modifier (SUMO) proteins to histone lysine residues is thought to be a repressive mark for transcription (Nathan *et al.*, 2003). Remarkably, chromatin can also be regulated at the molecular level, such as by *cis-trans* isomerisation of proline 38 of histone H3, catalysed by the proline isomerase Fpr4 (Nelson *et al.*, 2006). The isomerisation results in structural changes in the preceding N-terminal region of the protein and affects the ability of the adjacent lysine 36 residue to be methylated, which is a mark for transcriptionally active chromatin (Nelson *et al*., 2006).

*1.6 Histone methylation*

In contrast to histone acetylation, methylation does not affect the overall charge of the histone. Rather, the addition of a methyl group is thought to increase the basicity and hydrophobicity of the modified residue, resulting in a greater affinity of histone for DNA (Nakayama *et al.*, 2001). Histone methylation can be a mark of both active and silent chromatin, depending on the residue of the histone tail being

modified, as well as the methylation states (of mono-, di- or tri-) of the residues. Both lysine and arginine residues of the histone tail can be methylated. Methylation of histone arginine residues is performed by arginine methyltransferases, with S-adenosylmethionine (SAM) being the methyl donor. Similarly, SAM also provides the methyl moiety for the methylation of histone lysine residues, catalysed by histone lysine methyltransferases (HKMTs). All of the HKMTs characterised so far, with SUV39H1, a H3K9 methyltransferase as the founding member (Rea *et al.*, 2000), contain the SET catalytic domain. An exception to this is the histone H3K79 methyltransferase Dot1. Although Dot1 does not contain a SET domain, the histone H3K79 residue which Dot1 methylates is located within the globular histone core; therefore, Dot1 may be different in the sense that it does not methylate residues of the histone N-terminal tail, unlike other HKMTs (Nguyen & Zhang, 2011).

*1.7 Methylation of histone H3K4*

In yeast, methylation of histone H3K4 is performed by the COMPASS (Complex Proteins Associated with Set1) complex with Set1 as the main catalytic subunit that is responsible for all three forms of mono-, di- and tri- H3K4 methylation (Roguev *et al.*, 2001, Krogan *et al.*, 2002, Schneider *et al.*, 2005). *Drosophila* has three homologues of yeast Set1 (dSet1, Trithorax and Trithorax-related) and these exist and function in three COMPASS-like H3K4 methyltransferase complexes (Mohan *et al.*, 2011). In mammals, each of these genes is further duplicated resulting in six homologues (SET1A and SET1B are homologues of dSet1; MLL1 and MLL2 are homologues of Trithorax; and MLL3 and MLL4 are homologues of Trithorax-related) that give rise to six COMPASS-like complexes (Shilatifard, 2012).

Early findings found a correlation between H3K4 methylation and gene activation (Strahl *et al.*, 1999, Santos-Rosa *et al.*, 2002) and subsequent development of high-resolution interrogation techniques such as ChIP-Chip and ChIP-seq revealed the positive correlation of H3K4me3 with transcription start sites (TSSs) and active gene transcription. This feature of H3K4me3 appears to be conserved across organisms and is observed in mammals, plants, yeast and filamentous fungi (Pokholok *et al.*, 2005, Barski *et al.*, 2007, Zhang *et al.*, 2009, Connolly *et al.*, 2013). The presence of H3K4me1, me2 and me3 all correlated with gene transcription, however, the distributions of H3K4me2 and H3K4me1 differ from that of H3K4me3 (Fig. 1.5). In yeast, H3K4me2 peaks at the middle of genes, and H3K4me1 peaks near the 3' end of genes (Pokholok *et al*., 2005). Yet in Fusarium, both H3K4me2 and H3K4me3 peak near TSSs, and overlapping distributions between the two were observed, highlighting the differences that could exist in different fungi (Connolly *et al*., 2013).

Although generally a mark for active chromatin, H3K4 trimethylation has been shown to be required for the repression of silenced loci in yeast, such as the telomeric regions, the *HML*, *HMR* and the rDNA loci. With the use of reporter strains, Nislow *et al.* (1997) first showed the requirement of Set1 in this respect in silencing telomeric genes including the *HML* locus. Subsequently, Briggs *et al.* (2001) showed the involvement of Set1 in rDNA silencing, and importantly, that H3K4 methylation is present at the rDNA locus and that only *set1* constructs that can restore H3K4 methylation can restore the rDNA silencing defects in Δ*set1*, demonstrating the role of H3K4 methylation in silencing. Subsequent studies reported similar roles for Set1, the COMPASS complex and H3K4me3 in telomeric, centromeric, *HML* and rDNA silencing (Krogan *et al.*, 2002, Kanoh *et al.*, 2003, Fingerman *et al.*, 2005). Studies in yeasts have also shown

a role for Set1 in telomere maintenance, but interestingly, while deletion of *set1* in budding yeast shortened the telomeres by about 50 bp, deletion of *set1* in fission yeast extended the telomeres by about 120 bp (Nislow *et al*., 1997; Kanoh *et al*., 2003).

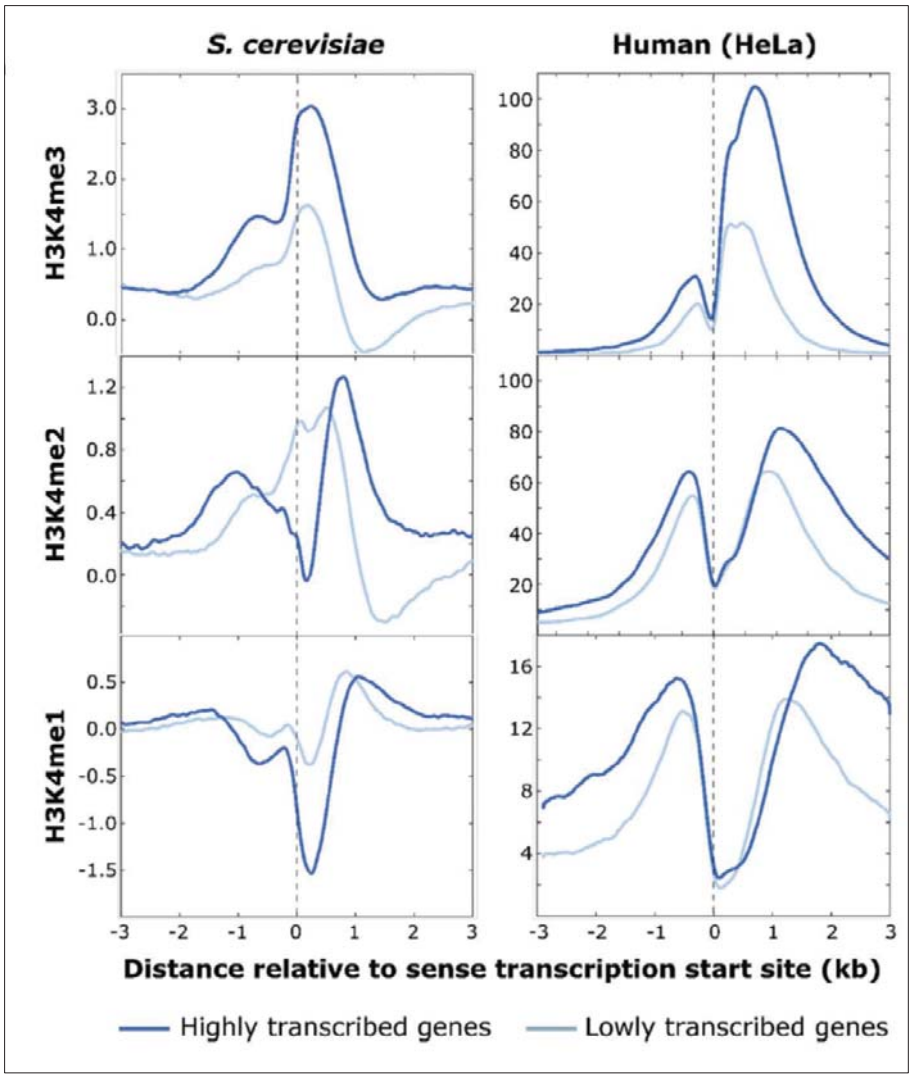


**Figure 1. 5. Distribution of H3K4 methylation around yeast and human genes.** X-axes show distance relative to the transcription start site (zero). Figure taken from Howe *et al*., 2017.

*1.8. Methylation of histone H3K9*

Methylation of histone H3K9 is associated with gene silencing (Bannister *et al.*, 2001). In *Drosophila*, it was initially discovered that integrating or juxtaposing a gene normally found in euchromatin into a heterochromatin region effectively silences the gene, a phenomenon known as position-effect variegation (PEV) (Wakimoto, 1998). Genetic analyses identified several suppressors of this phenomenon, which are referred to as Su(var) (suppressor of variegation) genes. The homologue of *Drosophila* Su(var)3-9 in human, SUV39H1, was subsequently shown to be a histone H3K9 methyltransferase (Rea *et al*., 2000). High-resolution ChIP-sequencing revealed that the distributions of H3K9me2/me3 and H3K27me2/me3 in human cells are inversely correlated with gene expression, reflecting the association of both marks with

silent genes (Fig. 1.6). In contrast, the correlation of H3K9me1 and H3K27me1 with active genes suggests that they are marks associated with transcription (Barski *et al*., 2007).

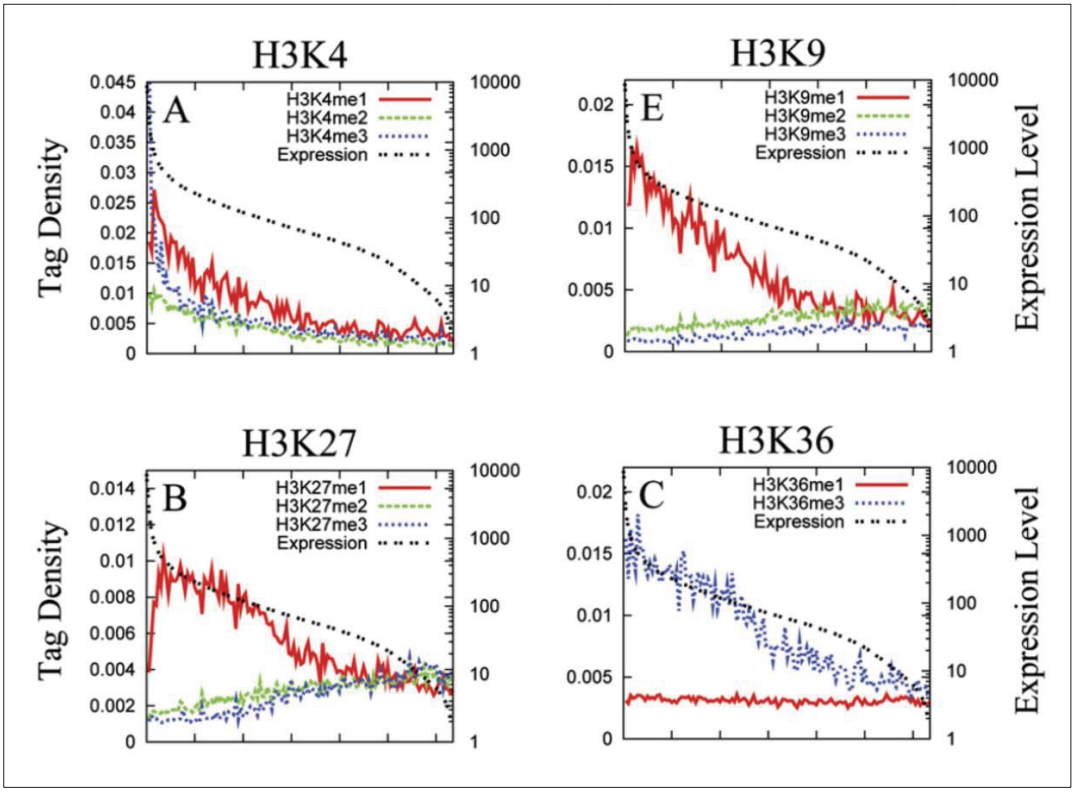


**Figure 1. 6. Correlation of histone methylation with gene transcription in human cells.** X-axes (left to right) represent groups of genes ordered by their expression from high to low. Right Y-axes indicate expression level of the gene and left Y-axes indicate level of histone methylation. Figure taken from Barski *et al*., 2007.

Methylated H3K9 was shown to be the binding site for another dominant suppressor of PEV, Heterochromatin Protein 1 (HP1), a protein that also localises to the heterochromatin and contributes to its establishment and maintenance (Eissenberg *et al.*, 1990, Bannister *et al.*, 2001, Lachner *et al.*, 2004, Maison & Almouzni, 2004). HP1 is a marker for heterochromatin and undergoes a very rapid turnover between its free and H3K9me-bound states turnover (Cheutin *et al.*, 2003), but the exact mechanisms by which HP1 induces heterochromatin formation are unclear. HP1 interacts with many different proteins so it is thought that these interacting proteins are involved in the generation and maintenance of heterochromatin (Lomberk *et al.*, 2006, Fanti & Pimpinelli, 2008). However, the chromoshadow domain of HP1, which mediates its dimerisation also serves to physically bridge proximally methylated and HP1-bound nucleosomes, thereby favouring the spread of heterochromatin (Canzio *et al.*, 2011). Keller *et al.* (2012) showed that rather than being transcriptionally silent; transcription still takes place within heterochromatin but that transcripts are captured by HP1 for subsequent degradation. Although both H3K9me3 and HP1 are associated with heterochromatin and gene silencing, H3K9me3 can also be found on active promoters (Squazzo *et al.*, 2006, Vakoc *et al.*, 2006), and recently HP1 has also been shown to bind to the TSS regions of active genes to induce their expression (Shoji *et al.*, 2014).

Heterochromatin can be further classified into constitutive and facultative heterochromatin. Constitutive heterochromatin forms at regions rich in sequence repeats and transposable elements and is generally marked by H3K9me3. By contrast, facultative heterochromatin is marked by H3K27me3 and as its name implies, refers to silent regions where the chromatin is highly compacted, but where decondensation can take place in the presence of specific signals such as during certain developmental stages, in order to allow for transcription to occur. In pathogenic fungi, genes encoding effector proteins are often found close to transposable elements, and H3K9me3 is an important silencing mark for these genes in the fungal pathogen *Leptosphaeria maculans* (Soyer *et al.*, 2014). In *Neurospora crassa*, H3K9me3-marked regions are mostly devoid of genes, and H3K9me3 colocalises with, and is required for DNA methylation (Tamaru & Selker, 2001, Lewis *et al.*, 2009, Jamieson *et al.*, 2013). Similarly, mutants of HP1, the reader of the H3K9me3 mark, lack DNA methylation, suggesting that HP1 links H3K9me3 and DNA methylation in the fungus (Freitag *et al.*, 2004).

### *1.9 Methylation of histone H3K27*

First described in *Drosophila*, the Polycomb group (PcG) refer to proteins or genes whose mutations result in phenotypes mimicking those of the *Polycomb* mutant, having defects in the fly body segmentation (Lewis, 1978, Margueron & Reinberg, 2011). Polycomb group (PcG) proteins function as two distinct complexes; the Polycomb repressive complex 1 (PRC1) and 2 (PRC2). The core components of PRC2 are conserved across species, comprising three proteins in *Drosophila*: the SET-domain containing protein E(z) (Enhancer of zeste), Su(z)12 (Suppressor of zeste) and Esc (Extra sexcombs). PRC2 is a histone H3K27 methyltransferase and E(z) is responsible for the catalytic activity of the complex (Cao *et al.*, 2002, Czermin *et al.*, 2002). The resulting H3K27me3 residue serves as a binding site for PRC1, the larger of the two PRC complexes, which in turn brings about stabilisation and compaction of the chromatin (Shao *et al.*, 1999, Cao *et al.*, 2002). No PRC1 components have been identified in any fungi to date, thus it is unclear how H3K27-dependent compaction of the chromatin is achieved in these organisms (Connolly *et al*., 2013). However, the observation that H3K27me3 marks are redistributed in the genome in the absence of H3K9me3 suggests that there is crosstalk between H3K27me3 and H3K9me3 (Basenko *et al*., 2015).

PcG proteins and H3K27 methylation are known to regulate numerous genes and processes, but their regulatory roles were initially studied most intensively in the field of developmental biology, particularly in the regulation of *Hox* genes. Transcriptionally silent *Hox* genes are rich in H3K27 trimethylation and this silencing is also dependent on the presence of a functional E(z) catalytic subunit (Müller *et al.*, 2002). In *Drosophila* embryos, *Hox* genes are derepressed when PcG proteins are removed; however, re-repression can take place if the proteins are reintroduced within a few cell generations, indicating that these marks are also inherited (Beuchle *et al.*, 2001). H3K27 methylation is important in X chromosome inactivation (XCI), the random but crucial process in which the second X chromosome in female cells is silenced. Mice embryos with a null mutation in *eed* (the mouse homologue of *ezh*) had impaired XCI and acquired two active X chromosomes (Wang *et al.*, 2001). Further, both PRC2 and H3K27 trimethylation were shown to accumulate on the inactivated X chromosomes in a Xist-dependent manner very early during the initiation process (Plath *et al.*, 2003, Silva *et al.*, 2003).

In *N. crassa*, H3K27me3 marks silent genes and its distribution is highest at the subtelomeric regions (Jamieson *et al.*, 2013). This distribution of H3K27me3 is important for the genome architecture and mutants lacking H3K27me2/me3 have disrupted tethering of the telomeres to the nuclear membrane (Galazka *et al.*, 2016). H3K27me3 and H3K9me3 form almost no overlap in this fungus and cover distinct regions of the genome (Jamieson *et al.*, 2013). Interestingly, in the absence of H3K9me3 (by disruption of the H3K9 methyltransferase in *N. crassa*), H3K27me3 is redistributed into the constitutive heterochromatic regions which were marked by H3K9me3, but this redistribution of H3K27me3 does not compensate for silencing (Basenko *et al.*, 2015). In *Fusarium graminearum*, H3K27me3 similarly marks subtelomeric regions, but also regions with low conservation and synteny with other Fusarium species, whereas regions with high synteny are marked by H3K4me2 (Connolly *et al.*, 2013). Strikingly, although genes for the H3K9 and H3K27 methyltransferases are found across many fungi, they are not found in the model yeast *Saccharomyces cerevisiae* (Freitag, 2017). Instead, the yeast makes up for the absence of these heterochromatic marks by generating heterochromatin with the silent information regulator (SIR) proteins (Wang *et al.*, 2016).

### *1.10 Methylation of histone H3K36*

Methylation of H3K36 is performed by the SET domain-containing protein Set2. In many fungi including *S. cerevisiae*, *Saccharomyces pombe* and *N. crassa*, Set2 is required for H3K36 mono-, di- and trimethylation (Strahl *et al.*, 2002, Adhvaryu *et al.*, 2005, Morris *et al.*, 2005), although surprisingly, deletion of *kmt3* (*set2*) in *M. oryzae* was not found to affect H3K36me3 levels (Pham *et al.*, 2015). By contrast, the Set2 homologue in mammals, Setd2, catalyses only H3K36 trimethylation *in vivo* (Edmunds *et al.*, 2008, Yuan *et al.*, 2009). In these systems, other H3K36 methyltransferases, of which there are eight, catalyse the different forms of H3K36 methylation (Wagner & Carpenter, 2012). The mammalian nuclear receptor SET domain-containing 1 (NSD1) specifically catalyses H3K36 mono- and dimethylation(Li *et al.*, 2009, Lucio-Eterovic *et al.*, 2010).

In general, H3K36 trimethylation correlates with gene expression and has roles in regulating transcriptional elongation, suggesting that the mark is involved in transcriptional activation (Fig. 1.6). However, in *F. graminearum*, ChIP-seq analysis found no association between H3K36 methylation and active transcription (Connolly *et al.*, 2013). In yeast, deletion of Set2 resulted in transcriptional elongation defects and accumulation of RNA polymerase II at 3' end of genes (Kizer *et al.*, 2005). This could be explained by the interaction of Set2 with RNA polymerase II via the WW and C-terminal SRI domain of Set2. This interaction is important for transcription elongation, but H3K36 methylation is also important in this aspect as only Set2 constructs that restored H3K36 methylation could rescue the Δ*set2* phenotype (Li *et al.*, 2002, Kizer *et al.*, 2005). The distribution of H3K36me3 peaks towards the 3' end of genes and this also appears to be conserved in filamentous fungi (Connolly *et al.*, 2013) (Fig. 1.7).

Correlations of Set2 and H3K36 methylation with gene repression have also been observed, in fact, Set2 was initially characterised as a transcriptional repressor (Strahl *et al.*, 2002). A possible link between H3K36me3 with gene silencing is provided by the observation that the DNA methyltransferase Dnmt3a binds to H3K36me3 via its PWWP domain, and that this interaction is important for the enzymatic activity of Dnmt3a (Dhayalan *et al.*, 2010). H3K36me3 also binds the chromodomain of Eaf3, a subunit of the

Rpd3S histone deacetylase complex that is involved in gene repression (Keogh *et al.*, 2005). In yeast, deletion of *set2* was found to result in silencing of the telomeric and rDNA loci (Ryu *et al.*, 2014). In support of this, deletion of *set2* increased the recruitment of Net1 and Sir2 to the rDNA loci; Net1 and Sir2 are components of the RENT (regulator of nucleolar silencing and telophase exit) complex that mediates rDNA silencing (Ryu & Ahn, 2014).

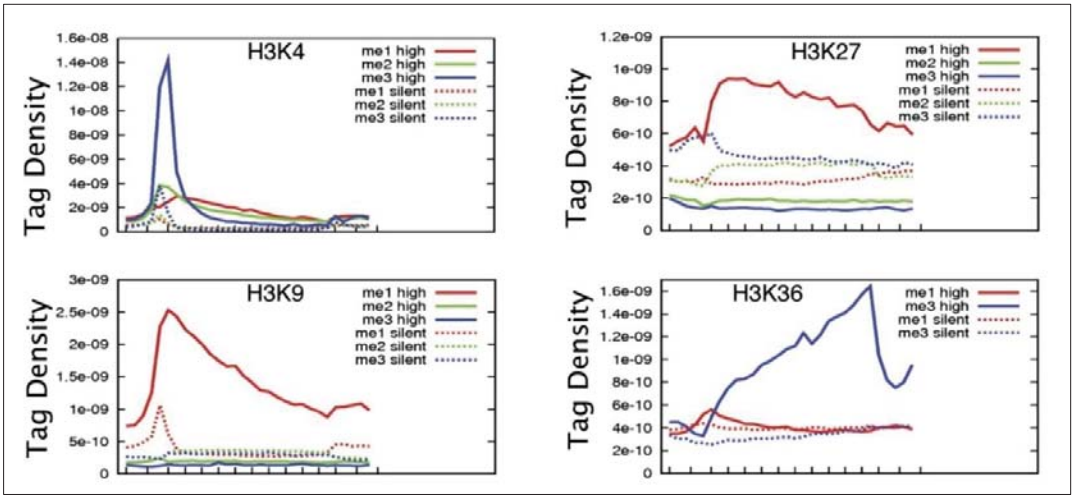


**Figure 1. 7. Histone methylation profiles at active and silent gene regions.** The data represent composite profiles of histone marks at 1000 genes in the human T-cell. Transcriptionally active genes are enriched in H3K4 trimethylation at promoter regions. H3K9, H3K27, H2BK5 and H4K20 monomethylation peak at 5' regions of active genes, but H3K36 trimethylation peaks at 3' regions. In comparison, silent genes have increased H3K27 methylation marks. Taken from Barski *et al*. (2007).

*1.11 Histone demethylation by JmjC proteins*

Methylation of histones was originally thought to be an irreversible modification, but was later proposed that these modifications could be removed by clipping of the N-terminal histone tails which contain the modified residues. However, such a mechanism does not offer a very dynamic regulation of histone methylation (Klose & Zhang, 2007). In 2004, a peptidyl arginine deiminase enzyme, PADI4 was discovered which catalyses the demethylimination of methylated arginine residues into citrulline (Cuthbert *et al.*, 2004). PADI4 is not considered as a true histone demethylase as it does not produce an unmodified arginine, but it indicated that a dynamic regulation of histone methylation was possible.

Shortly after, the discovery of the first *bona fide* histone demethylase was reported that was capable of reverting methyllysine to an unmodified lysine. The enzyme, LSD1 catalyses the oxidation of the ammonium group of a methyllysine, requiring flavin adenine dinucleotide (FAD) as a cofactor in the reaction and generating formaldehyde as a by-product (Fig. 1.8A) (Shi *et al.*, 2004). LSD1 can specifically recognise and demethylate H3K4me1/me2 *in vitro*, but it needs to form a complex with other proteins, such as CoREST (restin corepressor), in order to recognise and demethylate H3K4me1/me2 in a nucleosomal context.

Jumonji-C (JmjC) domain-containing proteins represent the second class of histone demethylases distinct from LSD1 that can catalyse the oxidative demethylation reactions of lysine and arginine residues. In 2006, several proteins of this class were reported that catalyse the demethylation of histone H3K9 and H3K36

residues. These include the human JmjC domain-containing histone demethylase 1A (JHDM1) that converts mono- and dimethyllysine (H3K36me1/me2) to unmethylated lysine (Tsukada *et al.*, 2006). Others include JHDM3A and Jumonji domain-containing protein 2A (JMJD2A) that are capable of demethylating histone H3K9me3/K36me3 (Klose *et al.*, 2006b, Whetstine *et al.*, 2006), and JHDM2A that demethylates H3K9me2/me3 (Yamane *et al*., 2006). All of these enzymes catalyse the demethylation of methyllysine in an iron Fe(II) and α-ketoglutarate (α-KG) dependent reaction (Fig. 1.8B) and mutagenesis studies showed that the catalytic activity of JmjC proteins reside within the JmjC domain (Chen *et al.*, 2006, Yamane *et al.*, 2006, Li *et al.*, 2010). Within this domain are three conserved residues (two histidine and one aspartate/glutamate) which interact with Fe(II), and two other residues (a lysine, and another phenylalanine, threonine or tyrosine) which bind to the α-KG co-factor.

Over the next few years, an intense effort by the scientific community to search for other JmjC demethylases resulted in the identification of novel JmjC demethylases with diverse target histone specificities. A new nomenclature was consequently suggested to account for the somewhat inconsistent naming of these proteins (Table 1.1) (Allis *et al.*, 2007). In this nomenclature, the first histone lysine demethylase, LSD1, is given the name KDM1 (lysine demethylase 1), while the remaining JmjC lysine demethylases were named KDM2-KDM6. Currently, the list can be expanded to include the KDM7 group of H3K9/K27 dual-specificity demethylases (Tsukada *et al.*, 2010) and the KDM8 group of H3K36me2 demethylase (Hsia *et al.*, 2010). As LSD1 can only demethylate mono- and dimethyllysine, the JmjC proteins also represent the only group of demethylases that can demethylate trimethyllysine.

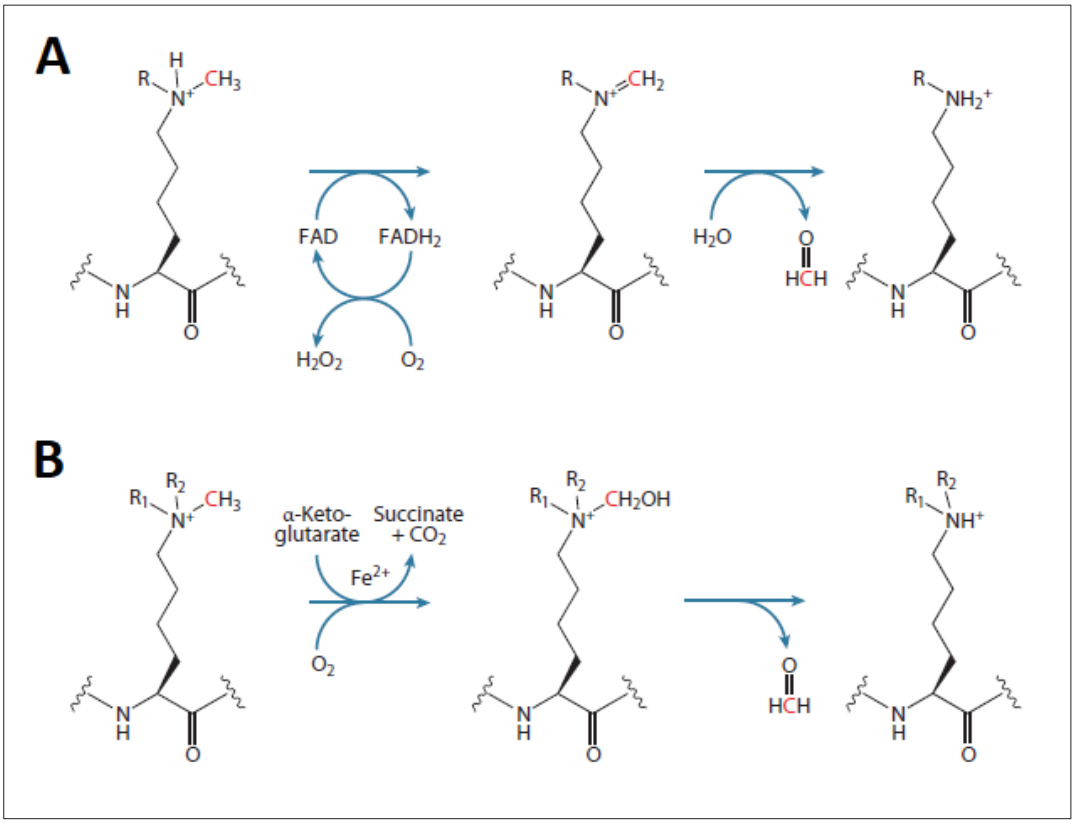


**Figure 1. 8. Demethylation reactions catalysed by LSD1 and JmjC proteins.** The demethylated carbons catalysed by (A) LSD1 and (B) JmjC proteins are indicated in red. Figure is taken from Mosammaparast & Shi (2010).

**Table 1. 1. A new nomenclature for lysine demethylases.** Taken from Allis *et al.* (2007).

| New Name | Human | *D. melanogaster* | *S. cerevisiae* | *S. pombe* | Substrate Specificity | Function |
|---|---|---|---|---|---|---|
| KDM1 | LSD1/BHC110 | Su(var)3-3 | | SpLsd1/Swm1/ Saf110 | H3K4me1/2, H3K9me1/2 | Transcription activation and repression, hetero-chromatin formation |
| KDM2 | | | Jhd1 | | H3K36me1/2 | Transcription elongation |
| KDM2A | JHDM1a/FBXL11 | | | | H3K36me1/2 | |
| KDM2B | JHDM1b/FBXL10 | | | | H3K36me1/2 | |
| KDM3A | JHDM2a | | | | H3K9me1/2 | Androgen receptor gene activation, spermatogenesis |
| KDM3B | JHDM2b | | | | H3K9me | |
| KDM4 | | | Rph1 | | H3K9/ K36me2/3 | Transcription elongation |
| KDM4A | JMJD2A/JHDM3A | | | | H3K9/ K36me2/3 | Transcription repression, genome integrity |
| KDM4B | JMJD2B | | | | H3K9/ H3K36me2/3 | Heterochromatin formation |
| KDM4C | JMJD2C/GASC1 | | | | H3K9/ K36me2/3 | Putative oncogene |
| KDM4D | JMJD2D | | | | H3K9me2/3 | |
| KDM5 | | Lid | Jhd2 | Jmj2 | H3K4me2/3 | |
| KDM5A | JARID1A/RBP2 | | | | H3K4me2/3 | Retinoblastoma-interacting protein |
| KDM5B | JARID1B/PLU-1 | | | | H3K4me1/2/3 | Transcription repression |
| KDM5C | JARID1C/SMCX | | | | H3K4me2/3 | X-linked mental retardation |
| KDM5D | JARID1D/SMCY | | | | H3K4me2/3 | Male-specific antigen |
| KDM6A | UTX | | | | H3K27me2/3 | Transcription activation |
| KDM6B | JMJD3 | | | | H3K27me2/3 | Transcription activation |

*1.12 Regulation of fungal secondary metabolism by histone modifications*

The first studies looking at the chromatin level of fungal secondary metabolite gene regulation analysed the role of histone acetylation in this aspect. In *Aspergillus*, acetylation of histone H4 was found to positively correlate with the expression of the aflatoxin cluster genes (Roze *et al.*, 2007), and deletion of a histone deacetylase, *hdaA*, led to the upregulation of genes of the sterigmatocystin (ST) and penicillin (PN) clusters, but not the terrequinone A cluster (Shwab *et al.*, 2007). Interestingly, the ST and PN clusters, like the *ltm* and *eas* clusters in *E. festucae*, are located subtelomerically in *Aspergillus nidulans*, about 90 kb and 30 kb away from the telomeric ends of the chromosomes. The terrequinone A cluster on the other hand, is found approximately 700 kb away from the telomere. This suggests that HdaA may specifically regulate subtelomeric SM clusters and may have a role in regulating the *E. festucae EAS* and *LTM* secondary metabolite clusters, which are located about 10 kb away from the telomeres. The HdaA homologue in *S. cerevisiae* also shows a preferential activity towards subtelomeric regions (Robyr *et al.*, 2002).

Deletion of *cclA* in *A. nidulans*, which encodes a component of the COMPASS complex of H3K4 methyltransferase resulted in significant derepression of secondary metabolism in the fungus and led to the identification of novel secondary metabolites (Bok *et al.*, 2009). H3K4me2/me3 levels at some of these genes were reduced in the mutant as expected; but interestingly, this was also accompanied by a

reduction in H3K9me2/me3 levels. Thus, although H3K4me2/me3 is typically a mark for active genes, it was proposed that both methylation profiles function to repress these secondary metabolite genes (Bok *et al*., 2009). Similarly, deletion of *cclA* in *Aspergillus fumigatus* resulted in the derepression of secondary metabolite genes and increased production of gliotoxin and other secondary metabolites (Palmer *et al.*, 2013), and recently, deletion of *cclA* in Fusarium also affected secondary metabolite expression (Studt *et al.*, 2017). On the other hand, deletion of *kdmB*, encoding the H3K4me3 demethylase in *A. nidulans*, resulted in the reduced expression of secondary metabolite genes (Gacek-Matthews *et al.*, 2016). Thus, although generally a mark of active genes, these studies point to a repressive role of H3K4me2/me3 on secondary metabolite gene clusters in fungi.

The H3K9 methyltransferase ClrD, as well as the HP1 homologue, HepA in *A. nidulans* have been shown to repress the silent ST cluster genes during the active growth phase of the fungus (Reyes-Dominguez *et al*., 2010). In *E. festucae*, deletion of *clrD* also derepresses the silent *EAS* and *LTM* clusters in culture (Chujo & Scott, 2014). Deletion of *hep1*, enoding the HP1 homologue in *F. graminearum* resulted in lower H3K9me3 occupancy levels at secondary metabolite (SM) genes and increased expression of the aurofusarin cluster, as well as production of the corresponding metabolite, aurofusarin (Reyes-Dominguez *et al.*, 2012). However, expression of the trichothecene (TC) cluster genes and subsequent production of the metabolite, deoxynivalenol, were downregulated, suggesting a repressive role for Hep1 on the TC cluster genes (Reyes-Dominguez *et al*., 2012).

Connolly *et al*. (2013) observed that 75% of silent genes (n = 4,449) in *F. graminearum* are enriched for H3K27me3. This histone mark was prominent around the subtelomeric, non-syntenic regions of the fungus. Deletion of the E(z) H3K27 methyltransferase homologue, *kmt6*, abolished H3K27 trimethylation in the mutant and brought about derepression of 32 of the 45 secondary metabolite clusters in the fungus; whereas only 5 of these clusters were constitutively-expressed in the wild-type strain. (Connolly *et al*., 2013). In *E. festucae*, deletion of *ezhB*, which encodes the homologue of *F. graminearum* KMT6, also resulted in derepression of secondary metabolite genes in culture (Chujo & Scott, 2014).

The telomeric regions in *N. crassa* are also enriched for H3K27me3 and H3K9me3 marks (Jamieson *et al.*, 2013). However, while H3K27me3 covers 774 genes or approximately 6.8% of the genome, all of which are silent, the regions covered by H3K9me3 are primarily A:T-rich and devoid of genes. Deletion of the E(z) homologue, *set-7* in *N. crassa*, abolished H3K27me3 and brought about the derepression of 130 genes in the mutant (Basenko *et al.*, 2015). Both studies in *F. graminearum* and *N. crassa* also found that for many silent genes, removal of H3K27 trimethylation alone, a mark for facultative heterochromatin, is insufficient to cause their derepression.

LaeA (loss of aflR expression-A) is a master regulator of secondary metabolism that is required for the production of ST, PN, lovastatin and gliotoxin, genes for which are all organised in clusters in the Aspergillus species (Bok & Keller, 2004, Bok *et al.*, 2006a). In a whole genome analysis, LaeA was shown to influence expression of 9.5% of the 9,626 genes in *A. fumigatus*, and positively regulate up to 40% of SM genes (Perrin *et al.*, 2007). LaeA is a nuclear protein and contains an S-adenosylmethionine (SAM) binding domain. Mutations within this domain mimic a Δ*laeA* phenotype (Bok *et al.*, 2006b). These data suggest that LaeA is a putative methyltransferase; however, biochemical evidence is still lacking for this hypothesis. Interestingly, in *A. nidulans*, LaeA counteracts ClrD-mediated H3K9 trimethylation and

subsequent binding of HepA at the *aflR* promoter (Reyes-Dominguez *et al.*, 2010). Therefore, LaeA likely activates *aflR* expression by preventing heterochromatin formation at the *aflR* locus. However, absence of H3K9me3 and HepA at the *aflR* locus in the *clrD* and *hepA* mutants, respectively, are not sufficient to activate *aflR* expression, suggesting that LaeA also activates *aflR* via additional mechanisms (Reyes-Dominguez *et al*., 2010). LaeA also regulates a wide range of secondary metabolite pathways across different fungal species and is intimately linked to the velvet family of proteins and regulation of fungal secondary metabolism by light (Bayram & Braus, 2011).

The first study looking at the role of chromatin regulation of secondary metabolism in *E. festucae* analysed the effects of H3K9 and H3K27 methylation in the fungus (Chujo & Scott, 2014). The authors showed that H3K9me3 and H3K27me3 occupancies at the promoter regions of *eas* and *ltm* genes (which are preferentially expressed by the fungus only *in planta*) are significantly lower *in planta* compared to axenic culture. Deletion of *clrD*, encoding an H3K9 methyltransferase, and *ezhB*, encoding an H3K27 methyltransferase both resulted in the derepression of most of the *eas* and *ltm* genes. However, despite the significant upregulation of these genes, the final metabolites, lolitrem B and ergovaline, as well as their intermediates remained undetectable in culture, presumably because some pathway genes remained silent. The authors then tested the effects of the double *clrD*/*ezhB* deletion and found that the *eas* and *ltm* genes were further derepressed in this mutant. Interestingly, H3K9me3 levels in both the promoter and coding regions of the *eas* and *ltm* genes were reduced in the *ezhB* (H3K27 methyltransferase) mutant. And vice versa, H3K27me3 levels in these gene regions were also reduced in the *clrD* (H3K9 methyltransferase) mutant (Chujo & Scott, 2014). This crosstalk between H3K9me3 and H3K27me3 was also observed in *N. crassa* (Basenko *et al*., 2015).

### *1.13 Aims of this study*

The biosynthesis of many fungal secondary metabolites typically involves several enzymes in a given pathway and the genes for these enzymes are usually found in clusters in the genome, often close to the telomeres. This physical organisation of the genes render them particularly amendable to regulation at the chromatin level, which allows the simultaneous regulation of a subset of genes. Several studies have now demonstrated the importance of histone methylation in SM regulation but most have analysed the roles of histone methyltransferases in this respect. These methyltransferases, including the H3K4, H3K9 and H3K27 methyltransferases, typically function to repress secondary metabolism in fungi (Bok *et al*., 2009; Palmer *et al*., 2013; Chujo & Scott, 2014; Liu *et al*., 2015; Gu *et al*., 2017; Studt *et al*., 2017). Therefore, the corresponding histone demethylases are expected to play the opposite roles to the histone methyltransferases with respect to fungal secondary metabolism. When this study was initiated, there was no report on histone demethylases in filamentous fungi. The aim of this study was therefore to identify and characterise histone lysine demethylases in *E. festucae*, with the following objectives:

1. Identify candidate histone demethylase genes using a bioinformatics approach.
2. Characterise target histone specificity of candidate histone demethylases using a biochemical approach.
3. Determine the roles of the demethylase(s) in secondary metabolite gene regulation.

4. Determine the roles of the demethylase(s) in regulating the symbiotic interaction phenotype of *E. festucae*.

# Chapter 2: Materials and Methods

## 2.1 Biological materials

Bacterial and fungal strains, plasmids, and plant material used this study are listed in Table 2.1.

**Table 2. 1. List of organisms and plasmids used in this study.**

| Organism/Strain | Characteristics | Reference |
|---|---|---|
| ***E. coli*** | | |
| DH5α | F⁻, ϕ80*lacZ*, ΔM15, Δ(*lacZYA-argF*), U169, *recA1*, *endA1*, *hsdR17* ($r_k^-$, $m_k^-$), *phoA*, *supE44*, λ⁻, *thi-1*, *gyrA96*, *relA1* | Invitrogen |
| PN4246 | DH5α; pYL3 | Lukito, 2014 |
| ***E. festucae*** | | |
| PN2278 (Fl1) | Wild-type | Young *et al*., 2005 |
| PN3204 (*jmj1*-OE#15) | Fl1/pYL4; HygR | This study |
| PN3205 (*jmj1*-OE#13) | Fl1/pYL4; HygR | This study |
| PN3206 (*jmj2*-OE#23) | Fl1/pYL5; HygR | This study |
| PN3207 (*jmj2*-OE#22) | Fl1/pYL5; HygR | This study |
| *jmj3*-OE#23 | Fl1/pYL6; HygR | This study |
| *jmj3*-OE#14 | Fl1/pYL6; HygR | This study |
| *jmj4*-OE#24 | Fl1/pYL7; HygR | This study |
| PN3211 (*jmj4*-OE#5) | Fl1/pYL7; HygR | This study |
| PN3212 (*jmj5*-OE#1) | Fl1/pYL8; HygR | This study |
| *jmj5*-OE#19 | Fl1/pYL8; HygR | This study |
| *jmj6*-OE#12 | Fl1/pYL9; HygR | This study |
| *jmj6*-OE#23 | Fl1/pYL9; HygR | This study |
| *jmj7*-OE#13 | Fl1/pYL10; HygR | This study |
| *jmj7*-OE#15 | Fl1/pYL10; HygR | This study |
| *jmj8*-OE#5 | Fl1/pYL11; HygR | This study |
| *jmj8*-OE#4 | Fl1/pYL11; HygR | This study |
| PN3171 (Δ*kdmB*#309) | Fl1/Δ*kdmB*::P*trpC-hph*-T*trpC*; HygR | This study |
| PN3172 (Δ*kdmB*#332) | Fl1/Δ*kdmB*::P*trpC-hph*-T*trpC*; HygR | This study |
| PN3173 (Δ*kdmB*#343) | Fl1/Δ*kdmB*::P*trpC-hph*-T*trpC*; HygR | This study |
| PN3177 (Δ*kdmb*/*kdmB*#3) | Fl1/Δ*kdmB*/*kdmB*; pYL19; HygR, GenR | This study |
| PN3178 (Δ*kdmb*/*kdmB*#19) | Fl1/Δ*kdmB*/*kdmB*; pYL19; HygR, GenR | This study |
| PN3174 (Δ*jmj4*#68) | Fl1/Δ*jmj4*::P*trpC-nptII*-T*trpC*; GenR | This study |
| PN3175 (Δ*jmj4*#72) | Fl1/Δ*jmj4*::P*trpC-nptII*-T*trpC*; GenR | This study |
| PN3176 (Δ*setB*#83) | Fl1/Δ*setB*::P*trpC-nptII*-T*trpC*; GenR | This study |
| PN3220 (*setB*-OE#4) | Fl1/P*tef-setB*-FLAG-T*tub*;HygR | This study |
| PN3221 (*setB*-OE#9) | Fl1/P*tef-setB*-FLAG-T*tub*;HygR | This study |
| ***L. perenne*** | | |
| *L. perenne* cv. Samson | - | AgResearch |

| Plasmid | Characteristics | Reference |
|---|---|---|
| pSF15.15 (PN1862) | pSP72 containing 1.4-kb *Hind*III P*trpC-hph* from pCB1004 cloned into *Sma*I site. $Amp^R$; $Hyg^R$; *Nco*I-free P*trpC-hph* | S. Foster |
| pDB48 | pRS426 containing 2.2 kb insert of P*trpC-hph*-T*trpC* | D. Berry |
| pNR1 | P*oliC-nat1*-T*tub* | |
| pYL3 | pSF15.15 containing 2.8 kb *Bam*HI/*Pst*I insert of P*tef-pacC*$^c$-T*trpC* | Lukito *et al*., 2015 |
| pYL4 | pSF15.15 containing 5.5 kb insert of P*tef-jmj1*-T*trpC* | This study |
| pYL5 | pSF15.15 containing 6.7 kb insert of P*tef-jmj2*-T*trpC* | This study |
| pYL6 | pSF15.15 containing 5.6 kb insert of P*tef-jmj3*-T*trpC* | This study |
| pYL7 | pSF15.15 containing 2.9 kb insert of P*tef-jmj4*-T*trpC* | This study |
| pYL8 | pSF15.15 containing 1.1 kb insert of P*tef-jmj5*-FLAG-T*trpC* | This study |
| pYL9 | pSF15.15 containing 1.5 kb insert of P*tef-jmj6*-FLAG-T*trpC* | This study |

| | | |
|---|---|---|
| pYL10 | pSF15.15 containing 3.2 kb insert of P*tef-jmj7*-FLAG-T*trpC* | This study |
| pYL11 | pSF15.15 containing 1.2 kb insert of P*tef*-j*mj8*-FLAG-T*trpC* | This study |
| pYL12 | pcDNA3.1 containing FLAG | This study |
| pYL13 | pYL12 containing 4.1 kb insert of *jmj1* | This study |
| pYL14 | pYL12 containing 5.3 kb insert of *jmj2* | This study |
| pYL15 | pUC19 containing insert of 5'*kdmB-hph*-3'*kdmB* | This study |
| pYL19 | pSF17.1 containing 7.8 kb insert of P*kdmB-kdmB* | This study |
| pYL20 | pUC19 containing insert of 5'*jmj4-nptII*-3'*jmj4* | This study |
| pYL23 | pUC19 containing insert of 5'*setB-nptII*-3'*setB* | This study |
| pYL25 | pSF15.15 containing insert of P*tef-setB*-FLAG-T*tub* | This study |
| pYL30 | pDB48 containing 4.3 kb insert of P*setB-setB* | This study |

## 2.2 Media and Growth Conditions

All media were prepared with Nanopure water and sterilised by autoclaving at 121°C for 20 min. Where not specified otherwise, solid media were prepared by addition of 1.5% (w/v) bacteriological agar.

### *2.2.1 E. coli growth conditions*

*E. coli* strains were cultured overnight at 37°C on Luria-Bertani (LB) agar or in LB broth with shaking at 200 rpm. Where antibiotic selection was required, ampicillin or kanamycin was added to a concentration of 100 or 50 μg $mL^{-1}$, respectively. Cultures were kept at 4°C for short-term storage (<2 weeks) or in 50% (v/v) glycerol at -80°C for long-term storage.

### *2.2.2 E. festucae growth conditions*

For regular culture of *E. festucae*, strains were grown at 22°C for 7-14 days on PD agar, or 3-5 days in PD broth with shaking at 200 rpm. Where antibiotic selection was required, hygromycin or geneticin was added to a concentration of 150 or 200 μg $mL^{-1}$, respectively. For temperature stress experiments, strains were cultured on PD agar at 30°C for 20 days. Cultures were kept at 4°C for short-term storage (<6 months) or in 15% (v/v) glycerol at -80°C for long-term storage. For transformation of *E. festucae*, protoplasts were regenerated in soft regeneration (RG) agar and overlaid with RG agar containing antibiotics and maintained for 2-3 weeks. Strains cultured on Blankenship media (Blankenship *et al*., 2001) were maintained for 10-16 days.

### *2.2.3 L. perenne growth conditions*

*L. perenne* seedlings were germinated on 3% (w/v) water agar at 22°C for 7 days in the dark, followed by another 7 days in the dark after inoculation with fungal strains, and a further 7 days in the light before planting. Seedlings were then moved into root trainers containing commercial potting mix and maintained in a temperature (19°C) and light-controlled (16h/8h light/dark cycle) growth room. Plants were watered as necessary.

### *2.2.4 Luria-Bertani (LB) medium*

LB medium contained 1% (w/v) tryptone, 0.5% (w/v) yeast extract and 0.5% (w/v) NaCl, with pH of 7.0-7.5.

### *2.2.5 SOC medium*

SOC medium contained 2% (w/v) tryptone, 0.5% (w/v) yeast extract, 20 mM glucose, 10 mM $MgSO_4.7H_2O$, 10 mM NaCl, 2.5 mM KCl and 10 mM $MgCl_2$.

### *2.2.6 Potato dextrose (PD) medium*

PD medium contained 2.4% (w/v) potato dextrose.

### *2.2.7 Blankenship medium*

Blankenship medium (Blankenship *et al*., 2001) contained 15 mM sucrose, 5 mM glutamine, 0.6 µM thiamine, 80 mM $MgSO_4$, trace elements, and buffered with 30 mM $K_2HPO_4$ and 30 mM $KH_2PO_4$. Trace elements solution was made up as a 1000x stock at the following final concentrations: 3.6 µM $H_3BO_3$, 1 µM $CuSO_4$, 0.7 µM KI, 0.8 µM FeNa-EDTA, 1 µM $MnSO_4$, 0.5 µM $NaMoO_4$ and $ZnSO_4$. The media was modified by adding basal salts $K_2HPO_4$ and $KH_2PO_4$ to a combined concentration of 60 mM. The amount of each proton donor and acceptor was calculated using the Henderson-Hasselbalch equation and pH was measured using the pH meter before autoclaving. Basal salts were made up as 20x stocks and autoclaved separately. $MgSO_4$ was also autoclaved separately to prevent precipitation of salt. Thiamine, glutamine and sucrose were made up as a 40x stock solutions and filter-sterilised (0.2 µm) together with the trace elements. Solid Blankenship medium was made by adding the components separately to autoclaved agar previously cooled to 50°C.

### *2.2.8 Minimal synthetic media 3 (MSM3)*

MSM3 defined media (Chujo & Scott, 2014) contained 3.67 mM $KH_2PO_4$, 3.44 mM $K_2HPO_4$, 15 mM sucrose, 5 mM glutamine, 2 mM $MgSO_4$, 0.6 µM thiamine and trace elements (3.6 µM $H_3BO_4$, 1 µM $CuSO_4$, 0.7 µM KI, 0.8 µM FeNa-ethylenediaminetetraacetic acid, 1 µM $MnSO_4$, 0.5 µM $NaMoO_4$ and 0.4 µM $ZnSO_4$).

### *2.2.9 Water agar (seedling germination)*

Water agar for germination of seedlings contained 3% (w/v) bacteriological agar. Water agar for microscopy cultures contained 1.5% (w/v) bacteriological agar.

## 2.3 DNA Isolation

### *2.3.1 DNA quantification*

DNA was quantified by fluorometry using either the Qubit dsDNA BR Assay Kit (Thermo Fisher Scientific) or Qubit dsDNA HS Kit (Thermo Fisher Scientific). DNA purity was determined by spectrometry using the nanophotometer (Implen).

### *2.3.2 Isolation of plasmid DNA from E. coli*

For plasmid isolation, *E. coli* was inoculated into LB broth and grown at 37°C with shaking at 200 rpm to an optical density of 1.5-2.0 at 600 nm ($OD_{600}$). For miniprep purposes, plasmid DNA was isolated using the High Pure Plasmid Isolation Kit (Roche) according to the manufacturer's instructions. For midiprep purposes (mammalian cell transfection), plasmid DNA was isolated using the PureLink™ HiPure Plasmid Midiprep Kit (Thermo Fisher Scientific).

### *2.3.3 Isolation of DNA from E. festucae*

The method from Byrd *et al*. (1990) was modified for a more rapid smaller-scale DNA extraction from *E. festucae*. Mycelia were cultured in 200 µL PD broth for 3-4 days and pelleted by centrifugation at 25°C for 1 min at 6,000 rcf. The supernatant was discarded and 200 µL of extraction buffer was added. The sample was vortexed and incubated at 70°C for 30 min. The solution was neutralised with 200 µL of 5 M potassium acetate and incubated on ice for 10 min, followed by centrifugated at 4°C for 20 min at 16,000 rcf. The resulting supernatant was transferred to a new tube and DNA was precipitated with 0.7 vol of isopropanol,

incubated on ice for 10 min and centrifuged at 4°C for 15 min at 16,000 rcf. The resulting DNA pellet was washed with 70% ethanol and resuspended in 20 µL $H_2O$.

### *2.3.4 Restriction endonuclease digestion*

Restriction digests were performed using commercial restriction enzymes (Roche and NEB) according to the manufacturer's instructions.

### *2.3.5 Agarose gel electrophoresis*

DNA was separated on 0.7-2.0% agarose gels in 1x Tris/Borate/EDTA (TBE) buffer with a voltage of 2-4 volts per cm of gel length. DNA solution was loaded onto gels diluted 1:4 with loading dye solution (0.2% (w/v) bromophenol blue, 20% (w/v) sucrose, 1% (w/v) SDS and 5 mM EDTA). Gels were stained with ethidium bromide (1 µg $mL^{-1}$) for 10-30 min and bands were visualised with the Molecular Imager® Gel Doc™ XR+ System and the Image Lab™ Software (BioRad).

### *2.3.6 Purification of DNA and PCR product*

Ethidium bromide-stained DNA bands were visualised and excised on the Dark Reader™ Non-UV transilluminator DR-88M (400-500 nm). DNA was purified from agarose slices or from PCR reactions using the Wizard® SV Gel and PCR Clean-Up System (Promega).

### *2.3.7 Gibson assembly*

The method for Gibson assembly was adapted from Gibson *et al.* (2009). A 1:3 vector:insert ratio and a total DNA amount of 0.5 pmol was used. Reactions were carried out in 20 µL volumes in 2.5% PEG-8000, 50 mM Tris-HCl (pH 7.5), 5 mM $MgCl_2$, 5 mM DTT, 0.5 mM $NAD^+$, 0.1 mM dNTPs, 0.8 U T5 exonuclease (NEB), 0.5 U Phusion® DNA polymerase (Thermo Fisher Scientific), 80 U Taq DNA ligase (NEB). The reaction was incubated at 50°C for 1 h with ramp rate of 1.5°C/sec from room temperature.

### *2.3.8 DNA ligation*

Standard ligation of DNA was performed with T4 DNA ligase (Promega). For blunt end cloning 100 ng of vector and a 1:1 molar ratio of vector:insert DNA was used. Reactions were performed in 10 µL volumes with 2 U of T4 DNA ligase and an incubation time of 16 h at 15°C.

### *2.3.9 5´-Phosphorylation of oligonucleotides*

PCR products used for subsequent ligation reactions were treated with T4 polynucleotide kinase (PNK) (NEB). The reaction was carried out in a 10 µL volume with 1 U of T4 PNK for every 30 pmol of 5'termini in 1x T4 DNA ligase buffer (NEB).

### *2.3.10 DNA sequencing*

DNA for sequencing was sent to the Massey Genome Service. The BigDye™ Terminator (version 3.1) Ready Reaction Cycle Sequencing Kit (Applied Biosystems) was used. For sequencing of plasmids from Zero Blunt® TOPO® reactions, the manufacturer-supplied M13F/M13R primers were used. Samples were sent in a 20 µL total volume containing 4 pmol primers and 100-200 ng plasmid DNA, or 5-100 ng DNA from PCR reactions.

### *2.3.11 Southern blotting (DIG)*

For Southern analysis (Southern, 1975), 2.5-5 µg genomic DNA was used in the initial restriction digest and ethanol precipitated. DNA was separated on 0.8% agarose gel at 30 V. Gels were soaked in 0.25 M HCl for 15 min (depurination step) followed by 0.5 M NaOH/0.5 M NaCl for 30 min (denaturation step), and 0.5 M Tris, pH 7.4, 2.0 M NaCl for 30 min (neutralisation step). Gels were subsequently washed in 2x saline-sodium citrate buffer (SSC; 0.3 M NaCl, 30 mM Na+ citrate) for 2 min and placed on the blotting stand. Prewetted positively-charged nylon membrane (Roche) was placed over the gel, followed by three prewetted Whatman 3 MM filter paper. Paper towels were placed on top of the filter paper and weighted with approx. 500 g of weight on top of a flat piece of plastic plate. Gels were allowed to blot overnight and the resulting membrane washed in 2x SSC for 5 min and air-dried. DNA was crosslinked to the membrane by exposure to ultraviolet (254 nm; Cex-800 UV light cross-linker) for 2 min.

DNA probes were labelled with digoxigenin-dUTP and subsequently hybridised to the blotted membrane using the DIG High Prime kit (Roche) according to manufacturer's instructions. Hybridised probes were detected with alkaline phosphatase-conjugated anti digoxigenin Fab fragments and visualised with nitro blue tetrazolium chloride.

## 2.4 RNA isolation and manipulation

### *2.4.1 RNA quantification*

RNA was quantified by fluorometry using the Qubit dsDNA HS Assay Kit (Thermo Fisher Scientific). RNA purity was determined by spectrometry using the nanophotometer (Implen).

### *2.4.2 RNA isolation*

RNA was isolated from mycelia or plant pseudostem with TRIzol® (Invitrogen) according to the manufacturer's instructions. For mycelia samples, tissues from liquid culture were filtered with nappy liners and washed three times with H2O, then flash-frozen with liquid nitrogen and ground into a fine powder with mortar and pestle pre-cooled with liquid nitrogen. For plant samples, tillers of endophyte-infected ryegrass were cut close to the base and the outermost sheath layer was gently peeled and discarded. 1 cm sections of the pseudostem regions were cut and flash-frozen in liquid nitrogen. Samples were ground into a fine powder with a mortar and pestle pre-cooled with liquid nitrogen. Following isolation, RNA was resuspended in 1x RNAsecure™ solution (Ambion) and incubated at 60°C for 10 min to inactivate RNases.

### *2.4.3 DNase I treatment*

RNA used for RT-PCR (section 2.6.3) using the SuperScript™ II Reverse Transcriptase kit (Invitrogen) was first treated with RNase-free DNase I (NEB). 5 µg RNA was treated with 1 U of DNase I in a 50 µL reaction volume with 1x DNase I Reaction Buffer and incubated at 37°C for 10 min. DNase I was subsequently inactivated by addition of 5 mM EDTA and incubated at 75°C for 10 min. Concentration of RNA was determined again after a DNase I treatment.

## 2.5 Protein manipulation

### *2.5.1 Protein quantification*

Protein was quantified by fluorometry using the Qubit Protein Assay Kit (Thermo Fisher Scientific).

### *2.5.2 Nuclear fractionation*

Flash-frozen mycelia or plant pseudostem material were ground to a fine powder in liquid nitrogen with a mortar and pestle and 10 mL high glycerol buffer (70% v/v glycerol, 50 mM sucrose, 20 mM HEPES-

NaOH pH 7.4, 5 mM $MgCl_2$, 5 mM KCl, 1 mM DTT, 0.2 mM PMSF) was added. For plant samples, HGB additionally contained 1% Triton X-100. The resulting lysate was transferred to a 50 mL Falcon tube and centrifuged at 2,000 rcf for 1 h at 4°C. The supernatant was removed and the pellet was resuspended in 10 mL low glycerol buffer (10% v/v glycerol, 50 mM sucrose, 20 mM HEPES-NaOH pH 7.4, 5 mM $MgCl_2$, 5 mM KCl, 1 mM DTT, 0.2 mM PMSF) and centrifuged at 2,000 rcf for 20 min. The supernatant was removed and pellet resuspended in 1 mL TE buffer (pH 8) containing freshly added HALT Protease Inhibitor Cocktail (Thermo Fisher Scientific).

### *2.5.3 Acid-extraction of histones*

The nuclear fraction from Section 2.5.2 was sonicated at 20% power for 2 x 50 seconds (QSonica Q700). The lysate was centrifuged at 20,000 rcf for 30 min at 4°C to pellet cellular debris. To 1 mL of the resulting supernatant, 800 µL 0.4 M $H_2SO_4$ was added and the resulting mixture was incubated with rotation at 4°C for 1 h. The mixture was then centrifuged at 20,000 rcf for 30 min and the pellet discarded. To 1 mL of the resulting solution, 250 µL trichloroacetic acid was added and the solution incubated for 1 h at 4°C with rotation. Precipitated proteins were pelleted by centrifugation at 20,000 rcf for 30 min at 4°C and the pellet washed three times with ice-cold acetone. The resulting pellet was resuspended in SDS sample buffer (25% v/v glycerol, 100 mM Tris HCl pH 6.8, 2% w/v SDS, 0.01% w/v bromophenol blue, 0.5 M 2-β-mercaptoethanol) for loading onto SDS-PAGE gel.

### *2.5.4 SDS-PAGE and western blotting*

Protein samples in SDS sample buffer (Section 2.5.3) were separated by discontinuous gel electrophoresis through a 5% stacking gel and a 15% resolution gel in 1x running buffer (25 mM Tris, 192 mM glycine, 1% SDS) at 200 V for 50 min.

Following separation, the proteins were transferred to 0.2 µm nitrocellulose membrane (GE Healthcare) in transfer buffer (20% v/v methanol, 25 mM Tris, 192 mM glycine, 1% SDS) at 30 V for 70 min. The membrane was equilibrated in 1x TBST (20 mM Tris pH 7.6, 150 mM NaCl, 0.1% Tween 20) then blocked with 5% BSA in TBST for 1 h at room temperature. Primary antibody was added at 1:5,000 concentration and incubated overnight at 4°C. Washes were performed for 2 x 5 min followed by 2 x 10 min in TBST. Secondary antibody was added at 1:20,000 concentration in 1% BSA in TBST for 1 h at room temperature. After similar washing steps, the membrane was developed using the Amersham ECL Prime Western Blotting Detection Reagent (GE Healthcare) and imaged with the Fujifilm LAS-1000 CCD camera in an Intelligent Dark Box II.

Antibodies used in this study are listed in Table 2.2.

### *2.5.5 Chromatin immunoprecipitation (ChIP)*

For ChIP, mycelial or pseudostem samples were crosslinked with a final concentration of 0.75% formaldehyde for 10 min (with vacuum infiltration for pseudostem samples). Glycine was added to a final concentration of 125 mM and incubated for 5 min. The samples were washed three times with $H_2O$ and dried with paper towels. Samples were flash-frozen in liquid nitrogen and nuclear fractions were prepared according to Section 2.5.2. The resulting nuclear fractions in TE buffer (pH 8) were sonicated at 20% power for 4 x 1 min in ice. The lysate was then centrifuged at 20,000 rcf for 30 min at 4°C to clear debris and the pellet discarded. Protein concentration was determined according to Section 2.5.1. For sonication check, DNA was purified from 20 µg chromatin and separated on 1.5% agarose gel.

Chromatin was pre-cleared by incubating with 20 µL Protein G-agarose beads (Millipore) per mL of chromatin for 30 min at room temperature with rotation. The beads were removed by centrifugation at 1,500 rcf for 10 s and washed once with IP buffer (10 mM Tris HCl pH 8, 1 mM EDTA, 100 mM NaCl, 0.4%

IGEPAL CA-630 (Sigma), 1x HALT protease inhibitor). ChIP of culture samples was performed with 20 µg chromatin and ChIP of plant samples was performed with 80 µg chromatin to account for the lower fungal biomass *in planta*. Primary antibodies were added at a 1:25 dilution and incubated for 1 h at room temperature with rotation. To the reaction, 5 µL Dynabeads (Thermo Fisher Scientific), preblocked with 0.1 µg BSA per µL beads and 75 ng herring ssDNA (Sigma) for 1 h at room temperature, were added per µg primary antibody. Immunoprecipitation was carried out overnight at 4°C with rotation. The next day, the three washes were performed with IP buffer and beads-Ab-antigen were resuspended in 100 µL elution buffer (10 mM Tris-HCl pH 8, 1 mM EDTA, 0.2 mM NaCl). 2 µL RNase A (10 mg/mL) was added and crosslinking was reversed by incubating at 65°C for 2 h. 2 µL proteinase K (20 mg/mL) was added and samples incubated for another hour at 45°C. DNA was purified using the QIAquick PCR Purification Kit (Qiagen) and resuspended in 70 µL TE buffer (pH 8).

**Table 2. 2. Antibodies used in this study.**

| Type | Specificity | Manufacturer | Catalogue no. |
|---|---|---|---|
| Primary | α-H3 | Abcam | ab1791 |
| Primary | α-H3K4me1 | Abcam | ab8895 |
| Primary | α-H3K4me2 | Abcam | ab32356 |
| Primary | α-H3K4me3 | Abcam | ab8580 |
| Primary | α-H3K9me1 | Abcam | ab9045 |
| Primary | α-H3K9me2 | Abcam | ab1220 |
| Primary | α-H3K9me3 | Abcam | ab8898 |
| Primary | α-H3K27me1 | Abcam | ab113671 |
| Primary | α-H3K27me2 | Abcam | ab24684 |
| Primary | α-H3K27me3 | Millipore | #07-449 |
| Primary | α-H3K36me1 | Abcam | ab9048 |
| Primary | α-H3K36me2 | Abcam | ab9049 |
| Primary | α-H3K36me3 | Abcam | ab9050 |
| Primary | α-FLAG | Sigma | F1804 |
| Secondary | α-Rabbit (Cy5) | Thermo Fisher Scientific | A10523 |
| Secondary | α-Mouse (Cy3) | Thermo Fisher Scientific | A10521 |

## 2.6 Polymerase chain reaction (PCR)

Primers used for PCR in this study are listed in Table 2.3.

**Table 2. 3. Primers used for PCR in this study.**

| Name | Sequence (5'-3') | Purpose |
|---|---|---|
| YL58R | ACAGCGATTCGCGTGCCGATGTCATGGTTTGACGGTGATGTATGGAAGAT | pYL7 generation |
| YL59F | ATCTTCCATACATCACCGTCAAACCATGACATCGGCACGCGAATCGCTGT | pYL7 generation |
| YL59R | TGATTTCAGTAACGTTAAGTGGATCTCAATTCCACCAGAAGCTCACGCTA | pYL7 generation |
| YL61R | GAGCGCTCACGACGTCGGTCGACATGGTTTGACGGTGATGTATGGAAGAT | pYL4 generation |
| YL62F | ATCTTCCATACATCACCGTCAAACCATGTCGACCGACGTCGTGAGCGCTC | pYL4 generation |
| YL62R | TGATTTCAGTAACGTTAAGTGGATCTTACTGATACAGGTCTGTGGCAGCG | pYL4 generation |
| YL63R | TTGTGGCTGTTGACATTGGTGCCATGGTTTGACGGTGATGTATGGAAGAT | pYL5 generation |
| YL64F | ATCTTCCATACATCACCGTCAAACCATGGCACCAATGTCAACAGCCACAA | pYL5 generation |
| YL64R | TGATTTCAGTAACGTTAAGTGGATCCTATTCGCCGTCTATCATGGCATCA | pYL5 generation |
| YL65F | AGGCAGAGGAAGGACGGCGGAGTAGGATCCACTTAACGTTACTGAAATCA | pYL6 generation |
| YL66F | ATCTTCCATACATCACCGTCAAACCATGCCAACATCACTTCACCCTCAGG | pYL6 generation |

| | | |
|---|---|---|
| YL66R | TGATTTCAGTAACGTTAAGTGGATCCTACTCCGCCGTCCTTCCTCTGCCT | pYL6 generation |
| YL79F | GAAAATCATTCCTACTAAGATGGGTAATCATCGATGAATTCGAGCTCGGT | pSF15 with TtrpC O/H |
| YL79R | CATCCTTTGACCACCGTTTGCTACCATCAGATCTGCCGGTCTCCCTATAG | pSF15 with Ptef O/H |
| YL80F | CTATAGGGAGACCGGCAGATCTGATGGTAGCAAACGGTGGTCAAAGGATG | Ptef with pSF15 O/H |
| YL81F | ATCAGTAAGATCCACTTAACGTTACTGAAATCA | TtrpC with jmj1 O/H |
| YL81R | TCGATGATTACCCATCTTAGTAGGAATG | TtrpC with pSF15 O/H |
| YL82F | ATAGGATCCACTTAACGTTACTGAAATCA | TtrpC with jmj2 O/H |
| YL83F | AGTAGGATCCACTTAACGTTACTGAAATCA | TtrpC with jmj3 O/H |
| YL84F | ATTGAGATCCACTTAACGTTACTGAAATCA | TtrpC with jmj4 O/H |
| YL134F | GATTACAAGGACGACGATGACAAG | pcDNA Fwd |
| YL134R | CATGGTGGCGGCCCT | pcDNA Rev |
| YL135F | TAGATCCCGGGTGGGAT | pcDNA Fwd |
| YL135R | CTTGTCATCGTCGTCCTTG | pcDNA Rev |
| YL136F | TCGACCGACGTCGTGAGC | jmj1 for pcDNA |
| YL136R | CTGATACAGGTCTGTGGCAGCG | jmj1 for pcDNA |
| YL137F | GCACCAATGTCAACAGCC | jmj2 for pcDNA |
| YL137F | TCGCCGTCTATCATGGC | jmj2 for pcDNA |
| YL140F | GATCCACTTAACGTTACTG | TtrpC Fwd |
| YL141F | ATGGATTACAAGGACGACGATGACAAGCACGTAATGAACAGGACATCGCTTC | pYL8 generation |
| YL141R | GTTTGATGATTTCAGTAACGTTAAGTGGATCTCATCTGAACCACCAATTCAC | pYL8 generation |
| YL142F | CTATAGGGAGACCGGCAGATCTGATGGTAGCAAACGGTGGTCAAAGG | Ptef Fwd |
| YL142R | CTTGTCATCGTCGTCCTTGTAATCCATGGTTTGACGGTGATGTATGGAAGAT | Ptef Rev with FLAG/ATG |
| YL143F | ATGGATTACAAGGACGACGATGACAAGCCGTCCGTTGTCTTGA | pYL9 generation |
| YL143R | GATTTCAGTAACGTTAAGTGGATCTTAGGGAACATCATTGTCG | pYL9 generation |
| YL144F | ATGGATTACAAGGACGACGATGACAAGCCCATCAACCAAGTGC | pYL10 generation |
| YL144R | GATTTCAGTAACGTTAAGTGGATCTTAAACTCCGTCTGCCGCAAG | pYL10 generation |
| YL145F | ATGGATTACAAGGACGACGATGACAAGGCATCGTCTGGAAATG | pYL11 generation |
| YL145R | ATGATTTCAGTAACGTTAAGTGGATCTCAGCTTTGTATAGAACTAAAAAC | pYL11 generation |
| YL164 | TTCGCCGTCTATCATGGC | jmj2 for pcDNA Rev |
| YL170F | CAAGAGGAGAAGCTCTGATGCCGCATAGTTA | pUC19 for Δ*kdmB* |
| YL170R | GATAATAATGCAACGTGTGAAATACCGCACAGATG | pUC19 for Δ*kdmB* |
| YL186F | GTATTTCACACGTTGCATTATTATCCAGCCG | Δ*kdmB* 5' frag |
| YL186R | GTTCCAAGCTGAGGACAGATGCTCGTAGCC | Δ*kdmB* 5' frag |
| YL187F | CATCTGTCCTCAGCTTGGAACTGATATTGAAGGAG | Δ*kdmB* hph frag |
| YL187R | CTTGTCTCGGTGGAGATGTGGAGTGGG | Δ*kdmB* hph frag |
| YL188F | CACATCTCCACCGAGACAAGTCGAAGAATCTG | Δ*kdmB* 3' frag |
| YL188R | GCATCAGAGCTTCTCCTCTTGTACTCGCTAACC | Δ*kdmB* 3' frag |
| YL231F | TTGCATGCCTGCAGGTCGACTCTAGGCCGATATAAATGGAGCGCGCGTTG | pYL19 generation |
| YL231R | TCCTTCAATATCGGGGATCCTCTAGGCTAGTTGTCACTAACTCATTCTCCTCTTG | pYL19 generation |
| YL243F | GCGGTATTTCACACCGCATACATATGGCAGAAGGAGCAGAAGAAGGGAGAAG | Δjmj4 5' fragment |
| YL243R | AAAAGTGCTCCTTCAATATCGCCGTGACGAAATCAACGAG | Δjmj4 5' fragment |
| YL244F | CTCGTTGATTTCGTCACGGCGATATTGAAGGAGCACTTTTTGGGC | Δjmj4 nptII frag |
| YL244R | CTCGTCTCACGCTGCTAGTTTACCCATCTTAGTAGGAATGATTTTCGA | Δjmj4 nptII frag |
| YL245F | CATTCCTACTAAGATGGGTAAACTAGCAGCGTGAGACGAGAG | kdmH 3' fragment |
| YL245R | TGTACTGAGAGTGCACCATATTAATTAACACCTGTCAGCATTGCATTGGTTGCATT | kdmH 3' fragment |
| YL271F | GACGATGACAAGTGAGATCCACTTAACGTTACTGAAATCATCAAACAGC | pYL25 intermediate |
| YL271R | GTCCTTGTAATCATTCCACCAGAAGCTCACGCTAAAGCTG | pYL25 intermediate |
| YL279F | GATTACAAGGACGACGATGACA | pYL25 intermediate |
| YL279R | CATGGTTTGACGGTGATGTA | pYL25 intermediate |
| YL280F | AGGACATTGCGCAGGCGGCGGATTACAAGGACGACGATGACAAG | pYL25 generation |
| YL280R | ACCGCATGCTCATCATCCCGCATGGTTTGACGGTGATGTATGG | pYL25 generation |
| YL281F | TAATGATGATTACTAACAGAAGTAGATGCCGACCGGGAACC | pYL25 intermediate |
| YL281R | ATGAAACGATTCTCAACGATCTATTCCTTTGCCCTCGGACG | pYL25 intermediate |
| YL282F | GTCCGAGGGCAAAGGAATAGATCGTTGAGAATCGTTTCATCGG | pYL25 intermediate |

| | | |
|---|---|---|
| YL282R | GTTCCCGGTCGGCATCTACTTCTGTTAGTAATCATCATTAAGTCTTTTCTTGG | pYL25 intermediate |
| YL283F | TACATCACCGTCAAACCATGCGGGATGATGAGCATGCGGTCG | pYL25 generation |
| YL283R | TCATCGTCGTCCTTGTAATCCGCCGCCTGCGCAATGTCCT | pYL25 generation |
| YL286F | TCTGTGCGGTATTTCACACCGCATATTAATTAATGGTCCGAGCCTTTCCATCATTG AAAAAAAAAA | Δ*setB* 5' fragment |
| YL286R | GCCCAAAAAGTGCTCCTTCAATATCTCAGTCCCTCGTAGTAGCTGGTTGC | Δ*setB* 5' fragment |
| YL287F | GCAACCAGCTACTACGAGGGACTGAGATATTGAAGGAGCACTTTTTGGGC | Δ*setB* nptII fragment |
| YL287R | TCGTCTTCTAGCCTTTGCGCTTCCTTACCCATCTTAGTAGGAATGATTTTC | Δ*setB* nptII fragment |
| YL288F | AAAATCATTCCTACTAAGATGGGTAAGGAAGCGCAAAGGCTAGAAGACGA | Δ*setB* 3' fragment |
| YL288R | CAGATTGTACTGAGAGTGCACCATAACTAGTCGACGATTCTTGTCCCCTGACTACA TTCGGA | Δ*setB* 3' fragment |
| YL330F | TTGGCTGGTATGGGATAAGG | pYL30 generation |
| YL330R | TCCCATATTTTGGGCAAATC | pYL30 generation |

### *2.6.1 Standard PCR*

Standard PCR was performed with Taq DNA polymerase (Roche) in 10 to 50 µL reaction volumes containing 1x PCR reaction buffer, 200 µM of each dNTP, 0.2 µM of each primer, Taq DNA polymerase (0.5 U/50 µL reaction) and template DNA (100 pg plasmid DNA or 100 ng genomic DNA per 50 µL reaction volume). The reaction conditions were: one cycle at 94°C for 2 min; 35-45 cycles at 94°C for 15-30 s, 50-65°C for 30-60 s, 72°C for 1 min/1 kb; one cycle at 72°C for 10 min.

### *2.6.2 High-fidelity PCR*

Where proofreading DNA polymerase activity was required PCR was performed with Q5® (NEB) or Phusion® (Thermo Fisher Scientific) High-Fidelity DNA Polymerase. PCR was performed in 10 to 50 µL reaction volumes containing the appropriate 1x PCR buffer, 200 µM of each dNTP, 0.5 µM of each primer, DNA polymerase (1 U/50 µL reaction) and template DNA (100 pg plasmid DNA or 100 ng genomic DNA per 50 µL reaction volume). Two-step reaction conditions were: one cycle at 98°C for 30 s; 35 cycles at 98°C for 10 s and 72°C for 30 s/1 kb; one cycle at 72°C for 2 min. Three-step reaction conditions were: one cycle at 98°C for 30 s; 35 cycles at 98°C for 10 s, 50-68°C for 10-30 s, 72°C for 30 s/1 kb; one cycle at 72°C for 2 min.

### *2.6.3 Reverse-transcription PCR (RT-PCR)*

Synthesis of cDNA for RT-PCR was performed using SuperScript™ II Reverse Transcriptase (Invitrogen) according to manufacturer's instructions. 1 µg of RNA (DNase I-treated) was used in a 20 µL reaction volume with Oligo(dT) primers. For quantitative reverse transcription PCR (qRT-PCR), reverse transcription was performed with the QuantiTect Reverse Transcription Kit (Qiagen), according to the manufacturer's instructions. 1 µg of RNA was used in a 20 µL reaction volume. cDNA was diluted with TE buffer prior to use as template for qRT-PCR reactions.

### *2.6.4 Real-time quantitative PCR*

Real-time quantitative PCR was performed using the SsoFast™ EvaGreen® Supermix (Bio-Rad) in 96- or 384-well plates on the LightCycler® 480 Instrument II (Roche). Reaction volumes of 10 µL were used containing 1 µL DNA template, 1x SsoFast™ EvaGreen® Supermix and 0.5 µM of each forward and reverse primer. Experiments were performed with three biological replicates and two technical replicates.

Primers used for qPCR in this study are listed in Table 2.4. Primer efficiencies of RT-qPCR primers used for analysis of secondary metabolite genes have been previously determined to be satisfactory (Chujo & Scott, 2014).

### *2.6.5 Real-time quantitative PCR cycling conditions*

For real-time quantitative PCR (qPCR) with cDNA templates, an initial denaturation step was performed at 95°C for 30 s, followed by 40 cycles at 95°C for 5 s and 60°C for 10 s. A denaturation step of 98°C was used for experiments using DNA templates (genomic copy qPCR and ChIP-qPCR). A melt curve was performed from 65 to 95°C with a ramp rate of 0.4°C/s. Signal was acquired at the end of each extension step and during the melt curve.

### *2.6.6 Real-time quantitative PCR standard curve generation*

For absolute quantification, cDNA standards (80-120 bp) were prepared by PCR amplification with Phusion® High-Fidelity DNA Polymerase (Thermo Fisher Scientific) using the respective primer pairs, separated on 2% (w/v) agarose gel, excised and purified. Serial dilutions were prepared and concentrations of 10 aM to 10 pM were used in generating the standard curve (Chujo & Scott, 2014).

### *2.6.7 Real-time quantitative PCR data analysis*

For real-time quantitative reverse transcription PCR (qRT-PCR), target transcript levels were normalized against the levels of reference genes for 40S ribosomal protein S22 (EfM3.016650) and translation elongation factor 2 (EfM3.021210) (Chujo and Scott, 2014). For determination of copy number, the *pacC* gene, present as single-copy in the *E. festucae* genome (Lukito *et al*., 2014) was used for normalisation. For ChIP-PCR, qRT-PCR and genomic copy number qPCR, the relative template amounts were determined by relative quantification using the Ratio (reference/target) = $2^{Cp(ref)-Cp(target)}$ variation of the Livak method (Livak & Schmittgen, 2001). For qRT-PCR of secondary metabolite gene expression, the relative cDNA amounts between target and reference genes were calculated by absolute quantification by comparing the values interpolated from standard curves.

**Table 2. 4. Primers used for qPCR in this study.**

| Name | Sequence (5'-3') | Purpose |
|---|---|---|
| YL106F | TTCCATCACCTCCCAAGAAG | jmj1 copy number |
| YL106R | CCTTGGAATCCTCCTCATCA | jmj1 copy number |
| YL108F | TGATGGTAACGTCGACCAAA | jmj2 copy number |
| YL108R | ATCAAGCGCGTTTCTCTCAT | jmj2 copy number |
| YL110F | ATCGGCAAATGACACACAAA | jmj3 copy number |
| YL110R | TTCTCCGTGATGCATGGTTA | jmj3 copy number |
| YL112F | AGAAGGAGGAGGACGAGGAG | jmj4 copy number |
| YL112R | ACCGGTACGCGTAGAACTTG | jmj4 copy number |
| YL113F | GAGAATTCCAGCCACGCTAC | pacC copy number |
| YL113R | AACCATCACCAGGCAAAGAC | pacC copy number |
| YL165F | GACGGCAATTTCGATGATG | hph qPCR |
| YL165R | TTGTGTACGCCAGACAGTCC | hph qPCR |
| YL179F | ATCGGATGGAGAACTCAACG | jmj5 copy number |
| YL179R | CTGACATCGACACCAACGAT | jmj5 copy number |
| YL181F | GCAGTGACGACGACAATGAT | jmj6 copy number |
| YL181R | CTGACATCGACACCAACGAT | jmj6 copy number |
| YL183F | ATTGGCAGGTGAACTGGAAC | jmj7 copy number |
| YL183R | CTGACATCGACACCAACGAT | jmj7 copy number |
| YL185F | GATGGAGAAGGTTTCGTGGA | jmj8 copy number |
| YL185R | CTGACATCGACACCAACGAT | jmj8 copy number |
| YL224F | ACTGTCGGGCGTACACAAAT | kdmB copy number |
| YL224R | GGTTTCCACTATCGGCGAGT | kdmB copy number |
| YL284F | GAAGCGCAAAGGCTAGAAGA | setB copy number |
| YL284R | TCACTTGTCATCGTCGTCCT | setB copy number |

| | | |
|---|---|---|
| YL311F | GACAAGCGTATCGGCTTCA | gigA qPCR |
| YL311R | GGCTCCCTTGTAAGGCATTT | gigA qPCR |
| YL312F | TGTGACCACATCCTCACCTC | sspA qPCR |
| YL312R | GTTCGGAGCACAGAGTCACA | sspA qPCR |
| BH132 | GCAAATGCGGGTCCAACAAG | sspM qPCR |
| BH133 | GTCGTTGGGAGCATAACCGG | sspM |
| YL313F | ACGTGGTGAATGTGTTGGAT | EfM3.077740 qPCR |
| YL313R | TTCTGAATCCTCGGGAACAC | EfM3.077740 qPCR |
| YL314F | GGGAGAATTTCCATCCCAAT | EfM3.057200 qPCR |
| YL314R | GACCTTTTGTCCCGATCTCA | EfM3.057200 qPCR |
| YL315F | GAAATGCCGTGTTTTGGAAT | EfM3.057240 qPCR |
| YL315R | CCGATCTTTGTACCGCTTGT | EfM3.057240 qPCR |
| YL316F | ATTCATCGCGAAGTTCAAGG | EfM3.077600 qPCR |
| YL316R | CGCAAGTCCCCTCAAAGTTA | EfM3.077600 qPCR |
| YL317F | TCTGAGAAGATTTGGGTCAGC | EfM3.061530 qPCR |
| YL317R | CAGGTGTGCTGCTCCTAGTG | EfM3.061530 qPCR |
| YL318F | CGAGATCAGGGCCTTAAACA | EfM3.061540 qPCR |
| YL318R | GGACATCATAGCCGTCCAGT | EfM3.061540 qPCR |
| YL319F | AATAGCCTGGCCTGAAGACA | EfM3.053730 qPCR |
| YL319R | CCCTCATTGGTGACCACTCT | EfM3.053730 qPCR |
| YL320F | GAGATGAACGCCCTCAAAAA | EfM3.071140 qPCR |
| YL320R | TAGATCTTTTGCCCCTGCAC | EfM3.071140 qPCR |
| YL321F | GCAACCACACGAGATACCTG | EfM3.050660 qPCR |
| YL321R | CCAAGTCTGCGACAGTCAAG | EfM3.050660 qPCR |
| YL322F | GACAAGGGTCGGTGAAGAGA | EfM3.041160 qPCR |
| YL322R | TGACCTTGCCACAGTCCAC | EfM3.041160 qPCR |
| TC119 | AGTGAGCATGTACCGCAAAA | ltmE qPCR |
| TC120 | AATGAACCGGCTCAATTCTG | ltmE qPCR |
| TC121 | CCTCTTCCCGTTAAAGACTGC | ltmJ qPCR |
| TC122 | AACTCGTTTTAGTGGGCATGT | ltmJ qPCR |
| TC123 | TTGCAGCGCTGTCGTATAAT | ltmP qPCR |
| TC124 | CACAACTTTCGCTTGTGGAA | ltmP qPCR |
| TC191 | GGGAGAAAAGAGCTAGGGAGA | ltmQ qPCR |
| TC126 | GGCCTCAAAGCTTCTCTTCA | ltmQ qPCR |
| TC127 | AGGGTTCCCTTGATCTTTCA | ltmF qPCR |
| TC128 | CGTCAAATGACGATTGAAGC | ltmF qPCR |
| TC129 | TTCCACCTTGTGGGTCTAGG | ltmC qPCR |
| TC130 | TGTAACTCACGCGCTATGCT | ltmC qPCR |
| TC131 | CGAAAACGAGTAACGGCTTG | ltmB qPCR |
| TC132 | TGAGTGTAAGCCCTTAGACAAAGA | ltmB qPCR |
| TC133 | CGCGACATCCTTGACAAGTT | ltmG qPCR |
| TC134 | AAAAGTGTCTTTTATCGCAATGTTC | ltmG qPCR |
| TC135 | GCCGTGATGTTGCTTTGTAG | ltmS qPCR |
| TC136 | TTTGAGATACGAGTTCTAACTAGGC | ltmS qPCR |
| TC137 | TCTCTTCCCGTAGCAAGGAA | ltmM qPCR |
| TC138 | GAGTTCTGCCTGCCTTCATC | ltmM qPCR |
| TC139 | TGATTTATTGTGACTTTCGTTAGCA | ltmK qPCR |
| TC140 | CATGCATGACAGTGCCAAA | ltmK qPCR |
| TC290 | AGAGTTTGATCCACCGCATC | lpsB qPCR |
| TC291 | AAGCAACAAGCGAAAGCAAG | lpsB qPCR |
| TC317 | TCGGGTATCTCAACCCCTTA | easE qPCR |
| TC318 | TTTCCTTGCGTAGCATTGTG | easE qPCR |
| TC294 | TGGCTGCAGCTACAAATACG | easG qPCR |
| TC295 | CCTTCATCCGACCACGTAAC | easG qPCR |
| TC261 | TGCATTCTTTTGGATTAGCC | easA qPCR |
| TC262 | AACGAAATACAAAAGCCATACCA | easA qPCR |

| | | |
|---|---|---|
| TC296 | TCGGTAGGATAACCCAAGGAG | easH qPCR |
| TC297 | TGTCTCACGCTCGATTTCTG | easH qPCR |
| TC319 | ATGCCGGCGAGATTTAACTT | dmaW qPCR |
| TC320 | TCTCTTCATAATCTGCCTTACACG | dmaW qPCR |
| TC321 | TTCCCGCCCTTAATTTTCTC | cloA qPCR |
| TC322 | AAGCTGAAAGCGTCCAAAAG | cloA qPCR |
| TC323 | AGGCTTAGCAGCCACTCAAT | easC qPCR |
| TC324 | TGGTGGTGGAAAAAGAAACC | easC qPCR |
| TC303 | CAAGACCAAACCCAAAGCAT | easD qPCR |
| TC304 | ATTAACGTTGGAGCGAGTGC | easD qPCR |
| TC305 | CAGCTCCCTTACGGTATTGAA | lpsA qPCR |
| TC306 | GGACCATATCCCGGAACAG | lpsA qPCR |
| TC399 | AAAAAGCAACCGAATGCAAG | EF2 qPCR |
| TC400 | CGAGACGACATAACTACATGTATCAAA | EF2 qPCR |
| TC407 | TAGCTGGCGTTATGGAAAGG | 40S S22 qPCR |
| TC408 | CGATTGTGCGACTACTACCTCA | 40S S22 qPCR |
| TC207 | GAGTTGGAGGCTCTTCCCTA | ltmE ChIP |
| TC208 | TCTCCTGAATGTTTCCAATGC | ltmE ChIP |
| TC211 | GTAGCTGATTTGACTTGAATGGAA | ltmP ChIP |
| TC212 | TCTTTTATTCTGTAGATGCCAAGC | ltmP ChIP |
| TC215 | ACGTCGGCTAAAGGCAGATT | ltmC ChIP |
| TC216 | TTGCTTGAGTTGCTCTGCAT | ltmC ChIP |
| TC223 | TGCCACTGCGTGAGAGATAA | ltmM ChIP |
| TC224 | TCCAAGAACATTGATGTGTGC | ltmM ChIP |
| TC349 | TGTTGTTCTTGTCGTGGTATCC | easG ChIP |
| TC350 | GGTTCTGACGATTGTCCCATA | easG ChIP |
| TC351 | GAGCGCAAAGGTGACTTGTT | dmaW ChIP |
| TC352 | AAGAAGAGGACGAGCGGAAT | dmaW ChIP |
| TC353 | ACTATTGTTGACTGTTTCTCGTAGTCA | lpsA ChIP |
| TC354 | TTTGGCTGTAAAGATAGAGAAATCC | lpsA ChIP |
| TC391 | TGAGCATATATTCCCCCATGA | easE ChIP |
| TC392 | TTGACAATTGGATATTGGTAAATTC | easE ChIP |
| TC393 | TCACATTGTAGAGGCCCATGT | easA ChIP |
| TC394 | ACGTCCAGAGGATTTTTCCA | easA ChIP |
| YL346F | AGGGCACTCTTCTTGCTCAC | 40S22 ChIP |
| YL346R | GTTGTCGGGACGGAGATTC | 40S22 ChIP |
| YL347F | GATCAGAGAGAGGCCCAAGG | EF2 ChIP |
| YL347R | CATTGCGAGGAAGACTGGTT | EF2 ChIP |

## 2.7 Generation of constructs

### *2.7.1 Generation of jmj1-jmj8 overexpression constructs (pYL4-pYL11)*

The constructs for *jmj1-jmj4* overexpression (pYL4-pYL7) were each generated by assembling four fragments (vector backbone and P*tef*, CDS and T*trpC* fragments) using Gibson assembly. For all constructs, vector backbone was amplified from *Eco*RV-linearised pSF15.15 with adaptor primers YL79F/YL79R. P*tef* fragments were amplified from *Sph*I-linearised pYL3 with primers YL80F/YL61R (*jmj1*), YL80F/YL63R (*jmj2*), YL80F/YL65R (*jmj3*) and YL80F/YL58R (*jmj4*). The CDS regions were amplified from wild-type *E. festucae* Fl1 cDNA with primers YL62F/YL62R (*jmj1*), YL64F/YL64R (*jmj2*), YL66F/YL66R (*jmj3*) and YL59F/YL59R (*jmj4*). The T*trpC* fragments were amplified from *Sph*I-linearised pYL3 with primers YL81F/YL81R (*jmj1*), YL82F/YL81R (*jmj2*), YL83F/YL81R (*jmj3*) and YL84F/YL81R (*jmj4*).

The vectors for *jmj5-jmj8* overexpression (pYL8-pYL11) were generated in a similar manner, the CDS regions of *jmj5-jmj8* were amplified from wild-type Fl1 cDNA and using primers YL141F/YL141R,

YL143F/YL143R, YL144F/YL144R and YL145F/YL145R, respectively. These fragments, and 'universal' P*tef* (YL142F/YL142R) and T*trpC* (YL140F/YL81R) fragments were assembled into *Eco*RV-linearised pSF15.15 using Gibson assembly.

### *2.7.2 Generation of constructs for mammalian transfection (pYL13 and pYL14)*

Primers YL134F/134R were used to insert a FLAG sequence to pcDNA3.1 Primers YL136F/YL136R and YL137F/YL164 were used to amplify *jmj1* and *jmj2* CDS from wild-type *E. festucae* Fl1 cDNA, respectively. The fragments were blunt end ligated to a 5.4 kb fragment amplified from pYL12 with primers YL135F/YL135R to generate pYL13 and pYL14, respectively.

### *2.7.3 Generation of vectors for deletion and complementation of kdmB (pYL15 and pYL19)*

To generate the Δ*kdmB* vector (pYL15) primers YL186F/YL186R and YL188F/YL188R were used to amplify a 1.4 kb 5'-fragment of *kdmB* and a 0.9 kb 3'- fragment of *kdmB* from wild-type Fl1 genomic DNA. Primers YL187F/R were used to amplify the hygromycin cassette from pDB48. The fragments were assembled into a linear fragment of pUC19 amplified with primers YL170F/YL170R using Gibson Assembly.

To generate the Δ*kdmB* complement vector (pYL19), a 7.8 kb fragment *kdmB* CDS was amplified using primers YL231F/YL231R from wild-type gDNA. The fragment was assembled into *Xba*I-digested pSF17.1 by Gibson assembly.

### *2.7.4 Generation of vectors for deletion, complementation and overexpression of jmj4 and setB (pYL20, pYL23, pYL25 and pYL30)*

To generate the Δ*jmj4* vector (pYL20), primers YL243F/YL243R and YL245F/YL245R were used to amplify a 2.7 kb 5'-fragment of *jmj4* and a 2.1 kb 3'- fragment of *jmj4* from wild-type Fl1 genomic DNA. Primers YL244F/YL244R were used to amplify the geneticin cassette from pSF17.1. The fragments were assembled into an *Nde*I-linearised pUC19 fragment using Gibson Assembly.

To generate the Δ*setB* vector (pYL23), primers YL286F/YL286R and YL288F/YL288R were used to amplify a 2.5 kb 5'-fragment of *setB* and a 2.5 kb 3'- fragment of *setB* from wild-type Fl1 genomic DNA. Primers YL287F/YL287R were used to amplify the geneticin cassette from pSF17.1. The fragments were assembled into an *Nde*I-linearised pUC19 fragment using Gibson Assembly.

To generate the *setB* overexpression vector (pYL25), primers YL282F/YL282R were used to amplify a 0.8 kb T*tub* (tubulin terminator) fragment from pNR1 and ligated into a linear fragment of pYL7 amplified with primers YL281F/YL281R. An C-terminal FLAG sequence was then added with primers YL271F/271R to form the intermediate pYL22. A 6.0 kb fragment was amplified from pYL22 with primers YL279F/YL279R to form the intermediate pYL24. Finally, a 6.0 kb fragment was amplified from pYL24 with primers YL280F/YL280R and assembled with a 2.7 kb fragment of *setB* obtained from wild-type cDNA with primers YL283F/YL283R to generate pYL25.

The Δ*setB* complement vector (pYL30) was generated by blunt-end ligation of a 4.3 kb *setB* genomic sequence amplified from wild-type Fl1 genomic DNA with primers YL330F/330R and *Sna*BI-linearised pDB48.

## 2.8 Preparation of protoplasts and competent cells

### *2.8.1 Chemically competent E. coli*

50 mL of super optimal broth (SOB; 2% (w/v) tryptone, 0.5% (w/v) yeast extract, 0.05 % (w/v) NaCl, 2.5 mM KCl, 2 mM $MgCl_2$, pH adjusted to 7) was inoculated with a fresh overnight culture of *E. coli* and

incubated at 18°C for 20-50 hours with shaking at 200 rpm until mid-log phase was reached (A600 = 0.4-0.8). The cells were chilled on ice for 10 min and centrifuged at 4°C for 10 min at 6,000 rcf then resuspended in 17 mL ice-chilled transformation buffer (TB; 10 mM PIPES, 15 mM $CaCl_2$, 0.25 M KCl, pH adjusted to 6.7, and 0.18 M $MnCl_2$, 0.45 µm filter-sterilised) and incubated on ice for 10 min. The cells were again centrifuged at 4°C for 10 min at 6,000 rcf then resuspended in 4 mL ice-chilled TB. 300 mL of DMSO was added, mixed well, and 100 µL aliquots of cell suspension were flash-frozen in liquid nitrogen and stored at -80°C.

### *2.8.2 Protoplasts of E. festucae*

150 ml of PD broth was inoculated with a fresh culture of *E. festucae* and incubated at 22°C for 4 days with shaking at 150 rpm. Mycelia were filtered with a sterilised nappy liner and washed with sterile $H_2O$, followed by OM buffer (100 mM $Na_2HPO_4$, 100 mM $NaH_2PO_4$, 1.2 M $MgSO_4$, 100 mM $Na_2HPO_4$). 40 mL of 0.2 µm filter-sterilised lysing enzymes (Sigma L1412) was added and incubated overnight at 22°C with shaking at 80 rpm. Protoplasts were filtered with a sterilised nappy liner and 5 mL aliquots of protoplasts were overlaid with 2 mL of ST buffer (0.6 M sorbitol, 1 M Tris-HCl, pH 8) in a Corex tube. The cell suspension was centrifuged at 4°C for 5 min at 5,000 rcf then the resulting middle layer of protoplasts was removed to a fresh tube. The protoplasts were resuspended in 5 mL of STC buffer (1 M sorbitol, 50 mM $CaCl_2$, 1 M Tris-HCl, pH 8) centrifuged at 4°C for 5 min at 5,000 rcf. This step was repeated 2 more times and the protoplasts resuspended in 500 µL of STC buffer. A cell count was performed using the haemocytometer and a concentration of 1.25 x $10^8$ protoplasts per mL was made in STC buffer. 20 µL of 40% (w/v) PEG was added to 80 µL protoplasts, flash-frozen and stored at -80°C.

## 2.9 Bacterial and fungal transformation

### *2.9.1 E. coli transformation by heat-shock*

1-10 µL of DNA was added to 100 µL of chemically competent *E. coli* cells (Section 2.9.1) and incubated on ice for 20 min. The cells were heat-shocked at 42°C for 30 s and placed on ice for 2 min. 900 µL of SOC medium was added and the cells incubated at 37°C for 1 h with shaking at 200 rpm then plated on LB agar supplemented with the appropriate antibiotics and incubated overnight at 37°C.

### *2.9.2 E. festucae transformation*

*E. festucae* protoplasts were transformed using the method adapted from Itoh *et al.* (1994). 1-5 µg of DNA, 2 µL of spermidine (50 mM) and 50 µL of heparin (5 mg/mL) were added to 100 µL of *E. festucae* protoplasts (Section 2.9.3). The cells were incubated on ice for 30 min and 900 µL of 40% (w/v) PEG solution was added followed by incubation on ice for another 20 min. 50 µL of the cell suspension was added to 3.5 mL of soft RG agar pre-warmed to 50°C and poured on pre-solidified RG agar (5 mL). The plates were incubated for 24 h at 22°C and the following day overlaid with 15 mL of soft RG agar supplemented with the appropriate antibiotics. The plates were incubated at 22°C for another 2-3 weeks.

## 2.10 Cell culture and immunofluorescence

### *2.10.1 Cell culture and maintenance*

HeLa and MCF7 cells were grown in 75 $cm^2$ flasks at 37 °C with 5% $CO_2$ in a Hera cell 150 incubator. Upon confluence cells were passaged by washing twice with 10 mL PBS (Thermo Fisher Scientific) and adding 1.5 mL 0.25% Trypsin-EDTA (Thermo Fisher Scientific). Trypsinisation was performed for 3-5 min at 37°C and 8.5 mL Dulbecco's Modified Eagle Medium (DMEM; containing 10% foetal bovine serum (Thermo Fisher Scientific) and 1% penicillin/streptomycin (Thermo Fisher Scientific) was added.

### *2.10.2 Acid etch and poly-D-lysine coating of coverslips*

Coverslips (Electron Microscopy Sciences; 8 mm, #1.5 thickness) were acid etched in 1 M HCl overnight at 60 °C with shaking, washed 5 x for 5 min in sterilised $H_2O$, then incubated in poly-D-lysine (1 mg/mL) for 1 h at room temperature. Washes were performed with sterilised $H_2O$ for 3 x 5 min, then with 70% ethanol for 2 x 10 min, and with 100% ethanol for 2 x 10 min. Each side of the coverslips was further UV-sterilised for 20 min.

### *2.10.3 Transient transfection*

Cells were seeded in a 24-well plate on poly-D-lysine coated coverslip at 100,000 cells/well in 0.5 mL DMEM and grown overnight. Culture media was replaced the next day before transfection using the JetPEI® transfection reagent (Polyplus). The DNA-particle complex was prepared with 4 µL jetPEI per µg DNA according to manufacturer's instructions in a 100 µL reaction volume.

### *2.10.4 Immunofluorescence*

Cells grown on poly-D-lysine coated coverslips were harvested by washing with PBS containing CaCl2 and MgCl2 (Thermo Fisher Scientific) for 3 x 5 min. Cells were fixed in 4% formaldehyde in PBS for 15 min and washed with PBS for 2 x 10 min. Cells were then permeabilised with 0.2% Triton X-100 in PBS for 5 min and washed with PBS for 2 x 10 min. Cells were blocked with blocking buffer (1x PBS, 5% BSA, 0.5% Tween-20) for 30 min at room temperature. Primary antibodies were added and incubated overnight at 4°C. The next day, washes with wash buffer (1x PBS, 0.1% Triton X-100) were performed for 3 x 5 min. Secondary antibodies were added and incubated for 1 h at room temperature. Washes were performed again for 3 x 5 min with wash buffer, followed by 1 x 5 min with PBS. Cells were fixed again in 2% formaldehyde in PBS, and washes were performed for 3 x 5 min with PBS followed by 2 x 5 min with wash buffer. Post-staining was performed with 300 nM DAPI (Thermo Fisher Scientific) in PBS for 1 min and washed with PBS for 2 x 2 min. The coverslips were mounted on microscope slides with SlowFade® Gold Antifade Mountant (Thermo Fisher Scientific).

## 2.11 Plant manipulation

### *2.11.1 Seed sterilisation*

*L. perenne* seeds were surface sterilised by the method adapted from Latchs & Christensen (1985). Seeds were soaked in 50% (v/v) $H_2SO_4$ for 30 min, rinsed in sterile $H_2O$ and soaked in 50% (v/v) commercial bleach, rinsed well with sterile $H_2O$ and air-dried in the laminar flow cabinet.

### *2.11.2 Seedling inoculation*

*L. perenne* seedlings (7 d old germinated on water agar) were inoculated by the method adapted from Latch and Christensen (1985). A 2-3 mm longitudinal slit was made between the mesocotyl and coleoptile regions of the seedling and aseptically inoculated with a small amount of fungal mycelia.

### *2.11.3 Immunoblot detection of Epichloe infection*

*L. perenne* tillers were cut close to the base of the pseudostem and printed on a nitrocellulose membrane (GE Healthcare). The membrane was incubated in blocking solution (20 mM Tris, 10 mM HCl, 50 mM NaCl, 0.5 % non-fat milk powder, pH adjusted to 7.5) for 2 h at 25°C with gentle shaking. The membrane was then incubated overnight at 4°C with gentle shaking in blocking buffer containing 1:1,000 dilution of rabbit polyclonal antibody raised to *Neotyphodium lolii* Lp5 mycelium. The membrane was then washed three times with fresh blocking buffer and incubated with blocking buffer containing 1:2,000 dilution of anti-

rabbit alkaline phosphatase-conjugated secondary antibody (Sigma) for 2 h at 25°C with gentle shaking. The membrane was developed with the Fast Red chromogen (Sigma) for 10-20 min.

## 2.12 Microscopy

### *2.12.1 Fluorescence inverted microscopy*

For fluorescence microscopy of fungal hyphae, *E. festucae* cultures were grown on 1.5% (w/v) water agar. The agar slice was excised and placed on a microscope and a drop of calcofluor white (250 µg/mL) was added, and observed under the Stereomicroscope BX51 (Olympus) using with the U-MWU2 Ultraviolet excitation cube (wideband).

### *2.12.2 Confocal microscopy*

For confocal microscopy of fungal hyphae *in planta*, approx. 0.5 x 1 cm sections were obtained from the pseudostem region of endophyte-infected *L. perenne* plants and incubated in 95% ethanol for at least 24 h. The sample was then incubated in 10% (w/v) potassium hydroxide for 16 h and in 500 µL staining solution (0.008% aniline blue (Sigma), 0.001% WGA-AlexaFluor488 (Molecular Probes) 0.02% (v/v) Tween®-20 (Invitrogen), 0.15 M NaCl, 2 mM KCl, 10 mM $Na_2HPO_4$, 2 mM $KH_2PO_4$, pH adjusted to 7.4). The samples were analysed under the Leica SP5 DM6000B confocal microscope (Leica Microsystems). An excitation wavelength of 405 nm and acquisition window of 449 nm to 555 nm was set for aniline blue and an excitation wavelength of 488 nm and acquisition window of 498 nm to 558 nm was set for WGA-AlexaFluor488. Images were obtained of 5-10 µm-thick z-distances with a step size of approx. half of each image thickness. Images were processed with ImageJ as a maximum projection (z-stack).

## 2.13 Alkaloid analysis

Indole-diterpenes and ergot alkaloids were extracted either from infected pseudostem tissue of *L. perenne* and analysed by LC-MS/MS as previously described (Rasmussen *et al.*, 2012). The limits of detection and quantification for ergot alkaloids and indole-diterpenes were 0.2 ppm (0.5 ppm) and 2 units (5 units) respectively. Ergotamine was included as an internal standard for quantifying ergot alkaloids.

## 2.14 Bioinformatics

The genomic sequences of *E. festucae* were retrieved from the *E. festucae* Genome Projects database at the University of Kentucky (http://www.endophyte.uky.edu/) (Schardl *et al.*, 2013). Other fungal gene and protein sequences were retrieved from either the NCBI databases (http://www.ncbi.nlm.nih.gov/) or the Broad Institute database (https://www.broadinstitute.org/scientific-community/data). Protein domains were analysed with the SMART Web-based tool (http://smart.embl-heidelberg.de/) (Schultz *et al.*, 1998, Letunic *et al.*, 2014) using the default settings and multiple amino acid sequence alignments were generated with Clustal Omega (http://www.ebi.ac.uk/Tools/msa/clustalo/) (Goujon *et al.*, 2010, Sievers *et al.*, 2011) using the default settings. Phylogenetic trees were generated using the MEGA 6 software (http://www.megasoftware.net/) (Tamura *et al.*, 2013). Boxplots were generated by BoxPlotR (http://shiny.chemgrid.org/boxplotr/) (Spitzer *et al.*, 2014).

# Chapter 3: Characterisation of *E. festucae* JmjC proteins identified Jmj2 (KdmB) as a H3K4me3-specific demethylase.

## 3.1 Introduction

The methylation status of histones influences the chromatin structure which in turn is an important determinant of the expression of fungal secondary metabolite genes (Strauss & Reyes-Dominguez, 2011). *E. festucae* contains two important SM clusters, the *EAS* and *LTM* clusters, both of which are regulated by H3K9 and H3K27 methylation (Chujo & Scott, 2014). In axenic culture, genes of these clusters carry high levels of H3K9me3 and H3K27me3, but when the fungal cultures are inoculated into the host plant, there is a marked reduction in the levels of both marks. This leads to the hypothesis that there are corresponding demethylases for removing these marks *in planta*. Chujo & Scott (2014) additionally showed the presence of H3K4 and H3K36 methylation in *E. festucae*. Therefore, it is hypothesised that histone demethylases for histone H3K4, K9, K27 and K36 are present in this fungus.

To date, all histone demethylases characterised, with the exception of the amine oxidase LSD1, contain and rely on the JmjC domain for their oxidative demethylation activity. LSD1 was reported in 2004 and specifically demethylates H3K4me2 (Cuthbert *et al*., 2004). Palmer *et al*. (2013) reported that disruption of the *LSD1* homologue, *hdmA* in *A. nidulans* did not impact H3K4 methylation, development and secondary metabolism of the fungus. The JmjC domain-containing demethylases constitute a family of histone demethylases with a wider range of histone residue specificities that include methylated H3K4, H3K9, H3K27 and H3K36 (Cloos *et al*., 2006; Klose *et al*., 2006b; Tsukada *et al*., 2006; Whetstine *et al*., 2006; Yamane *et al*., 2006). Therefore, although *E. festucae* possesses the homologue of LSD1 (EfM3.034720), only the characterisation of JmjC demethylases is relevant to the aims of this study. At the commencement of this study no fungal demethylases were characterised so information was drawn from the mammalian JmjC proteins in order to identify candidate demethylases in *E. festucae*.

To this end, the first objective for this study is the identification and subsequent *in silico* characterisation of JmjC-domain containing proteins in *E. festucae*. The genes encoding the proteins of interest were overexpressed in *E. festucae* and the strains analysed by western blotting to test for reduction in global histone H3 methylation. Finally, the effects of the gene overexpression on *E. festucae* development and symbiotic interaction phenotype were analysed.

## 3.2 Results

### *3.2.1 Identification of JmjC proteins in E. festucae*

Putative JmjC domain containing proteins were first identified in the genome database of *E. festucae* strain Fl1 (http://www.endophyte.uky.edu/). The annotation of genes in the genome database is based on hits of the putative genes to several public protein databases, including the NCBI protein database, InterProScan and UniGene databases. A search of these annotations with the 'JmjC' and 'Jumonji' keywords identified a total of 8 *E. festucae* genes and these were designated *jmj1* to *jmj8*. Although the convention is to use letters for the genes (e.g. *jmjA*), these numeric designations were used to avoid confusion with known genes, e.g. JMJD. Subsequent BLAST searches of the *E. festucae* genome using the amino acid sequences of the JmjC domains of these proteins did not identify any additional unique hits, suggesting that all putative JmjC proteins in the fungus have been identified in the analysis. The eight proteins vary in their predicted sizes from 282 amino acids (31.7 kDa; Jmj8) to 1764 amino acids (198 kDa; Jmj2) (Fig. 3.1).

### *3.2.2 In silico characterisation of the E. festucae JmjC proteins.*

To gain a further understanding of the predicted JmjC proteins, BLAST searches were performed against the UniProtKB and NCBI non-redundant protein databases. For each of the proteins, homologues could be identified within the Fungi kingdom. This was to be expected for most fungal proteins, but interestingly, Jmj2 had surprisingly good homology with proteins across species, including fruit flies, mouse and human. In addition, homology was found for the full-length protein of Jmj2, and the hits identified were the KDM5 group of H3K4 demethylases. Good homology outside fungi was also found for Jmj1, but this was confined to the N-terminal JmjN and JmjC domains of the protein and not the entire protein. The hits for Jmj1 were to the KDM4 group of H3K9/K36 demethylases.

Jmj3 has excellent matches across the full-length protein but only within the ascomycetes. Outside of this group but still within the Fungi kingdom, good homology was found only for the JmjC domain, while outside fungi, only poor homology was found, which was also restricted to the JmjC domain of Jmj3. The homologue of Jmj3 in *N. crassa* is Dmm-1 (Honda *et al.*, 2010), and the two proteins share 52% amino acid identity. The study in *N. crassa* identified Dmm-1 as a JmjC-domain containing protein, however histone demethylase activity could not be demonstrated for the protein, although it is clearly involved in regulating the spread of DNA and H3K9 methylation. Strikingly, mutation of a crucial amino acid residue within the Fe(II)-binding site of the JmjC domain abolished the functions of Dmm-1 (Honda *et al*., 2010). Outside the Fungi kingdom, hits to the JmjC domain of Jmj3 were present but restricted to only three genera of amoebas (*Naegleria*, *Dictyostelium* and *Acytostelium*) (Appendix 22).

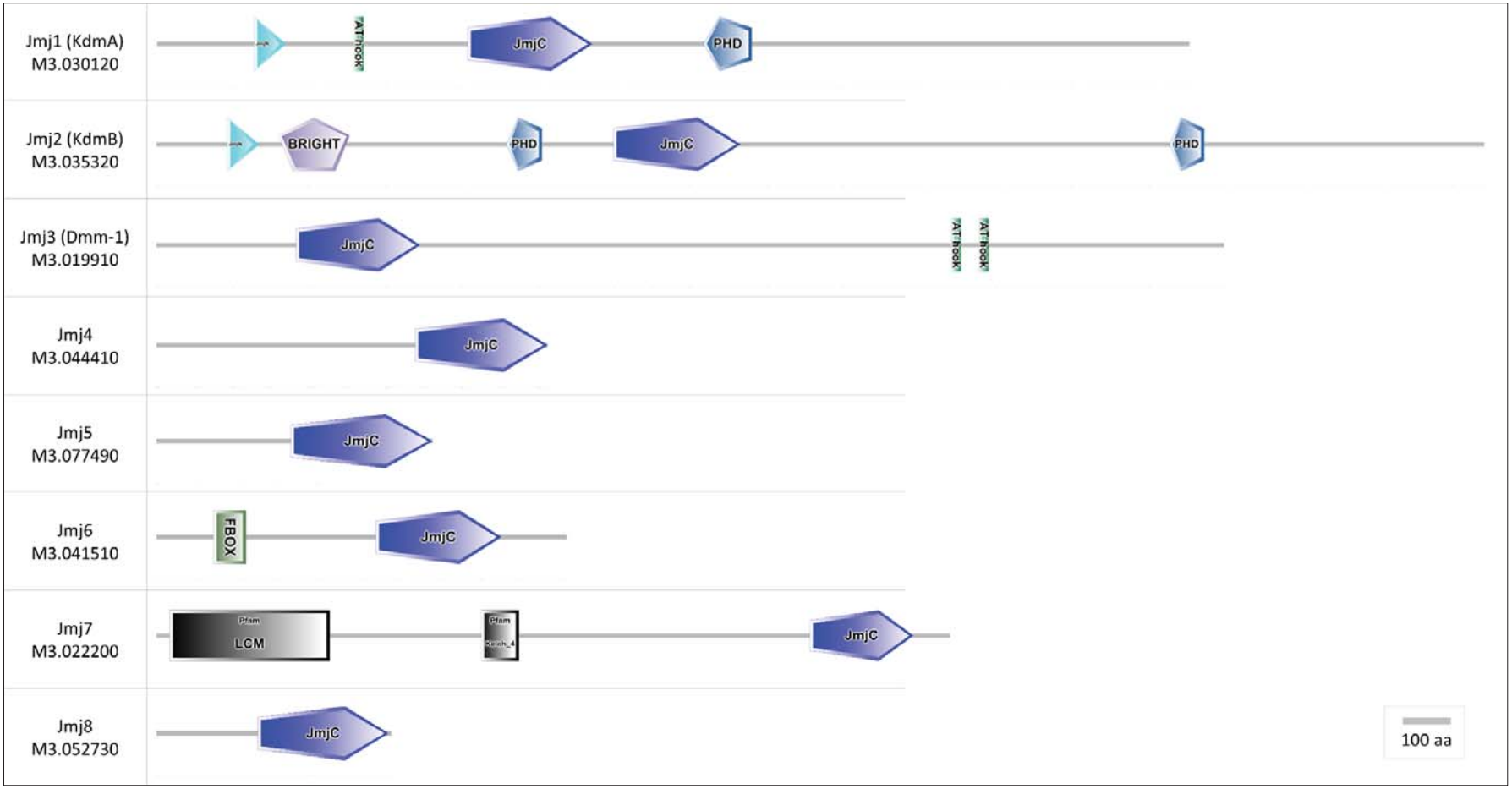


**Figure 3. 1. Domain composition of *E. festucae* JmjC proteins.** Domains were predicted by SMART (Schultz *et al*., 1998; Letunic *et al*., 2014). The numbers below the gene names refer to the M3 model numbers of the genes. JmjC domains are depicted by blue pentagons, JmjN domains in cyan triangles, and PhD domains in grey pentagons. Other domains depicted in the figure are AT hooks in Jmj1 and Jmj3, F-box domain of Jmj6, the leucine carboxylmethyltransferase domain and Kelch motif of Jmj7.

Jmj4, Jmj5 and Jmj8 are relatively smaller proteins (300-500 aa) that contain no other identifiable domain except for the JmjC domain (Fig. 3.1). Homologues of these proteins could be identified in fungi, but these were to uncharacterised proteins. Interestingly, hits to mammalian KDM8 proteins were identified for Jmj4 (Appendix 22). Human KDM8 (renamed from JMJD5; Jumonji domain-containing 5) was shown to be a histone H3K36me2 demethylase (Hsia *et al.*, 2010). The full-length protein of Jmj4 shares 34% amino acid identity with full-length KDM8, while the JmjC domains of the proteins share 48% amino acid identity, suggesting that the proteins are likely homologues (Fig. 3.2). The hits for Jmj8 were to JMJD7 proteins. The functions of JMJD7 were unknown at the time of this analysis, but a recent study has shown that both JMJD7 and KDM8 in *Mus musculus* are proteases that act to cleave histone tails containing methylated arginines (Liu *et al.*, 2017). Full-length Jmj8 shares 35% amino acid identity with full-length *M. musculus* JMJD7, while the JmjC domains of the proteins share 37% amino acid identity (Fig. 3.3). By comparison, there were no strong hits for Jmj5 to any proteins outside of the Fungi kingdom. The best of these hits, albeit weak, were mostly to KDM8 proteins. Jmj5 shares 21% (full-length) and 25% (JmjC domain) amino acid similarity with KDM8.

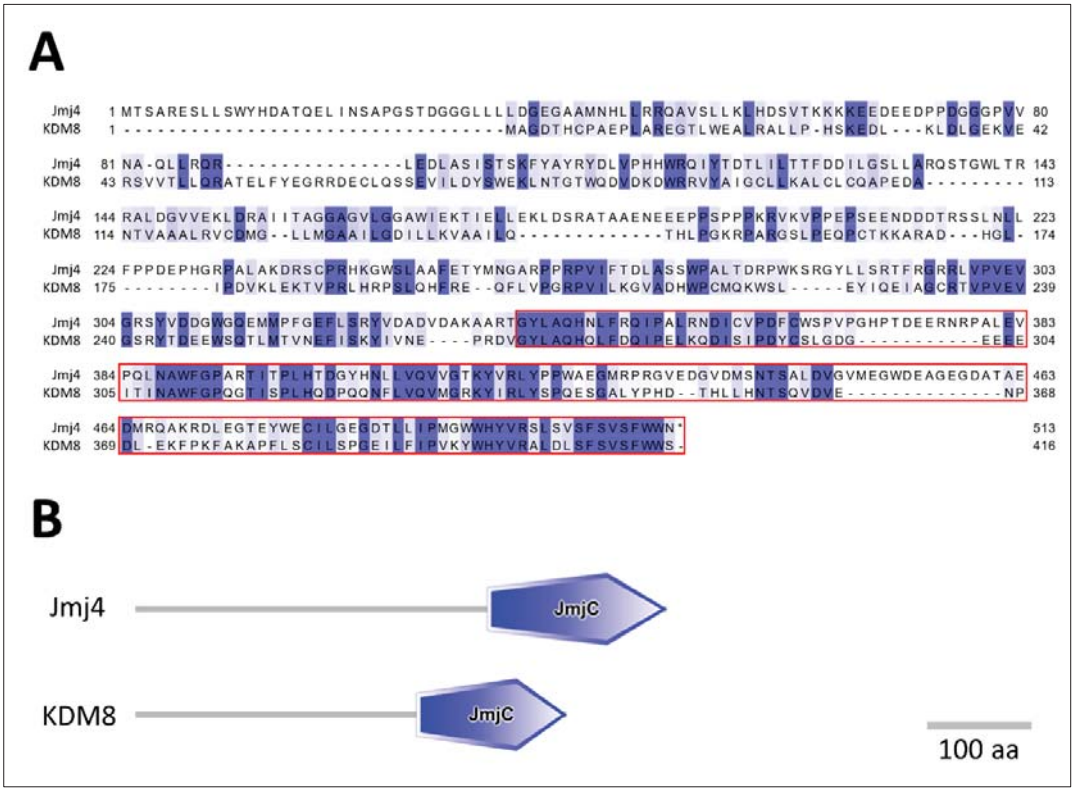


**Figure 3. 2. Similarity of *E. festucae* Jmj4 with KDM8.** (A) Amino acid alignment of Jmj4 and *H. sapiens* KDM8. The C-terminal JmjC domain is boxed in red. The alignment was generated with Clustal Omega. Identical residues are shown in dark blue and conservative changes in lighter blue. (B) Domain composition of Jmj4 and H. sapiens KDM8. C-terminal JmjC domain is indicated by blue pentagon. Accession codes of the sequences shown are EfM3.044410 (Jmj4) and Q8N371 (KDM8).

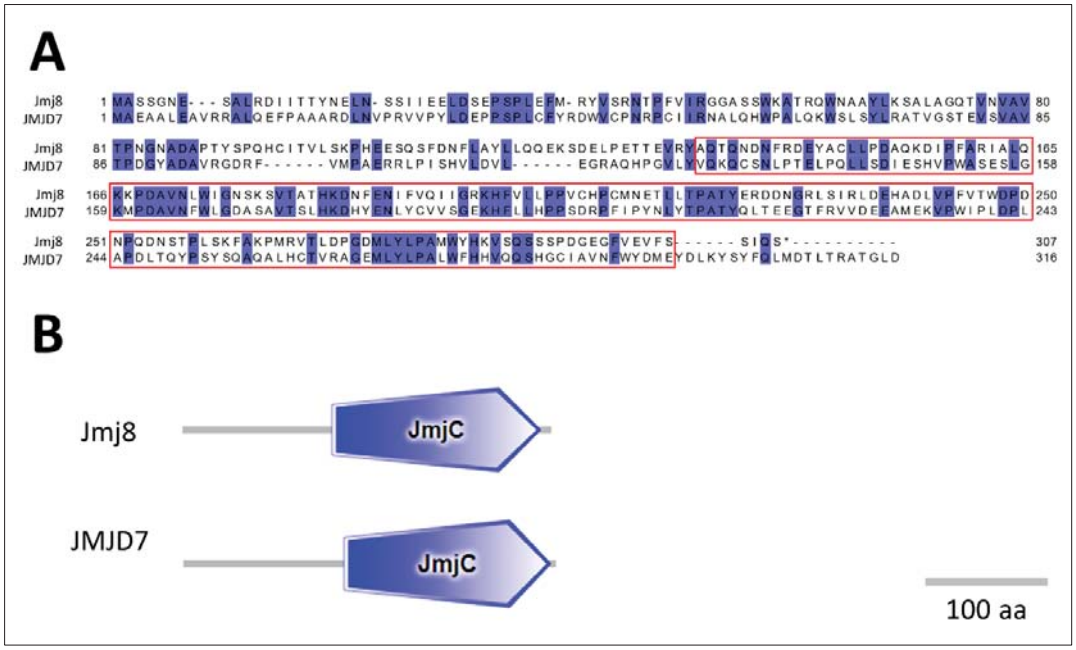


**Figure 3. 3. Similarity of *E. festucae* Jmj8 with JMJD7.** (A) Amino acid alignment of Jmj8 and *M. musculus* JMJD7. The C-terminal JmjC domain is boxed in red. The alignment was generated with Clustal Omega. Identical residues are shown in dark blue and conservative changes in lighter blue. (B) Domain composition of Jmj7 and KDM8. C-terminal JmjC domain is indicated by blue pentagon. Accession codes of the sequences shown are EfM3.052730 (Jmj8) and P0C872 (JMJD7).

The conservation of Jmj6 across taxa was also interesting. Excellent hits to the full-length protein could be identified across species, with the majority of the best matches found in the plant kingdom. In animals, moderate homology was present but this was confined to the JmjC domain of Jmj6. These hits were to JMJD6 proteins, enzymes which have bifunctional (histone) arginine demethylase as well as (protein) lysyl-hydroxylase activity, but not lysine demethylase activity. Hits to Jmj6 were also identified in bacteria, albeit with very poor homology and restricted to the JmjC domain of the protein. Interestingly, a single bacterium, *Chlamydia trachomatis*, appears to possess the full-length homologue of Jmj6, suggesting a possible horizontal gene transfer event. Jmj6 also contains an F-box domain (Fig. 3.1), which was first described in a mammalian cyclin and found to be important in mediating protein-protein interactions (Skaar *et al.*, 2013).

Finally, hits to Jmj7 in fungi were all predicted to be leucine carboxylmethyltransferases, and a leucine carboxylmethyltransferase domain was also predicted for the protein (Fig. 3.1). The homologue in *S. cerevisiae*, Tyw4 (tRNA yW-synthesizing protein 4) is an S-adenosyl-L-methionine-dependent carboxylmethyltransferase and likely catalyses the final reactions for the synthesis of wybutosine, a modified guanosine nucleoside that is found on eukaryotic phenylalanine tRNA (Noma *et al.*, 2006). Outside fungi, hits were only found to the carboxymethyltransferase domain of Jmj7, and these proteins were similarly predicted to be wybutosine modifying proteins (Appendix 22). Jmj7 also contains a Kelch motif found in proteins with diverse range of activities and functions, across many species ranging from poxviruses, bacteria, fruit flies to humans.

In summary, these analyses identified Jmj1 and Jmj2 as homologues of KDM4 and KDM5 demethylases, respectively. Jmj3 is the homologue of Dmm-1. Jmj6 appears to be an arginine demethylase and Jmj7 a leucine carboxylmethyltransferase. The JmjC domain of Jmj4 appears to have some similarity to the JmjC domains of KDM8 proteins, and Jmj8 protein has some homology to mammalian JMJD7 proteins. Jmj5 constitutes an entirely uncharacterised class of fungal proteins that do not contain any identifiable protein domains other than a single JmjC domain.

*3.2.3 Jmj1 and Jmj2 are homologues of A. nidulans KdmA and KdmB.*

There were no reports of histone demethylases in filamentous fungi when this study was initiated, but the H3K36 and H3K4 demethylases, KdmA and KdmB have since been reported in *A. nidulans* (Gacek-Matthews *et al.*, 2015, 2016). The homologues of these proteins in *E. festucae* are Jmj1 and Jmj2, respectively, and so these will also be referred to as KdmA and KdmB. Similar to what the above BLAST analyses have suggested, the Jmj1 homologue in *A. nidulans*, KdmA, belongs to the KDM4 group of demethylases, while the Jmj2 homologue in *A. nidulans*, KdmB, belongs to the KDM5 group of demethylases.

*E. festucae* KdmA shares 43% amino acid identity with *A. nidulans* KdmA (Fig. 3.4) and domain architecture between the two proteins is well conserved, with both having N-terminal JmjN and JmjC domains (Fig. 3.5). The JmjN domain is found only in JmjC domain-containing proteins. While its precise functions are still unclear, the domain is essential for the activity of the human H3K9me/K36me demethylase KDM4A as well as the *Drosophila* H3K4me3 demethylase Lid/dmKDM5 (Klose *et al*., 2006b; Li *et al*., 2010). Some of the KDM4 proteins also contain plant homeodomains (PHDs) (Fig. 3.5). Although there are no studies to date on the PHDs of KDM4, the PHDs of KDM5 proteins have been shown to recognise H3K4me3 and H3K9me3 (see next paragraph). The yeast Rph1 and rice JMJ705 proteins have C-terminal zinc finger domains, and interestingly, mammalian KDM4A additionally has double TUDOR domains at the C-terminal end (Fig. 3.5). These double TUDOR domains have been shown to produce a distinctive fold that recognises methylated H3K4 and H4K20 (Huang *et al*., 2006). Rph1 and JMJ705 also contain AT hooks, these are DNA binding motifs that bind to AT-rich DNA sequences (Fig. 3.5).

*E. festucae* KdmB shares 54% amino acid similarity with *A. nidulans* KdmB (Fig. 3.6), and the domain architecture of both proteins is well conserved (Fig. 3.7). The KDM5 proteins are H3K4me2/me3 demethylases that have an N-terminal JmjN domain, a PHD finger and a JmjC domain, and most have at least one PHD finger at the C-terminus (Fig. 3.7). The H3K4me3-binding functions of the PHD finger was first identified in the PHD fingers of INhibitor of Growth (ING) proteins and the nucleosome remodelling factor (NURF) complex (Shi *et al.*, 2006, Wysocka *et al.*, 2006). More recently, the first and third PHD fingers of mammalian KDM5B were shown to recognise unmethylated H3K4 (H3K4me0) and H3K4me3, respectively (Klein *et al.*, 2014). The N-terminal PHD finger of Lid (Fig. 3.7) also binds specifically to H3K4me2/me3 and is essential for the catalytic activity of the demethylase (Li *et al*., 2010). Although the PHD finger of PHF8 recognises H3K4me3 and is required for the demethylase activity of the protein, it also has a H3K9/K27 demethylase activity (Horton *et al.*, 2010). The authors further found that PHF8 demethylation of H3K9me2 is increased 12-fold when the H3K4 residue on the target H3 peptide is trimethylated. Thus, PHD fingers can be viewed as readers of H3K4 trimethylation and may direct JmjC proteins to the histones containing the modified residue in order to catalyse its demethylation, but it may

also serve to link this euchromatic mark with the demethylation of other heterochromatic marks, such as H3K9me3 and H3K27me3.

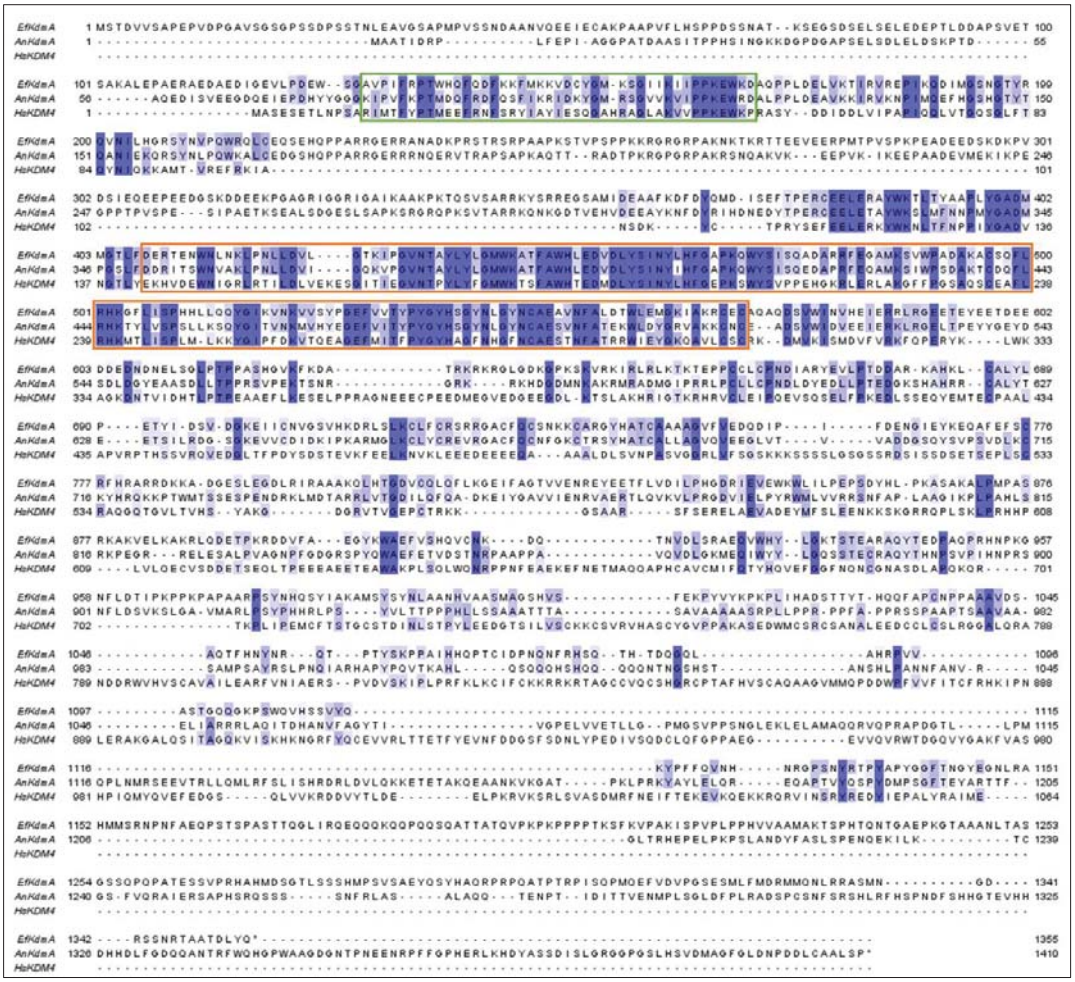

**Figure 3. 4. Amino acid alignment of *E. festucae*, *A. nidulans* and *H. sapiens* KDM4 proteins.** The N-terminal JmjN domain is boxed in green and JmjC domain in orange. Accession codes of the sequences shown are ANID_01060 (KdmA) and O75164 (KDM4A). The alignment was generated with Clustal Omega. Identical residues are shown in dark blue and conservative changes in lighter blue.

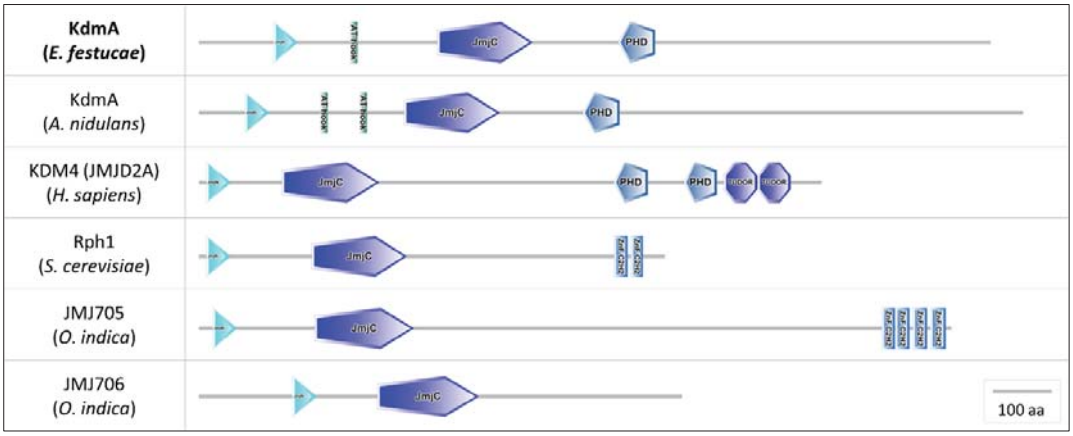


**Figure 3. 5. Domain composition of *E. festucae* KdmA and other KDM4 proteins.** In addition to N-terminal JmjN and JmjC domains, KDM4 proteins in some organisms contain zinc fingers and AT hook domains (DNA binding) as well as C-terminal PHD and TUDOR domains. The accession codes for the proteins shown are ANID_01060 (KdmB), O75164 (KDM4A), P39956 (Rph1), Os01g67970 (JMJ705) and Os10g42690 (JMJ706). Domains were predicted by SMART (Schultz *et al*., 1998; Letunic *et al*., 2014).

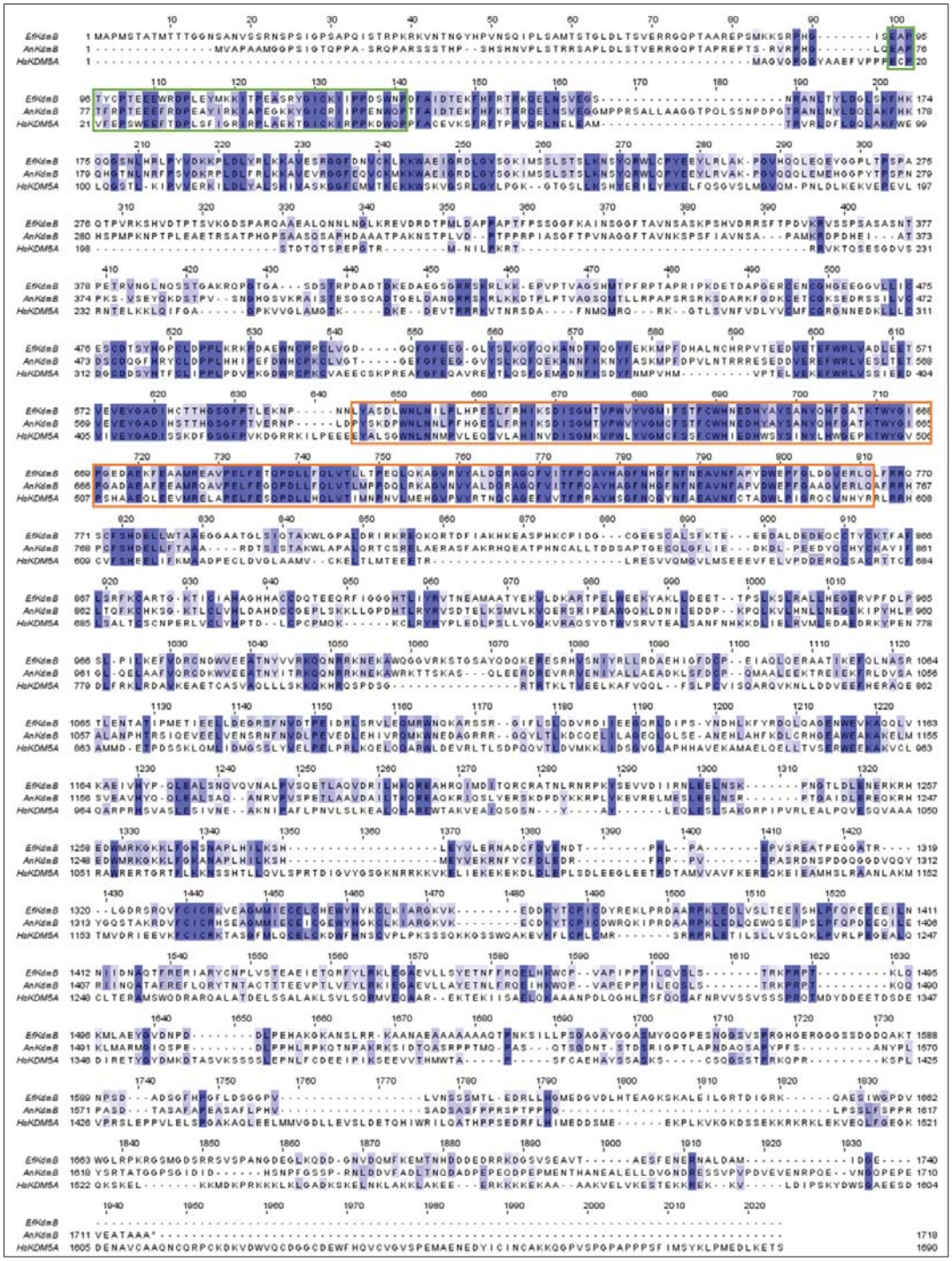


**Figure 3. 6. Amino acid alignment of *E. festucae*, *A. nidulans* and *H. sapiens* KDM5 proteins.** The N-terminal JmjN domain is boxed in green and JmjC domain in orange. Accession codes of the sequences shown are ANID_08211 (KdmB) and P29375 (KDM5A). The alignment was generated with Clustal Omega. Identical residues are shown in dark blue and conservative changes in lighter blue.

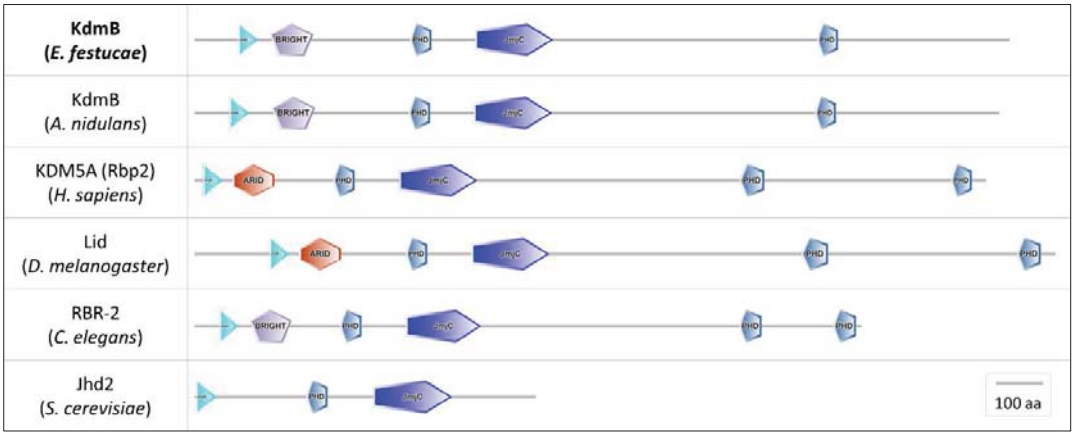


**Figure 3. 7. Domain composition of E. festucae KdmB and other KDM5 proteins**. All KDM5 proteins contain PHD fingers, in addition to a JmjC domain and an N-terminal JmjN domain. Some homologues can contain additional C-terminal PHD fingers. The accession codes for the proteins shown are ANID_08211 (KdmB) and P29375 (KDM5A), Q9VMJ7 (Lid), Q23541 (RBR-2) and P47156 (Jhd2). Domains were predicted by SMART (Schultz *et al.*, 1998; Letunic *et al.*, 2014).

### *3.2.4 The E. festucae JmjC proteins are likely catalytically active enzymes.*

The enzymatic activity of the JmjC domain relies on two essential cofactors; Fe(II) and α-ketoglutarate for its oxidative demethylation reaction. Binding of these molecules to the JmjC domain is coordinated by several key amino acid residues within the enzymatic pocket of the domain (Fig. 3.8). The conservation of these residues is an indicator of a catalytically active domain, and conversely, substitutions of the residues by non-active amino acids suggest the absence of enzymatic activity (Klose *et al.*, 2006a). To identify the conservation of these residues in the JmjC domains of the *E. festucae* proteins, a multiple amino acid sequence alignment was performed with other known demethylases. The results showed that all three Fe(II)-binding amino acid residues as well as the two α-ketoglutarate-binding amino acid residues of the JmjC domain are present in all eight *E. festucae* proteins, indicating that these proteins are likely to be enzymatically active (Fig. 3.9). However, JmjC domains do not exclusively catalyse the demethylation of histone residues. For example, factor inhibiting hypoxia (FIH), the first JmjC protein shown to be catalytically active, is an asparagine protein hydroxylase that hydroxylates hypoxia inducible factor 1 (HIF-1) (Lando *et al.*, 2002). Other non-histone demethylase proteins that contain a JmjC domain include the nucleolar MINA53/NO66 proteins, cytosolic phospholipases and heat shock proteins (Klose *et al.*, 2006a).

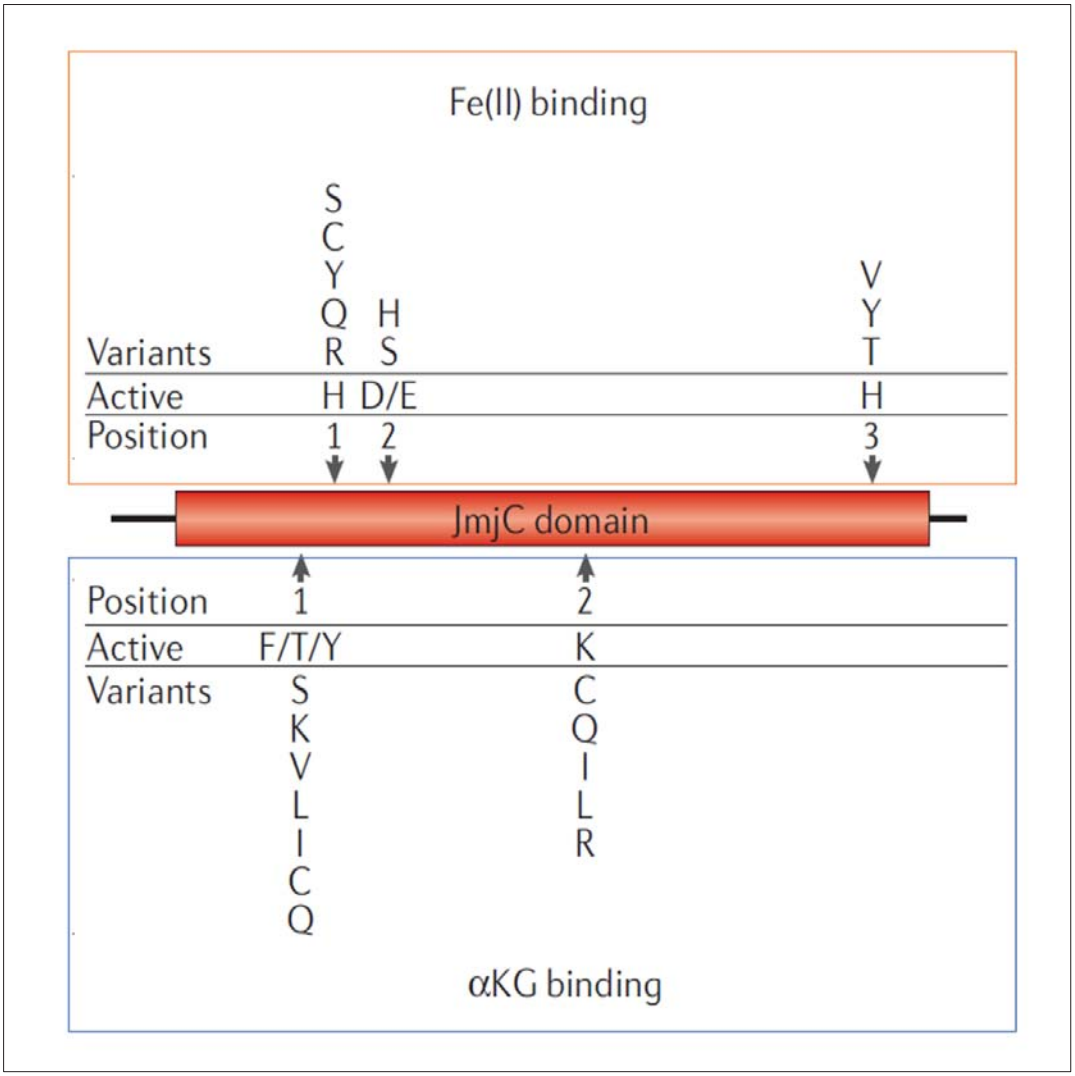


**Figure 3. 8. Key amino acid residues of the JmjC domain.** The active amino acids for Fe(II)-binding and αKG-binding as well as the non-active variants are shown. Figure is taken from Klose *et al*., (2006a).

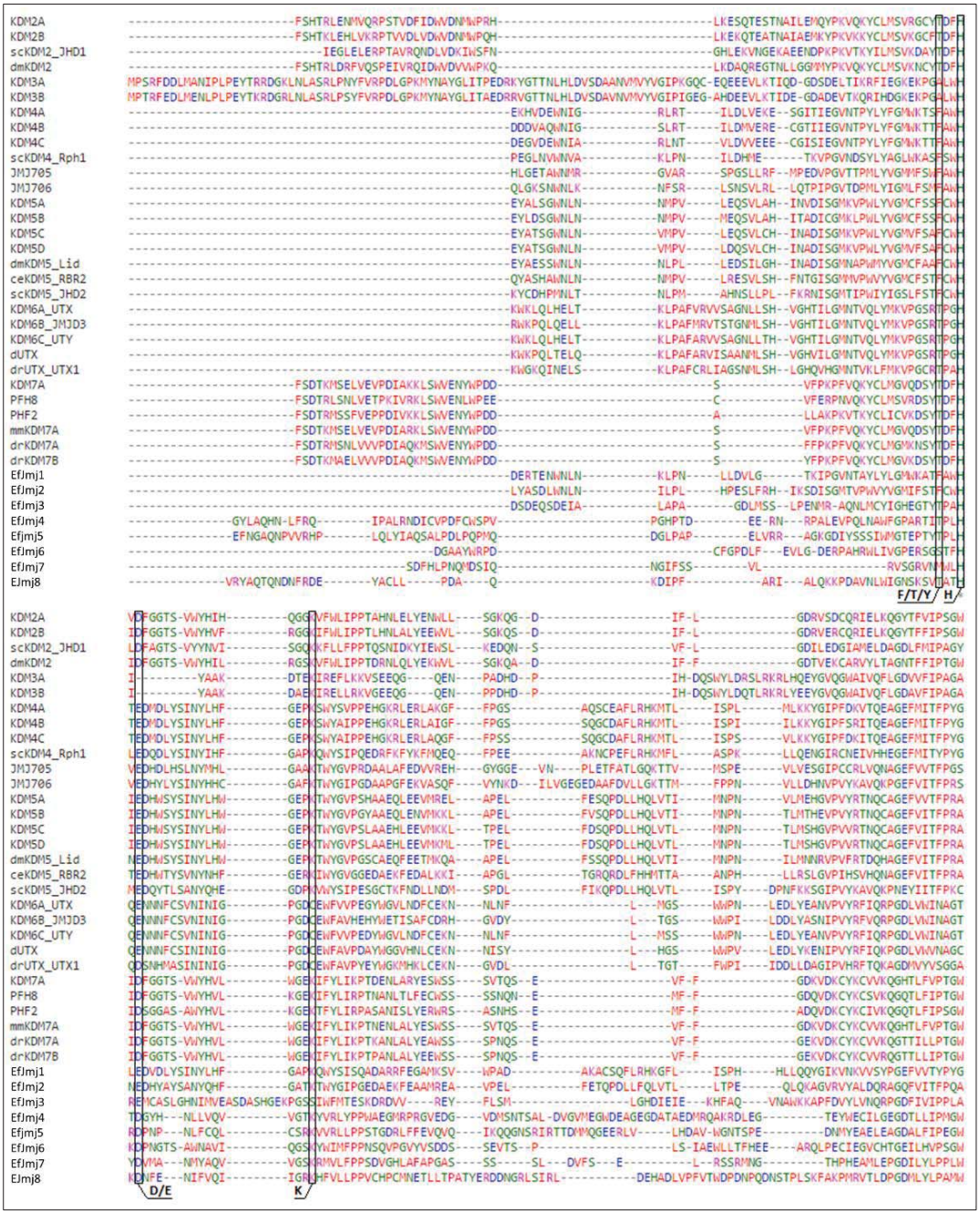
KDM2A
KDM2B
scKDM2_JHD1
dmKDM2
KDM3A
KDM3B
KDM4A
KDM4B
KDM4C
scKDM4_Rph1
JMJ705
JMJ706
KDM5A
KDM5B
KDM5C
KDM5D
dmKDM5_Lid
ceKDM5_RBR2
scKDM5_JHD2
KDM6A_UTX
KDM6B_JMJD3
KDM6C_UTY
dUTX
drUTX_UTX1
KDM7A
PFH8
PHF2
mmKDM7A
drKDM7A
drKDM7B
EfJmj1
EfJmj2
EfJmj3
EfJmj4
Efjmj5
EfJmj6
EfJmj7
EJmj8
F/T/Y
H
D/E
K


**Figure 3. 9. Multiple sequence alignment of the JmjC domains of Jmj1-Jmj8 with other characterised histone demethylases.** Shown in the figure are the first phenylalanine/threonine/tyrosine (F/T/Y) residues, predicted to be the αKG-binding residues. The next two amino acids shown are the first two of three Fe(II)-binding residues, histidine (H), and aspartate/glutamate (D/E). The third boxed residue, lysine (K) is the second αKG-binding residue. And the last histidine (H) is the third Fe(II)-binding residue.

*3.2.5 Predicted cellular localisation of the E. festucae JmjC proteins.*

Given that histones are strictly nuclear proteins, it is expected that histone demethylases would similarly be localised in the nucleus. Therefore, the *E. festucae* JmjC proteins were first analysed for the presence of classical (Importin α-dependent) nuclear localisation signals (NLS) by the cNLS Mapper (http://nls-mapper.iab.keio.ac.jp) (Kosugi *et al.*, 2009). The residual positions and sequences of the predicted monopartite and bipartite NLSs, the two major classes of classical NLS, as well as their scores are given in Table 3.1. Reporter experiments with GUS-GFP suggest that NLS with a score of 8 and above localise exclusively to the nucleus, while those with scores 1 or 2 are cytoplasmic (Kosugi *et al*., 2009). NLS with scores in-between these may localise to both compartments.

Several *E. festucae* proteins were initially used in the analysis as controls. The first is ProA, a zinc-finger transcription factor that has been shown to bind to *E. festucae* gene promoters (Tanaka *et al.*, 2013). An N-terminal monopartite NLS with a score of 8 was predicted for this protein (Table 3.1). The second is PacC, a zinc-finger transcription factor that localises to the nucleus in response to extracellular pH alkalinisation (Mingot *et al.*, 2001, Lukito *et al.*, 2015). A bipartite NLS with a score of 8.2 was predicted for this protein. Several histone H3 methyltransferases were also analysed and most had predicted NLS with reasonable scores (Table 3.1). This shows that analysis of *E. festucae* proteins with the prediction algorithm is relatively reliable. Interestingly, a weak (score of 4.7) NLS was predicted for the H3K9 methyltransferase ClrD. However, ClrD has been shown to be the H3K9 methyltransferase in *E. festucae* (Chujo & Scott, 2014), thus a negative result from this analysis does not necessarily rule out nuclear

localisation of the protein. Such proteins may instead have their nuclear import chaperoned directly by importin-β. Analysis of the JmjC proteins showed that KdmA, KdmB and Jmj3 had strongly predicted NLSs, while Jmj4, 5 and 8 had weak or no NLS predicted, and Jmj6 and 7 had moderate scores (Table 3.1).

**Table 3. 1.Predicted nuclear localisation signals (NLSs) in *E. festucae* JmjC proteins.**

| | | | |
|---|---|---|---|
| **ProA** (755 aa) | Predicted monopartite NLS | | |
| | Pos. | Sequence | Score |
| | 96 | IKNIIKRKKLA | 8 |
| **PacC** (591 aa) | Predicted bipartite NLS | | |
| | Pos. | Sequence | Score |
| | 218 | DRKRAFDMVDDFFGSAKRRQVD | 8.2 |
| **SetA** (1282 aa) | Predicted monopartite NLS | | |
| H3K34 methyltransferase | Pos. | Sequence | Score |
| | 493 | VPHMRKRLKNYGF | 9 |
| | 668 | HLAKRRKLN | 8 |
| | 814 | DRPSSKKRKLE | 14 |
| | 827 | LETALKRRKRSDEELF | 7 |
| | 1134 | QLKKRKKPVK | 7 |
| | Predicted bipartite NLS | | |
| | Pos. | Sequence | Score |
| | 815 | RPSSKKRKLEVSLETALKRRKRS | 16.4 |
| **ClrD** (188 aa) | Predicted bipartite NLS | | |
| H3K9 methyltransferase | Pos. | Sequence | Score |
| | 4 | ATKRHFFCHGQDGNDVEKDKCHWCQ LRSFP | 4.7 |
| **EzhB** (1158 aa) | Predicted monopartite NLS | | |
| H3K27 methyltransferase | Pos. | Sequence | Score |
| | 930 | RKRKRRLDED | 14 |
| **SetB** (894 aa) | Predicted monopartite NLS | | |
| H3K36 methyltransferase | Pos. | Sequence | Score |
| | 791 | QDLKRKREAD | 7 |
| **KdmA** (1354 aa) | Predicted monopartite NLS | | |
| | Pos. | Sequence | Score |
| | 627 | DATRKRKRGLG | 10 |
| | Predicted bipartite NLS | | |
| | Pos. | Sequence | Score |
| | 627 | DATRKRKRGLGDKGPKSKVRKI | 11.5 |
| **KdmB** (1740 aa) | Predicted monopartite NLS | | |
| | Pos. | Sequence | Score |
| | 419 | GRRSKRLKKE | 8.5 |

| | | | |
|---|---|---|---|
| | 488 | DPPLKRKPDAE | 7 |
| **Jmj3** (1399 aa) | Predicted monopartite NLS | | |
| | Pos. | Sequence | Score |
| | 864 | RARKRKAKRD | 11 |
| | 1075 | PIAKRPRGRPKKGF | 7 |
| **Jmj4** (512 aa) | Predicted monopartite NLS | | |
| | Pos. | Sequence | Score |
| | 197 | PPPKRVKVPPE | 5 |
| **Jmj5** (341 aa) | Predicted bipartite NLS | | |
| | Pos. | Sequence | Score |
| | 244 | RKVVRLLPPSTGDRLFFEVQVQIKQQG NS | 4 |
| **Jmj6** (505 aa) | Predicted monopartite NLS | | |
| | Pos. | Sequence | Score |
| | 465 | DKKSGKKRKWD | 6.5 |
| **Jmj7** (1036 aa) | Predicted monopartite NLS | | |
| | Pos. | Sequence | Score |
| | 368 | EPKRRFGDAF | 6 |
| | Predicted bipartite NLS | | |
| | Pos. | Sequence | Score |
| | 39 | VSKRSVENLYYPNEPHYFRYFVKKYQRR | 7.8 |
| | 117 | RHAALCDGVMFVDIDYPDLMRKKRSIV | 5.4 |
| **Jmj8** (306 aa) | None | | |

NLSs in *E. festucae* nuclear proteins (ProA, PacC, SetA, ClrD, EzhB and SetB) and JmjC proteins (Jmj1-Jmj8) were predicted using the cNLS Mapper (http://nls-mapper.iab.keio.ac.jp). The table shows the amino acid positions and sequences of the predicted NLSs, as well as the likelihood scores (see text).

The proteins were additionally analysed by PSORTII (https://psort.hgc.jp/) that predicts the cellular localisation of yeast and animal proteins (Nakai & Horton, 1999). The analysis similarly predicted strong nuclear localisation of the 'control' proteins, the transcription factors ProA and PacC, and the histone methyltransferases (Table 3.2). KdmA, KdmB and Jmj3, and to a lesser extent Jmj8, were also predicted to be nuclear. By contrast, Jmj5 was predicted to be mitochondrial and the remaining proteins Jmj4, 6 and 7 were predicted to be cytoplasmic.

Taken together, both prediction algorithms appear to agree in finding strong NLSs in the first three proteins, KdmA (Jmj1), KdmB (Jmj2) and Dmm-1 (Jmj3), weak or no NLSs in Jmj5 and Jmj6, and somewhat inconclusive prediction for Jmj7 and Jmj8. However, in determining nuclear localisation both algorithms rely on predicting the presence of classical NLSs, which are contained in many nuclear proteins chaperoned by importin-α, but as indicated, some nuclear proteins may be directly chaperoned by importin-β, or may be co-transported into the nucleus by another protein that in turn contain an NLS.

**Table 3. 2. Predicted cellular localisation of *E. festucae* JmjC proteins.**

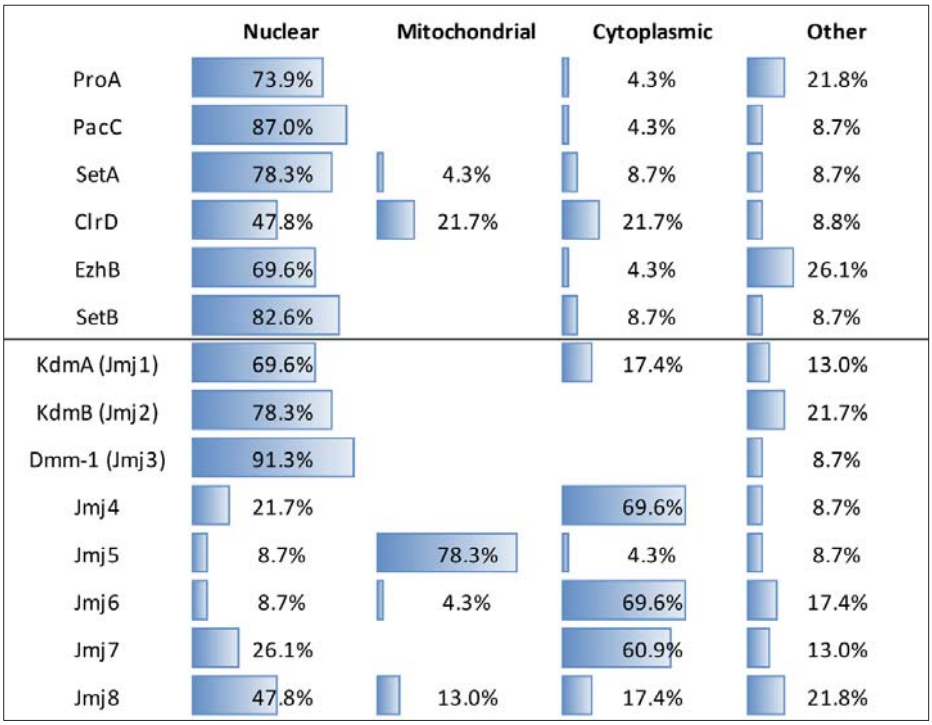

| | Nuclear | Mitochondrial | Cytoplasmic | Other |
|---|---|---|---|---|
| ProA | 73.9% | | 4.3% | 21.8% |
| PacC | 87.0% | | 4.3% | 8.7% |
| SetA | 78.3% | 4.3% | 8.7% | 8.7% |
| ClrD | 47.8% | 21.7% | 21.7% | 8.8% |
| EzhB | 69.6% | | 4.3% | 26.1% |
| SetB | 82.6% | | 8.7% | 8.7% |
| KdmA (Jmj1) | 69.6% | | 17.4% | 13.0% |
| KdmB (Jmj2) | 78.3% | | | 21.7% |
| Dmm-1 (Jmj3) | 91.3% | | | 8.7% |
| Jmj4 | 21.7% | | 69.6% | 8.7% |
| Jmj5 | 8.7% | 78.3% | 4.3% | 8.7% |
| Jmj6 | 8.7% | 4.3% | 69.6% | 17.4% |
| Jmj7 | 26.1% | | 60.9% | 13.0% |
| Jmj8 | 47.8% | 13.0% | 17.4% | 21.8% |

Localisation of the proteins was predicted using PSORTII (https://psort.hgc.jp/). Percentages refer to the likelihood of the proteins being localised in the given compartments. The category of 'other' in the table includes cellular compartments such as cytoskeletal, plasma membrane and vacuoles.

*3.2.6 Transcriptomic analysis of the E. festucae JmjC proteins.*

Presently, several transcriptomic data of wild-type as well as mutant *E. festucae* strains both in culture and *in planta* are available. Most of these studies were done with the aim of identifying key symbiotic genes, utilising symbiotic mutants of the fungus, such as Δ*noxA* (NADPH oxidase), Δ*proA* (zinc-finger transcription factor), Δ*sakA* (MAP kinase) and Δ*hepA* (heterochromatin protein 1) (Tanaka *et al*., 2006; Eaton *et al*., 2010; Eaton *et al*., 2015; Chujo *et al*., in preparation). To predict the importance of the eight *E. festucae* JmjC proteins in symbiosis of the fungus, the expression data of the genes encoding the demethylase proteins were retrieved from these data sets. It is hypothesised that a significant change in expression of a gene in a symbiotic mutant of the fungus implicate either a causal or consequential effect of the gene. In other words, it is hypothesised that the gene may be misregulated due to the breakdown in symbiosis, or the misregulation of the gene is what causes the breakdown in symbiosis. Using a cut-off of >2 as an arbitrary significant fold change, the analysis showed that among the eight genes, only *jmj4* appeared to be consistently downregulated among the symbiotic mutants, thus suggesting a possible involvement of this gene in the fungal-grass symbiosis (Table 3.3). None of the other genes encoding JmjC proteins show any significant and consistent change in expression across the symbiotic mutants.

The normalised read/kilobase/million mapped reads (RPKM) values shows how highly expressed a gene is in the culture conditions. In the wild-type strain in axenic culture, RPKM values for actin G and GAPDH are 480 and 580, respectively, whereas RPKM values for secondary metabolite genes, such as those of the

*EAS* and *LTM* clusters, are zero in comparison. The RPKM values for *kdmA*, *kdmB* and *jmj3* are about 8, suggesting that these genes are expressed at basal levels and may not be important for culture growth conditions (Table 3.3). A comparison of these values with their expression *in planta* further gives an indication of how important these genes are under either condition. In this case, *jmj3* is differentially expressed by 3-fold in the plant, whereas *jmj5* is differentially expressed by 2-fold in culture (Table 3.3).

**Table 3. 3. Expression of *E. festucae* genes encoding JmjC proteins and other histone modifiers in wild-type symbiotic mutants of the fungus.**

| Gene | Δ*noxA* *(in planta)* | Δ*proA* *(in planta)* | Δ*sakA* *(in planta)* | Δ*hepA* *(in planta)* | WT RPKM (in culture) | Fold WT Plant / WT culture |
|---|---|---|---|---|---|---|
| *kdmA* (*jmj1*) | -1.20 | 1.26 | 1.00 | -1.06 | 7.85 | 1.88 |
| *kdmB* (*jmj2*) | 1.47 | 1.80 | -1.08 | 1.28 | 8.10 | 1.36 |
| *dmm*-1 (*jmj3*) | -1.29 | 1.38 | -1.35 | 1.62 | 7.76 | **2.91** |
| *jmj4* | -1.98 | **-2.37** | **-2.35** | 1.06 | 39.94 | -1.64 |
| *jmj5* | 1.21 | **3.28** | -1.41 | -1.11 | 46.45 | **-2.07** |
| *jmj6* | 1.24 | 1.32 | 1.03 | -1.69 | 23.26 | -1.12 |
| *jmj7* | 1.00 | 1.49 | **-2.06** | -1.37 | 26.59 | -1.24 |
| *jmj8* | -1.64 | 1.05 | -1.05 | 1.07 | 14.29 | 1.73 |

Data were retrieved from Tanaka *et al*. (2006); Eaton *et al*. (2010); Eaton *et al*. (2015) and Chujo *et al*. (in preparation). Otherwise indicated, values are fold difference of the expression values in the mutant over the wild-type strain. Significant (fold change >2) values are underlined and in bold, with upregulation in green and downregulation in red.

### *3.2.7 Phylogenetic analysis of E. festucae JmjC proteins.*

These analyses described above revealed very little about the functions of Jmj4, Jmj5 and Jmj8, which are proteins found exclusively in fungi, relatively small in size, contain only a JmjC domain, and also appear to lack NLSs. A phylogenetic analysis was thus performed with the *E. festucae* proteins and >30 characterised histone demethylases in order to determine which histone demethylases these proteins bear most resemblance to. In addition, putative JmjC proteins in yeast and other filamentous fungi; *A. nidulans*, *A. fumigatus*, *N. crassa* and *F. graminearum* (http://www.broadinstitute.org/scientific-community/data) were also retrieved and included in the analysis to provide additional insights, such as whether the proteins are specific to filamentous fungi. The tree generated using full-length sequences of the proteins did not reveal much insight as sequence variability between the proteins was too high. However, the tree constructed with only the JmjC domain sequences of the proteins showed that the KDM2-8 demethylases formed distinct clades, indicating that the JmjC domains between the KDM groups are sufficiently distinct and can be used with confidence to characterise the proteins (Fig. 3.10).

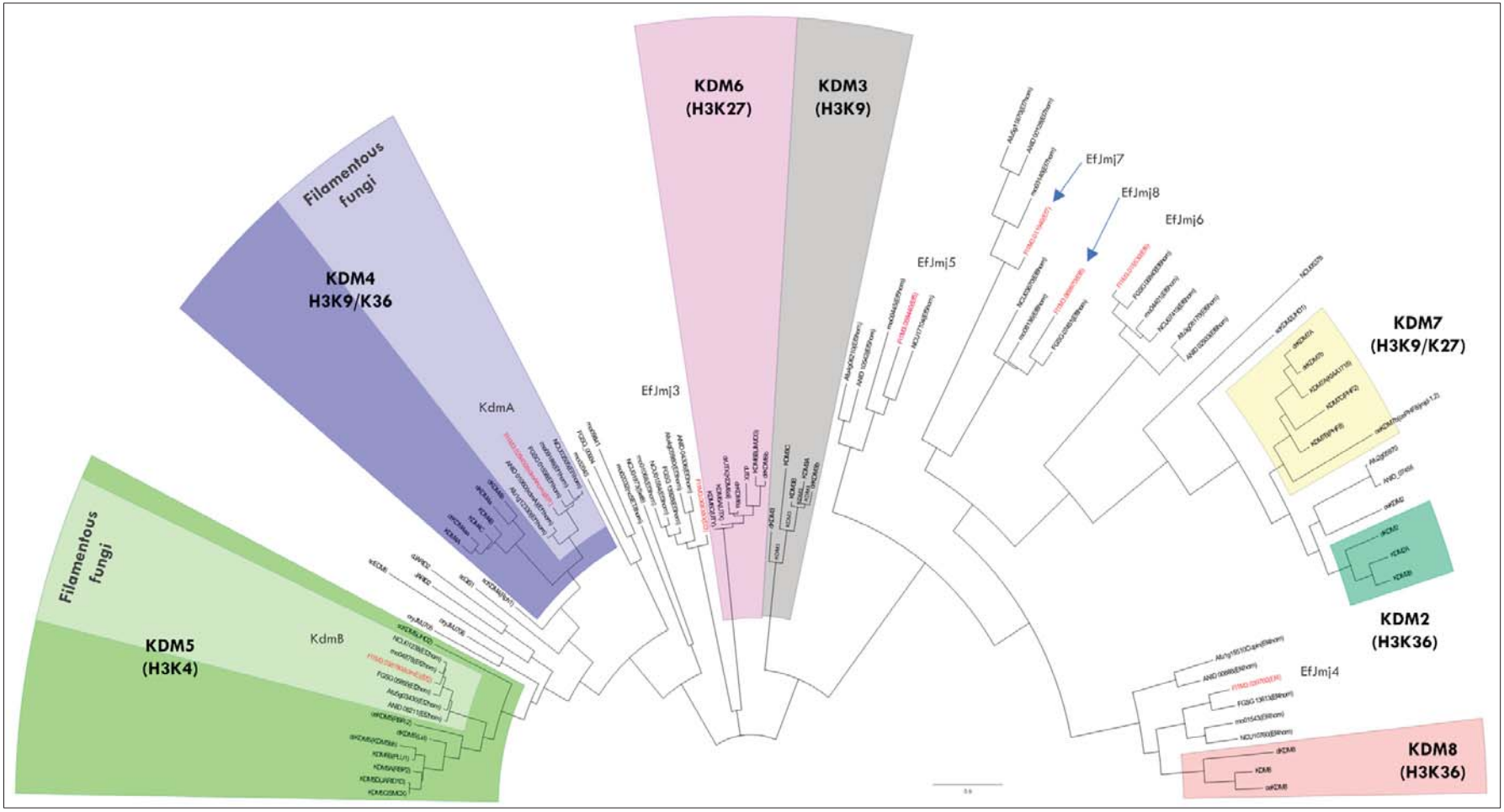


**Figure 3. 10. Phylogenetic tree of *E. festucae* JmjC proteins with characterised histone lysine demethylases.** The *E. festucae* proteins are shown in red font. Amino acid sequences were aligned using ClustalO. The evolutionary history was inferred using the Maximum Likelihood method based on the JTT matrix-based model (Jones *et al*., 1992). The tree is drawn to scale, with branch lengths measured in the number of substitutions per site. The analysis involved 98 amino acid sequences and evolutionary analyses were conducted in MEGA7 (Kumar *et al.*, 2016).

In this tree, the fungal homologues of KDM4 (KdmA) and KDM5 (KdmB) fall within the same clades as the mammalian proteins but formed as distinct sub-clades within them (Fig. 3.10). There appear to be no homologues of the mammalian KDM2, 3, 6 and 7 demethylases in fungi, but the JmjC domain of Dmm-1 (Jmj3) appears most similar to that of the KDM6 group of H3K27 demethylases.

The tree also shows that Jmj5, 6 and 7 are unrelated to any of the characterised histone lysine demethylases. These proteins did not fall into any of the known group or with demethylases of the budding yeast *S. cerevisiae*, suggesting that these proteins are sufficiently distinct. However, homologues Jmj4-Jmj7 are present in filamentous fungi and form separate clades that are distinct from the metazoan and other known demethylases. Interestingly, the fungal homologues of Jmj4 segregated most closely to the KDM8 proteins and appear to be the possible fungal homologues of these demethylases (Fig. 3.10).

### *3.2.8 Insights from H3K27me-deficient filamentous fungi.*

Identification of the H3K9 and H3K27 demethylases in *E. festucae* was the original objective of this study. However, the above analyses revealed that most of the metazoan H3K9/K27 demethylases are strikingly distinct from the fungal proteins. Additionally, metazoan KDM6 (H3K27 demethylase) proteins contain N-terminal tetratricopeptide repeats (TPR) (Fig. 3.11). Such repeats can be found in some *E. festucae* proteins but were not found in JmjC domain-containing proteins. In an attempt to identify the H3K27 demethylase in *E. festucae*, it was hypothesised that fungi which do not sport H3K27 methylation should likewise not possess the corresponding H3K27 demethylase. Unlike *E. festucae* which sports H3K27 methylation (Chujo and Scott, 2014), at least two other Ascomycetes (*A. nidulans*, *A. fumigatus*) are known not to utilise H3K27 methylation (Connolly *et al*., 2013, Gacek-Matthews *et al*., 2015). It may thus be possible to predict candidate *E. festucae* H3K27 demethylases based on the absence of their homologues in these fungi.

The previous phylogenetic tree in Fig. 3.10 shows that two proteins, Jmj5 and Jmj8 are particularly interesting in this aspect. The Aspergillus homologues of Jmj5 segregated as slightly separate clades from the other filamentous fungus homologues of the protein, and no Aspergillus homologues were found in the Jmj8 clade. To confirm this, the amino acid sequences of Jmj5 and Jmj8 were used in a tBLASTn search against the genomes of *A. nidulans* and *A. fumigatus*.

Hits to the full-length protein of Jmj5 was identified in both Aspergilli (Fig. 3.12A). The *A. fumigatus* protein (NCBI reference: XM_747110) and the *A. nidulans* protein (XM_656839) share 49% and 45% amino acid identity with Jmj5, respectively. Both Aspergilli proteins only share such high amino acid identity with Jmj5 and not with other *E. festucae* Jmj proteins, indicating that they are the most likely homologues of Jmj5. Interestingly, no homologue was identified for Jmj8 in both Aspergilli (Fig. 3.12B). A weak hit was identified in *A. fumigatus*, but the protein was the previously identified homologue of Jmj5 (see above) and shares only 27% amino acid identity with Jmj8.

Taken together, these analyses identified that fungi deficient in H3K27 methylation lack the homologue for *E. festucae* Jmj8, although they possess homologues for the other *E. festucae* Jmj proteins. This may suggest that Jmj8 could be the H3K27 demethylase in *E. festucae*, although there could be other evolutionary reasons for the absence of a Jmj8 homologue in these fungi.

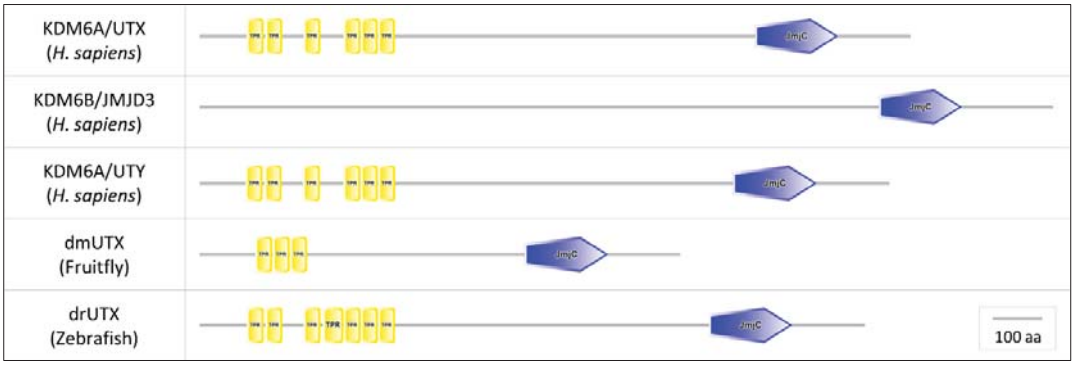


**Figure 3. 11. Domain composition of KDM6 proteins.** JmjC domains are depicted by blue pentagons and tetratricopeptide repeats in yellow. The accession codes for the proteins used are O15550 (KDM6A), O15054 (KDM6B), O14607 (KDM6C), Q76NQ3 (dmUTX) and A1L1S9 (drUTX). Domains were predicted by SMART (Schultz *et al.*, 1998; Letunic *et al.*, 2014).

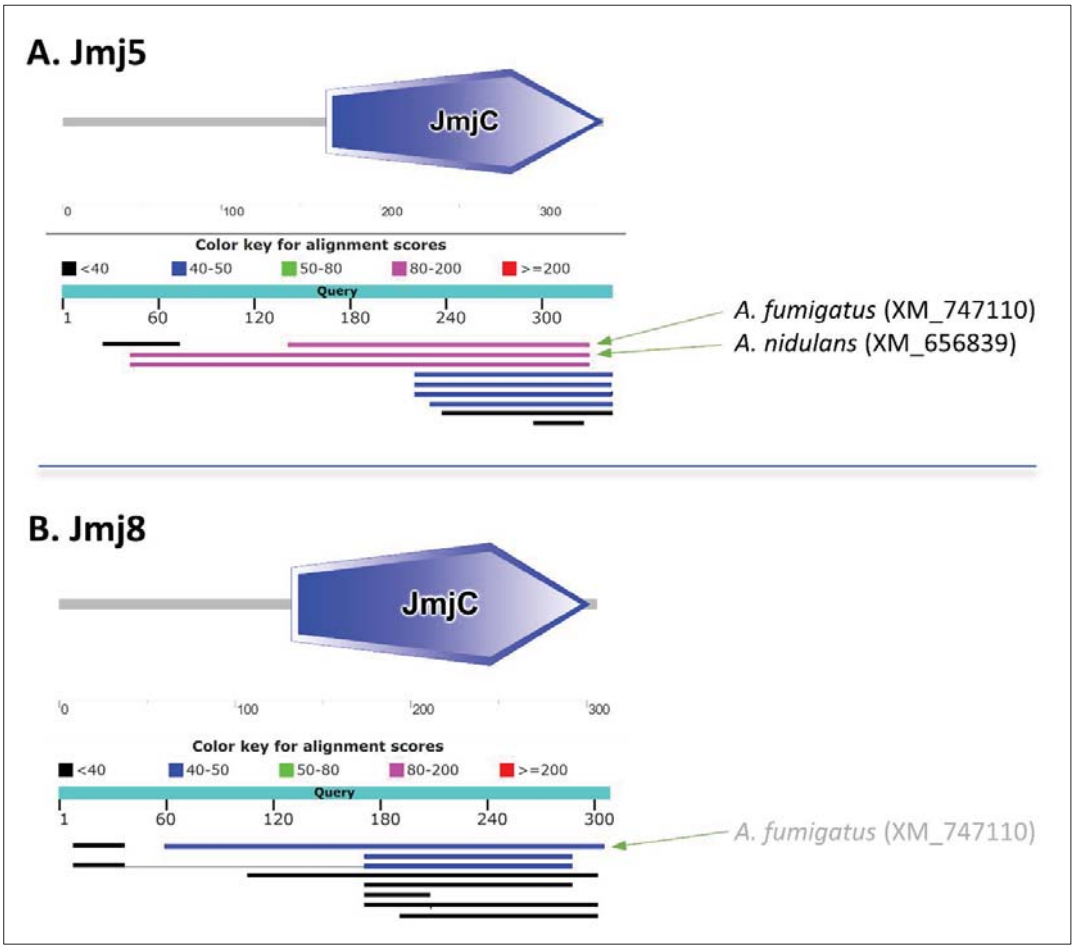


**Figure 3. 12. BLAST analyses of Jmj5 and Jmj8 against the genomes of H3K27me-deficient fungi.** Amino acid sequences of Jmj5 and Jmj8 were used in a tBLASTn analysis against the *A. nidulans*, *A. fumigatus* and *U. maydis* genomes in the NCBI database.

*3.2.9 Generation of jmj1-jmj8 overexpression strains.*

Given the aim of the study is to screen for histone lysine demethylases in *E. festucae*, the candidate histone demethylase genes were overexpressed so as to be able to detect reduced histone methylation in the mutants. To this end, the full-length cDNA sequences of Jmj1-Jmj8 were placed under the control of the constitutive *tefA* promoter (P*tefA*) and the *trpC* terminator (T*trpC*), in a pSF15 ($Hyg^R$) backbone vector and transformed into wild-type *E. festucae* (Fig. 3.13) This strategy has been successfully shown to drive expression of target genes at sufficiently high levels in *E. festucae* (Takemoto *et al.*, 2006, Lukito *et al.*, 2015).

Although some proteins, such as Jmj6 and Jmj7 were less likely to be histone demethylases, this was not known for sure. Therefore, overexpression strains for all eight Jmj proteins were generated. To this end, 8 plasmids, pYL4 to pYL11, were prepared for overexpression of *jmj1-jmj8*, respectively. Plasmid maps for these are provided in the appendices and detailed cloning procedures of the plasmids are given in Materials and Methods (Section 2.7.1). Sequence integrity of all plasmids was confirmed by Sanger sequencing.

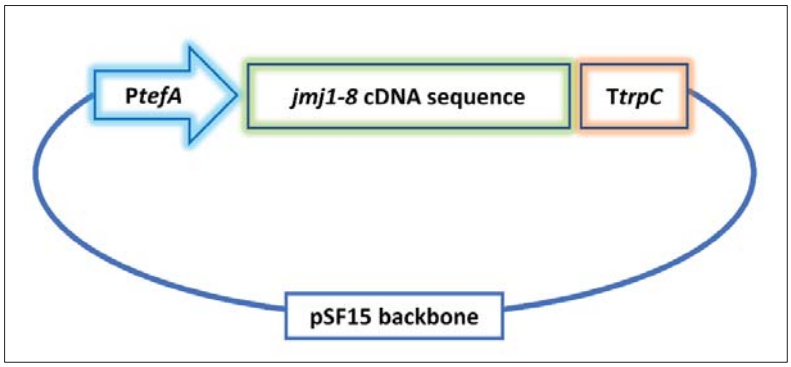


**Figure 3. 13. Schematic of the strategy for overexpression of *jmj1-jmj8*.** Full-length cDNA sequences of *jmj1-jmj8* were placed under the control of the constitutive *tefA* promoter and *trpC* terminator in a pSF15 backbone. Figure is not drawn to scale.

Following transformation, the resulting transformants were first screened by PCR to confirm presence of the full-length genes (Fig. 3.14). The copy number of the integrated constructs in the mutants that contain full-length constructs were subsequently determined by quantitative PCR (qPCR). This was found to range from 2 (reflecting integration of a single integrated construct plus the native gene) to about 80 in some transformants (Fig. 3.14). From these data, two strains; one having high-copy and another having low-copy number, were selected for each mutant for confirmation of gene overexpression by RT-qPCR. The low-copy number strain was selected to minimise possible ectopic gene disruptions caused by random integration of the constructs, while the high-copy number strain was selected to maximise the impact of the gene overexpression. The expression levels in these strains were found to correlate with the copy number of the constructs (Fig. 3.14). For clarity, only data for the final two mutants that were used for further analyses in this study are presented, although more than 20 transformants for each of the constructs were screened at the initial stage.

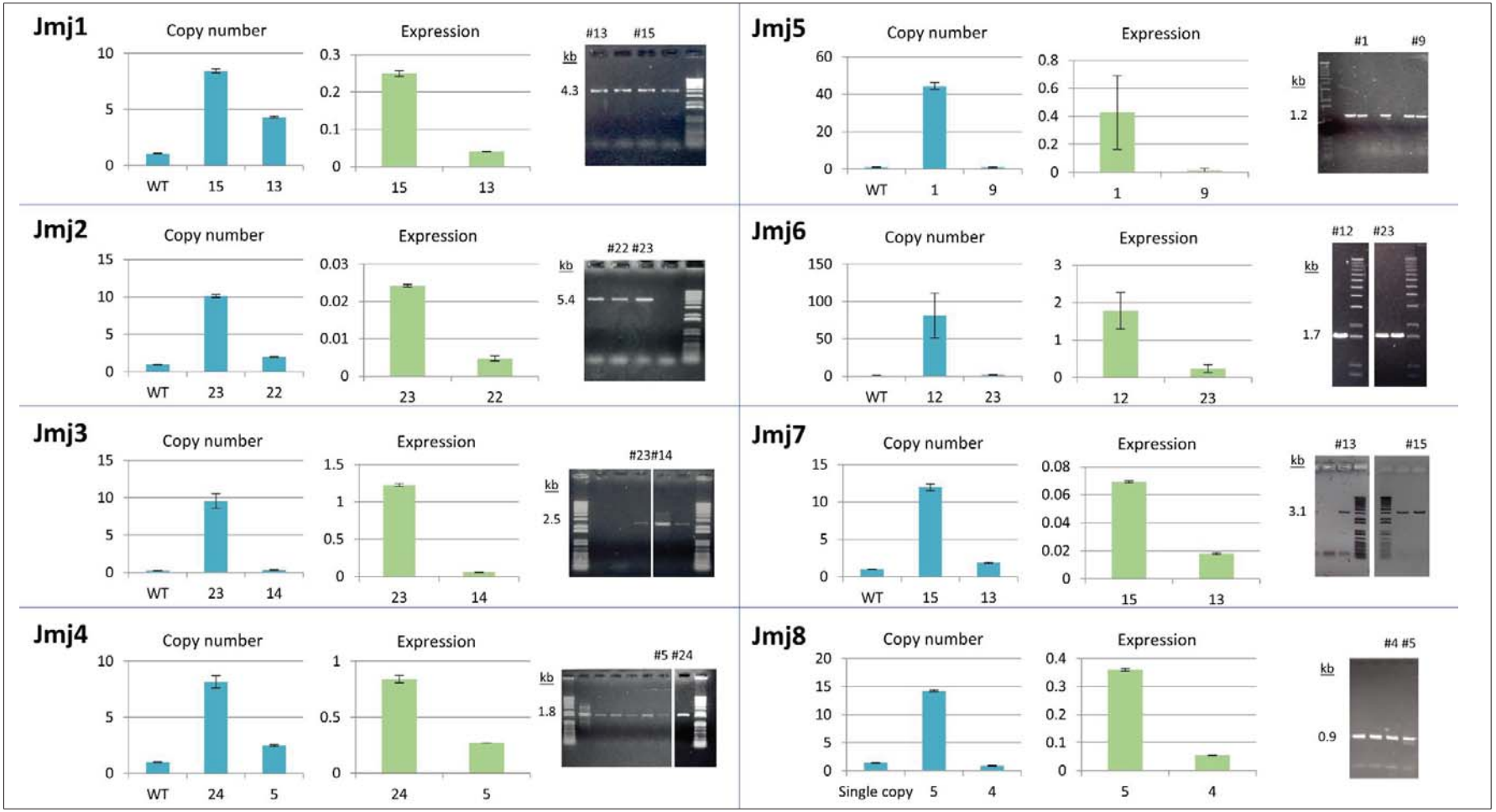


**Figure 3. 14. Copy number and expression of *jmj1-jmj8* overexpression strains.** Y-axes in blue charts represent copy number fold single-copy *pacC* gene, Y-axes in green chart represent transcript level fold 40S ribosomal protein 22 mRNA. Both values expressed relative to the wild-type levels as determined by qPCR. Error bars represent S.D. from two technical replicates. Gel images show presence of full-length constructs as amplified by PCR. Primers used for the analyses are given in Table 2.4.

*3.2.10 Culture phenotypes of the overexpression mutants.*

The effect of overexpression of the genes on development was next analysed by analysing the radial growth and colony morphology of the strains on PD agar. No difference in colony morphology from wild-type was observed for the strains except for *jmj2*-OE#23 that showed a slight reduction in radial growth (Fig. 3.15). However, the second independent strain, *jmj2*-OE#22, did not show any reduction in radial growth. Given that *jmj2*-OE#23 expresses the *jmj2* gene at a higher level than strain #22, it is possible that the culture phenotype of strain #23 is due to the higher expression of the gene, however this was not confirmed with additional mutants. Taken together, these analyses suggest that overexpression of the *jmj1-jmj8* does not influence *E. festucae* development.

*3.2.11 Western blot analysis identified Jmj2 (KdmB) as an H3K4me3-specific demethylase.*

To determine if overexpression of the JmjC proteins leads to demethylation of histone H3 residues, the global (total) histone methylation levels in the strains were analysed by western blotting. The blot was performed on acid-extracted histones from strains cultured in PD medium. Given that the first four proteins, Jmj1-Jmj4, were the most likely histone lysine demethylases, these were first analysed for all three forms (mono-, di- and tri-) of histone H3K4, K9, K27 and K36 methylation. Jmj3 (Dmm-1) was included in the analysis as although the *N. crassa* homologue did not show demethylase activity, the protein influences spreading of H3K9me3 in the fungus (Honda *et al*., 2010), thus it would be interesting to test if the *E. festucae* homologue has detectable demethylase activity. As additional controls for the analysis, deletion mutants of the H3K9 and H3K27 methyltransferases *clrD* and *ezhB* respectively (Chujo & Scott, 2014) were included and these showed the expected reduction in H3K9 and H3K27 di- and trimethylation levels (Fig. 3.16).

The *jmj1* (*kdmA*) overexpression strains did not show reduced methylation of any of the H3 residues analysed (Fig. 3.16). This is similar to *A. nidulans*, where the demethylase activity of KdmA was only demonstrable at secondary metabolite gene loci and not at the global level (Gacek-Matthews *et al*., 2015). Interestingly, the blot showed that H3K4me3 levels were reduced in the *jmj2* (*kdmB*) overexpression strains, in line with the prediction of Jmj2 as the KDM5 homologue in the fungus. No reduction in H3K9 methylation was observed in the *jmj3* (*dmm*-1) overexpression strains, confirming that the Dmm-1 homologue in *E. festucae*, as in *N. crassa*, likely does not possess histone demethylase activity. The *jmj3* overexpression strains did not show any reduction in the other histone marks, but interestingly one of the *jmj4* overexpression strains, the high-copy strain (#24), appeared to show a significant reduction in H3K27me2 (Fig. 3.16). This reduction was not observed in the single-copy strain (#5). Although It is possible that only the high-copy strain expresses Jmj4 at sufficiently high levels to achieve the reduction in H3K27me2 levels, this needs to be confirmed further. Given that samples for the *jmj4* strains were loaded at slightly lower amounts (compare H3 lanes with wild-type), the apparent reduction in other marks such as H3K9me1 and H3K9me2 also needs to be confirmed further (Fig. 3.16).

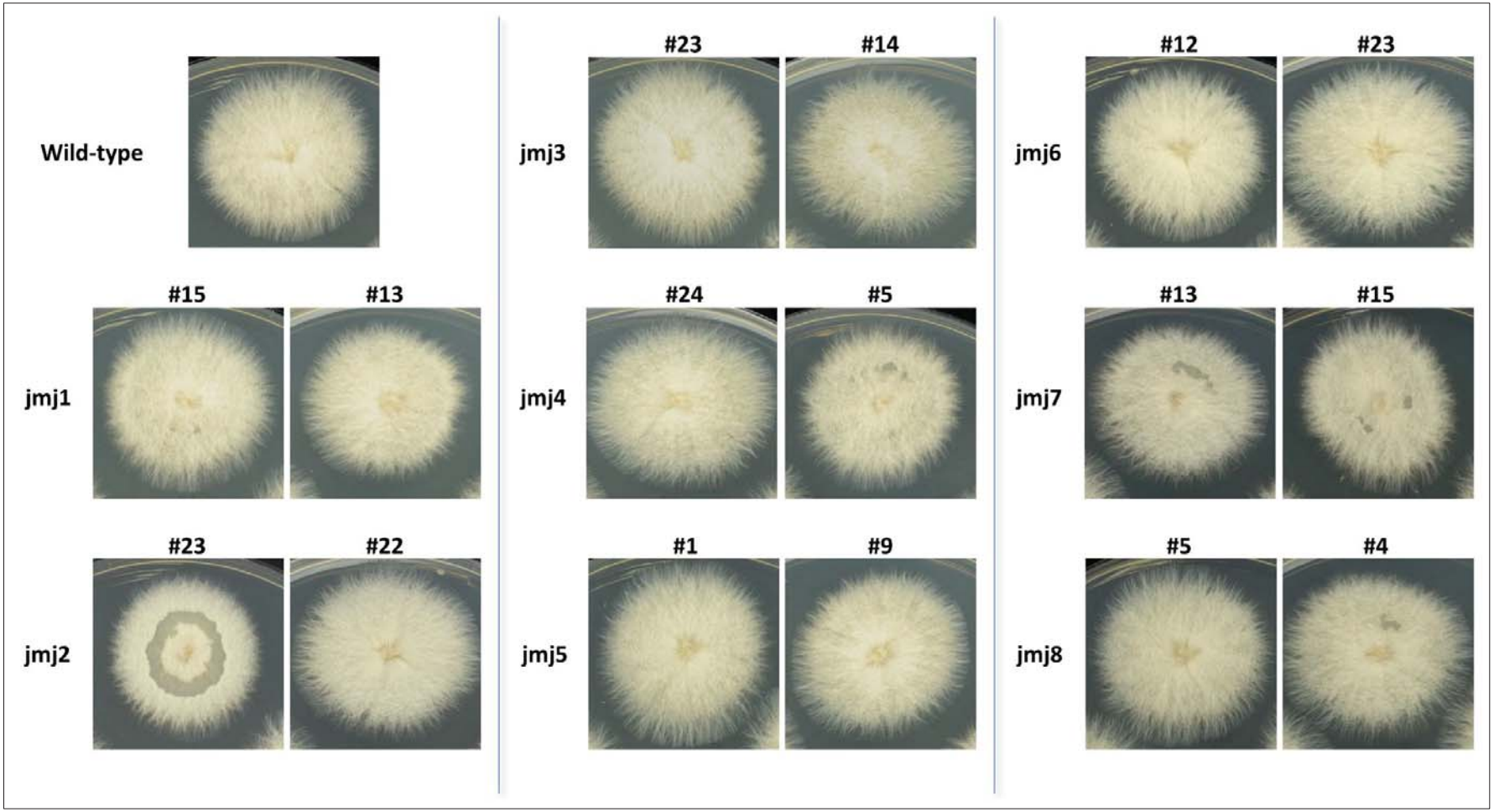


**Figure 3. 15. Culture morphology of *jmj1-jmj8* overexpression mutants on PDA.** Two independent strains of wild-type and *jmj1-jmj8* overexpression mutants were inoculated on 2.4% PDA and photographed after incubation at 22°C for 11 days.

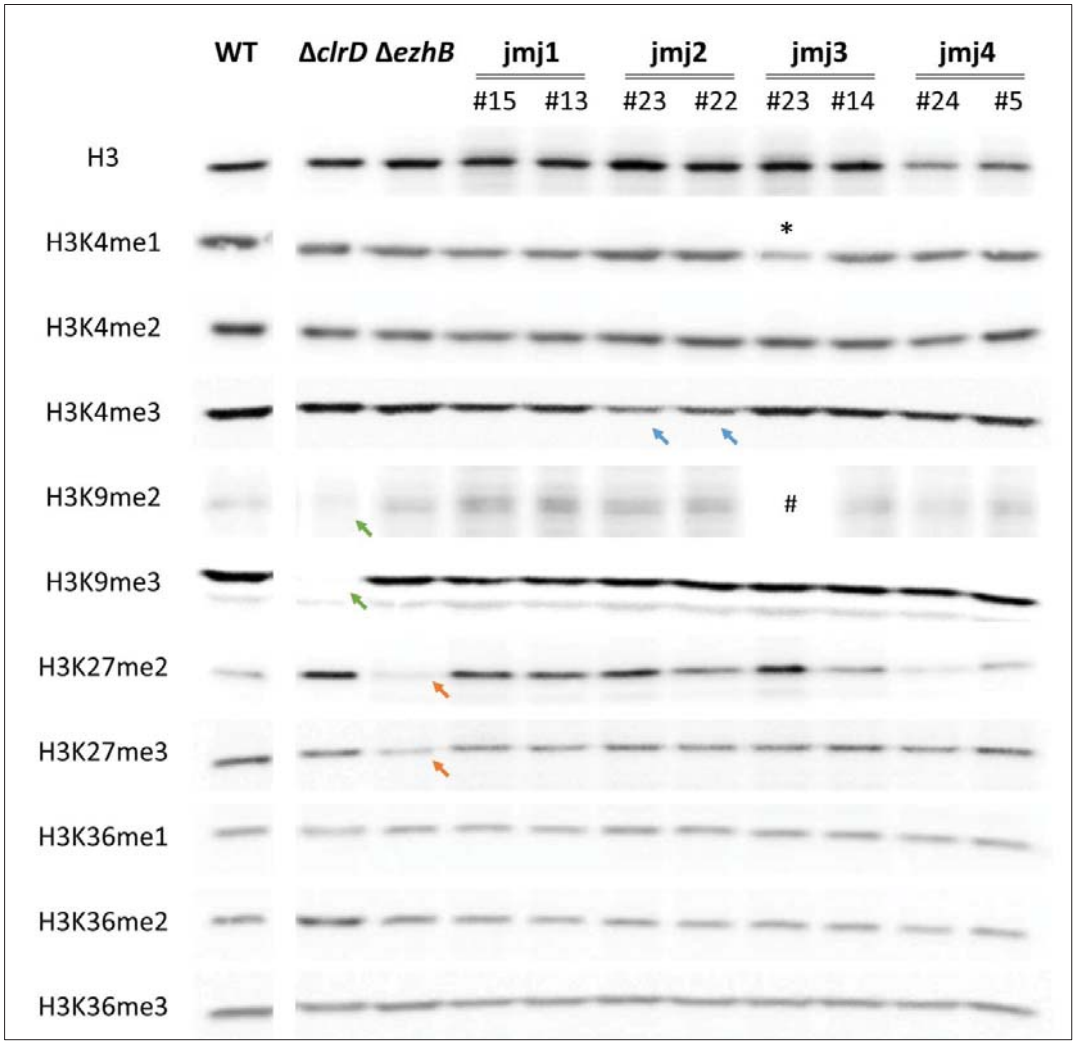


**Figure 3. 16. Western blot analysis of *jmj1-jmj4* overexpressing mutants.** Each row is from the same gel with lanes for samples not relevant for this analysis removed. Reduced H3K4me3 levels in *jmj2* overexpression strains are indicated by blue arrows. Reduced H3K9me2/me3 and H3K27me2/me3 in control strains Δ*clrD* and Δ*ezhB* (see text) are indicated by green and red arrows, respectively. Histones were acid-extracted from nuclear fractions of *E. festucae* cultured in PD media, separated by SDS-PAGE and probed with the indicated primary antibodies (Table 2.2) and visualised with the ECL method. All samples were loaded at equal volumes except: (*) sample was loaded at half volume and (#) no samples were loaded.

Having identified the H3K4me3-demethylase (Jmj2) in *E. festucae*, efforts were now directed towards its characterisation, and *jmj5* and *jmj8* overexpression were only analysed for reduction in H3K9me3. Given that Jmj6 and Jmj7 are unlikely to be histone demethylases, the overexpression strains for these genes were also excluded from analysis. Western blot analysis of the *jmj5* and *jmj8* strains showed no reduction in H3K9me3 levels in these strains, although loss of H3K9me3 was observed in the control Δ*clrD* strain (Fig. 3.17).

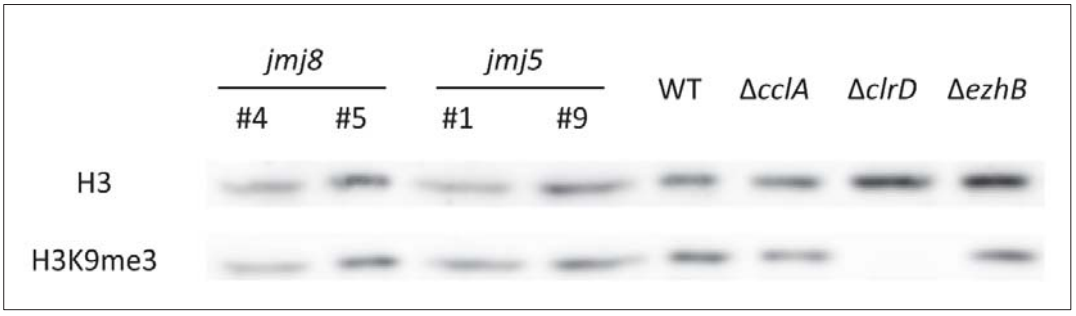


**Figure 3. 17. Western blot analysis of *jmj5* and *jmj8* overexpressing mutants.** Histones were acid-extracted from nuclear fractions of *E. festucae* cultured in PD media, separated by SDS-PAGE and probed with the indicated primary antibodies (Table 2.2) and visualised with the ECL method. All samples were loaded at equal volumes.

*3.2.12 Overexpression of E. festucae KdmA and KdmB in mammalian cells.*

As there was no report of a H3K4me3 demethylase in filamentous fungus when this study was initiated, additional experimental evidence was sought to substantiate the demethylase activity of KdmB. One of the approaches used in mammalian systems to demonstrate activity of KDMs is to express the enzyme and measure the level of histone methylation by immunofluorescence (Cloos *et al*., 2006; Klose *et al*., 2006b; Tsukada *et al*., 2006; Whetstine *et al*., 2006; Yamane *et al*., 2006). Given the high degree of conservation (90% amino acid identity) between *E. festucae* and *H. sapiens* histone H3 (Fig. 3.18), and the degree of similarity between *E. festucae* KdmB with mammalian KDM5 (Fig. 3.6), it is hypothesised that *E. festucae* KdmB is able to recognise and demethylate *H. sapiens* histone H3K4. Thus, the *E. festucae* protein was expressed in the human carcinoma HeLa cell line to test its activity towards H3K4.

To this end, plasmid pYL14 (Appendix 15) containing the *E. festucae* FLAG-tagged KdmB (Jmj2) cDNA sequence under the control of the constitutive CMV (cytomegalovirus) promoter was prepared and transfected into HeLa cells (Fig. 3.19). The presence of FLAG was used as a marker for successful transfection and expression. The histone methylation level in transfected HeLa cells was then compared to that of untransfected cells. The analysis revealed no difference between the methylation levels of cells expressing KdmB and untransfected cells (Fig. 3.20). To confirm this, three experimental timepoints (24h, 48h and 72h post-transfection) were used and similar results were obtained.

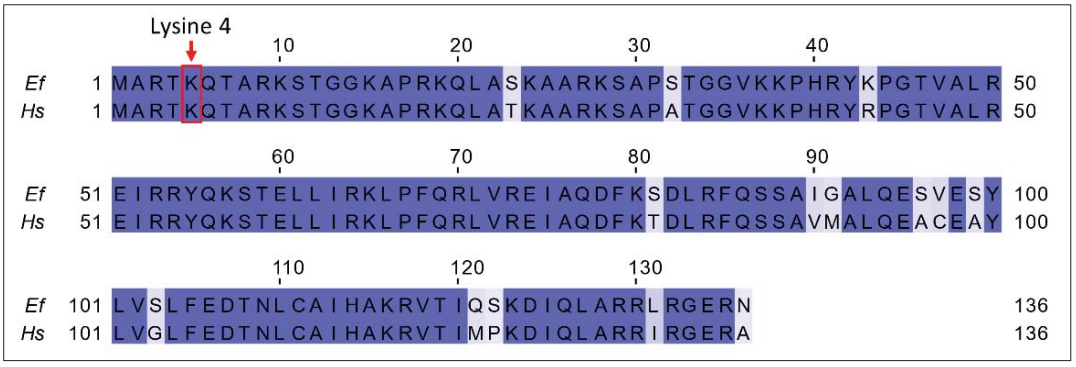


**Figure 3. 18. Amino acid alignment of *E. festucae* and human histone H3**. Accession codes of the sequences shown are EfM3.022140 (*E. festucae*) and P68431 (*H. sapiens*). The alignment was generated with Clustal Omega.

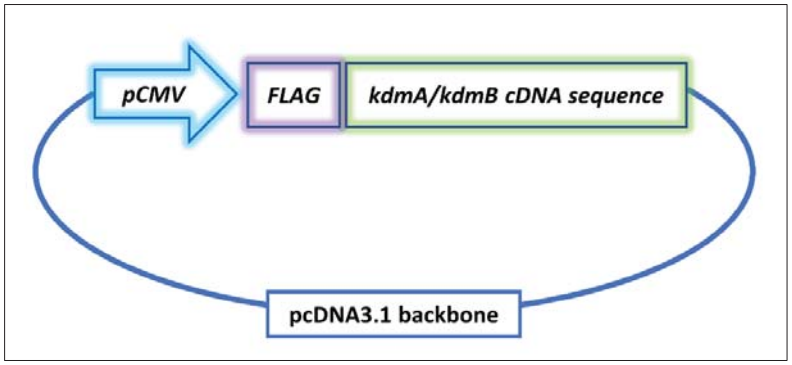


**Figure 3. 19. Schematic of the strategy used for overexpression of *kdmA* and *kdmB* in mammalian cells.** Full-length cDNA sequences of *kdmA* or *kdmB* were placed under the control of the constitutive CMV promoter in a pcDNA3.1 backbone. Figure is not drawn to scale.

Although the results of these experiments suggest an inability of *E. festucae* KdmB to demethylate mammalian histone H3, further experiments are required to optimise and confirm this finding. One possible issue to address is full-length expression of the construct. Given the protein has FLAG at its N-terminus, its full-length expression neds to be confirmed. The N-terminal tagging option was selected as tag placement can affect protein folding, and seminal studies performing similar immunofluorescence experiments had opted for the N-terminal placement of tags (Kloos *et al*., 2006; Tsukada *et al*., 2006). To confirm expression of full-length KdmB a western blot analysis of the cells would be required, but this was not pursued as the KdmB homologue in *A. nidulans* had then been shown by mass spectrometry and *in vitro* CT-nucleosome assay to as an H3K4me3 demethylase (Gacek-Matthews *et al*., 2016).

Given that the KDM4 homologues of Jmj1 (KdmA) are dual H3K9/K36 demethylases, a similar experiment in HeLa cells was performed to test for possible H3K9/K36 demethylase activity of KdmA. To this end, plasmid pYL13 was prepared (Section 2.7.2) and HeLa cells transfected and processed for immunocytofluorescence. The results did not demonstrate any H3K9me3, H3K27me3, nor H3K36me1/me2 demethylase activity for *E. festucae* KdmA on mammalian histones (Fig. 3.21). As KdmA was similarly N-terminally FLAG tagged, western blot analysis is also required to confirm the full-length expression of the protein, but this was not performed as the focus of the study was directed towards KdmB and H3K4 methylation in *E. festucae*.

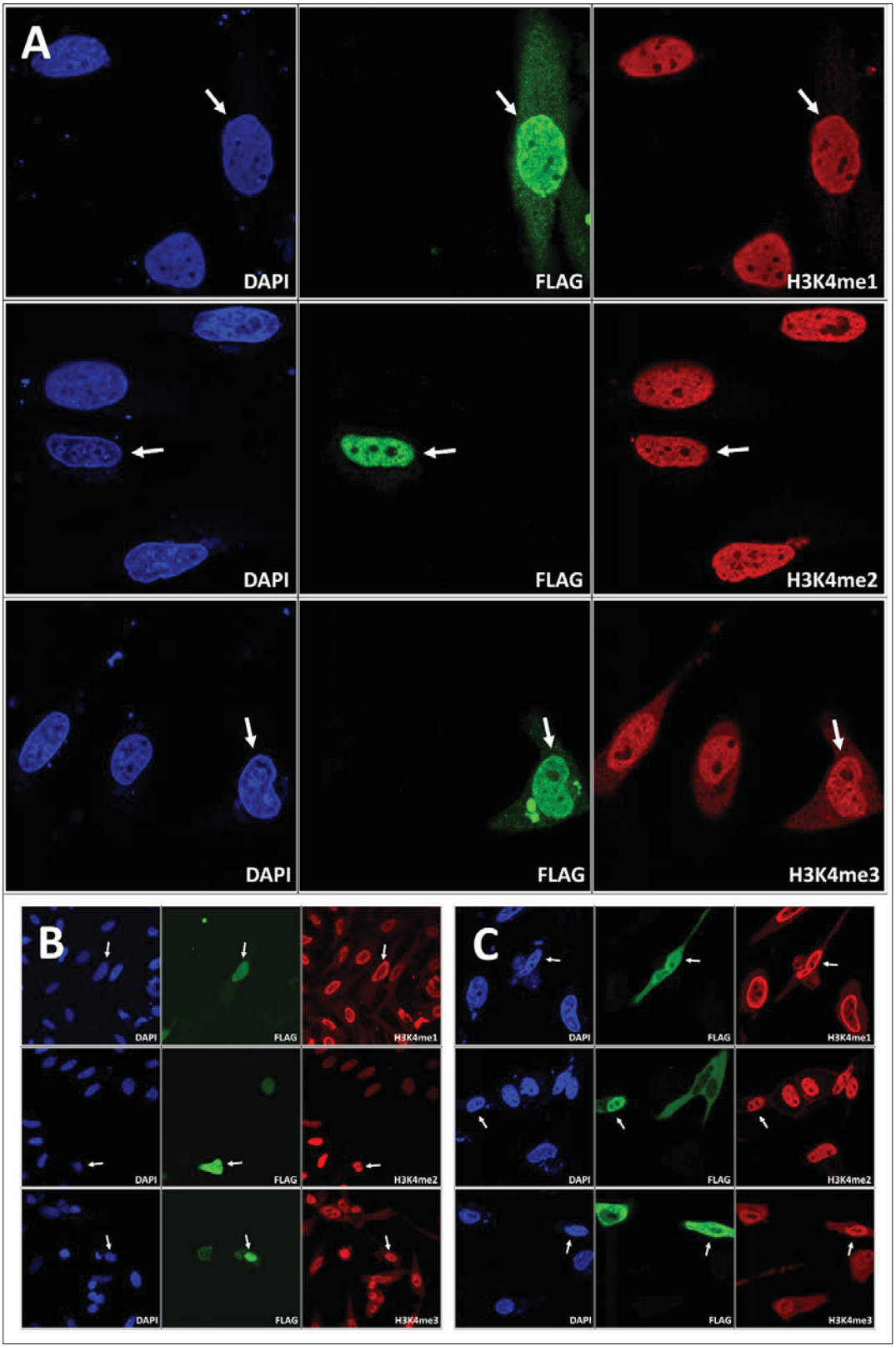


**Figure 3. 20. Overexpression of *E. festucae* KdmB in HeLa cells did not result in reduction in H3K4 methylation levels.** Full-length FLAG-tagged *kdmB* was expressed in HeLa cells. Transfected cells that express FLAG are indicated by arrows. Cells were fixed at (A) 24 h, (B) 48 h and (C) 72 h post-transfection and stained with the indicated antibodies (Table 2.2). DAPI was used to stain nuclei.

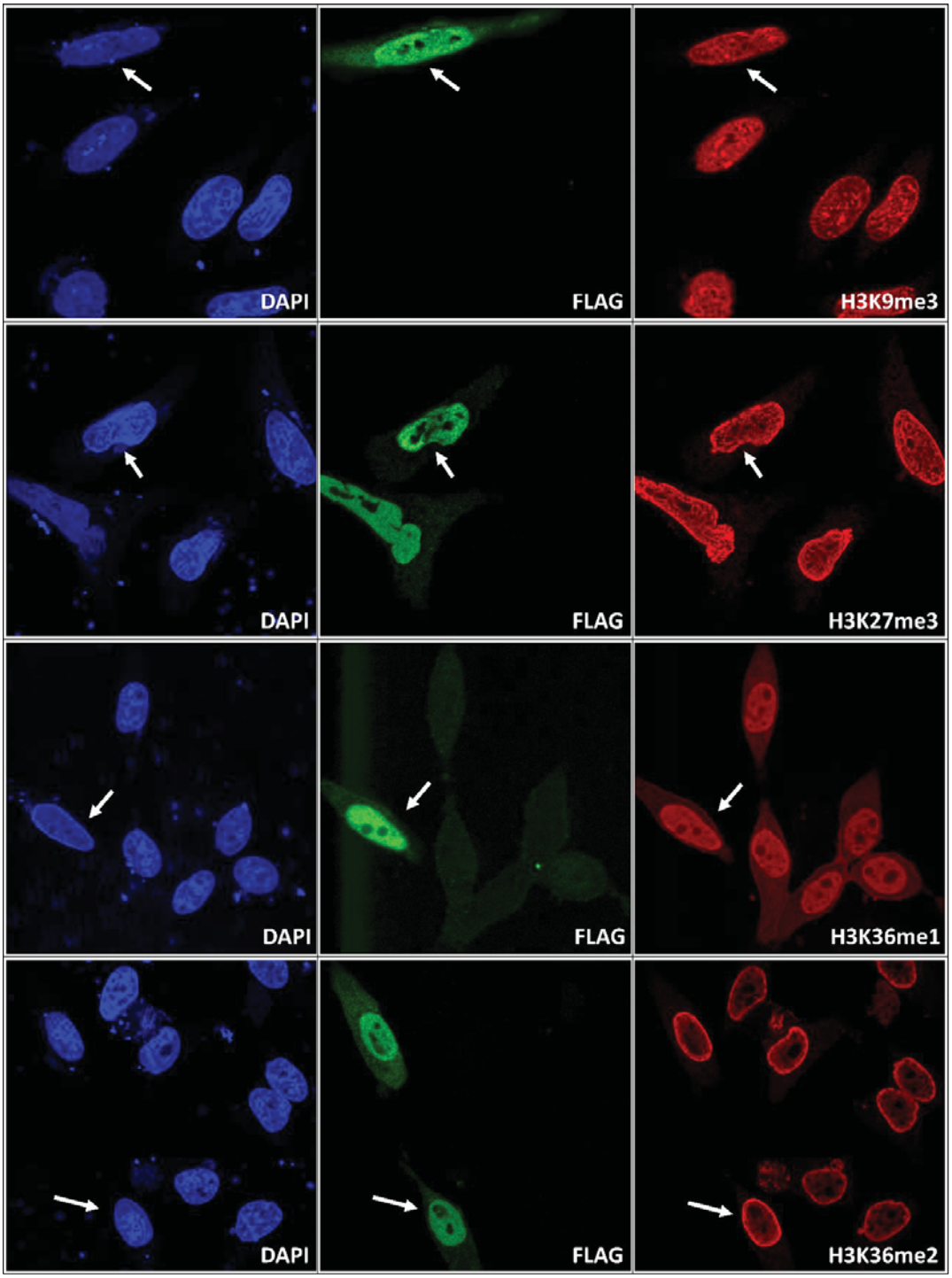


**Figure 3. 21. Overexpression *of E. festucae KdmA* in HeLa cells does not result in reduction of H3K36 methylation levels.** Full-length FLAG-tagged *kdmA* was overexpressed in HeLa cells. Transfected cells that express FLAG are indicated by arrows. Cells were fixed at 24 h post-transfection for H3K9me3 and H3K27me3 staining, and 72 h post-transfection for H3K36me2/me3 staining. The antibodies used for the experiment are listed in Table 2.2. DAPI was used to stain nuclei.

*3.2.13 Overexpression of jmj1-jmj8 does not affect symbiosis of E. festucae with perennial ryegrass.*

The strains were subsequently inoculated into *L. perenne* and the plant phenotypes of infected plants analysed to determine if overexpression of these genes impacted the symbiosis. In addition, given that deletion of the H3K9 or H3K27 methyltransferase in *E. festucae* has been shown to result in a change in the symbiotic interaction phenotype (Chujo & Scott, 2014), with the H3K9 mutant losing its ability to infect and the H3K27 mutant giving rise to hypertillered host plants, it may be possible to identify the H3K9/K27 demethylase in *E. festucae* from the host phenotype of the *jmj* overexpression strains. However, the analysis showed that none of the *jmj1-jmj8* overexpression strains had a change in the interaction phenotype (Fig. 3.22). Measurements of the tiller number and length of the mutant-infected plants additionally revealed no difference from the wild-type infected plants (Fig. 3.23). Although a few strains showed statistically significant changes, these were seen in only one strain (the lower expressing strain) and not consistently observed in the second, higher-expressing strains. Thus, these mild differences were thought to arise from experimental variance rather than a true phenotype of the mutation.

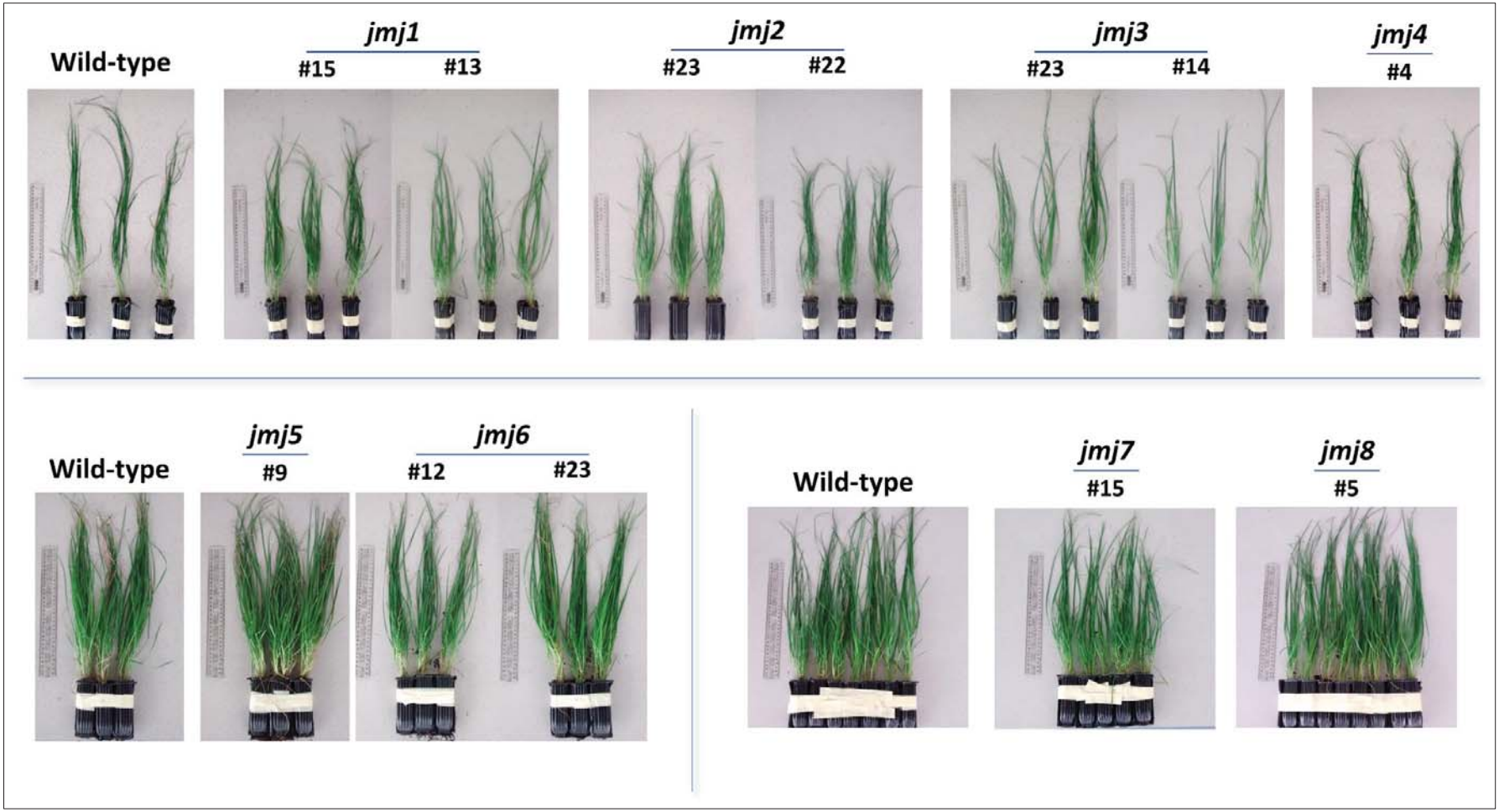


**Figure 3. 22. Whole plant interaction phenotype of *L. perenne* infected with wild-type and *jmj1-jmj8* overexpression mutants of *E. festucae*.** *L. perenne* seedlings were inoculated with the indicated strains and grown under controlled environment conditions (Section 2.11.2). Infection status was confirmed by immunoblotting (Section 2.11.3) and representative plants were photographed at 14 weeks post inoculation.

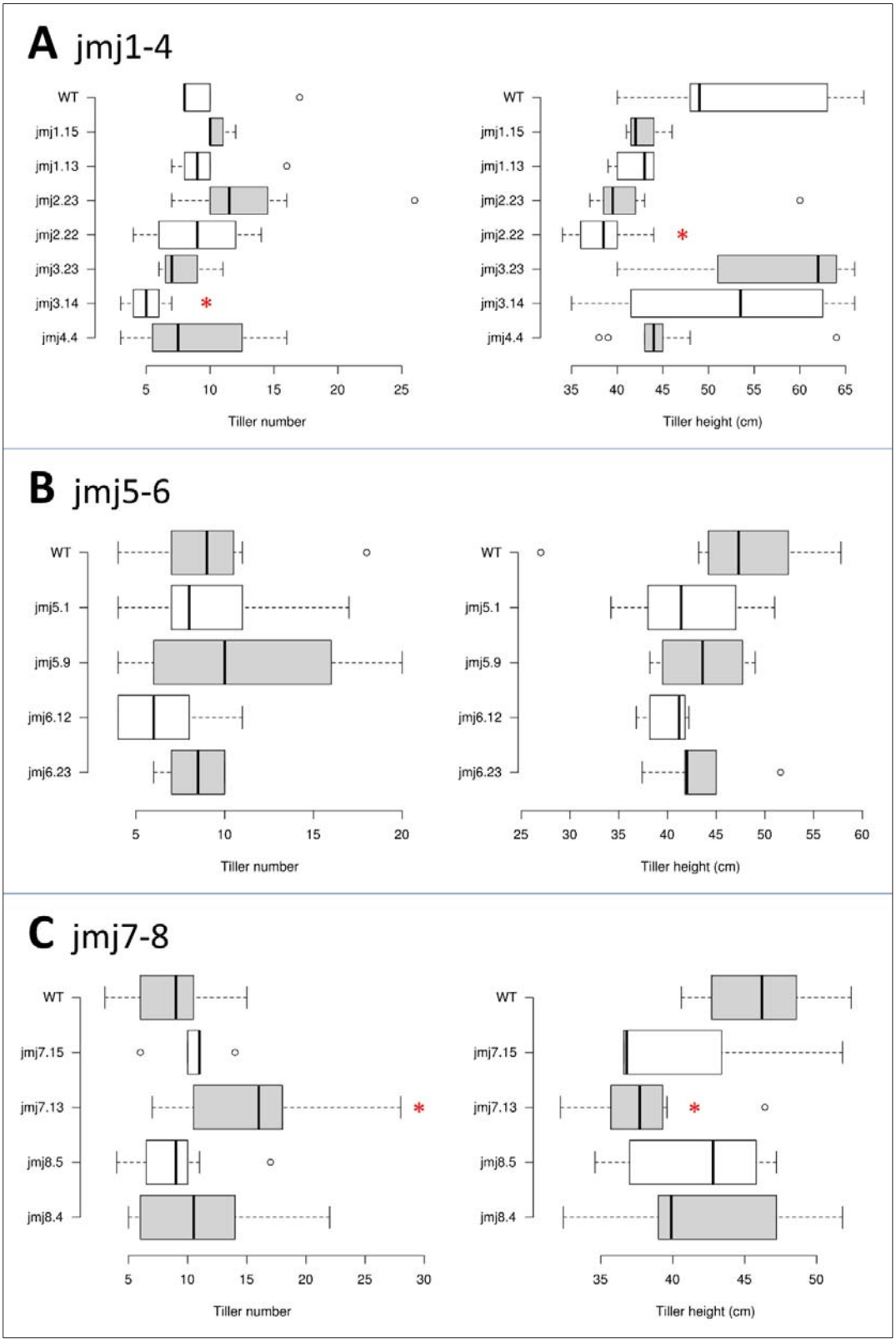


**Figure 3. 23. Tiller analysis of plants infected with the *jmj1-jmj8* overexpression strains.** Boxplot of the tiller number and tiller length of plants infected with the indicated strains. (A) *jmj1* to *jmj4* infected plants at 14 wpi. (B) *jmj5* and *jmj6* plants at 18 wpi. (C) *jmj7* and *jmj8* plants at 13 wpi. **P* = <0.05 (two-tailed t-test).

### 3.3 Discussion

In this study, using the JmjC domain as a signature of candidate demethylase, eight JmjC proteins (Jmj1 to Jmj8) were identified in *E. festucae*. These putative proteins vary considerably in length and domain composition. Jmj8 is about 300 amino acid in length and contains only an identifiable JmjC domain, while Jmj2 is about 1800 amino acid in length and contains several different protein domains in addition to the JmjC domain. The conservation of critical residues of the JmjC domain in all eight proteins suggest that these proteins are catalytically active.

BLAST analyses subsequently ruled out Jmj6 and Jmj7 as candidate histone lysine demethylases, as these proteins are likely to be an arginine demethylase and a leucine carboxylmethyltransferase, respectively. By contrast, the analyses identified significant homology for *E. festucae* Jmj1 and Jmj2 with metazoan KDM4 (H3K9/K36) and KDM5 (H3K4) demethylases, respectively. Nuclear localisation was predicted only for Jmj1, Jmj2, and Jmj3 and to a lesser extent Jmj8. None of the remaining JmjC proteins was predicted to be nuclear. Thus, Jmj1 and Jmj2 represent the two most likely candidates for *bona fide* demethylases in *E. festucae*. The third and final candidate for a *bona fide* histone demethylase, Jmj4, has homology to metazoan KDM8 proteins, which are H3K36me2 demethylases. On the other hand, Jmj3 is a homologue of *N. crassa* Dmm-1, which does not have histone demethylase activity (Honda *et al*., 2010), and Jmj8 has weak homology to JMJD7 proteins, which are also not histone demethylases. The final protein, Jmj5, could be an interesting candidate for a novel class of histone demethylase. Jmj5 is a small, 340 amino acid protein that does not appear to contain any other domain except for a JmjC domain. Phylogenetic analysis showed that it is specific to the Fungi kingdom and its homologues in other fungi are entirely uncharacterised.

Interestingly, the phylogenetic analysis also suggests that some Aspergillus species lack homologues of Jmj5 and Jmj8. BLAST analyses subsequently confirmed that filamentous fungi utilising H3K27 methylation possess the genes for Jmj8, but Aspergilli deficient in H3K27 methylation do not contain homologues of Jmj8, suggesting that it could be the H3K27-specific demethylase. However, *S. cerevisiae* Rph1 was shown to possess a H3K9 demethylase activity, although H3K9 methylation has not been observed in the yeast (Klose *et al*., 2007). Therefore, although this analysis suggests that Jmj8 could be the H3K27 demethylase in *E. festucae*, it is important to note that absence of a demethylase in a fungus not utilising the corresponding methylation is not necessarily the case.

The analyses in this chapter did not identify the H3K9 and H3K27 demethylases in *E. festucae*, except for Jmj1, which is the homologue of metazoan KDM4 that has dual H3K9/K36 demethylase activity. *E. festucae* and other filamentous fungi do not possess homologues of the metazoan H3K9- and H3K27-specific demethylases; the KDM3 and KDM6 family of proteins, respectively. Interestingly, Lu *et al.* (2011) showed that the KDM4 homologue in *Arabidopsis*, JMJ12, is specific for H3K27me2/me3, and Li *et al.* (2013) showed that the KDM4 homolog in rice, JMJ705, is also specific for H3K27me2/me3. Thus, both studies suggest that substrate specificity of the JmjC demethylases can vary dramatically between kingdoms and that the KDM homologues in fungi may not necessarily have the same substrate specificity as their metazoan or plant counterparts. Additionally, JmjC demethylases are additionally capable of having more than one target residue specificity, as evidenced by the dual target specificities of the mammalian KDM4 family (H3K9/K36), as well as the KDM7 (H3K9/K27) proteins. Therefore, it is possible

that *E. festucae* KdmA and KdmB possess histone specificities that are different from the metazoan counterparts.

The genes for all eight Jmj proteins were overexpressed in wild-type *E. festucae* and no culture or plant phenotype was observed for the strains. The first four (*jmj1-jmj4*) overexpression strains were comprehensively analysed for reduction in histone methylation marks by western blotting. These experiments identified Jmj2 (KdmB) as the H3K4me3-specific demethylase in *E. festucae*, which is consistent with identification of KdmB in *A. nidulans* as a H3K4me3 demethylase by mass spectrometry (Gacek-Matthews *et al*., 2016). No measurable change in total H3K36 methylation was observed by *jmj1* (*kdmA*) overexpression, which is again consistent with the findings in *A. nidulans*, in which the H3K36 demethylase activity of KdmA was only demonstrable at the locus level and not at the global level (Gacek-Matthews *et al*., 2015). KdmA and KdmB were additionally overexpressed in mammalian cell in this study but immunofluorescence analyses did not demonstrate any demethylase activity for the proteins, suggesting that Jmj1 and Jmj2 are not active on mammalian histone. However, in order to be sure of this conclusion the expression of full-length Jmj1 and Jmj2 must be determined in the cells by western blotting.

Taken together, the analyses in this chapter identified *E. festucae* KdmA as a homologue of KDM4 and *E. festucae* KdmB as a homologue of KDM5 with demonstrable H3K4me3-specific demethylase activity *in vivo*. *E. festucae* Jmj4 is likely to be a homologue of mammalian KDM8, a H3K36me2 specific demethylase and *E. festucae* Jmj5 and Jmj8 are potentially interesting candidates for novel classes of histone demethylase. Similar to the findings in *N. crassa* (Honda *et al*., 2010), no demethylase activity could be demonstrated for the Dmm-1 homologue in *E. festucae*, Jmj3.

# Chapter 4: H3K4 trimethylation modulated by CclA and KdmB is associated with repression of subtelomeric secondary metabolite genes.

## 4.1 Introduction

In the previous chapter, KdmB was identified as the H3K4me3 demethylase in *E. festucae*, belonging to the KDM5 family of H3K4 demethylases. Also called the JARID1 family (Jumonji, AT-rich interactive domain), KDM5 family proteins typically possess an N-terminal JmjN domain, an ARID/BRIGHT (DNA binding) and several PHD (histone binding) domains in addition to a JmjC domain (Fig. 3.5). The ARID/BRIGHT domain is required for the demethylase activity of mammalian RBP2 (KDM5A) (Tu *et al.*, 2008), while the single N-terminal PHD finger, as well as the JmjN domain of *S. cerevisiae* Jhd2 are required for the demethylase activity of the protein (Huang *et al.*, 2010). Jhd2 is distinct from *E. festucae* KdmB and other KDM5 proteins as it is much shorter and lacks the multiple C-terminal PHD fingers found in other KDM5 proteins (Fig. 3.5). Interestingly, there appears to be a conserved requirement of the N-terminal PHD finger for the enzymatic activity of KDM5 proteins. Similar to Jhd2, the N-terminal PHD finger of, but not the two C-terminal PHD fingers, is required for the demethylase activity of *Drosophila* Lid (Li *et al*., 2010).

*S. cerevisiae* Jhd2 is capable of demethylating all three forms of methylated H3K4 (Ingvarsdottir *et al.*, 2007, Huang *et al.*, 2010) and opposes Set1 function with respect to telomeric silencing. Whereas deletion of *set1* disrupted telomeric silencing, deletion of *jhd2* enhanced telomeric silencing. Further, overexpression of *jhd2* recapitulated the defects in telomeric silencing seen in *set1* mutants (Liang *et al.*, 2007). Jhd2 also demethylates H3K4 at the rDNA locus, and loss of *jhd2* significantly enhanced rDNA silencing, thus illustrating the role of the demethylase at silent loci (Ryu *et al*., 2014).

In yeast, the Set1/COMPASS complex catalyses the mono-, di- and trimethylation of H3K4 (Roguev *et al*., 2001; Krogan *et al*., 2002). Set1 as the catalytic subunit contains an N-terminal SET methyltransferase domain and is required for all forms of H3K4 methylation. However, the other seven members of the complex are required for specific forms of H3K4 methylation. Swd1 (Cps50) and Swd3 (Cps30) are involved in the assembly of the complex and thus are required for all forms of H3K4 methylation, while Sdc1 (Cps25), Spp1 (Cps40) and Bre2 (Cps60/CclA) are required specifically for trimethylation of H3K4 (Schneider *et al.*, 2005, Shilatifard, 2012). *Bre2* was initially described in a genetic screen for yeast mutants that were sensitive to brefeldin A (BFA), an inhibitor of Golgi and endoplasmic reticulum transport (Murén *et al.*, 2001). Interestingly, a subsequent study found that mutation of *set1*, as well as other members of the COMPASS complex resulted in similar sensitivity to BFA (South *et al.*, 2013). In *A. nidulans*, deletion of the *bre2* homologue, *cclA* resulted in the reduction of H3K4me2/me3 levels at cryptic secondary metabolite genes that is accompanied by activation of the genes (Bok *et al*., 2009). Deletion of *cclA* in *A. fumigatus* which similarly resulted in loss of H3K4me2/me3 also led to increased secondary metabolite expression (Palmer *et al*., 2013). In *Fusarium*, deletion of *cclA* resulted in the specific reduction of H3K4me3 and not H3K4me2, but both positively and negatively affected secondary metabolite expression (Studt *et al*., 2017). Thus, CclA and H3K4 methylation appears to be associated with secondary metabolite repression.

Many fungal secondary metabolite clusters are located subtelomerically. The definition of 'subtelomeric' is somewhat arbitrary, but one study puts this as within 350 kb of the telomere (Chiara *et al.*, 2015). In this sense, the cryptic gene clusters upregulated in *A. nidulans* Δ*cclA* are approximately 200 kb and 500 kb from the telomeres (Bok *et al*., 2009). In comparison, the *eas* and *ltm* genes in *E. festucae* are about 10 – 90 kb away from the telomeres. Studies in yeast have implicated a role of Set1, COMPASS complex and H3K4 methylation in telomeric silencing (Nislow *et al.*, 1997, Bryk *et al.*, 2002, Fingerman *et al.*, 2005). Strong evidence for this was the observation that deletion of COMPASS subunits that resulted in the abrogation of H3K4 methylation; Δ*set1*, Δ*swd1* (*cps50*) and Δ*swd3* (*cps30*) also disrupted telomeric silencing, while deletion of COMPASS subunits that did not abrogate H3K4 methylation; Δ*sdc1* (*cps25*), Δ*spp1* (*cps40*) and Δ*cclA* (*bre2*/*cps60*) did not disrupt telomeric silencing (Krogan *et al*., 2002). However, this study utilised an antibody against general H3K4 methylation, so no distinctions were made between H3K4 mono-, di- and trimethylation. In a series of elegant experiments, Fingerman *et al*. (2005) utilised *set1* mutants that were defective only in H3K4me3 to show that the mark is required for silencing of rDNA, *HML*, *HMR* loci and a telomeric reporter gene. Additionally, in a Δ*set1* mutant which lacked H3K4 methylation and was disrupted in telomeric silencing, only *set1* constructs that restored H3K4 methylation could rescue the telomeric silencing defect of the mutant (Briggs *et al*., 2001).

In light of the role of COMPASS and H3K4 methylation in telomeric silencing and the subtelomeric location of the *EAS* and *LTM* clusters in *E. festucae*, it is hypothesised that these clusters are regulated by H3K4 methylation. In this chapter, this hypothesis was tested by examining deletion and overexpression strains of the genes for the COMPASS subunit CclA and the H3K4me3 demethylase KdmB. The role of CclA and KdmB in regulating H3K4 methylation in *E. festucae* was first analysed by western blot. Subsequently, expression of the SM genes was analysed by RT-qPCR and ChIP-qPCR to measure the levels of histone methylation at the SM loci.

## 4.2 Results

*4.2.1 CclA and KdmB are regulators of global H3K4me3 in E. festucae.*

Given that KdmB is a H3K4me3 demethylase, further characterisation of the role of H3K4 methylation in *E. festucae* was sought by including mutants of the H3K4 methyltransferase in the study. H3K4 methylation in the model yeast, *S. cerevisiae* is catalysed by COMPASS, a complex of 8 proteins with Set1 as the main catalytic subunit (Miller *et al.*, 2001, Roguev *et al.*, 2001, Krogan *et al.*, 2002). Through BLAST analyses, homologues of 6 of these yeast proteins (Set1, Bre2, Swd1, Spp1, Swd3 and Sdc1) can be identified in *E. festucae* but not for Swd2 (Cps35) and Shg1 (Fig. 4.1).

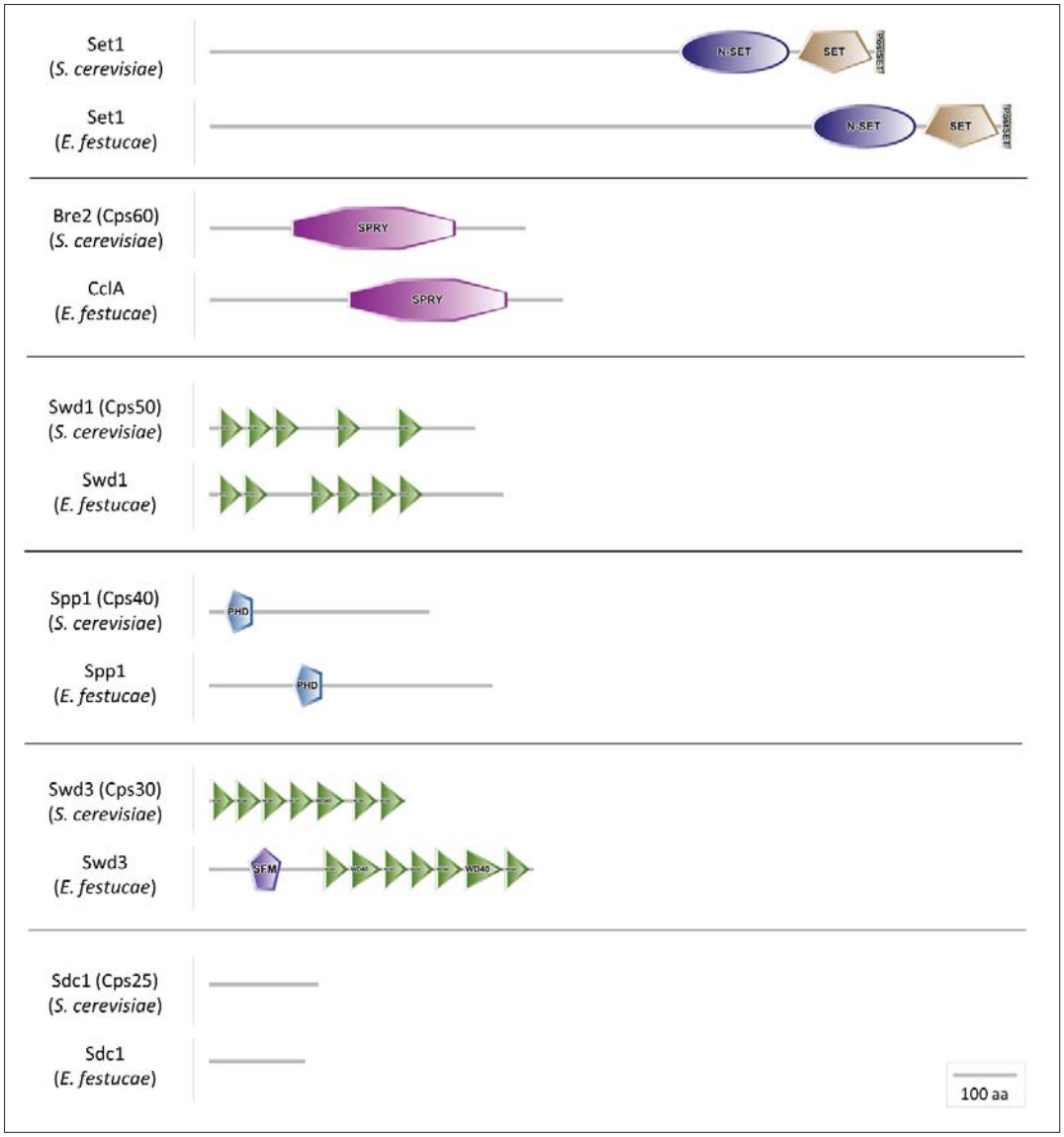


**Figure 4. 1. Homologues of yeast COMPASS proteins in *E. festucae*.** Domains were identified with SMART (Schultz *et al.*, 1998; Letunic *et al.*, 2014). N-SET, SET and POST-SET domains are conserved in both Set1 proteins. The SPRY domain in Bre2 is also conserved in CclA. WD40 repeats in Swd1 and Swd3 proteins are indicated by green triangles. The PHD domain is conserved in the Spp1 proteins. *E. festucae* Swd3 has an additional splicing factor motif (SFM) indicated by the purple pentagon, while Sdc1 proteins have no identifiable domain. The accession codes of the proteins used are P38827/EfM3.052640 (Set1), P43132/EfM3.021140 (Bre2/CclA), P39706/ EfM3.065870 (Swd1), Q03012/EfM3.018120 (Spp1), P38123/EfM3.061990 (Swd3) and Q03323/EfM3.061750 (Sdc1).

Disruption of *set1* in several filamentous fungi including *A. nidulans*, *F. graminearum*, *F. verticillioides* and *M. oryzae* was found to result in severe developmental defects, reflecting the importance of H3K4 methylation in the organisms (Govindaraghavan *et al.*, 2014, Liu *et al.*, 2015, Pham *et al.*, 2015, Gu *et al.*, 2017). In *E. festucae*, attempts to disrupt the *set1* gene were unsuccessful, suggesting that this gene is essential (T. Chujo, pers comm). Although Set1 is required for all three forms of H3K4 methylation, some components of the COMPASS complex, such as CclA and Sdc1, are required specifically for H3K4me3 (Schneider *et al*., 2005). Therefore, in this study mutants of *cclA* (courtesy of T. Chujo), and *kdmB* were used to study the role of H3K4me3 in *E. festucae*.

Analysis of the Δ*cclA* strains for changes in H3 methylation marks showed that similar to the *kdmB* overexpression mutants, the Δ*cclA* mutants showed specific reduction in H3K4me3, with minimal alterations in the levels of the other methylation marks analysed (Fig. 4.2). Introduction of the wild-type gene into Δ*cclA*#15 restored global H3K4me3 to the wild-type levels (Fig. 4.3A). To confirm the role of CclA and KdmB in regulating H3K4me3, the entire experiment was repeated with only the *cclA* and *kdmB* mutants. H3K4me3 reduction was consistently seen in both Δ*cclA* and *kdmB* overexpression mutants, establishing CclA and KdmB as regulators of global H3K4me3 in *E. festucae* (Fig. 4.3B).

Interestingly, a study in yeast has shown that Jhd2 (homologue of KdmB) is regulated at the protein level by ubiquitination and subsequent degradation by the proteasome. Jhd2 is normally undetectable in the cell, but inhibition of the proteasome for 30 minutes allowed Jhd2 to accumulate to high levels, indicating that Jhd2 is continually kept at low levels by sustained degradation by the proteasome (Mersman *et al.*, 2009). However, the results above in *E. festucae* show that overexpression of *kdmB* under the *tefA* promoter must lead to sufficiently high protein levels to result in demethylation of H3K4me3. Otherwise, it is possible that KdmB, which contains a much longer C-terminal region than Jhd2 (Fig. 3.5) is regulated in a different manner from Jhd2 in yeast.

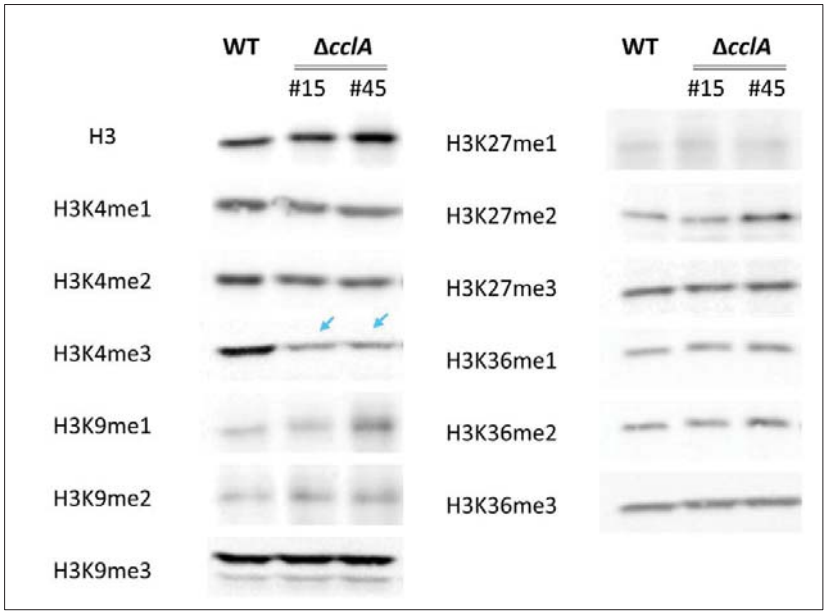


**Figure 4. 2. Western blot analysis of Δ*cclA* mutants.** Reduced H3K4me3 levels in the Δ*cclA* strains are indicated by blue arrows. Histones were acid-extracted from nuclear fractions of *E. festucae* cultured in PD media, separated by SDS-PAGE and probed with the indicated primary antibodies (Table 2.2) and visualised with the ECL method.

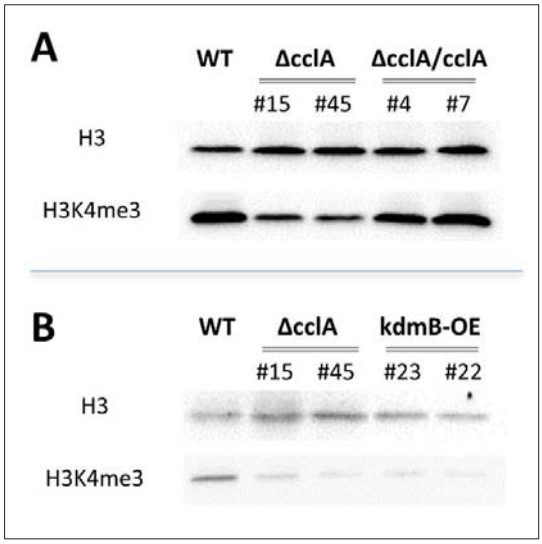


**Figure 4. 3. Western blot analysis of Δ*cclA* and *kdmB* overexpression mutants.** (A) Introduction of the wild-type *cclA* into Δ*cclA*#15 restores H3K3me3 to wild-type levels. (B) Loss of *cclA* and overexpression of *kdmB* lead to reduction in H3K4me3. Histones were acid-extracted from nuclear fractions of *E. festucae* cultured in PD media, separated by SDS-PAGE and probed with the indicated primary antibodies (Table 2.2) and visualised with the ECL method.

### *4.2.2 Loss of cclA does not affect E. festucae development.*

In Aspergillus and Fusarium, deletion of *cclA* leads to a reduction in colony radial growth (Palmer *et al*., 2013; Studt *et al*., 2017). Interestingly, deletion of *cclA* in *E. festucae* did not affect growth (Fig. 4.4). Growth of the mutants was also tested on PDA supplemented with NaCl to test if loss of cclA affects growth under salt stress, and on Blankenship media (Blankenship *et al*., 2001) buffered at pH 5, 6.5 and 8

to test if CclA is important for growth under pH stress. No difference in colony radial growth was observed for the Δ*cclA* mutants compared to wild-type (Fig. 4.4).

To observe the hyphal morphology of the mutants, the strains were cultured on nutrient-limiting water agar, stained with calcofluor white which binds chitin in the cell wall, and analysed under the inverted fluorescence microscope. No difference was observed in the morphology of hyphae of the Δ*cclA* mutant, and mutant hyphae fused with each other just as well as wild-type (Fig. 4.5). The *kdmB* overexpression mutants were similarly analysed and no differences in hyphal morphology or hyphal fusion were observed to that of wild-type.

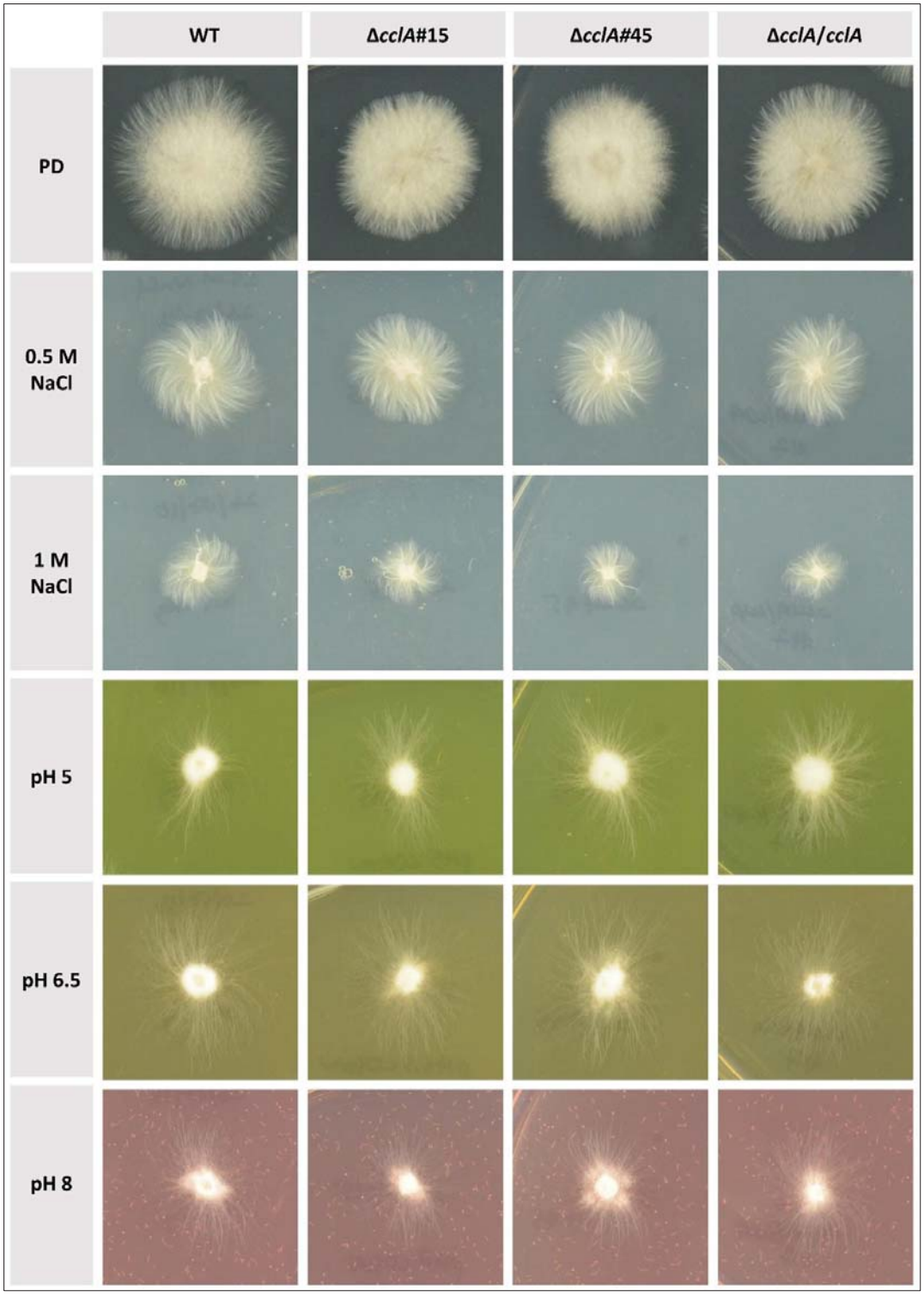


**Figure 4. 4. Culture phenotype of *cclA* mutants.** Strains were cultured for 10 days on 2.4% PD or supplemented with the indicated concentrations of NaCl. For pH tests strains were cultured on Blankenship media (Blankenship *et al.*, 2001) buffered with 60 mM phosphate buffer.

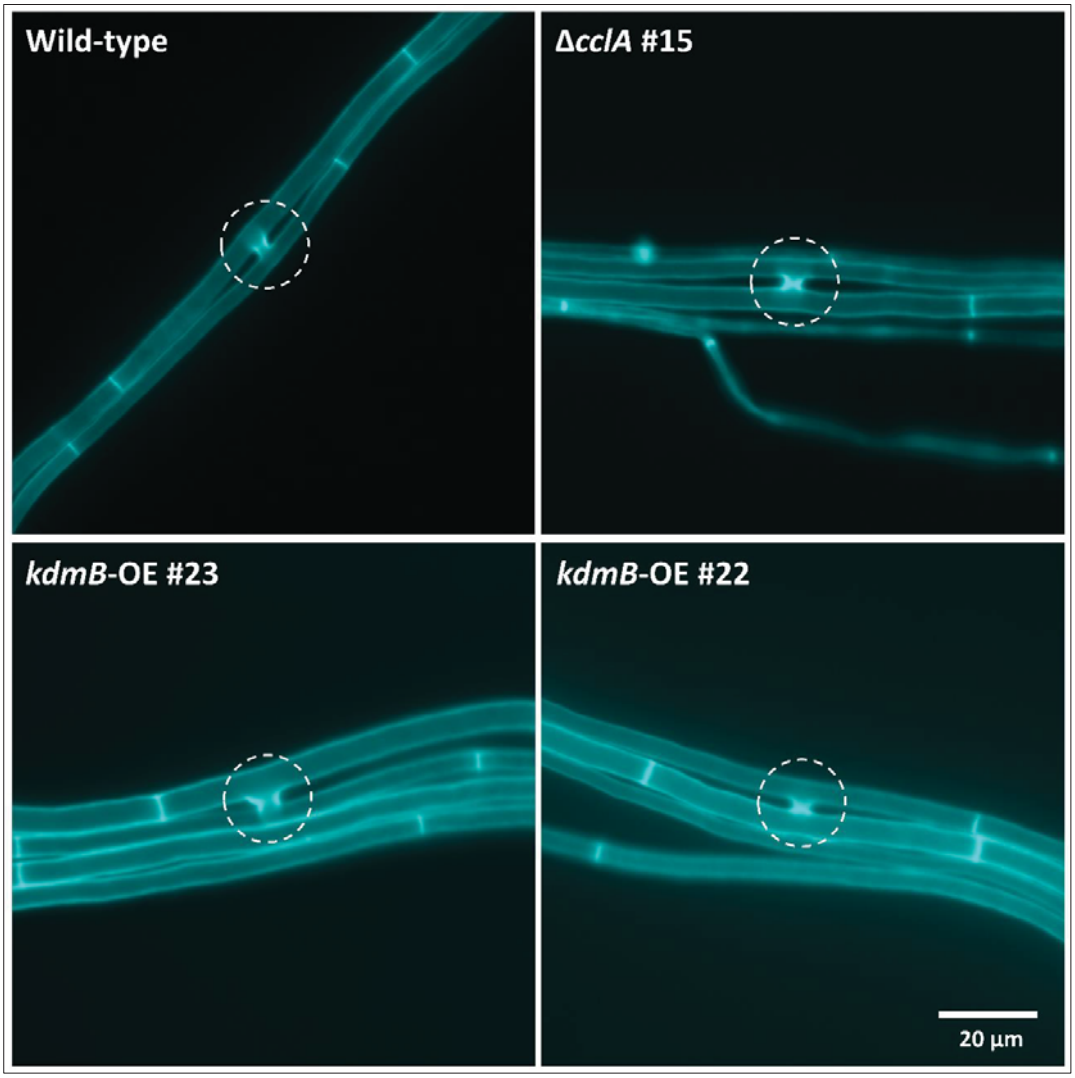


**Figure 4. 5. Hyphal morphology and fusion events in Δ*cclA* and *kdmB* overexpression strains.** Mycelia was cultured on water agar for 12 days, stained with calcofluor white and observed under the fluorescence microscope. Hyphal fusion events are indicated by white circles.

*4.2.3 CclA represses the subtelomeric eas and ltm genes in culture.*

CclA appears to have an exclusively repressive function over secondary metabolite clusters in Aspergillus (Bok *et al.*, 2009, Palmer *et al.*, 2013, Shinohara *et al.*, 2016), but interestingly, CclA in Fusarium has both repressive and activation functions, depending on the SM loci in question (Studt *et al.*, 2016). The role of CclA in regulating *E. festucae* SM clusters was tested by looking at the expression of the two known *E. festucae* SM clusters, the *EAS* and *LTM* clusters which are located ~10 kb from the telomeres of chromosomes I and III respectively (Fig. 1.1). Genes of the both clusters are typically silent in axenic culture, but culturing in MSM3 medium induces a low expression of the genes (Chujo & Scott, 2014). When tested using this medium, deletion of *cclA* was observed to cause significant derepression of the *eas* and *ltm* genes (Fig. 4.6).

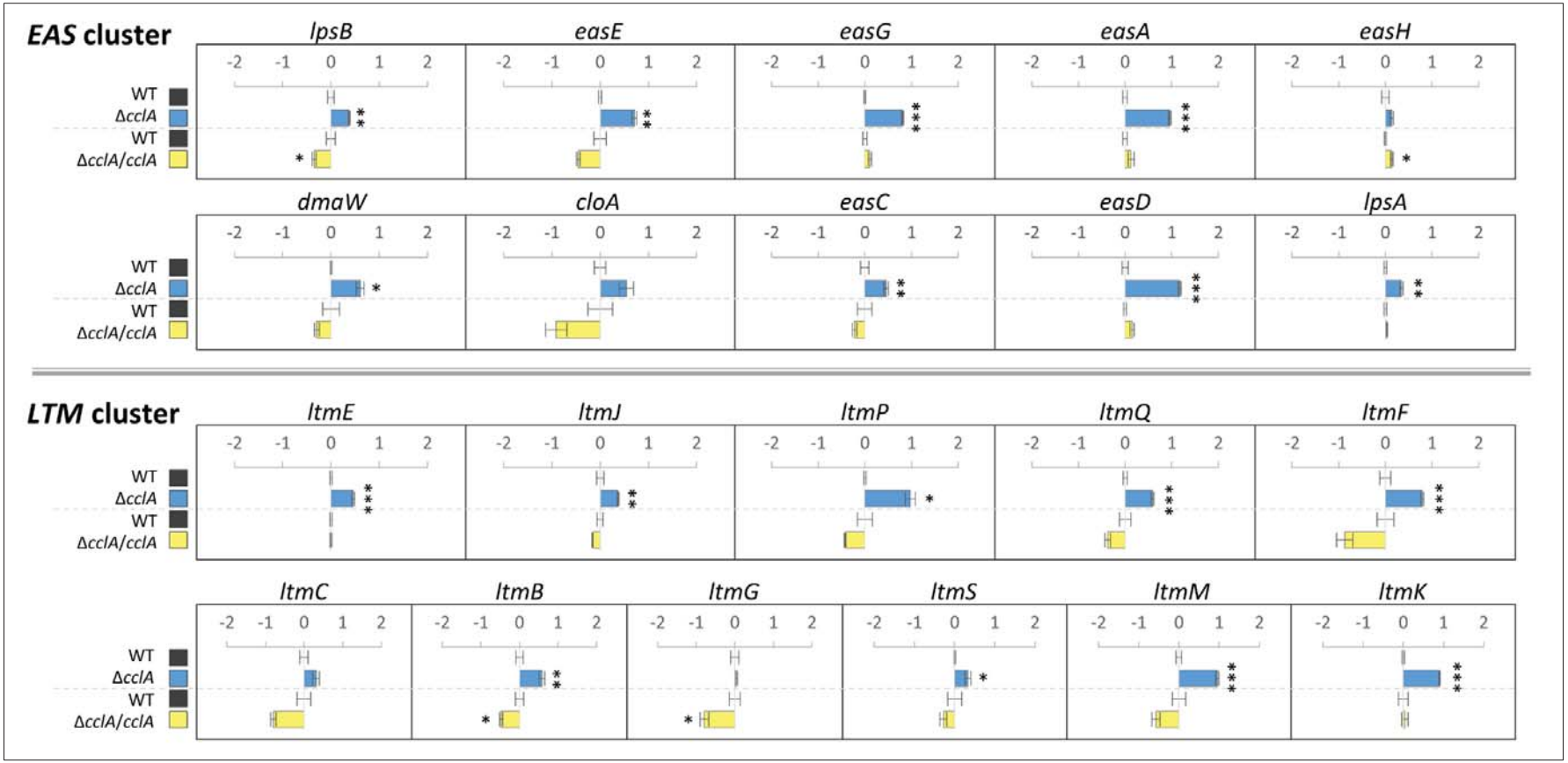


**Figure 4. 6. CclA represses the subtelomeric *EAS* and *LTM* clusters.** Derepression of *eas* and *ltm* genes in Δ*cclA* strains grown in axenic culture with MSM3 media. Introduction of the wild-type gene restores repression of these genes. Introduction of the wild-type gene restored expression of the genes in a separate independent experiment indicated by dashes. Steady state transcript levels of the genes were analysed by RT-qPCR and normalised to that of the 40S ribosomal protein S22 reference gene. Bars represent log10 ± SEM (n = 3). *P < 0.05, **P < 0.01 and ***P < 0.001 (two-tailed unpaired t-test).

Among the ten *eas* genes analysed, *easH* and *cloA* were not significantly derepressed in the Δ*cclA* mutant. Interestingly, *cloA* was also the only gene consistently not derepressed in the Δ*clrD* (H3K9 methyltransferase), Δ*ezhB* (H3K27 methyltransferase) (Chujo & Scott, 2014) and Δ*hepA* (heterochromatin protein 1) (Chujo *et al*., unpublished) mutants. Among the *ltm* genes, only *ltmG* was not significantly derepressed in the Δ*cclA* mutant (Fig. 4.6). This gene was also not derepressed in the Δ*ezhB* mutant, but was strongly derepressed in the Δ*clrD* mutant. These observations highlight the differences and similarities between the different layers of regulation of H3K4, H3K9 and H3K27 methylation over the *eas* and *ltm* genes. In general, deletion of *cclA* resulted in the derepression of a greater number of the *eas* and *ltm* genes compared to deletion of *clrD* and *ezhB*. However, the level of gene derepression was greater in both the *clrD* and *ezhB* deletion strains compared to the Δ*cclA* strain.

Introduction of the wild-type gene into the Δ*cclA* mutant reversed the observed gene derepression with the exception of *easH*, showing that this phenotype could be complemented. Interestingly, the complement strain had even lower transcript levels for many of the genes analysed (Fig. 4.6). Determination of the copy number and expression of the *cclA* gene showed that the strain used (Δ*cclA*/*cclA*#7) carries 8 copies of the gene and expresses at 11 times higher than the wild-type strain (Fig. 4.7), thus indicating that overexpression of CclA further silences the SM genes and provides additional evidence for a repressive role of CclA on these genes. Although derepression of the genes in the Δ*cclA* mutant can be as high as 15 times the expression in wild-type for some genes (e.g. *easG*), this is still a low level of expression compared to the derepression seen in the wild-type strain *in planta*, where expression of some *ltm* genes can be several orders of magnitudes higher than the expression in culture (Fig. 4.8).

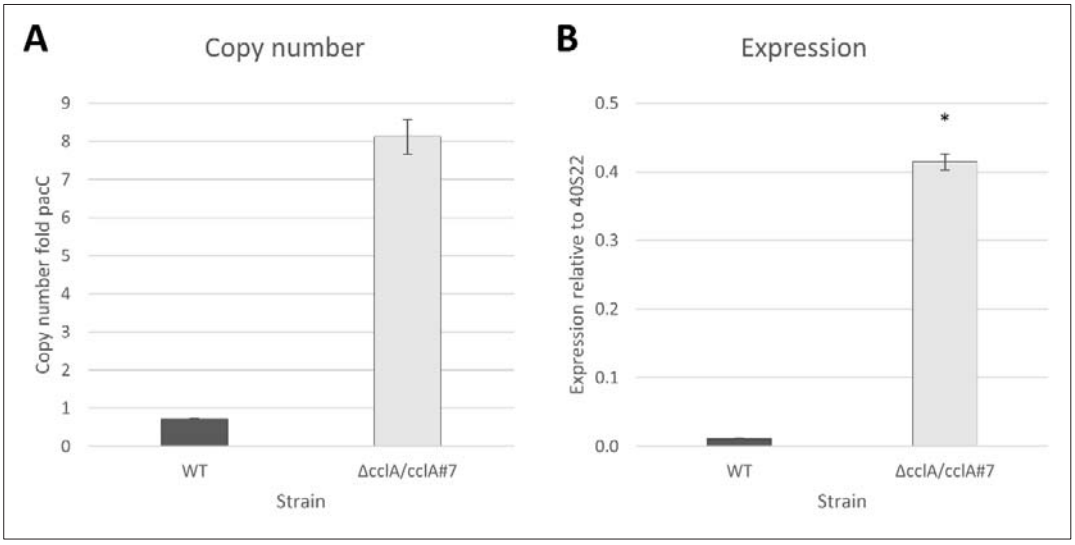


**Figure 4. 7. Copy number and expression analysis of Δ*cclA*/*cclA* strain.** (A) Genomic copy number of *cclA* in wild-type and Δ*cclA*/*cclA*#7. (B) Expression level of *cclA* in wild-type and Δ*cclA*/*cclA*#7. Copy number was determined by quantifying the amount of target DNA present relative to that of single-copy *pacC* gene by qPCR. Transcript levels were quantified by RT-qPCR and normalised to that of the 40S ribosomal protein S22 reference gene. Primers used in the analysis are listed in Table 2.4. Error bars represent ± SEM (n = 3). **P* < 0.05 (two-tailed t-test).

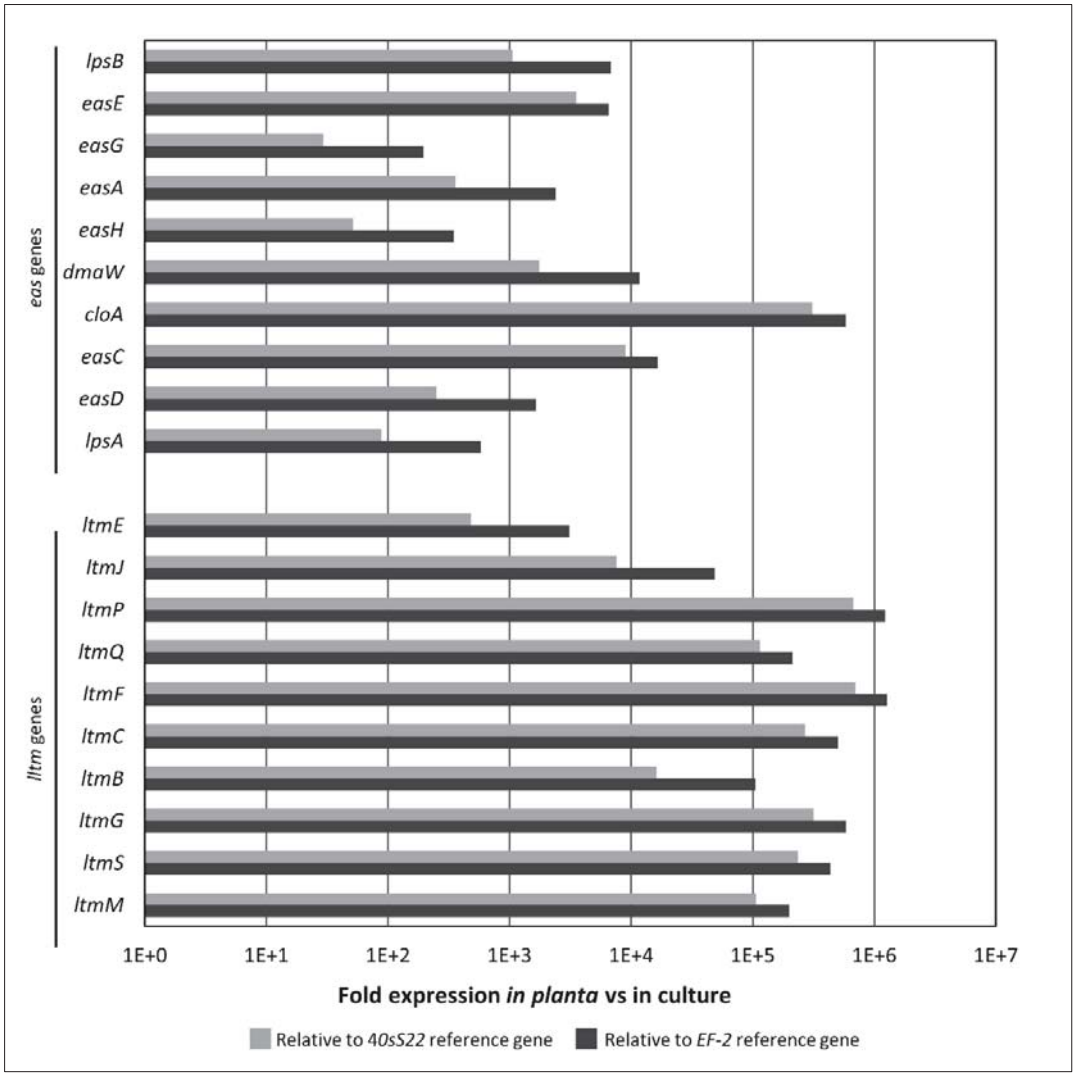


**Figure 4. 8. Fold expression of *eas* and *ltm* genes in wild-type *E. festucae in planta* and in axenic culture. For** culture conditions mycelia were grown in MSM3 media. For plant conditions, wild-type *E. festucae* was inoculated into perennial ryegrass and pseudostem material was harvested at 16 weeks post inoculation. Steady state transcript levels were determined by RT-qPCR and calculated relative to two reference genes; 40S ribosomal protein S22 and elongation factor 2, shown in light and dark grey respectively. Three biological replicates were used for each condition, i.e. fold difference is calculated from the average of three biological replicates of plant conditions, over the average of three biological replicates of culture conditions.

*4.2.4 CclA promotes H3K4 trimethylation at the eas and ltm gene promoters.*

Given that CclA is responsible for H3K4 trimethylation in *E. festucae*, it was next tested if CclA represses the SM genes by increasing H3K4me3 levels at the gene loci. H3K4me3 peaks near the transcription start sites (TSSs) in *F. graminearum* (Connolly *et al*., 2013). However, there is presently no information on the TSSs of the *eas*/*ltm* genes. An analysis of *E. festucae* transcriptomic data (Eaton *et al*., 2010) suggests that transcription begins at around -35 to -340 relative to ATG (with a median of -170) for the *eas* genes, while for the *ltm* genes, transcription starts at -15 to -310 (median of -60). Based on these observations, the 0 to -150 regions of the genes were selected for ChIP analysis. Chromatin was sonicated to lengths of 100-500 bp (Fig. 4.9) and primers for qPCR were designed to generate products of 80-120 bp in size.

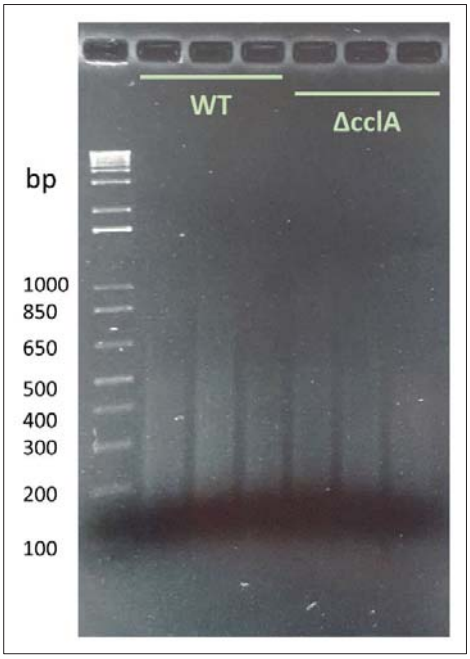


**Figure 4. 9. Size of DNA fragments used for culture ChIP.** DNA was isolated from 20 µg sonicated chromatin and separated on a 1.5% agarose gel. The gel shows three biological replicates of each strain. The majority of sheared DNA fragments were within 100-500 bp.

At the identical growth conditions that promoted SM derepression, H3K4me3 levels at both *eas* and *ltm* gene promoters were consistently lower by about a factor of half in the Δ*cclA* mutant compared to the wild-type strain (Fig. 4.10A). This suggests that derepression of the SM genes was due to a reduction in H3K4me3 levels. By contrast, H3K4me3 levels were not reduced at the *S22* reference genes, but was reduced at the *EF-2* gene. To test if the reduction in H3K4me3 level at *EF-2* in the Δ*cclA* strain had an impact on transcription, expression of the gene was compared to that of *S22* in the exact culture conditions used for the ChIP study. The analysis revealed no difference in the expression of the gene between Δ*cclA* and the wild-type strain, indicating that if there were a reduction in H3K4me3 at the *EF-2* gene in the Δ*cclA* mutant, this did not lead to changes in the expression of the gene (Fig. 4.11). Unlike the SM genes, none of these housekeeping genes are located near the telomeres in *E. festucae* (Winter *et al*., unpublished). Being housekeeping genes, the expression of these genes would also be expected to be higher than the SM genes. In fact, *40S22* and *EF-2* were expressed at three to seven orders of magnitudes higher than the SM genes in the test conditions used (Fig. 4.12). The ChIP analysis also showed that levels of H3K4me3 at the housekeeping genes were much higher than at the SM genes, this is consistent with the general correlation of H3K4me3 with active genes (Santos-Rosa *et al*., 2002), (Fig. 4.10A).

In *A. nidulans*, derepression of cryptic SM genes in the Δ*cclA* mutant of the fungus was accompanied not only by reduced levels of H3K4me3, but also by reduced levels of H3K9me3 at the SM genes (Bok *et al*., 2006). In addition, reduction in H3K9me3 and H3K27me3 levels have been observed to accompany derepression of the *eas* and *ltm* genes in *E. festucae* (Chujo & Scott, 2014). The levels of these marks were analysed in this study to rule out the possibility that the observed gene derepression in the Δ*cclA* mutant was due to reduction in these repressive marks. However, no changes in the levels of H3K9me3 and H3K27me3 were observed in the Δ*cclA* mutant at the *eas* and *ltm* genes, as well as at the reference genes

(Fig. 4.10B and C). Consistent with the expectation that euchromatic and highly transcribed genes carry low levels of repressive histone marks, H3K9me3 and H3K27 levels at the reference genes were also significantly lower than at the SM genes (Fig. 4.10B and C). Taken together, these results suggest that H3K4me3 is a repressive mark for the subtelomeric SM genes in *E. festucae*, and that CclA plays a role in maintaining repressive levels of the mark that is important for the silencing of these genes in culture conditions.

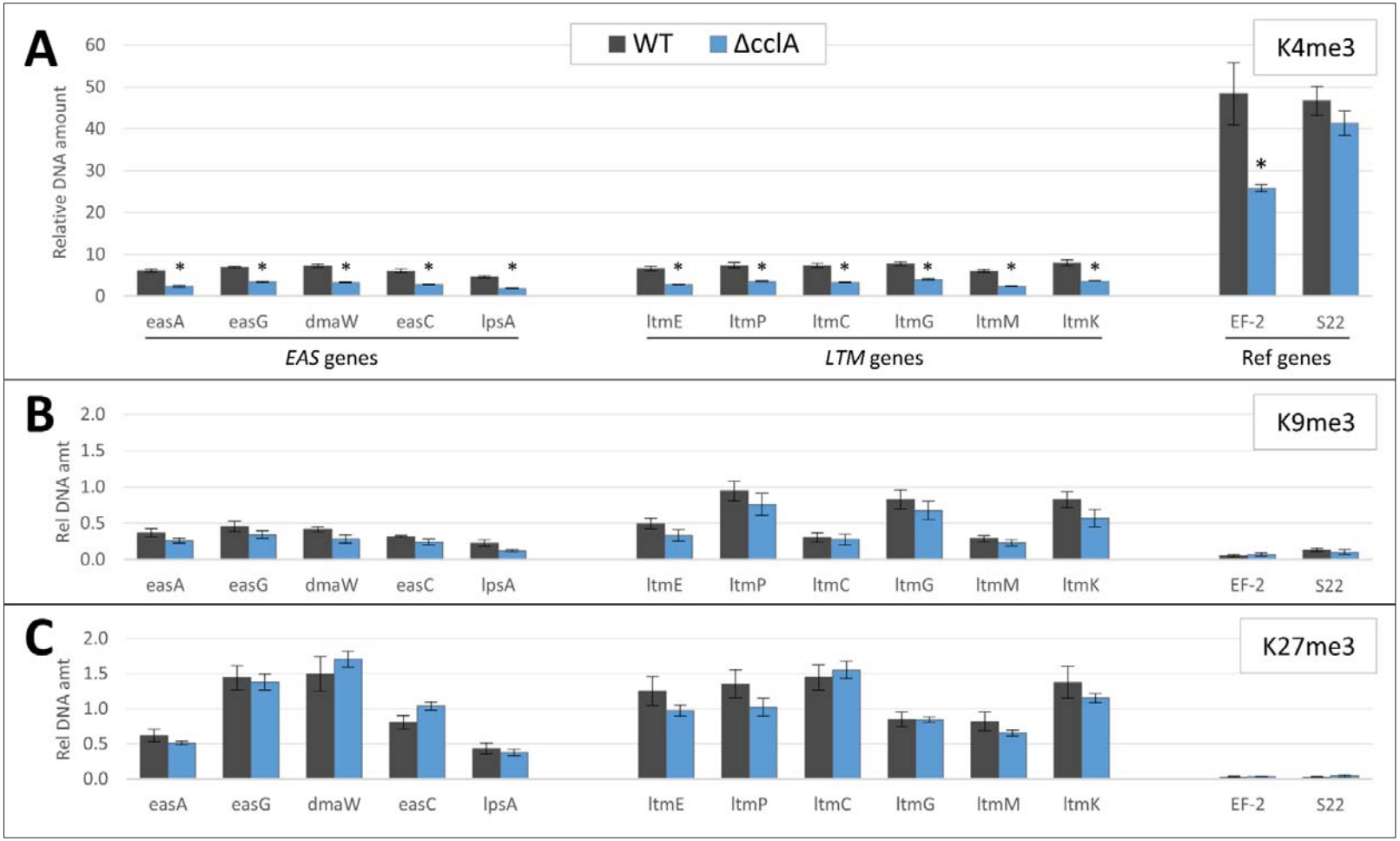


**Figure 4. 10. CclA promotes H3K4 trimethylation at the *eas* and *ltm* genes.** (A) H3K4me3, (B) H3K9me3 and (C) H3K27me3 levels at promoter regions of the genes were analysed ChIP-qPCR. ChIP was performed on chromatin obtained from nuclear fractions of mycelia cultured in MSM3 media for 9 days and immunoprecipitated DNA was quantified relative to input by qPCR. Antibodies and primers used are provided in Tables 2.2 and 2.4. Bars represent ± SEM (n = 3). *$P < 0.05$ (two-tailed t-test).

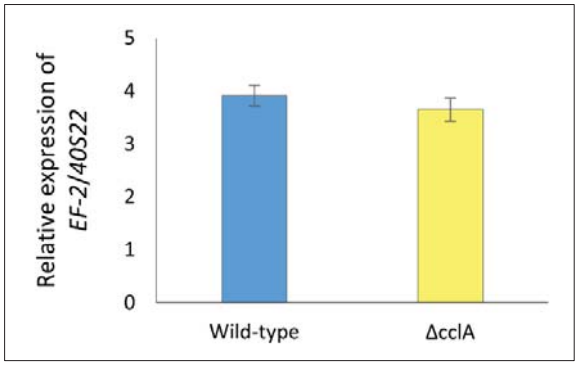


**Figure 4. 11. Expression level of *EF-2* relative to *40S22* in MSM3 media.** The steady state transcript levels of reference genes elongation factor 2 and 40S ribosomal S22 in the culture conditions used for ChIP (Fig. 4.10) was determined by RT-qPCR. Strains were cultured in MSM3 media for 9 days. Error bars are ± SEM (n = 3).

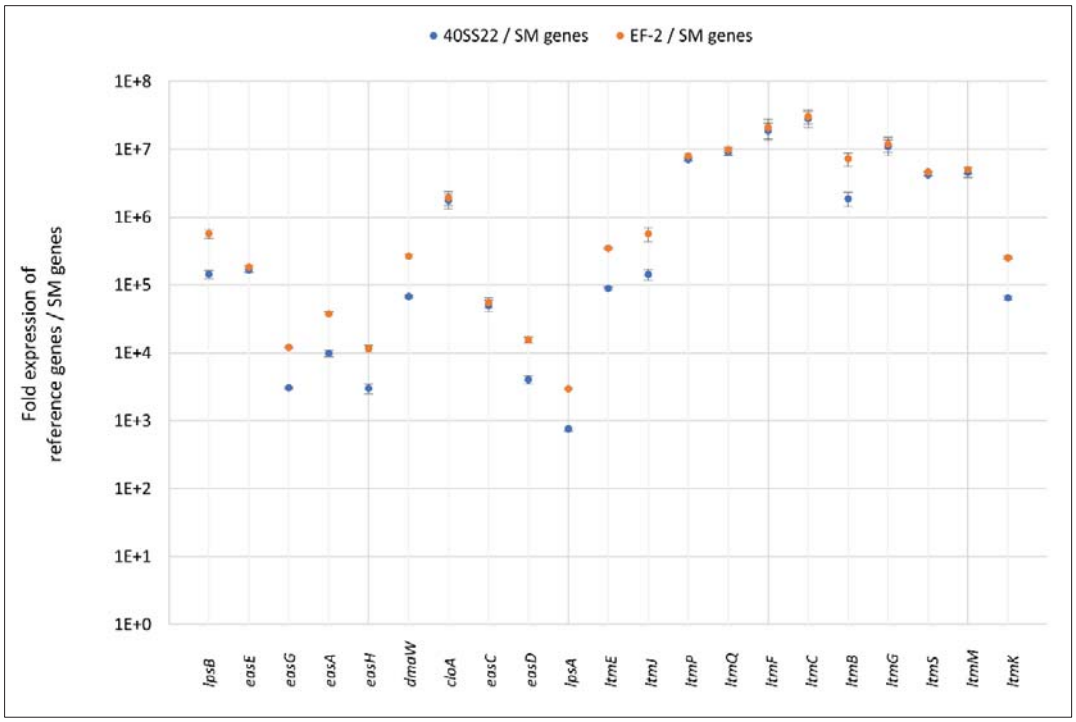


**Figure 4. 12. Fold expression of *40S22* and *EF-2* reference genes relative to the *eas*/*ltm* genes.** Transcript levels of the genes in the wild-type strain cultured in MSM3 media for 9 days were determined by RT-qPCR. Error bars are ± SEM (n = 3).

*4.2.5 Overexpression of kdmB does not affect the expression of eas and ltm genes in culture.*

Given that overexpression of *kdmB* in *E. festucae* achieved a similar effect as deletion of *cclA* on global H3K4me levels (Fig. 4.3), expression of the SM genes was analysed in the *kdmB* overexpression strains to test if the *EAS* and *LTM* clusters are similarly derepressed in these strains. Unlike deletion of *cclA*, overexpression of *kdmB* did not result in clear derepression of the genes (Fig. 4.13). Only two genes; *easC* and *ltmG*, showed a mild derepression that was consistent between the two *kdmB*-OE strains. Additionally, *easA*, *lpsA* and *ltmS* were on the contrary more repressed in one or the other *kdmB*-OE

strains in comparison to wild-type (Fig. 4.13). Thus, given the absence of any significant changes in gene expression in the other SM genes in the *kdmB*-OE mutants, it was concluded that overexpression of *kdmB* does not lead to derepression of SM genes in axenic culture.

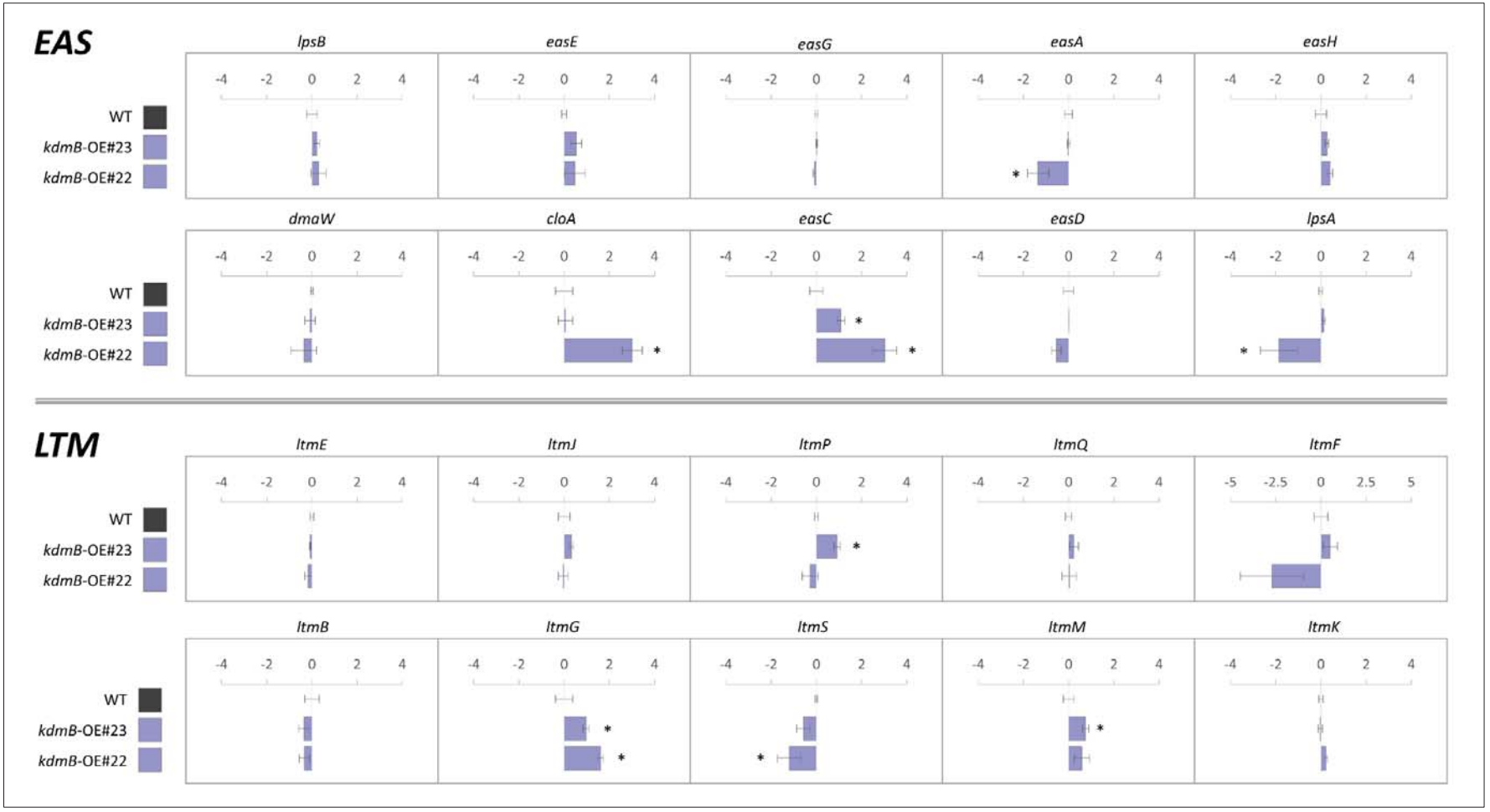


**Figure 4. 13. Expression of *eas* and *ltm* genes in *kdmB* overexpression strains.** Steady state transcript levels of the genes were analysed by RT-qPCR and normalised to that of the 40S ribosomal protein S22 reference gene. Bars represent log2 ± SEM (n = 3). *$P < 0.05$ (two-tailed t-test).

*4.2.6 KdmB is required for derepression of eas and ltm genes in planta.*

The *eas* and *ltm* genes in *E. festucae* undergo a remarkable transcriptional switch *in planta* that drives their expression from basal levels in culture to massive levels in the host plant. Recent transcriptomic analysis showed that the 11 genes of the *LTM* cluster are among the 40 most highly expressed genes *in planta*, accounting for roughly 1.5% of the total fungal transcripts (Chujo *et al*., unpublished). Therefore, if H3K4me3 is acting in silencing these clusters then these marks would need to be removed *in planta*. Present literature suggests that removal of H3K4me3 can only be performed by either the KDM5 proteins or by the KDM2 group of H3K36/H3K4me3 demethylases. As homologues of KDM2 do not appear to be present in *E. festucae* or other filamentous fungi, KdmB is likely to be the only demethylase capable of demethylating H3K4me3 in *E. festucae*. Thus, to test if H3K4me3 is removed from the SM genes upon activation of the genes *in planta*, the *kdmB* gene in *E. festucae* was disrupted by replacement with the hygromycin resistance gene. Out of about 350 transformants screened, 12 were found to be 'clean' deletion strains as shown by Southern blot analysis (Fig. 4.14). One of these mutants, Δ*kdmB*#332, had the wild-type gene reintroduced in order to generate the complement strain. The Δ*kdmB*/*kdmB*#3 complement strain was shown to have a single copy integration and expresses the *kdmB* gene at a similar level to the wild-type strain (Fig. 4.15). The Δ*kdmB*#332 and Δ*kdmB*/*kdmB*#3 strains were subsequently inoculated into perennial ryegrass plants and transcript level of the SM genes was determined by RT-qPCR using RNA isolated from the pseudostem regions of infected plants, where fungal biomass is highest.

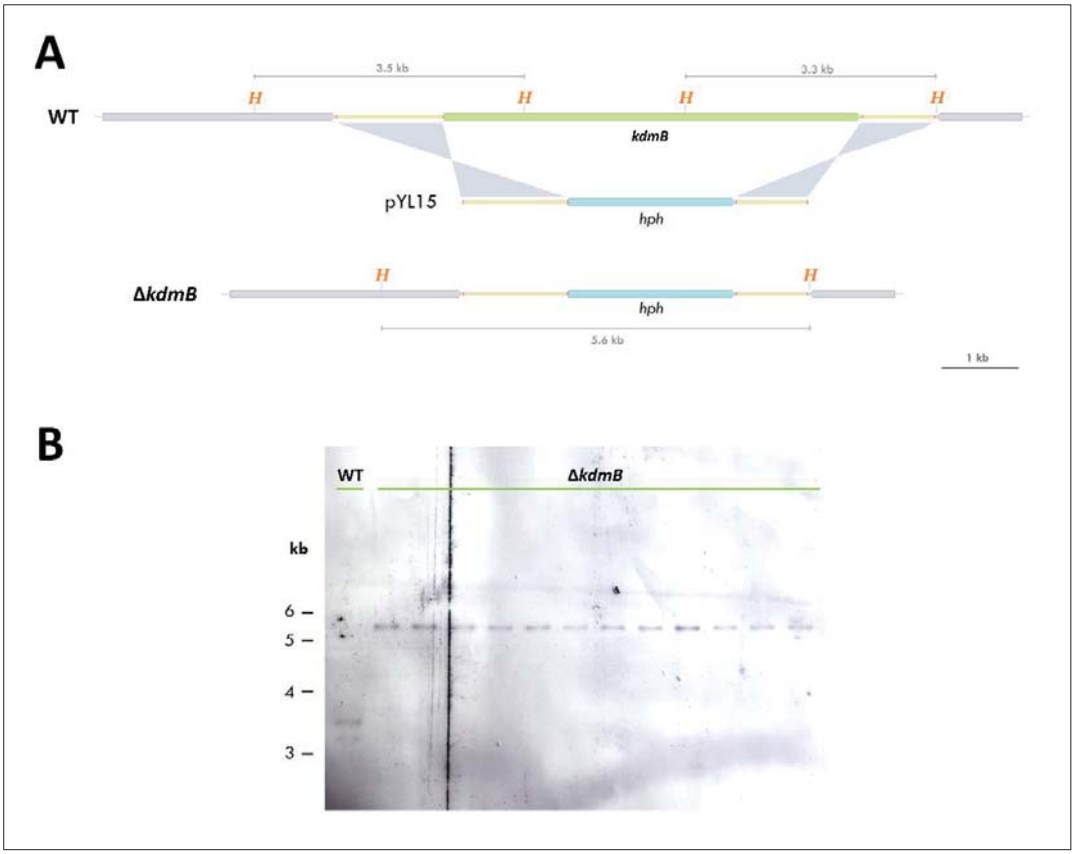


**Figure 4. 14. Strategy for deletion of *kdmB* in *E. festucae* and confirmation by Southern blot analysis.** (A) Physical map of the wild-type *kdmB* genomic locus, linear insert of *kdmB* replacement construct pYL15, and the Δ*kdmB* mutant locus, showing restriction sites for *Hin*dIII and homologous regions in yellow. (B) NBT/BCIP stained Southern blot of *Hin*dIII genomic digests (1 µg) of *E. festucae* wild-type and Δ*kdmB* deletion strains probed with digoxigenin (DIG)-11-

dUTP labelled linear product of pYL15 amplified with primers YL169F/YL169R. Sizes in kilobases of hybridising bands are indicated on the left.

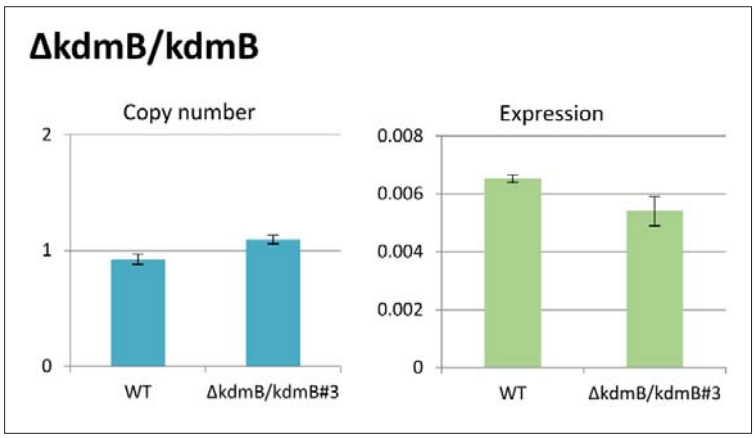


**Figure 4. 15. Copy number and expression of *kdmB* in Δ*kdmB*/*kdmB* complement strain.** Copy number determined by qPCR is expressed relative to the copy number *pacC* in wild-type (single copy). Expression level determined by RT-qPCR is expressed relative to that of the 40S ribosomal S22 reference gene. Error bars represent S.D. from two technical replicates. Primers used for the analyses are given in Table 2.4.

The analysis revealed that loss of KdmB resulted in drastically reduced expression of almost all of the *eas* and *ltm* genes, supporting the hypothesis that KdmB is required for derepression of the clusters *in planta* (Fig. 4.16). Introduction of the wild-type *kdmB* gene reversed this downregulation, confirming that the effects were due to the absence of KdmB. Given the high levels of *eas*/*ltm* gene expression *in planta*, the reduction in gene expression (e.g. up to 65% reduction for *ltmJ*) in the Δ*kdmB* mutant represents a huge reduction in the actual transcript abundancy. Consistent with this, measurement of the metabolite levels by LC-MS/MS showed that the mg $kg^{-1}$ levels of paxilline, a shunt product of the lolitrem pathway, as well as lolitrem B, the main pathway product (Saikia *et al.*, 2012), were significantly reduced by 67% and 70%, respectively in the Δ*kdmB* mutant (Fig. 4.17A). Subsequent comparisons of the relative peak areas in the analysis showed that most of the intermediate metabolites of the lolitrem pathway and all of the end metabolites were also significantly reduced in the Δ*kdmB* mutant relative to wild-type (Fig. 4.18).

In comparison, there were no significant differences in the levels of ergot alkaloids, including chanoclavine, agroclavine and lysergic acid, intermediates of the ergovaline pathway, and ergovaline, the main product of the pathway (Schardl *et al*., 2012) (Fig. 4.17B). The *ltm* genes are among the most highly expressed *E. festucae* genes *in planta* and are expressed at a few orders of magnitude higher than the *eas* genes (Fig. 4.8). Thus, this may explain why a difference was observed in the levels of the indole diterpenes (lolitrem), but not with the ergot alkaloids (ergovaline), as the lower expression of the *eas* genes means a smaller reduction in the actual transcript abundancy for the ergovaline biosynthetic enzymes in the Δ*kdmB* mutant. There were also no differences in the levels of peramine, the third major secondary metabolite in *E. festucae*, between the wild-type and Δ*kdmB* mutant (Fig. 4.17C). Peramine is synthesised by a single enzyme encoded by the *perA* gene in *E. festucae* that is not found subtelomerically (Tanaka *et al*., 2006; Winter *et al*., unpublished). Therefore, this suggests that deletion of *kdmB* specifically alters the expression of subtelomeric secondary metabolite clusters and not all secondary metabolite genes in *E. festucae*.

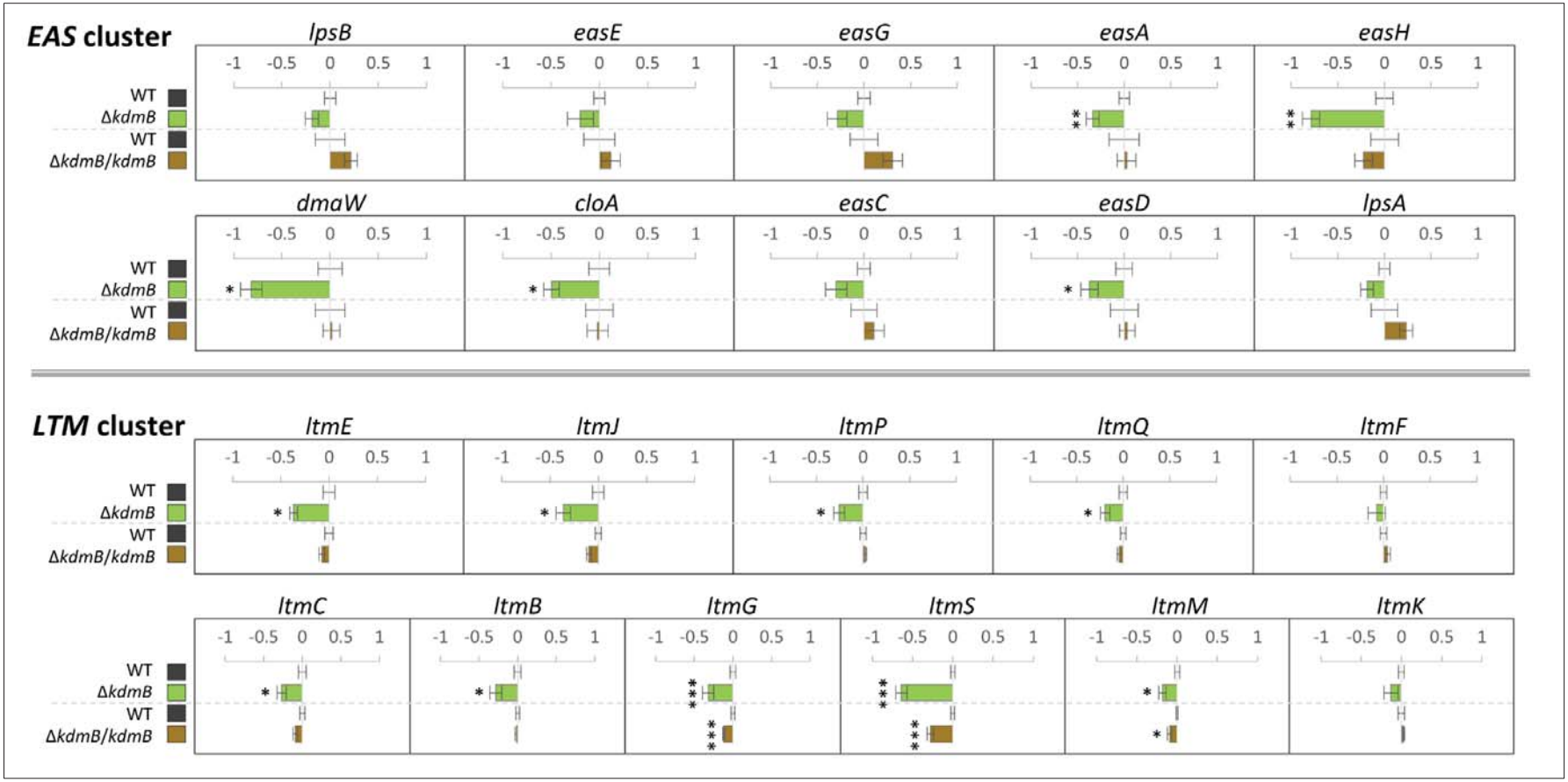


**Figure 4. 16. KdmB derepresses the subtelomeric *EAS* and *LTM* clusters *in planta*.** Loss of *kdmB* resulted in reduced expression of *eas* and *ltm* genes *in planta*. Introduction of the wild-type gene restored expression of the genes in a separate independent experiment indicated by dashes. Steady state transcript levels of the genes in pseudostem tissue of infected perennial ryegrass at 16 weeks post-inoculation were determined by RT-qPCR and normalised to that of the 40S ribosomal protein S22 reference gene. Bars represent log10 ± SEM (n = 4). *P < 0.05, **P < 0.01 and ***P < 0.001 (two-tailed unpaired t-test).

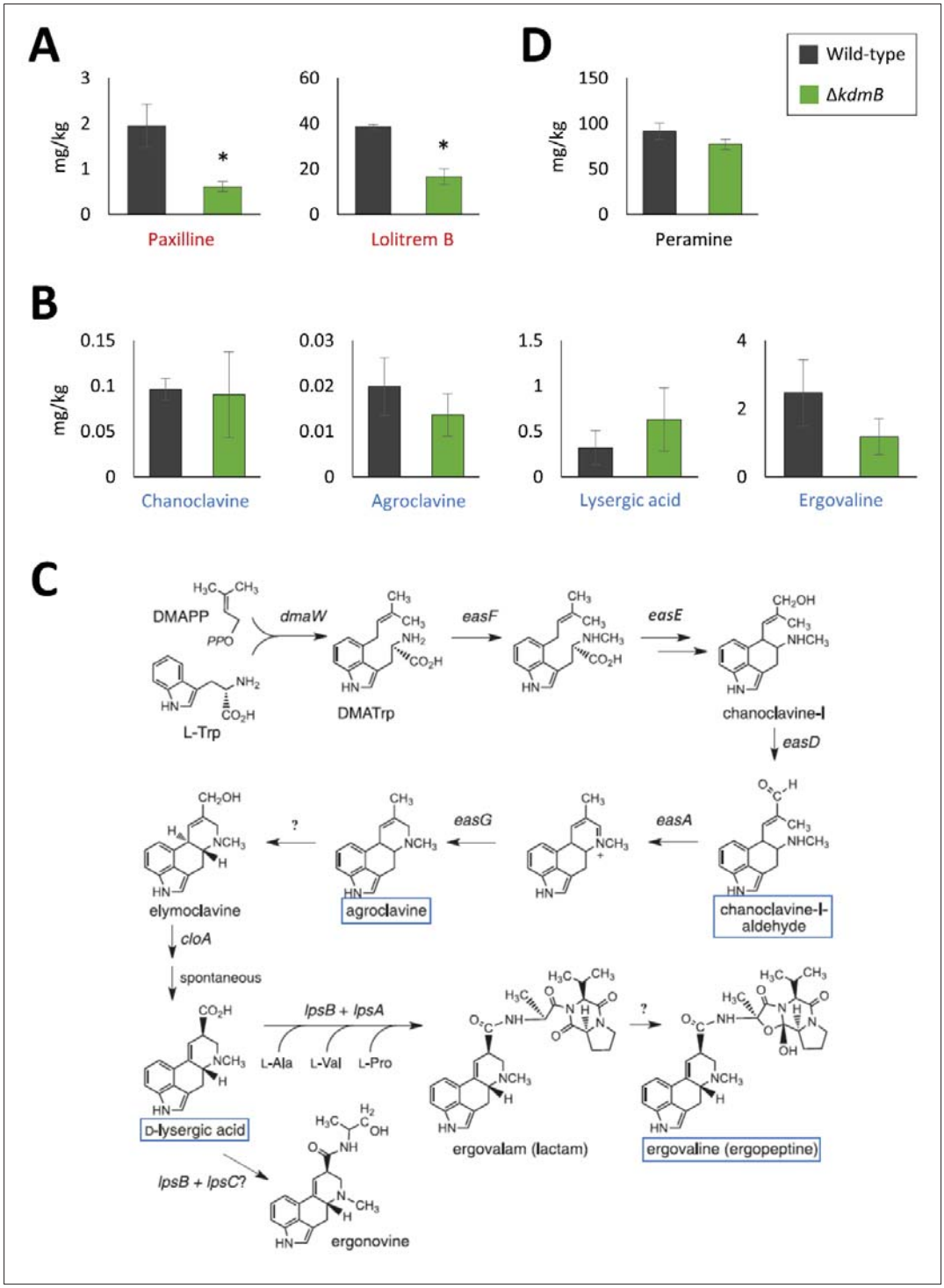


**Figure 4. 17. LC-MS/MS analysis of *E. festucae* secondary metabolites in ryegrass plants infected with wild-type and Δ*kdmB* mutant.** Levels of (A) Indole diterpenes, (B) ergot alkaloids and (D) peramine levels were determined in wild-type and Δ*kdmB* infected perennial ryegrass plants at 16 weeks post-inoculation. (C) The ergovaline biosynthetic pathway showing the metabolites analysed, figure is modified from Schardl *et al*. (2012). Values were normalized to plant tissue dry weight and ppm determined using internal standards. Bars represent mean ± SEM (n = 4). * $P < 0.05$ (two-tailed t-test).

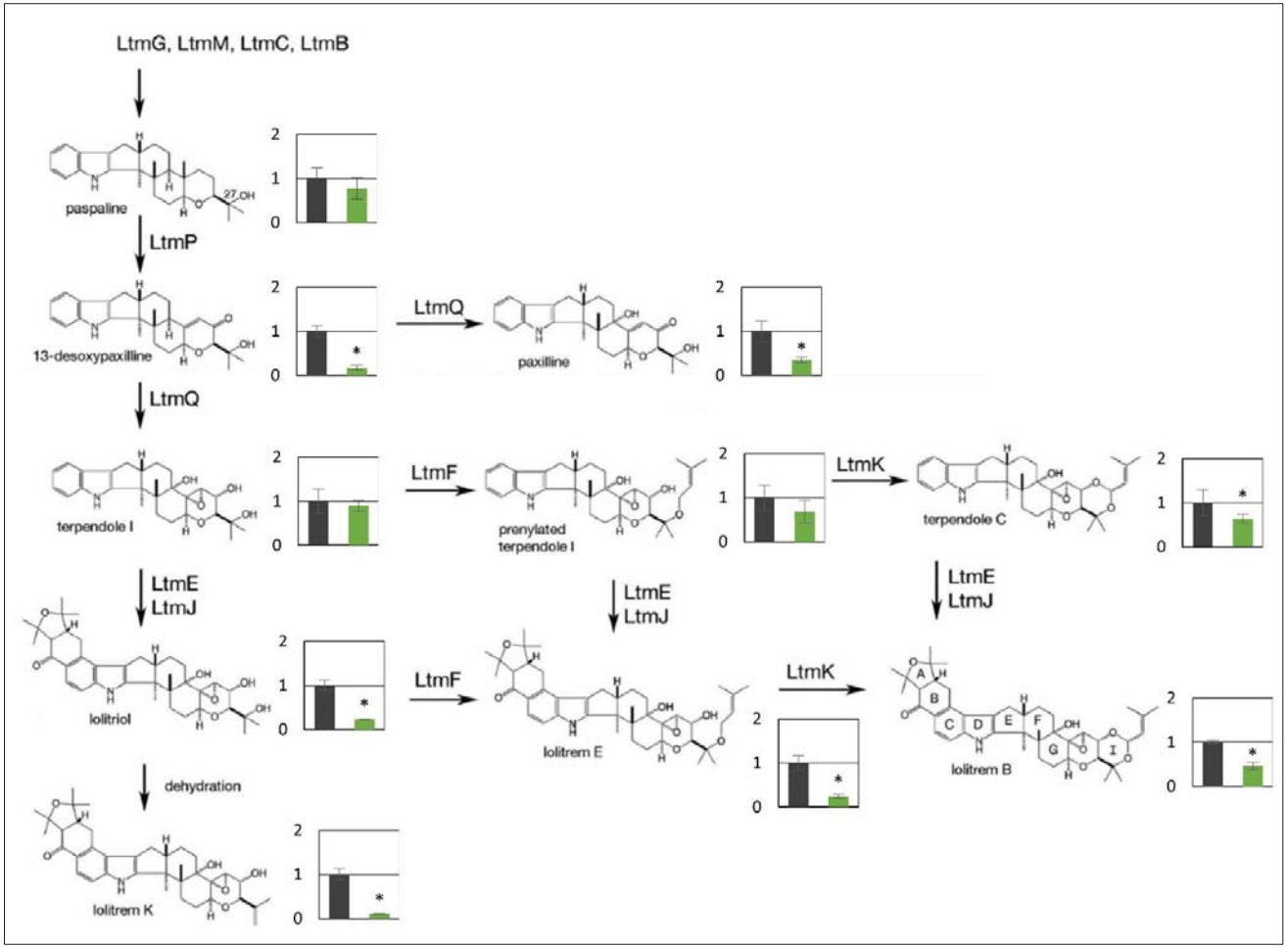


**Figure 4. 18. LC-MS/MS analysis of lolitrem pathway metabolites in ryegrass plants infected with wild-type and Δ*kdmB* mutant.** Metabolite levels were determined in wild-type and Δ*kdmB* infected perennial ryegrass plants at 16 weeks post-inoculation. Relative peak areas of the metabolites were normalised to sample weights and values are shown relative to the wild-type levels. Bars represent mean ± SEM (n = 4). * $P < 0.05$ (two-tailed t-test).

*4.2.7 KdmB demethylates H3K4me3 at the eas and ltm gene promoters.*

The results above have shown that KdmB is required for derepression of the *eas* and *ltm* genes *in planta*. Thus, it was determined next if KdmB derepresses the SM genes by demethylating H3K4me3 at the gene loci. To test this hypothesis, wild-type and Δ*kdmB* strains were inoculated into perennial ryegrass and ChIP-qPCR was performed on pseudostem sections of infected plants at 16 weeks post inoculation. Chromatin was sonicated to lengths of 100-1000 (Fig. 4.19) and the same promoter regions analysed in previous culture ChIP were analysed in this experiment.

The results showed that in the Δ*kdmB* mutant, H3K4me3 levels at the SM gene promoters were significantly higher compared to the wild-type, by about 3.3-fold on average, in keeping with the inability of the mutant to remove H3K4me3 from these loci (Fig. 4.20A). H3K4me3 levels at the reference genes were also higher in the Δ*kdmB* mutant, but by about 1.6-fold on average. This may suggest that widespread H3K4me3 methylation followed by demethylation occurs during the shift from axenic culture to *in planta* growth. It was not investigated whether the higher levels of H3K4me3 led to changes in expression of the housekeeping genes in the Δ*kdmB* mutant. However, previous in culture analyses have shown that higher H3K4me3 levels at the housekeeping genes did not lead to any change in the gene expression (Fig. 4.11).

Analysis of the H3K9me3/K27me3 repressive marks showed that H3K9me3 levels at the SM genes were unperturbed by the loss of KdmB (Fig. 4.20B). On the other hand, a reduction in H3K27me3 levels was observed in the Δ*kdmB* mutant (Fig. 4.20C). It is unclear what the significance of this is, as a decrease in H3K27me3, a heterochromatic and repressive mark, is typically associated with gene activation, whereas the SM genes were downregulated in the Δ*kdmB* mutant. Nevertheless, these results show that the reduced expression of the SM genes in the Δ*kdmB* mutant could not be explained by a change in levels of repressive H3K9me3/K27me3 marks. Thus, consistent with the findings of the culture experiments, these findings suggest that H3K4me3 is a repressive mark for the *eas*/*ltm* genes and its removal by KdmB is required to allow complete derepression of the genes *in planta*.

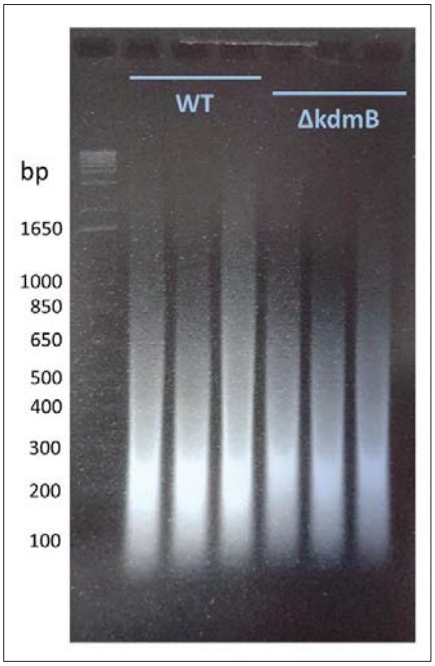


**Figure 4. 19 Average size of DNA fragments used for plant ChIP.** Chromatin isolated from ryegrass pseudostem infected of WT and Δ*kdmB* was sonicated (Section 2.5.5) and DNA was isolated from 20 µg chromatin and separated on a 1.5% agarose gel. The majority of sheared DNA fragments were within 100-1000 bp.

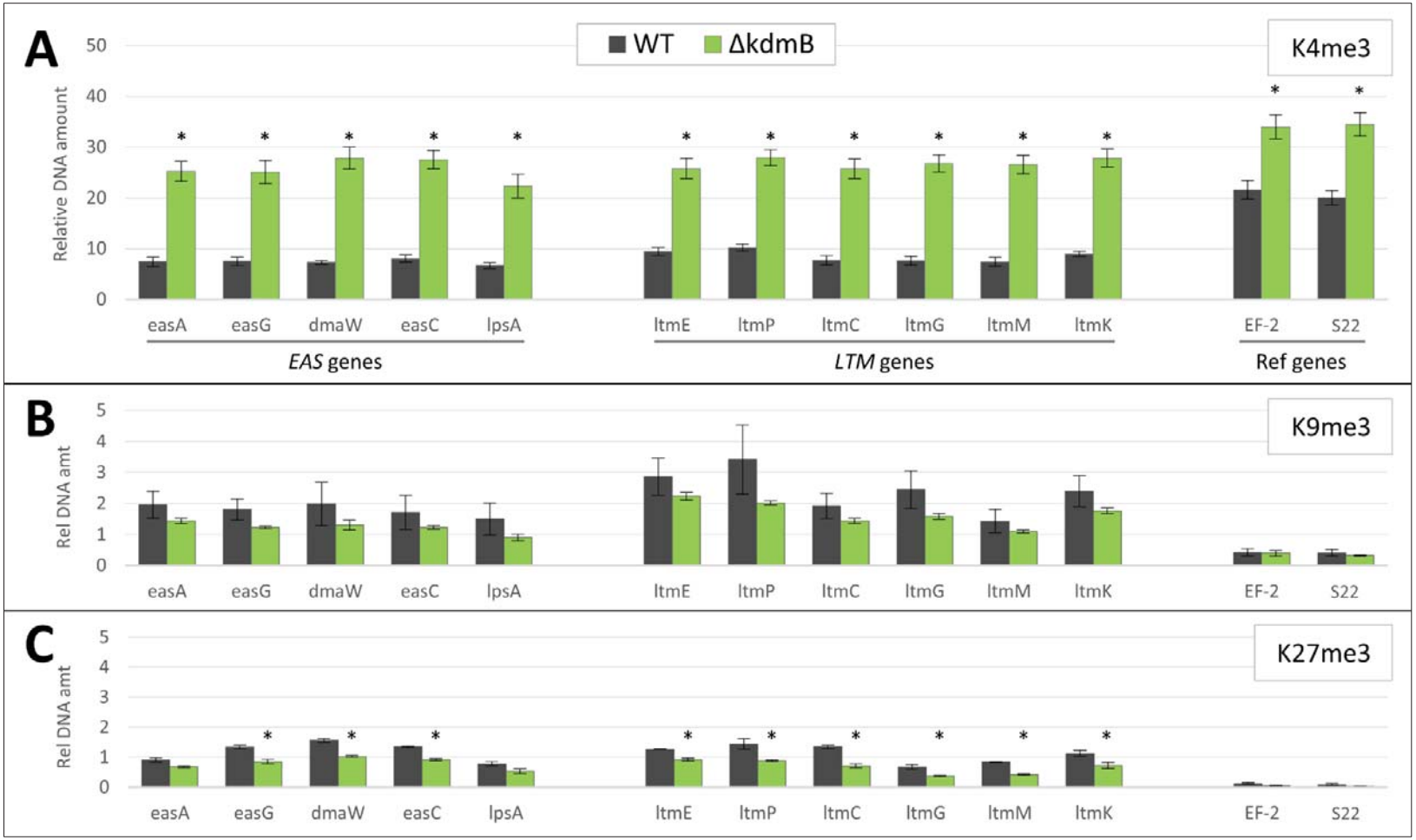


**Figure 4. 20. The *eas* and *ltm* genes are targeted for H3K4me3 demethylation by KdmB *in planta*.** (A) H3K4me3, (B) H3K9me3 and (C) H3K27me3 levels at promoter regions of the genes were analysed ChIP-qPCR. ChIP was performed on chromatin obtained from nuclear fractions of infected ryegrass pseudostem at 16 weeks post-inoculation and immunoprecipitated DNA was quantified relative to input by qPCR. Antibodies and primers used are provided in Table 2.4. Bars represent ± SEM (n = 3). *$P < 0.05$ (two-tailed t-test).

*4.2.8 Role of KdmB in regulating other telomeric genes.*

In this study, the importance of H3K4me3 in telomeric silencing and the role of the H3K4me3 demethylase KdmB in counteracting this was demonstrated by looking at two clusters (*EAS* and *LTM*) located about 10 kb from the telomeres of chromosomes I and III in *E. festucae*. Other studies in yeast have shown similar roles for KdmB by using reporter genes that were integrated proximal to one or two telomeres (Liang *et al*., 2007; Ryu & Ahn, 2014). However, it is not known if KdmB or H3K4me3 regulate telomere silencing across all telomeres in general or if it is locus-dependent. To address this question in *E. festucae*, the expression of subtelomeric genes from several chromosomes was analysed in the Δ*kdmB* mutant. To this end, genes located up to 50 kb from the fourteen telomeres of the seven *E. festucae* chromosomes were first identified, this was enabled by the recent chromosomal assembly of the *E. festucae* genome (Winter *et al*., unpublished). Subsequently, one gene on each chromosome arm was selected that lies closest to the telomere but which has a significant upregulation *in planta* vs. in culture in the transcriptome data set (Chujo *et al*., unpublished). Due to these selection factors, only eleven genes out of the fourteen telomeres in the fungus fit the criteria. These genes lie anywhere from 1.6 to 50 kb from the telomere. The expression levels of these genes were then determined in the Δ*kdmB* mutant *in planta* to test if derepression of these genes is lost.

The analysis showed that out of the eleven genes, eight had reduced expression in the Δ*kdmB* mutant compared to the wild-type (Fig. 4.21). With the remaining three genes, one was not downregulated, and two were downregulated but could not be complemented with the wild-type gene. As a comparison, the expression of three of the most highly expressed fungal genes *in planta* were analysed, these genes are similarly silent in culture and preferentially expressed *in planta* (Chujo *et al*., unpublished). None of these genes are telomeric (Winter *et al*., unpublished), and interestingly, all three are predicted to encode small and secreted proteins. The first, *gigA*, encodes a secreted protein that is further processed into small octa- and nona-cyclic peptides (Johnson *et al.*, 2013b) and has a fold-difference in expression (in *planta* vs. in culture) of 9,500 and accounts for approximately 6% of the total fungal steady-state level of transcripts *in planta*. The other two, *sspA* and *sspM*, are also predicted to be small secreted proteins and have fold differences in expression of 12,000 and 7,500 times and account for ~1% and ~0.3% of total fungal steady state level of transcripts *in planta*, respectively. Despite the high level of expression of these genes *in planta* compared to culture, their expression did not depend on KdmB (Fig. 4.21). The expression levels of *gigA* and *sspM* were not different between the wild-type, Δ*kdmB* and Δ*kdmB*/*kdmB* strains, however, the expression of *sspA* was unexpectedly reduced in the complement strain, suggesting that KdmB may act to repress the gene, although as previously determined, the complement strain has a single copy integration of *kdmB*, and expresses the gene at a similar level as the wild-type strain (Fig. 4.15). Given that the wild-type strain did not show similar repression of *sspA*, and the *kdmB* deletion strain did not show the opposite derepression, the observed repression of *sspA* in the complement strain was likely not a function of KdmB. It is possible that the complement strain has a disruptive integration of the construct into a gene that encodes a regulator of *sspA* expression, or that the results are due to variations in the host plant genotypes. Taken together, these results show that proper activation of most subtelomeric genes depend on KdmB, and suggest that KdmB counteracts telomeric silencing at telomeric genes in general. However, a more comprehensive analysis with e.g. RNAseq is required to confirm this hypothesis.

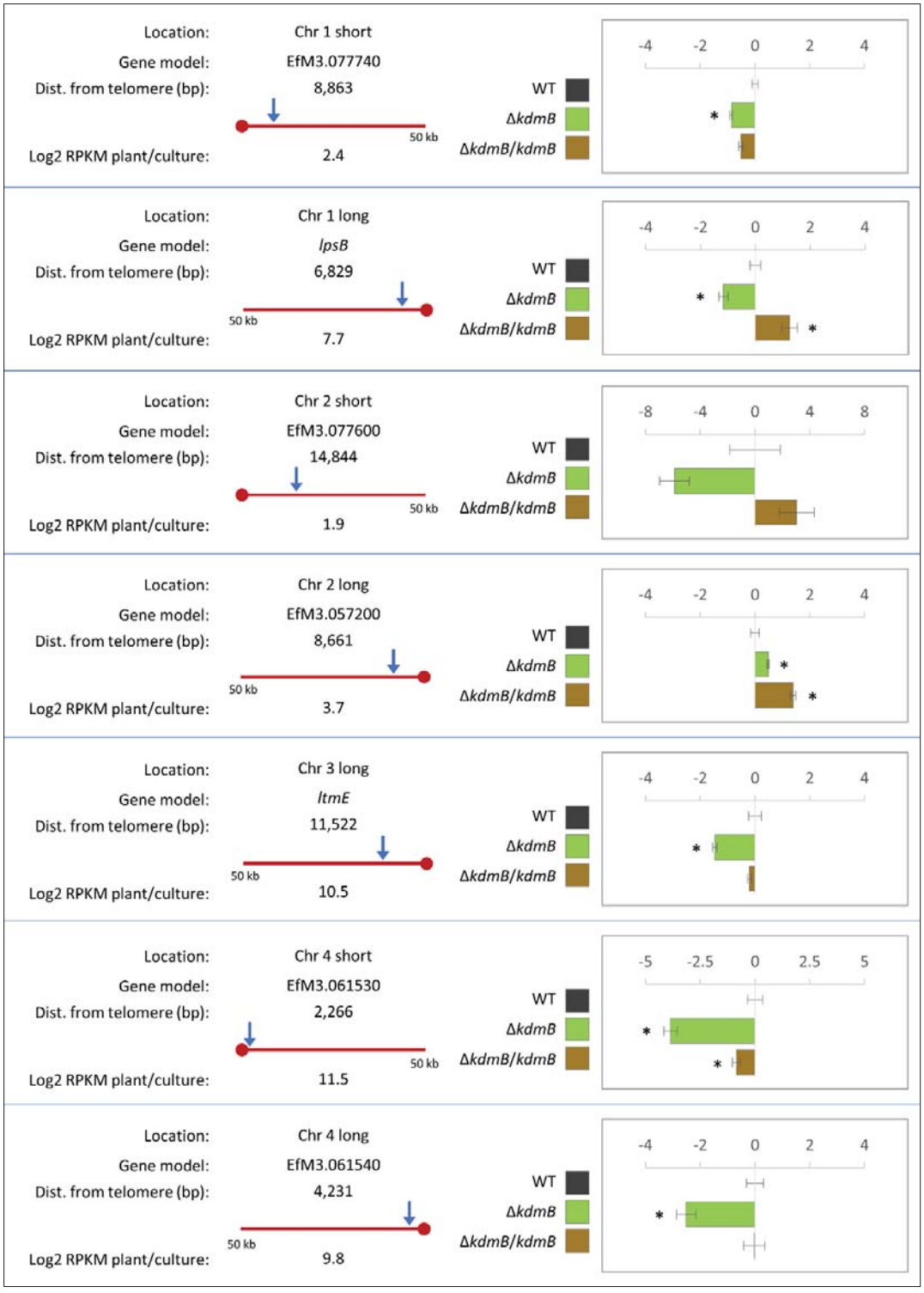
Location:
Chr 1 short
Gene model:
EfM3.077740
Dist. from telomere (bp):
8,863
50 kb
Log2 RPKM plant/culture:
2.4
WT
ΔkdmB
ΔkdmB/kdmB
-4 -2 0 2 4
Location:
Chr 1 long
Gene model:
lpsB
Dist. from telomere (bp):
6,829
50 kb
Log2 RPKM plant/culture:
7.7
WT
ΔkdmB
ΔkdmB/kdmB
-4 -2 0 2 4
Location:
Chr 2 short
Gene model:
EfM3.077600
Dist. from telomere (bp):
14,844
50 kb
Log2 RPKM plant/culture:
1.9
WT
ΔkdmB
ΔkdmB/kdmB
-8 -4 0 4 8
Location:
Chr 2 long
Gene model:
EfM3.057200
Dist. from telomere (bp):
8,661
50 kb
Log2 RPKM plant/culture:
3.7
WT
ΔkdmB
ΔkdmB/kdmB
-4 -2 0 2 4
Location:
Chr 3 long
Gene model:
ltmE
Dist. from telomere (bp):
11,522
50 kb
Log2 RPKM plant/culture:
10.5
WT
ΔkdmB
ΔkdmB/kdmB
-4 -2 0 2 4
Location:
Chr 4 short
Gene model:
EfM3.061530
Dist. from telomere (bp):
2,266
50 kb
Log2 RPKM plant/culture:
11.5
WT
ΔkdmB
ΔkdmB/kdmB
-5 -2.5 0 2.5 5
Location:
Chr 4 long
Gene model:
EfM3.061540
Dist. from telomere (bp):
4,231
50 kb
Log2 RPKM plant/culture:
9.8
WT
ΔkdmB
ΔkdmB/kdmB
-4 -2 0 2 4


**Figure 4. 21. Expression of subtelomeric genes and other highly expressed genes in the Δ*kdmB* mutant *in planta*.** Loss of *kdmB* resulted in reduced expression of some subtelomeric genes *in planta* but not in other highly expressed genes. Location of the genes with respect to the telomere is shown by the blue arrows. Figures are drawn to scale. Steady state transcript levels of the genes in pseudostem of infected perennial ryegrass were analysed by RT-qPCR and normalised to that of the 40S ribosomal protein S22 reference gene. Bars represent log2 ± SEM (n = 3). *$P < 0.05$ (two-tailed T-test).

*4.2.9 CclA and KdmB are not required for the symbiotic interaction of E. festucae with its host.*

Having established the roles of these proteins in regulating the symbiotically important secondary metabolites, the role of these proteins in regulating symbiosis of *E. festucae* with its host, *L. perenne* was analysed. Examination of perennial ryegrass plants infected with Δ*cclA* and Δ*kdmB* mutants indicated that none of the strains gave rise to host phenotypes that were different from those infected with the wild-type strain (Fig. 4.22). Consistent with the previous results (Fig 3.22), no change in the host plant phenotype was observed with the *kdmB* overexpression strains. However, analysis of tiller height and number of the plants showed that in comparison to the wild-type infected plants, Δ*kdmB* and *kdmB*-OE infected plants had longer tillers, while Δ*kdmB*-infected plants had fewer tillers (Fig. 4.23). These differences were statistically significant but were mild and not apparent at the whole plant level of examination. In addition, analysis of the pseudostem tissue by confocal microscopy did not reveal any change in the cellular phenotypes of the Δ*cclA* and Δ*kdmB* mutants *in planta* (Fig. 4.24). Therefore, taken together, these results suggest that regulators of H3K4me3 in *E. festucae*; CclA and KdmB are not important for the establishment or maintenance of the symbiotic interaction of *E. festucae* with perennial ryegrass.


**Figure 4. 22. Regulators of H3K4 methylation in *E. festucae* are not important for symbiosis.** Whole plant phenotype of perennial ryegrass plants infected with the indicated strains at 16 weeks post inoculation. Plants were grown under controlled environment conditions (Section 2.11.2) and infection status was confirmed by immunoblotting (Section 2.11.3).

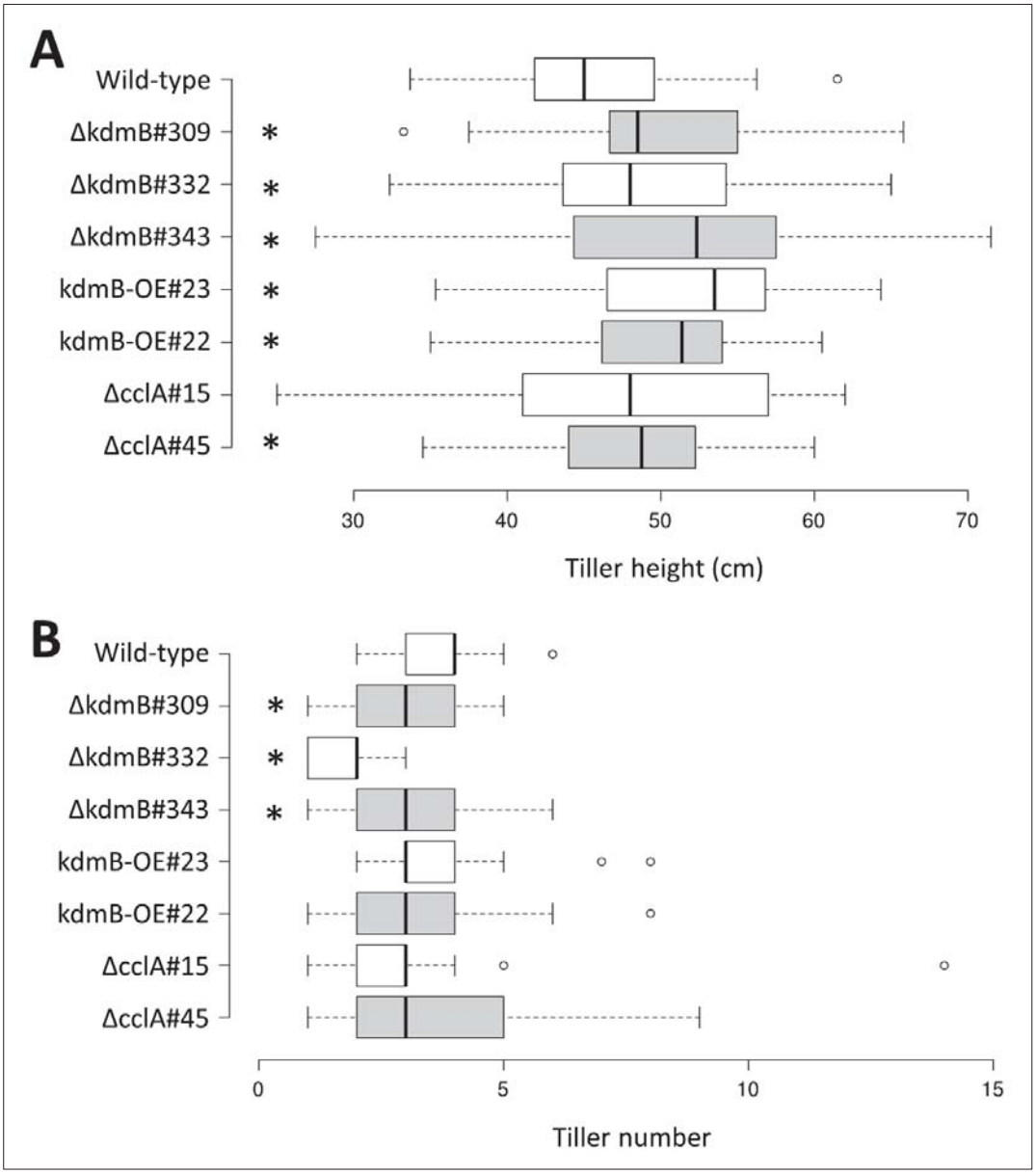


**Figure 4. 23. Tiller analysis of plants infected with H3K4me3 mutants.** (A) Boxplot of the tiller height of infected plants. (B) Boxplot of tiller number of infected plants. Plants were analysed at 16 weeks post inoculation. *P = <0.05 (two-tailed t-test).

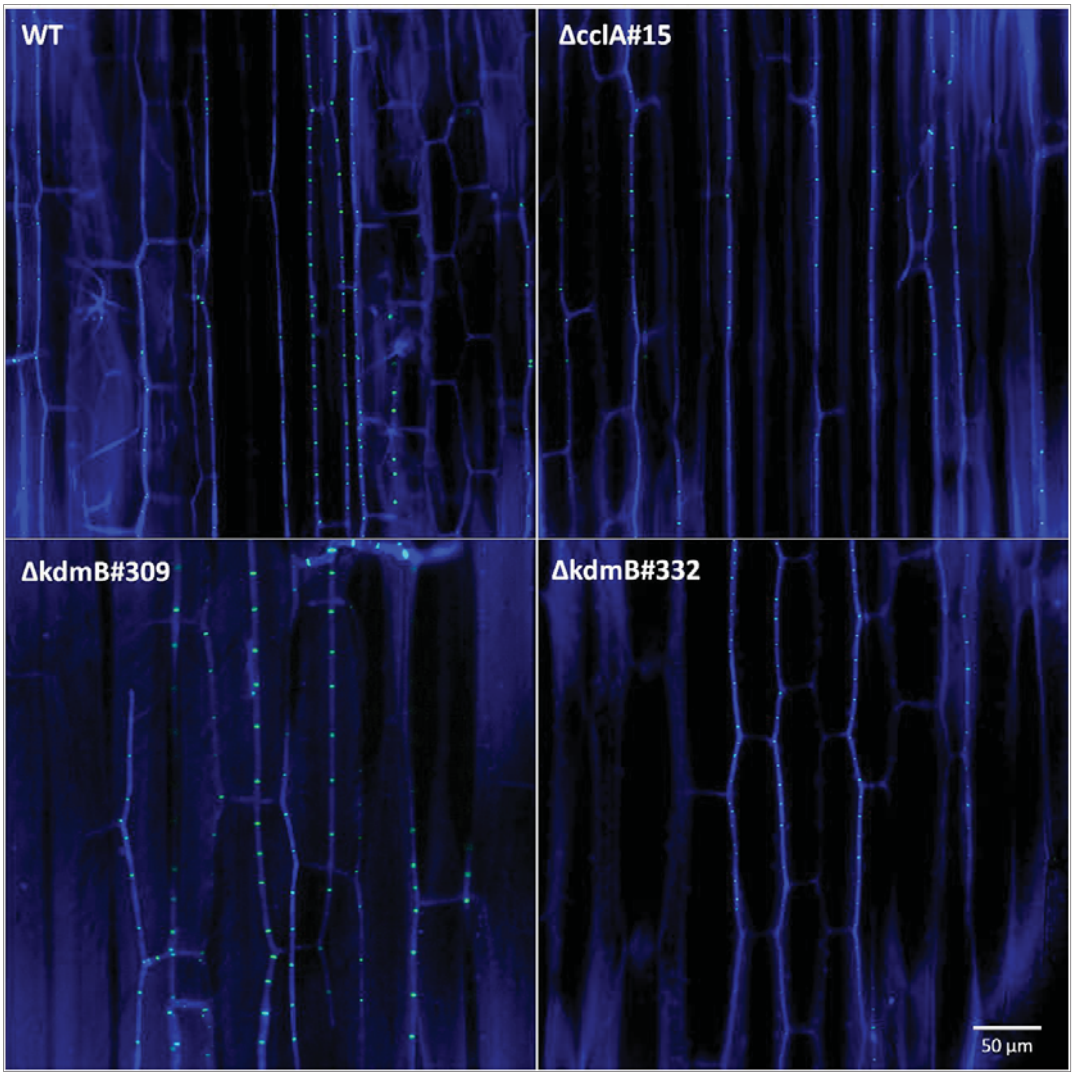


**Figure 4. 24. Hyphal morphology of *cclA* and *kdmB* mutants in planta.** Confocal depth series images of longitudinal pseudostem sections of plants infected with the indicated strains at 16 weeks post inoculation. Images are 5 µm maximum intensity projections (Z-stacks) of composite images. Aniline blue was used to stain fungal cytoplasm, visualised in blue; and WGA/AlexaFluor488 was used to stain fungal septa, visualised in green.

### 4.3 Discussion

In this study, deletion of *cclA* in *E. festucae* which caused the specific reduction in global H3K4me3 levels also resulted in the derepression of the subtelomeric *eas* and *ltm* genes in culture. The role of COMPASS and H3K4 methylation in telomeric silencing was first observed in the initial characterisation of Set1 (Nislow *et al*., 1997). More detailed studies revealed that mutants of the COMPASS complex were similarly defective in telomeric silencing, but importantly, this defect correlated with the ability of the mutants to methylate H3K4. Krogan *et al*. (2002) showed that mutants of COMPASS subunits that still maintain H3K4 methylation retained the ability to silence a subtelomeric reporter gene, but mutants lacking H3K4 methylation were severely disrupted in telomeric silencing. Deletion of *set1* or substitution of lysine 4 of histone H3 to arginine (H3K4R) resulted in defects in rDNA silencing (Bryk *et al*., 2001), and in addition, only *set1* constructs that restored H3K4 methylation could rescue the rDNA silencing defects in a Δ*set1* mutant (Briggs *et al*., 2001). Fingerman *et al*. (2005) additionally showed that H3K4me3 is specifically required for proper silencing of the rDNA and telomeric loci. Most of these studies utilised yeast strains that have the *URA3* gene inserted ~20 kb from the end of chromosome VII as a reporter gene (Gottschling *et al.*, 1990). By comparison, the first genes of the *EAS* and *LTM* clusters in *E. festucae*, *lpsB* and *ltmE*, respectively, lie ~10 kb from the ends of chromosomes I and III, while the entire clusters which each comprise 11 genes are up to ~90 kb from the telomeres (Fig. 1.1). Therefore, these clusters, which are tightly silenced in axenic culture conditions may serve as an equally, if not more effective tool for the study of telomeric silencing.

Derepression of almost all of the *eas* and *ltm* genes in culture was observed in the Δ*cclA* mutant, and measurement of H3K4me3 levels at these genes showed significantly lower levels of the mark in the mutant. On the other hand, the levels of H3K9me3 and H3K27me3, marks which have been shown to repress these genes (Chujo & Scott, 2014), were unaffected by *cclA* deletion. This suggests that derepression of the genes in the Δ*cclA* mutant was brought about specifically by the reduction in H3K4me3 levels. Nevertheless, these results do not exclude the possibility that CclA additionally regulates these genes via H3K4me3-independent pathways, further studies dissecting the roles of CclA domains would clarify this. Only a single SPRY domain is identifiable in CclA and its yeast/metazoan homologues. This domain of CclA is highly conserved across kingdoms, and is thought to be important for protein-protein interactions. The human homologue of CclA, ASH2L, functions as a heterodimer with RbBP5 (homologue of yeast Swd1) and surprisingly, a H3K4-methyltransferase activity was detectable in the ASH2L/RbBP5 complex, while a weak H3 methyltransferase activity was detected in just the SPRY domain of ASH2L and a short RbBP5 peptide (Cao *et al*., 2010). In addition, stoichiometric analysis indicated that all cellular Bre2 (CclA) in yeast is incorporated into the COMPASS complex (Roguev *et al*., 2001). Given these findings, it is likely that CclA represses the *eas* and *ltm* genes in *E. festucae* by maintaining repressive levels of H3K4me3 at these genes, and not by H3K4me3-independent means.

It was then hypothesised that if H3K4me3 is acting as a repressive mark at these SM loci, these marks would need to be removed for derepression *in planta*. Subsequent analysis of the Δ*kdmB* mutant *in planta* showed that in the absence of the demethylase, there was a lower expression of the *eas* and *ltm* genes. In line with the inability of the mutant to demethylate H3K4me, this reduction in gene expression was also accompanied by accumulation of H3K4me3 at the gene promoter regions. These results are consistent with a repressive role of H3K4me3 at the SM genes. However, H3K4me3 levels at the

housekeeping genes, including those genes used for RT-qPCR normalisation were similarly increased in the Δ*kdmB* mutant. It was not possible to test if this increase resulted in any change in the gene expression, as all of the genes analysed similarly had an increase in H3K4me3 levels. However, in culture, H3K4me3 levels at the *EF-2* gene was higher in the wild-type strain compared to the Δ*cclA* mutant but this did not lead to a change in the expression of the gene. In addition, *40S22* and *EF-2* were initially selected as reference genes due to their stabile expression in wild-type *E. festucae* as well as in the Δ*sakA*, Δ*noxA*, Δ*proA* and Δ*hepA* mutants, all of which had a profound change in the symbiotic interaction phenotype and caused severe stunting of the host plants. With the exception of Δ*proA*, these mutants also had significant changes in secondary metabolite gene expression *in planta*, but nevertheless stabile expression of *40S22* and *EF-2* (Chujo & Scott, 2014; Eaton *et al*., 2015). Thus, it is considered unlikely that expression of the reference genes was altered in the Δ*kdmB* strain.

Analysis of H3K9me3/K27me3 levels in the Δ*kdmB* mutant showed that there was no concomitant increase in these repressive marks that could account for the reduced SM gene expression, suggesting that the downregulation of these genes is due to the higher levels of H3K4me3. Active marks such as histone H3 acetylation were not analysed in this study, thus the possibility cannot be excluded that the observed transcriptional changes are due to changes in activating marks. Notably, interactions between mammalian KDM5A, KDM5B and *Drosophila* Lid with histone deacetylases (HDACs) and HDAC-interacting proteins have been documented (Hayakawa *et al.*, 2007, Moshkin *et al.*, 2009, Xie *et al.*, 2011). Deletion of *kdmB* in *A. nidulans* was also found to increase total H3 acetylation in this fungus (Gacek-Matthews *et al*., 2016). Hence, it is possible that KdmB regulates the *eas*/*ltm* genes by other mechanisms independent of H3K4me3-demethylation, such as by indirectly influencing H3 acetylation. However, HDACs can also be recruited by methylated H3K4. The yeast Rpd3L HDAC complex is recruited by H3K4me2/me3 via the plant homeodomains (PHDs) of Pho23 and Cti6, and the deacetylation activity of the HDAC complex is essential for the Set1-mediated repression of the *PHO5* gene (Wang *et al.*, 2011). H3K4me3 also recruits the mSin3a-HDAC1 complex via the PHD of ING2 (inhibitor of growth) that is subsequently required for repression of cyclin D1 following DNA damage (Shi *et al*., 2006). Finally, the Rpd3S HDAC complex is recruited by H3K4me2/me3 for Set1-mediated repression of *GAL1* (Pinskaya *et al.*, 2009). It is therefore possible that similar mechanisms are in play in the repression of *eas*/*ltm* genes caused by deletion of *kdmB* and subsequent H3K4me3 accumulation. It would be interesting to test if introduction of a demethylase-inactive KdmB into the Δ*kdmB* mutant can rescue the downregulation of *eas*/*ltm* gene expression, thus determining whether KdmB regulates these genes via a H3K4me3-dependent manner.

As expected, the downregulation of *ltm* genes in the Δ*kdmB* mutant resulted in a significant reduction in the levels of a number of intermediates and final products of lolitrem B biosynthesis *in planta*. By comparison, there was little to no difference in the production of the ergot alkaloid pathway metabolites between the wild-type and Δ*kdmB* strain. One possible explanation for this result is the fact that the *eas* genes are expressed at several orders of magnitudes lower than the *ltm* genes, hence the reduction in *eas* genes transcripts caused by *kdmB* deletion is much lower than the reduction in *ltm* transcripts. The levels of the third known class of *E. festucae* secondary metabolite, peramine, was not affected by deletion of *kdmB*. Given that the metabolite levels do not change it is likely that expression of the peramine biosynthetic gene, *perA*, is similarly unaffected though this was not measured. Unlike the *eas* and *ltm* genes, *perA* is not found subtelomerically in *E. festucae* (Winter *et al*., unpublished), suggesting that KdmB preferentially regulates subtelomeric secondary metabolite genes in *E. festucae*. This is further supported

by results of the subtelomeric gene expression analysis. Out of the eleven subtelomeric genes selected from each chromosome end, ten were found to require KdmB for their full expression, suggesting that KdmB preferentially induces the expression of subtelomeric genes. It would be interesting to measure the levels of H3K4me3 at these genes to confirm if KdmB also upregulates these genes by demethylating H3K4me3. These findings are consistent with those previously reported in yeast, in which deletion of *jhd2* silences the subtelomerically-integrated *URA3* reporter gene, while overexpression of *jhd2* activates the gene (Liang *et al*., 2007; Ryu & Ahn, 2014).

H3K4me3 is a mark intimately associated with gene transcription (Santos-Rosa *et al*., 2002), however studies to date have yet to provide concrete evidence for an instructive role of H3K4me3 on gene transcription. Consequently, it has been suggested that rather than being a causative mark, trimethylation of histone H3K4 may rather be a consequence of active gene transcription (Howe *et al.*, 2017). On the other hand, an increasing number of studies have reported a repressive role of H3K4 methylation, particularly at silent loci, but also at euchromatic genes such as *PHO5* and *GAL1* in *S. cerevisiae* (Carvin & Kladde, 2004). The repressive role of H3K4me3 may be due to the ability of the mark to recruit proteins involved in gene repression such as HDACs, but also chromatin remodelling complexes such as Isw2p that functions as transcriptional repressors (Goldmark *et al.*, 2000, Santos-Rosa *et al.*, 2003). Taken together, this study provides strong evidence for a repressive role of H3K4me3 at subtelomeric secondary metabolite loci in a mutualistic fungal symbiont. In culture, the *E. festucae* COMPASS subunit CclA promotes trimethylation of H3K4 at subtelomeric *eas*/*ltm* genes which contribute to gene repression, while *in planta*, these marks are removed by the H3K4me3 demethylase KdmB to allow for complete derepression of the genes (Fig. 4.25). Deletion or overexpression of *kdmB* did not affect the culture and symbiotic interaction phenotypes of *E. festucae*, indicating that the protein is a specific regulator of telomeric and secondary metabolite genes.

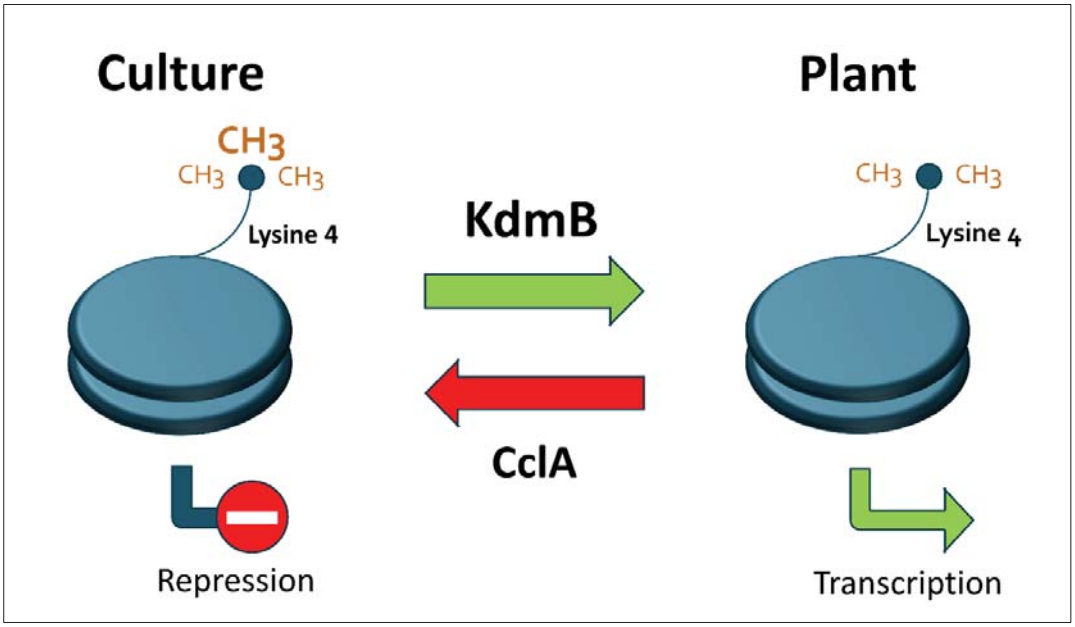


**Figure 4. 25. Model showing regulation of subtelomeric *eas* and *ltm* genes in *E. festucae* by CclA, KdmB and H3K4me3.** In culture, CclA mediates H3K4 trimethylation at the promoter regions of the *eas* and *ltm* genes, and this leads to repression of the genes. *In planta*, where the genes are massively upregulated, H3K4me3 at the gene promoters are demethylated by KdmB to allow for derepression of the genes.

# Chapter 5: SetB, an H3K36me3 methyltransferase is required for *E. festucae* to infect perennial ryegrass.

## 5.1 Introduction

The phylogenetic analysis in Chapter 3 showed that *E. festucae* Jmj4 is most similar to mammalian KDM8, a demethylase specific for H3K36me2 (Hsia *et al*., 2010) (Fig. 3.10). The proteins share a high degree of amino acid identity in the JmjC domains as well as the full-length sequences (Fig. 3.2). This suggests that Jmj4 is likely a homologue of KDM8 despite the fact that there was no change in any of the common methylation marks in an overexpression mutant of this strain (Fig 3.16).

JMJD5 (KDM8) was initially identified as a candidate in a tumour suppressor screen (Suzuki *et al.*, 2006). The protein was subsequently shown to demethylate the repressive H3K36me2 mark at the cyclin A1 gene to activate its transcription, thus KDM8 is thought to have a role in the regulation of cell cycle progression (Hsia *et al*., 2010). In fungi, methylation of H3K36me1, me2 and me3 are catalysed by the SET domain–containing protein Set2. Set2 in budding yeast is not essential (Strahl *et al*., 2002). In fission yeast, deletion of *set2* resulted in increased susceptibility to DNA damage (Pai *et al.*, 2014), while in *N. crassa*, disruption of *set2* or an H3K36L substitution resulted in developmental defects, poor conidiation and sterility (Adhvaryu *et al*., 2005). These results suggest that Set2 and H3K36 methylation have important functions in fungal development.

In this chapter, the roles of Jmj4, SetB and H3K36 methylation in *E. festucae* development and symbiotic interaction phenotype were investigated through the use of deletion and overexpression strains of *jmj4* and *setB* (homologue of *set2*).

## 5.2 Results

### *5.2.1 Generation of E. festucae Δjmj4 and ΔsetB mutants.*

In order to further characterise Jmj4, the gene was deleted in *E. festucae* by replacement with the geneticin resistance gene. Out of approximately 150 transformants screened, one was a 'clean' deletion mutant (Δ*jmj4*#72), and another (Δ*jmj4*#68) a 'clean' mutant with tandem insertion of the construct, as shown by Southern blot analysis (Fig. 5.1).

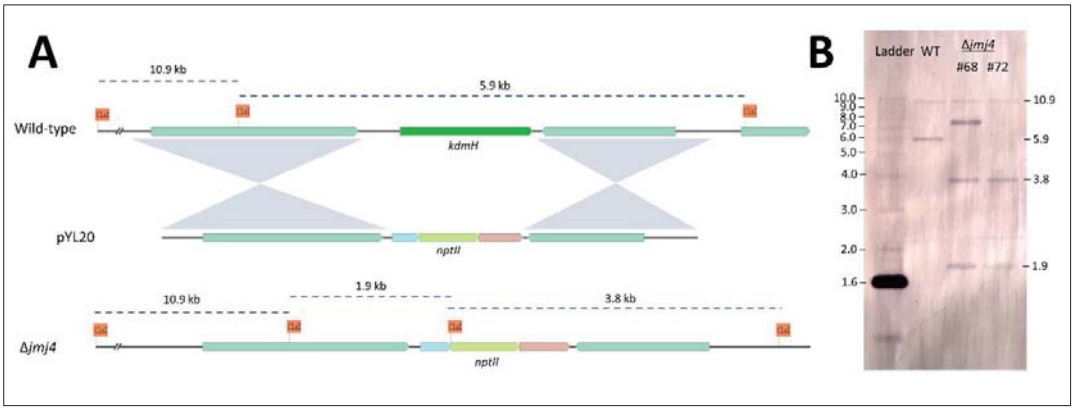


**Figure 5. 1. Strategy for deletion of *jmj4* in *E. festucae* and confirmation by Southern blot analysis.** (A) Physical map of the wild-type *jmj4* genomic locus, linear insert of *jmj4* replacement construct pYL20, and the Δ*jmj4* mutant locus, showing restriction sites for *Cla*I and homologous regions. (B) NBT/BCIP stained Southern blot of *Cla*I genomic digests (1 µg) of *E. festucae* wild-type and Δ*jmj4* deletion strains probed with digoxigenin (DIG)-11-dUTP labelled linear product of pYL20. Sizes in kilobases of hybridising bands are indicated on the left.

Given that Jmj4 is likely to be the H3K36me2-demethylase, the H3K36 methyltransferase was also identified in *E. festucae* in order to further characterise the role of H3K36 methylation in *E. festucae*. In both budding and fission yeast, as well as *N. crassa*, H3K36 methylation is catalysed by the SET domain containing protein Set2 (Strahl *et al*., 2002; Adhvaryu *et al*., 2005; Morris *et al*., 2005). A tBLASTn search performed using Set2 from *S. cerevisiae* identified a single homologue in *E. festucae*, designated as SetB. The protein shares 39% amino acid identity and similar domain structure and composition as is found in *S. cerevisiae* Set2 (Fig. 5.2A). *E. festucae* SetB contains the AWS (associated with SET), SET (catalytic), Post-SET and SRI (Set2-Rpb1-interacting) domains found in all Set2 proteins, and a WW (2x tryptophan) domain found in most Set2 proteins. Interestingly, *E. festucae* SetB additionally contains a TFS2N domain that in fungi seem to be conserved only in Set2 from *F. graminearum* and *N. crassa* (Fig. 5.2B). The TFS2N is one of the domains of the transcription elongation factor S-II (TFIIS) and is found at the N-terminal end of the protein.

The *setB* gene was subsequently deleted in *E. festucae* by replacement with the geneticin resistance gene. A single clean mutant was obtained out of about 80 transformants screened (Fig. 5.3). In addition, the *setB* gene was also overexpressed in *E. festucae*. To this end, two high-copy mutants, *setB*-OE#4 and #9 were selected for further experiments (Fig. 5.3C).

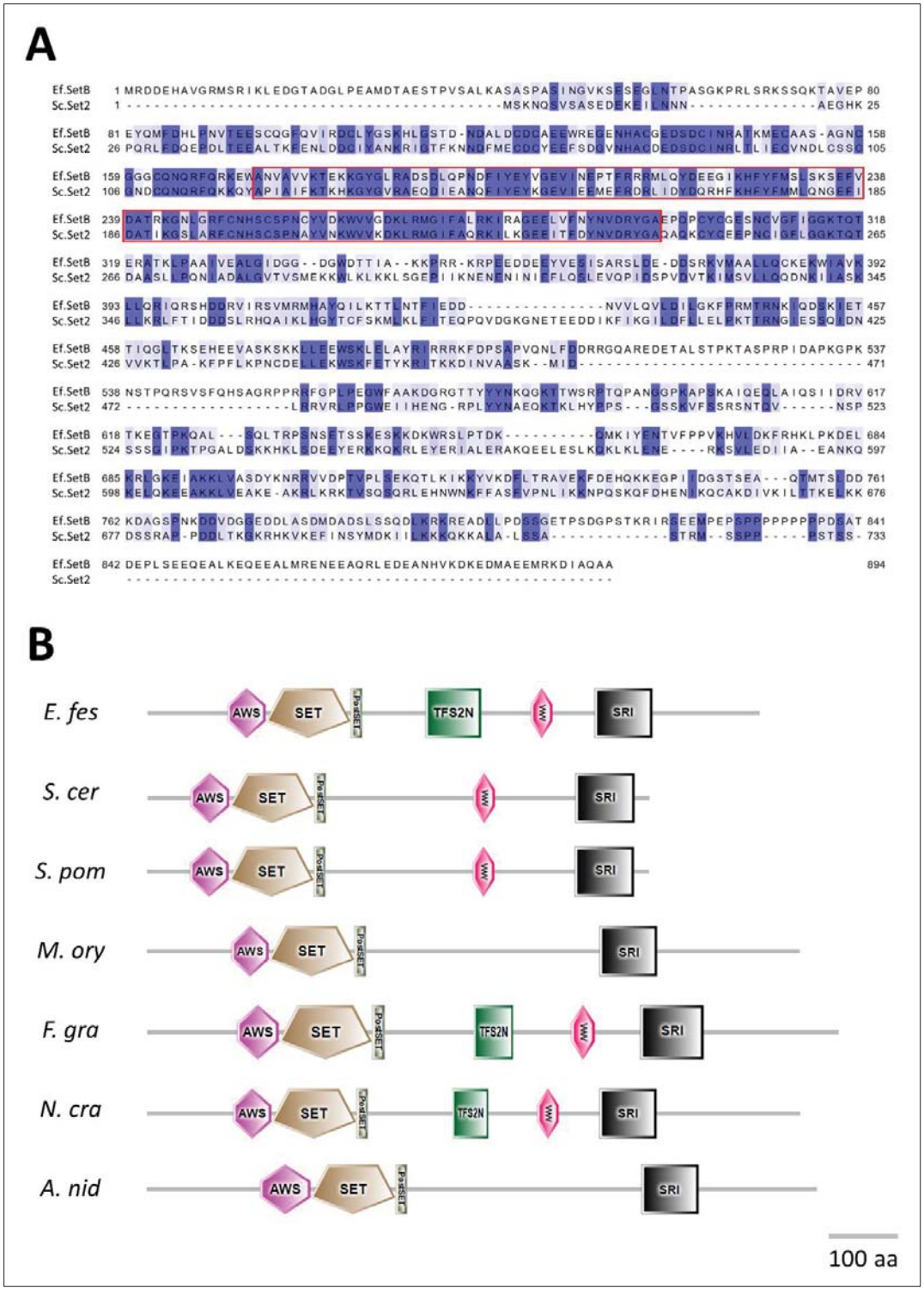


**Figure 5. 2 Similarity of *E. festucae* SetB with *S. cerevisiae* Set2.** (A) Amino acid alignment of SetB and Set2. The alignment was generated with Clustal Omega. Identical residues are shown in dark blue and conservative changes in lighter blue. The N-terminal SET domain is boxed in red. (B) Domain composition of *E. festucae* SetB and homologues from other fungi. Accession codes of the sequences shown are EfM3.042710 (Jmj4), Q8N371 (ScSet2), O14026 (SpSet2), G4MUF3 (MoSet2), Q4IB50 (FgSet2), Q7RZU4 (NcSet2) and Q5ASA5 (AnSet2).

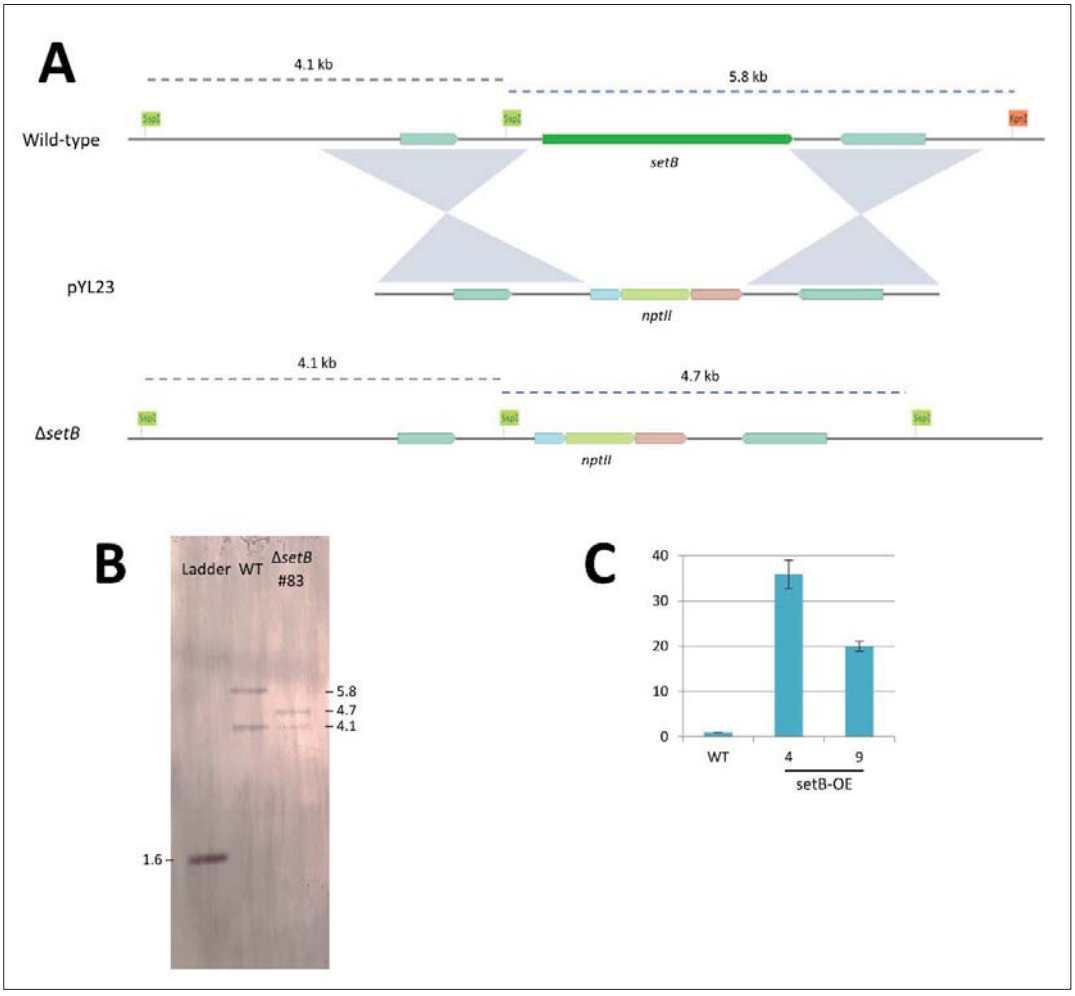


**Figure 5. 3. Strategy for deletion of *setB* in *E. festucae* and confirmation by Southern blot analysis.** (A) Physical map of the wild-type *setB* genomic locus, linear insert of *setB* replacement construct pYL20, and the Δ*setB* mutant locus, showing restriction sites and homologous regions. (B) NBT/BCIP stained Southern blot of *Kpn*I/*Ssp*I genomic digests (1 µg) of *E. festucae* wild-type and Δ*setB* deletion strains probed with digoxigenin (DIG)-11-dUTP labelled linear product of pYL23. Sizes in kilobases of hybridising bands are indicated on the left. (C) Copy number of *setB* overexpression strains as determined by qPCR relative to the copy number of *pacC*, shown relative to the wild-type. Error bars represent S.D. from two technical replicates. Primers used for the analyses are given in Table 2.4.

*5.2.2 SetB is required for normal development of E. festucae.*

To investigate the role of SetB in *E. festucae* development, radial growth of the strains was compared to the wild-type on PD agar. Deletion of *setB* was found to severely impact radial growth of *E. festucae* and introduction of the wild-type gene rescued this phenotype, showing this mutation could be complemented (Fig. 5.4). On the other hand, deletion of *jmj4* had no effect on radial growth of *E. festucae*. The culture phenotypes of *jmj4* overexpression strains were analysed previously (Fig. 3.14), and no difference was observed in colony radial growth and morphology of the mutants from wild-type.


**Figure 5. 4. Culture phenotype of H3K36 mutants.** Strains were cultured for 10 days on 2.4% PDA.

*5.2.3 SetB is required for H3K36 trimethylation in E. festucae.*

Knockdown of Setd2 in human and mice specifically reduces H3K36 trimethylation levels and not H3K36me1/me2 (Sun *et al.*, 2005, Edmunds *et al.*, 2008). By contrast, Set2 in *S. cerevisiae*, *S. pombe* and *N. crassa* is required for all forms of H3K36 mono-, di- and trimethylation (Strahl *et al*., 2002; Adhvaryu *et al*., 2005; Morris *et al*., 2005). Surprisingly, deletion of *setB* in *E. festucae* was found to specifically reduce, but not abolish H3K36me3, while H3K36me1 and me2 levels were not affected in the mutant. This suggests that the role of Set2 in regulating H3K36 methylation in *E. festucae* is drastically different than in other fungi, and also suggests the presence of another active H3K36 methyltransferase responsible for H3K36me1/me2 in *E. festucae* (Fig. 5.5). The effect of *jmj4* overexpression was re-analysed using two additional independent mutants to those used in Section 4.2.4, and no reduction in H3K36 marks was again observed in the strains (Fig. 5.5).


**Figure 5. 5. SetB is required for H3K36 trimethylation.** Histones were acid-extracted from nuclear fractions of *E. festucae* cultured in PD media, separated by SDS-PAGE and probed with the indicated primary antibodies (Table 2.2) and visualised with the ECL method.

*5.2.4 SetB is required for infectivity of E. festucae.*

Next, to determine the symbiotic phenotype of the mutants, the strains were inoculated into perennial ryegrass. At 12 weeks post-inoculation, pseudostem tissues of the plants were immunoblotted for presence of *E. festucae* to determine the infection status. Surprisingly, all plants inoculated with Δ*setB* consistently tested negative for infection in two independent experiments (Fig. 5.6A and B). Introduction of the wild-type gene into the Δ*setB* mutant re-established the infection phenotype (Fig. 5.6C). To confirm the absence of endophyte in these plants, ten Δ*setB*-inoculated plants were taken for further microscopy analysis. Samples were stained with wheat germ agglutinin, Alexa Fluor 488 conjugate (WGA-488), which binds to chitin in the fungal cell wall, and aniline blue that stains both plant and fungal cell wall by binding to callose and 1,3-beta-glucan. In the wild-type infected plants, fungal hyphae stained by aniline blue are visible with additional WGA-488 staining of the fungal septa, however, no fungal hyphae could be discerned in all 10 Δ*setB*-infected plant samples (Fig. 5.7). Hyphae could be identified in the Δ*setB* complement strain, similar to the wild-type strain. These results confirm that deletion of *setB* abolishes the ability of *E. festucae* to infect the host plant. On the other hand, overexpression of *setB*, deletion of *jmj4* and overexpression of *jmj4* (as determined previously) had no effect on the symbiotic interaction phenotype (Fig. 5.8). Tiller length and number of the plants were not significantly different between the Δ*jmj4*- and wild-type-infected plants, whereas tiller number of Δ*jmj4*#68- and tiller length of Δ*jmj4*#72-infected plants were significantly different. However, there were no significant differences for the other independent strains of the mutants (Fig. 5.9).

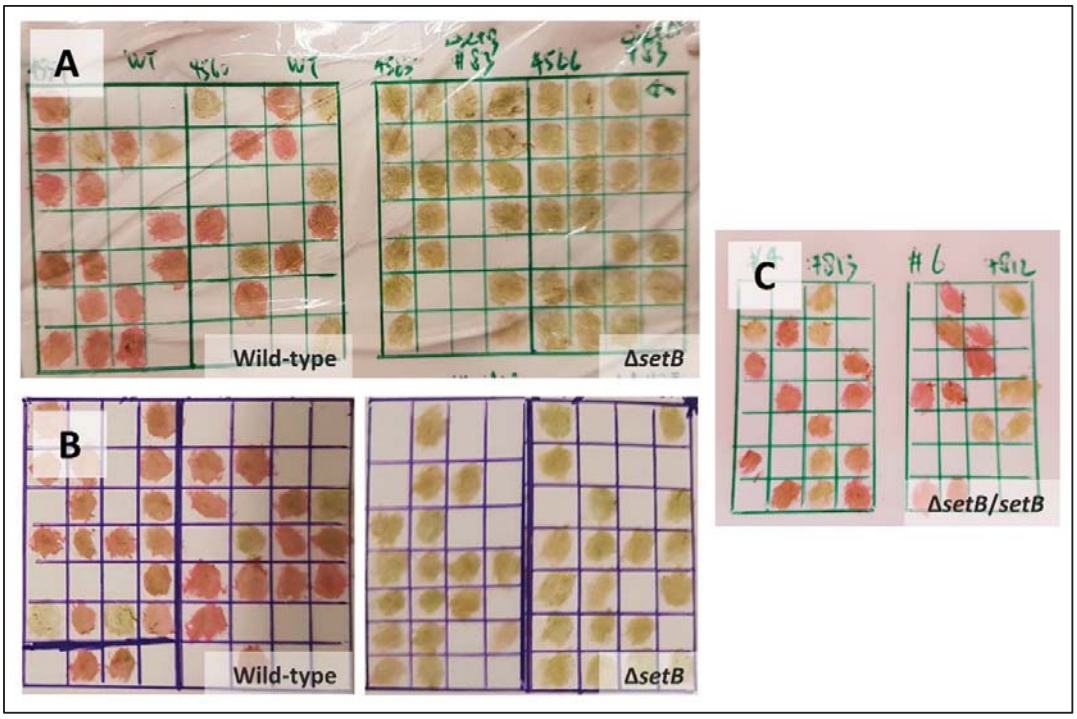


**Figure 5. 6. Immunoblot of Δ*setB* plants.** (A and B) Results of two independent inoculation experiments with wild-type and Δ*setB* mutant (C) Experiment with two independent Δ*setB*/*setB* complement strains (Δ*setB*/*setB*#4 and #6). Pseudostems were blotted onto nitrocellulose membrane and probed with antibody raised against *E. festucae*. Red pigment indicates presence of endophyte as determined by secondary alkaline phosphatase-conjugated antibody staining and Fast Red TR/Naphthol.

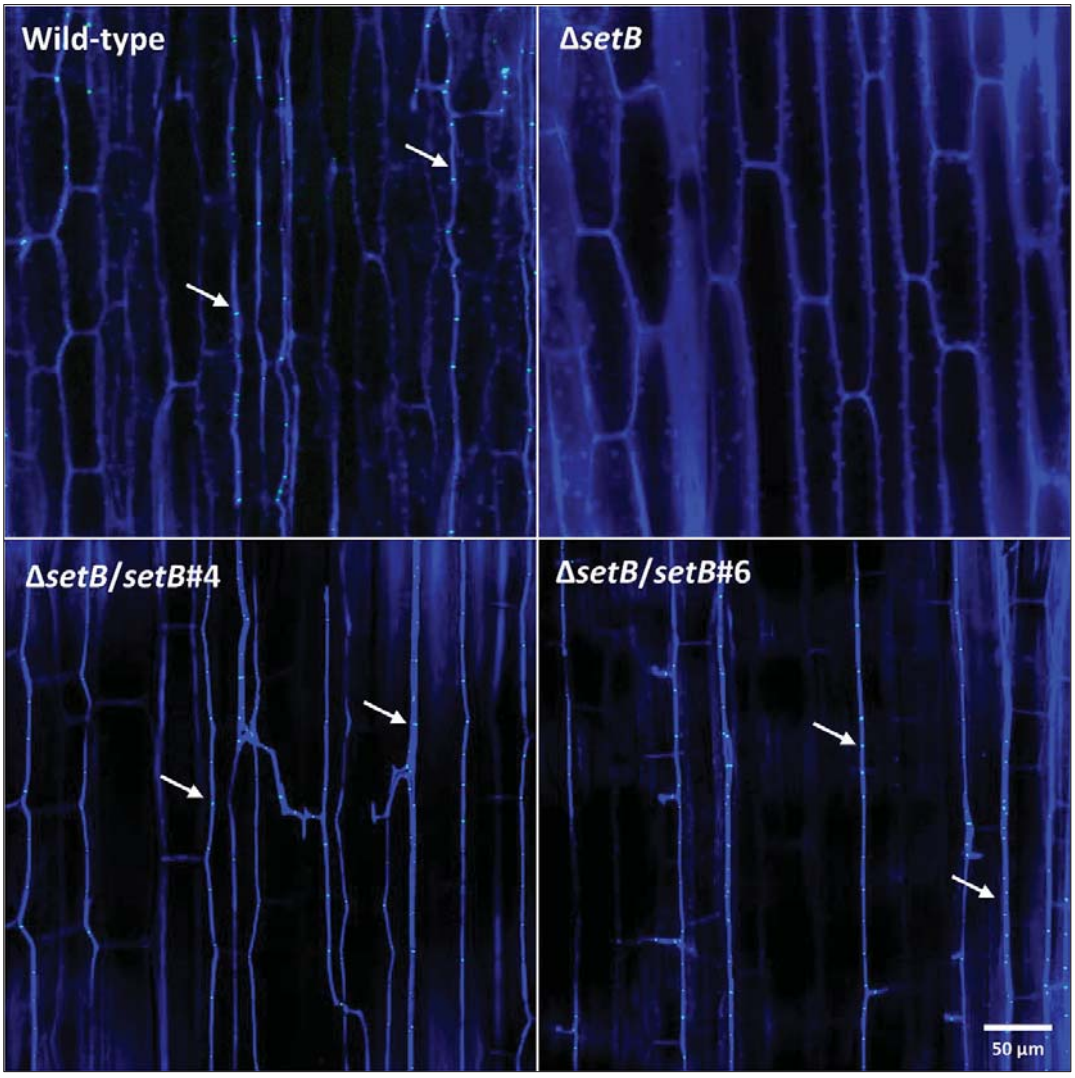


**Figure 5. 7. Confocal microscopy of plant samples inoculated with wild-type and Δ*setB* mutant.** Pseudostem samples were stained with aniline blue and wheat germ agglutinin-Alexa Fluor 488 conjugate and analysed by confocal microscopy. Image of Δ*setB* plant is representative of a total of 10 independent plant samples analysed. *E. festucae* hyphae are indicated by arrows. Images are 5 µm *z*-section and scale bar represents 50 µm.

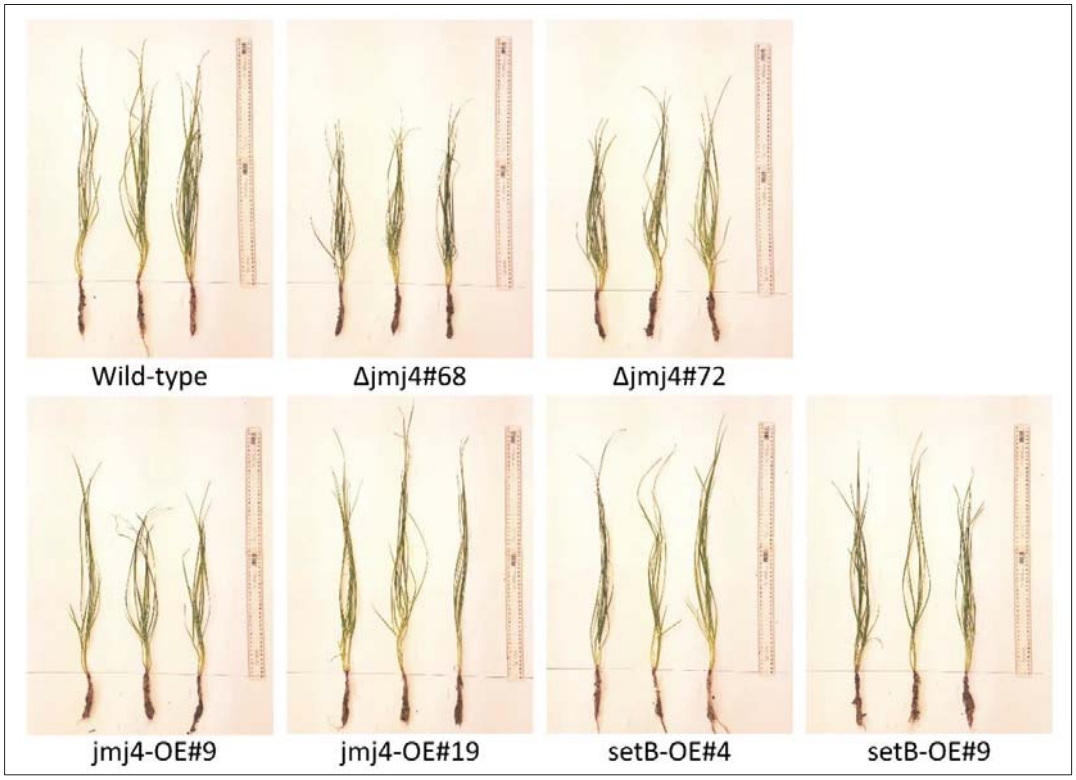


**Figure 5. 8. Phenotype of plants infected with *jmj4* and *setB*-OE strains.** Whole plant phenotype of perennial ryegrass plants infected with the indicated strains at 16 weeks post inoculation. Plants were grown under controlled environment conditions (Section 2.11.2) and infection status was confirmed by immunoblotting (Section 2.11.3).

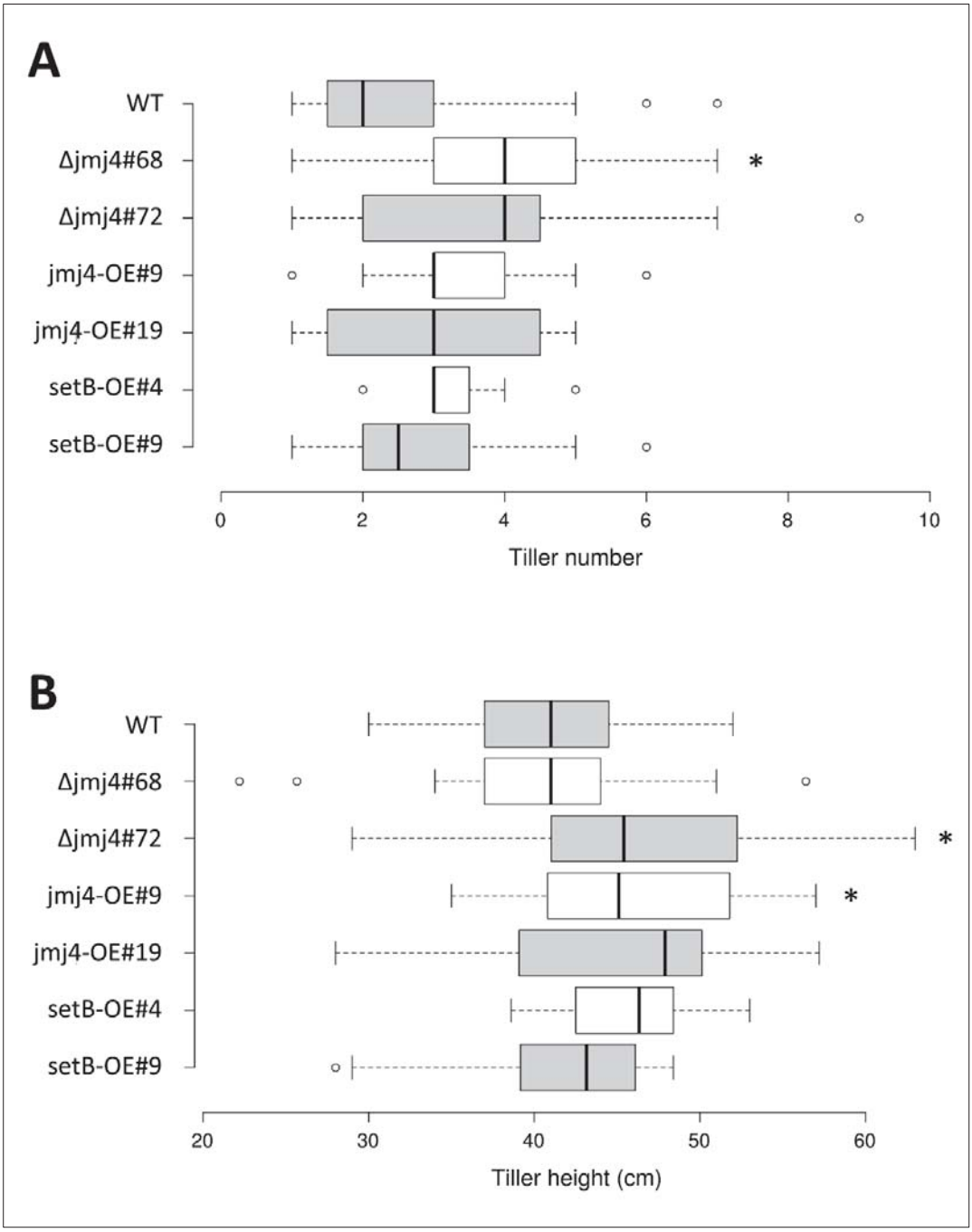


**Figure 5. 9. Tiller analysis of plants infected with *jmj4* and *setB*-OE strains.** (A) Boxplot of the tiller height of infected plants. (B) Boxplot of tiller number of infected plants. Plants were analysed at 16 weeks post inoculation. *$P$ = <0.05 (two-tailed t-test).

### 5.3 Discussion

In this study, *E. festucae* Jmj4, the most likely homologue of mammalian KDM8 was characterised. Although KDM8 is a demethylase specific for H3K36me2, no reduction in H3K36 methylation was found for the *jmj4* overexpression strains. Overexpression of Jmj proteins has been demonstrated to be a working strategy to identify candidate histone demethylases in *E. festucae*, as shown by the identification of KdmB as a H3K4me3-specific demethylase, and overexpression of KDM8 in mammalian cells similarly resulted in detectable reduction in global H3K36me2 levels (Hsia *et al*., 2010). However, as a previous study of KdmA in *A. nidulans* has shown, histone demethylases can exhibit locus-specific activity that is not apparent at the global histone level (Gacek-matthews *et al*., 2015). Therefore, it would be interesting to test the activity of Jmj4 at the gene level by ChIP, as well as on H3 peptides or nucleosomes *in vitro*. Deletion and overexpression of *jmj4* were not found to affect *E. festucae* development and symbiotic interaction phenotype, suggesting that Jmj4 is not important in these processes.

On the other hand, deletion of *setB* in *E. festucae* resulted in a severely reduced radial growth. Consistent with a developmental role of Set2, disruption of *set*-2 in *N. crassa* similarly resulted in poor growth, conidiation and infertility (Adhvaryu *et al*., 2005). Deletion of *kmt3* (*set2*) in *M. oryzae* similarly resulted in reduced growth and conidiation (Pham *et al*., 2015). In *N. crassa* and *S. cerevisiae* and *S. pombe*, Set2 is required for all forms of H3K36 mono-, di- and trimethylation (Strahl *et al*., 2002; Adhvaryu *et al*., 2005; Morris *et al*., 2005). However, western blot analysis of *E. festucae* Δ*setB* showed that Set2 in *E. festucae* is specifically required for H3K36me3 but not for H3K36me1/me2. This is in contrast to all other fungi analysed to date. In this respect, the role of *E. festucae* Set2 in H3K36 methylation also appears to be more similar to that of mammalian Setd2 proteins, which catalyse only H3K36 trimethylation *in vivo* (Sun *et al*., 2005; Edmunds *et al*., 2008). The specificity of *E. festucae* SetB for H3K36 trimethylation also suggests the presence of another active H3K36 methyltransferase responsible for H3K36 mono- and dimethylation in this fungus. In mammals, there are a total of eight distinct H3K36 methyltransferases, some of which are responsible for H3K36me1/me2 (Wagner & Carpenter, 2012). One of these, human ASH1L (ASH1-like), a homologue of *Drosophila* ASH1 (Absent, small, or homeotic disc1), is a Trithorax family protein that possesses H3K36me1, me2 and a relatively weaker H3K36me3 methyltransferase activity (Tanaka *et al.*, 2007, An *et al.*, 2011). *E. festucae* as well as several other filamentous fungi possess the homologue for Ash1, which is related to Set2 and contains AWS, SET, and post-SET domains (Freitag, 2017). It is possible that Ash1 mediates H3K36 mono- and dimethylation, while SetB mediates H3K36 trimethylation in *E. festucae*. Recently, the Ash1 homologue in *F. fujikuroi* was characterised. Deletion of the gene had less impact on H3K36me3 levels compared to deletion of *set2*, which severely reduced H3K36me3 levels (*setB*), while H3K36me2 levels were only slightly reduced in both mutants, and H3K36me1 was not analysed (Janevska & Tudzynski, 2017). These results suggest that indeed, Set2 appears to be the major H3K36me3 methyltransferase in *F. fujikuroi*.

An important aspect of the present study is the finding that SetB is required for infection of *E. festucae* in perennial ryegrass. Closer microscopic examination of the host plant tissues post-inoculation showed that the host was completely free of any Δ*setB* hyphae. On the other hand, overexpression of *setB* had no impact on the symbiotic interaction. Interestingly, deletion of the *setB* homologue in *M. oryzae* similarly resulted in reduced appressorium formation and pathogenicity (Pham *et al*., 2015), suggesting that SetB is crucial for both fungal pathogenicity and symbiosis. Taking into consideration the method of inoculation

used in this study, in which an open wound is made in the host seedling and *E. festucae* hyphae is subsequently embedded within the wound, it is considered less likely that the Δ*setB* mutant has lost the ability to penetrate or enter its host. Rather, it is possible that the Δ*setB* mutant is susceptible to the host defence resulting in clearance from host tissues. It would be interesting to track the growth of the mutant at the early stages of infection and to analyse the expression of host defence genes to confirm this hypothesis. Additionally, given the role of SetB in regulating H3K36me3 and the role of this mark in transcription, the infection phenotype of the Δ*setB* mutant could be due to a lack of expression of *E. festucae* host defence-suppressing factors, or overexpression of *E. festucae* host defence-eliciting factors. Strikingly, deletion of the gene for H3K9 methyltransferase, ClrD, similarly resulted in an inability of *E. festucae* to establish infection in perennial ryegrass (Chujo & Scott, 2014). Thus, a future transcriptomic study of the mutants at the early infection stages would potentially shed light on fungal regulatory factors of infection and/or identify host-specific factors, and examination of the similarities and differences between the early infection stages of the Δ*clrD* and Δ*setB* strains will add to the current understanding of how *E. festucae* establishes infection in the host plant.

## Chapter 6: Conclusions and future directions

Histone methylation is now firmly established as an important regulatory layer of secondary metabolite genes in fungi. However, the majority of studies have looked at the roles of histone methyltransferases in this respect. Therefore, the aims of these studies were to identify histone lysine demethylases in *E. festucae*, and to determine their roles in secondary metabolite regulation in this fungus.

To this end, eight candidate JmjC domain proteins were identified in *E. festucae*. Subsequent bioinformatics characterisation identified two; Jmj1 (KdmA) and Jmj2 (KdmB), as the most likely candidates for histone demethylases based on their similarity to mammalian KDM4 and KDM5, respectively. Another two proteins, Jmj6 and Jmj7 were ruled out as candidate KDMs. Of the remaining four, Jmj4 was probably the homologue of mammalian KDM8, a H3K36me2 demethylase, and Jmj8 the homologue of JMJD7. *E. festucae* Jmj3 is a homologue of *N. crassa* Dmm-1 and the last protein, Jmj5, represents an uncharacterised class of JmjC proteins that is restricted to kingdom Fungi.

Consequently, these proteins were overexpressed in *E. festucae* to test for a demethylase activity. The culture and symbiotic phenotypes of all eight *jmj1-jmj8* overexpression strains were not different from the wild-type. Western blot analysis of the *jmj1-jmj4* overexpression strains subsequently led to the identification of Jmj2 (KdmB) as an H3K34me3-specific demethylase. The *jmj5* and *jmj8* overexpression strains were similarly analysed but no reduction in H3K9me3 levels was observed for either strain. It remains to be seen if H3K27me3 levels are reduced in these strains. Hence, at this stage the K9/K27 demethylase(s) in *E. festucae* (and in filamentous fungi) still remains elusive. It is possible that KdmA is the H3K9 demethylase in filamentous fungi given the dual H3K9/K36 substrate specificity of mammalian KDM4. It is also possible that Jmj8 is the H3K27 demethylase given the presence of Jmj8 homologues in filamentous fungi but the absence in *A. nidulans* which do not utilise H3K27 methylation. The strategy used in this study, of overexpression of candidate demethylases followed by western blot analysis of total histones has proven effective for the characterisation of KdmB. However, other strategies to screen for demethylases include *in vitro* incubation of the enzymes with calf histones or histone tail peptides and analysing the resulting methylation levels by western blot and/or mass spectrometry. Another strategy that has been widely used is immunofluorescence. This was performed for KdmA and KdmB in HeLa cells but no positive results showing demethylase activity for either proteins were obtained.

Based on the identification of KdmB as the H3K4me3 demethylase, the role of H3K4 was characterised further in *E. festucae* by studying mutants of the H3K4 methyltransferase complex. Deletion of the Set1 catalytic subunit of the COMPASS complex appears to be lethal in *E. festucae*, thus the gene for the CclA (Bre2/Cps60) subunit of the complex was deleted, which led to the significant reduction in global histone H3K4me3 levels in the fungus. CclA is important for the repression of secondary metabolite clusters in other filamentous fungi (Bok *et al*., 2009; Palmer *et al*., 2013), and H3K4me3 is an important repressive mark for telomeric loci in yeast (Fingerman *et al.*, 2005). Thus, it was hypothesised that CclA and H3K4me3 repress the silent (in axenic culture) and subtelomeric *EAS*/*LTM* clusters in *E. festucae*. In support of this hypothesis, deletion of *cclA* in axenic culture was found to result in the derepression of *eas* and *ltm* genes as well as significantly lower levels of H3K4me3 at the *eas*/*ltm* gene promoters, suggesting that CclA represses these genes by maintaining higher levels of H3K4me3. However, similar to deletion mutants of the H3K9 (ClrD) and H3K27 (EzhB) methyltransferases in *E. festucae*, transcript levels of the *eas*/*ltm* genes

in the Δ*cclA* mutant in culture were still lower by several orders of magnitudes compared to the wild-type strain *in planta*, when these genes are massively derepressed. This indicates that the trimethyl histone H3K4/K9/K27 marks at these genes are but a basal repressive layer and removal of these marks, although perhaps necessary, are insufficient to bring about maximal derepression. Additional activating factors, possibly plant derived signals and specific transcription factors for these clusters are required to bring the expression of these genes to the high levels seen *in planta*.

In the host plant, deletion of *kdmB* was found to result in suboptimal derepression of the genes and accumulation of H3K4me3 at the gene promoters. These findings are consistent with a repressive role of H3K4me3 at the *EAS*/*LTM* loci. As expected, the significant reduction in *ltm* gene expression (up to 65%) in the Δ*kdmB* mutant translated to a significant reduction in the levels of lolitrem pathway intermediates and end products. By comparison, the levels of ergot alkaloids and peramine were not affected by *kdmB* deletion. Lolitrem B production in an endophyte is undesirable as it is the causal agent of 'ryegrass staggers'. However, the toxicity of lolitrem B appears to be dose-dependent and low levels of the metabolite have negligible effects on muscle tissue. Lolitrem B given at 45 μg $kg^{-1}$ caused moderate tremors in sheep muscle tissue, but at 25 μg $kg^{-1}$ (a 40% reduction in dosage) it resulted in little to no tremors (Smith *et al.*, 1997). Thus, the 67% reduction in lolitrem B levels in the Δ*kdmB* infected plants may prove to be biologically and agriculturally significant, although it also depends on how much grass a sheep ingests. Results from field studies have shown that endophytes lacking lolitrem B but expressing ergovaline and peramine were equally effective as pest control compared to endophytes producing all three compounds (Popay *et al.*, 1995, Popay *et al.*, 1999, Johnson *et al.*, 2013a). Hence, this study shows that a promising approach in the context of endophyte improvement could be the disruption of *kdmB* in the fungus by genetic means, or inhibition of the demethylase by a selection of KDM5-specific inhibitors that are available (Maes *et al.*, 2015, Liang *et al.*, 2016).

The findings in this study led to a model in which H3K4me3 is a repressive mark for the subtelomeric *EAS* and *LTM* clusters in *E. festucae*. CclA is important for the maintenance of the levels of the mark for repression in culture while KdmB is required for demethylation of the mark for derepression of the genes *in planta*. The findings that Jhd2, the yeast homologue of KdmB is also important for counteracting telomeric silencing (Liang *et al*., 2007; Ryu & Ahn, 2014) led to the hypothesis that KdmB plays a similar role in counteracting silencing of other telomeric genes in *E. festucae*. This was tested by analysing the expression of telomeric genes selected from each chromosome end that are preferentially upregulated *in planta*. The results show that all but one of the genes analysed required KdmB for their optimal expression, thus suggesting that KdmB also mediates the derepression of other *E. festucae* telomeric genes in general.

The next part of this study looked at the role of H3K36 methylation in *E. festucae*. Bioinformatics analysis had identified *E. festucae* Jmj4 as a putative H3K36me2 demethylase based on its homology with mammalian KDM8. Although the *jmj4* overexpression mutants did not have detectable reduction in global levels of H3K36 methylation *in vivo*, it would be interesting for future studies to determine activity of the protein on histone substrates *in vitro*. To gain insight into the role of H3K36 methylation in this fungus, mutants of the H3K36 methyltransferase SetB were also analysed. SetB was found to be required specifically for H3K36 trimethylation and for normal development in *E. festucae*, and the loss of *setB* also prevented *E. festucae* from establishing infection of the host plant. This is similar to the inability of the

Δ*clrD* (H3K9 methyltransferase) mutant of *E. festucae* to infect perennial ryegrass (Chujo & Scott, 2014). Further examination of the fungal-host interaction of the Δ*setB* and Δ*clrD* mutants at the early stages of colonisation will advance our understanding of the infection process that *E. festucae* uses to colonise the host. In addition, it is likely that SetB and ClrD control the infection process by regulating the expression of target genes, therefore, further transcriptomic analysis of the mutants is also likely to result in the identification of *E. festucae* factors that are important for host-specificity, infection and symbiosis.

## Appendices

**Appendix 1. Plasmid map of pSF15.**

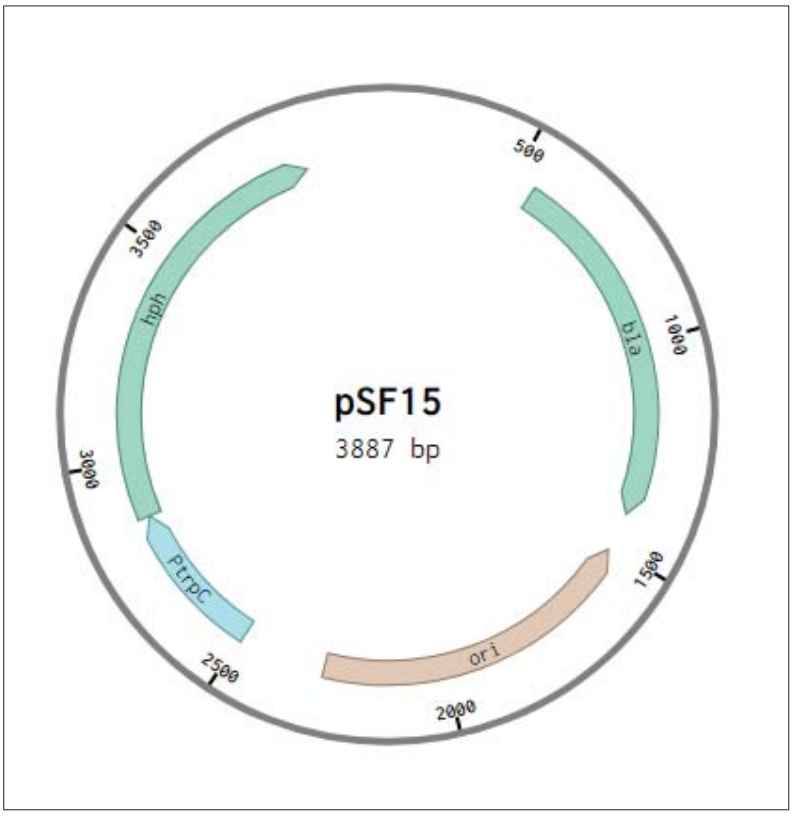

**Appendix 2. Plasmid map of pDB48.**

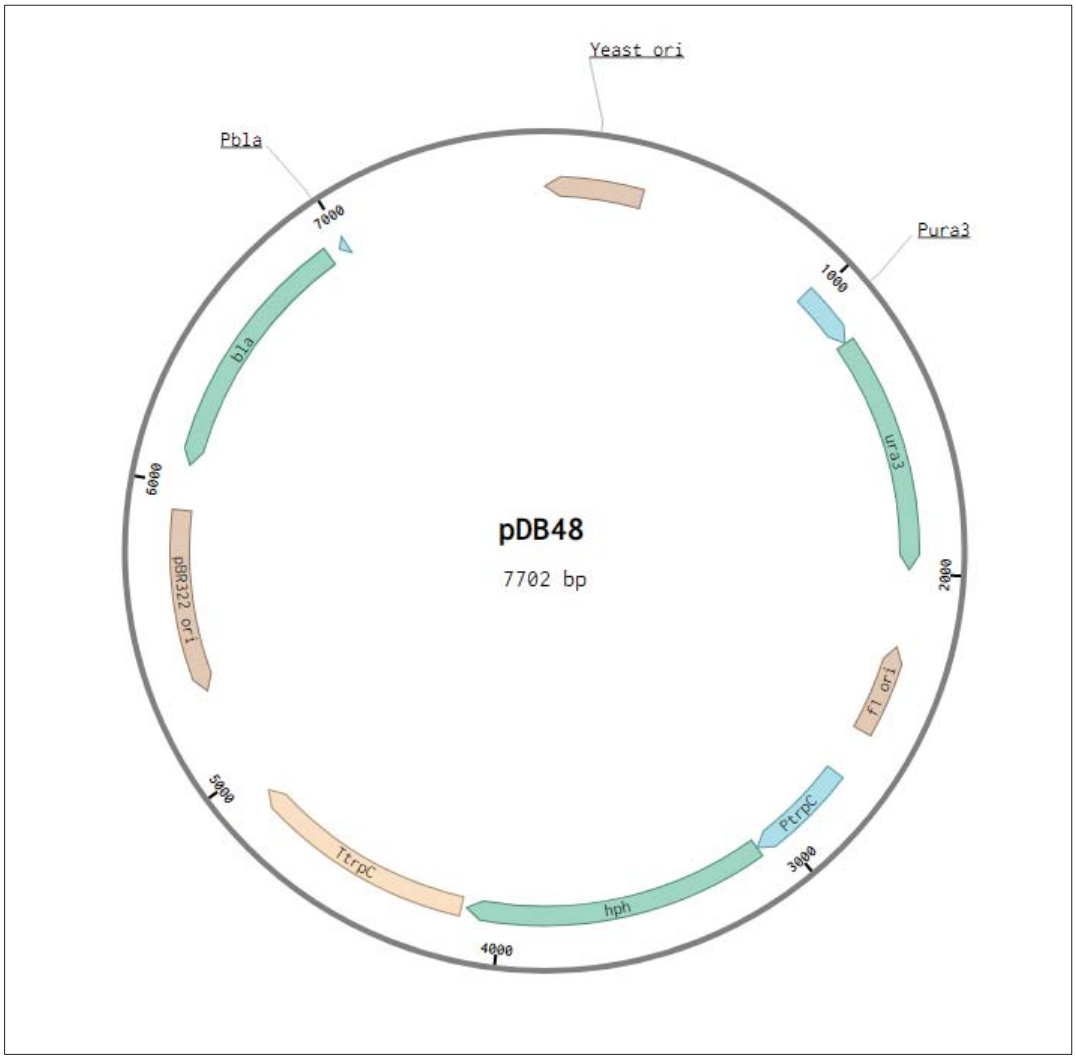

**Appendix 3. Plasmid map of pNR1.**

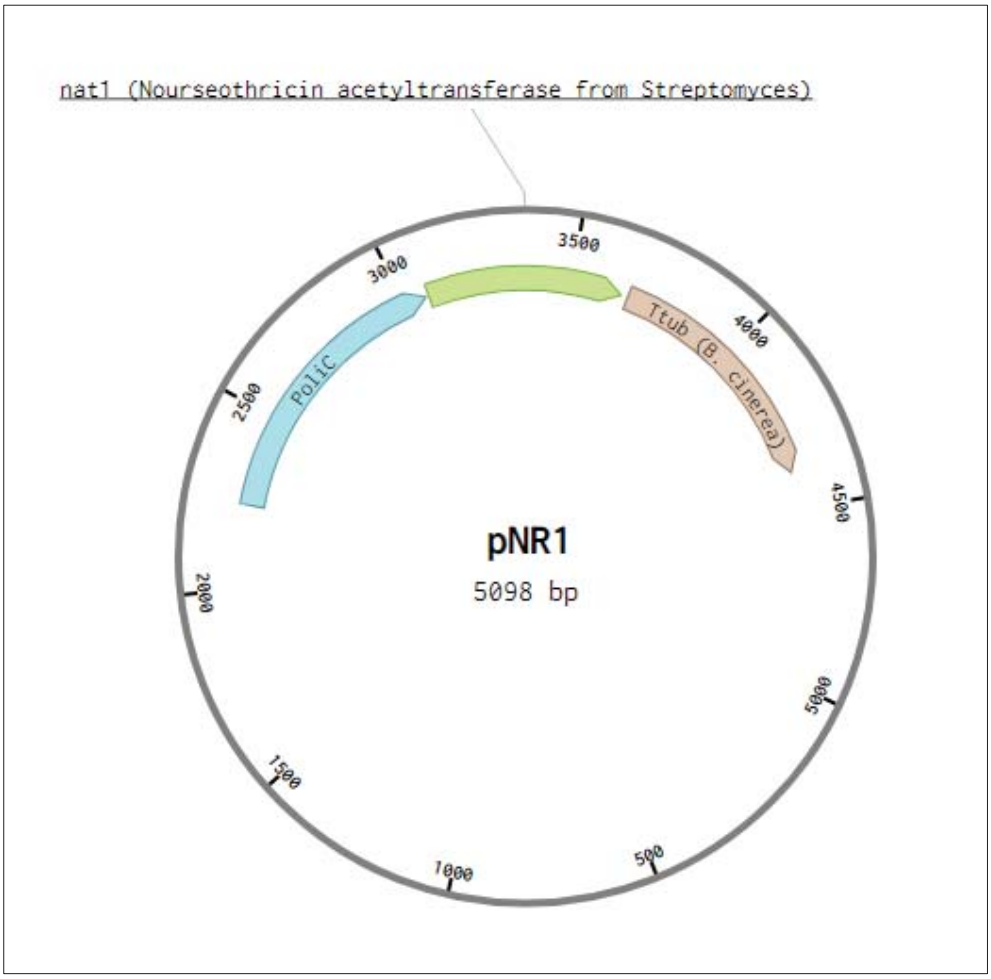

**Appendix 4. Plasmid map of pYL3.**

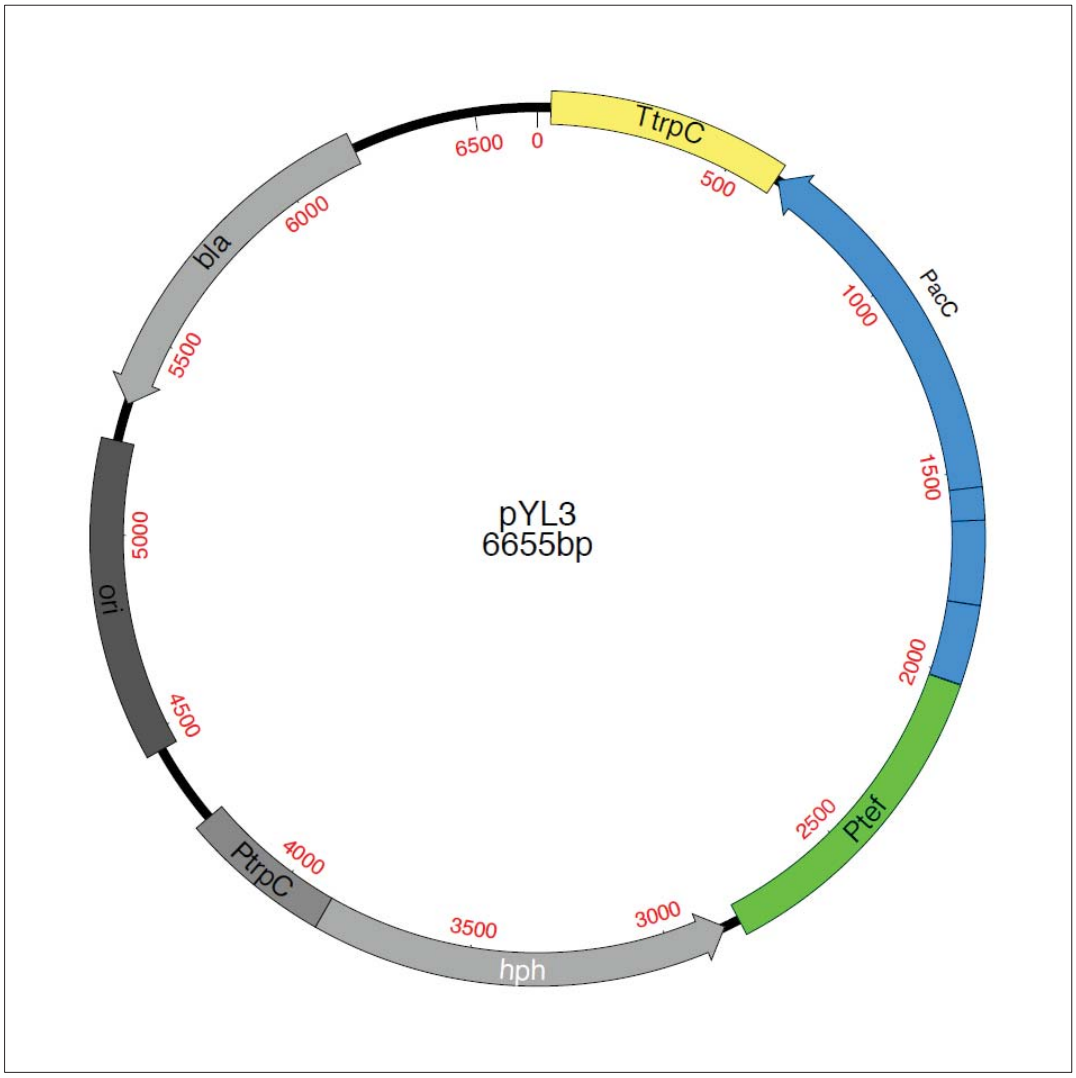

**Appendix 5. Plasmid map of pYL4.**

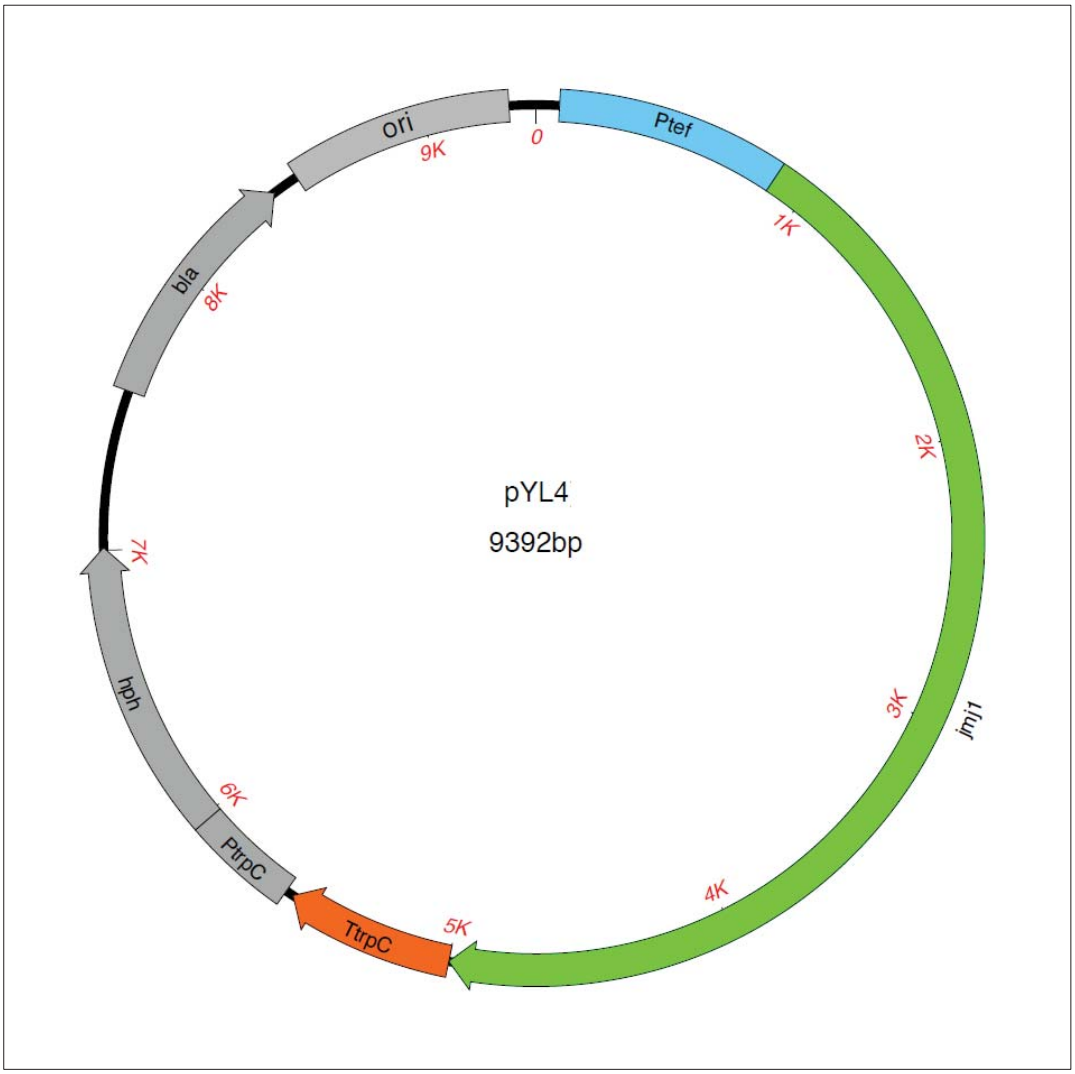

**Appendix 6. Plasmid map of pYL5.**

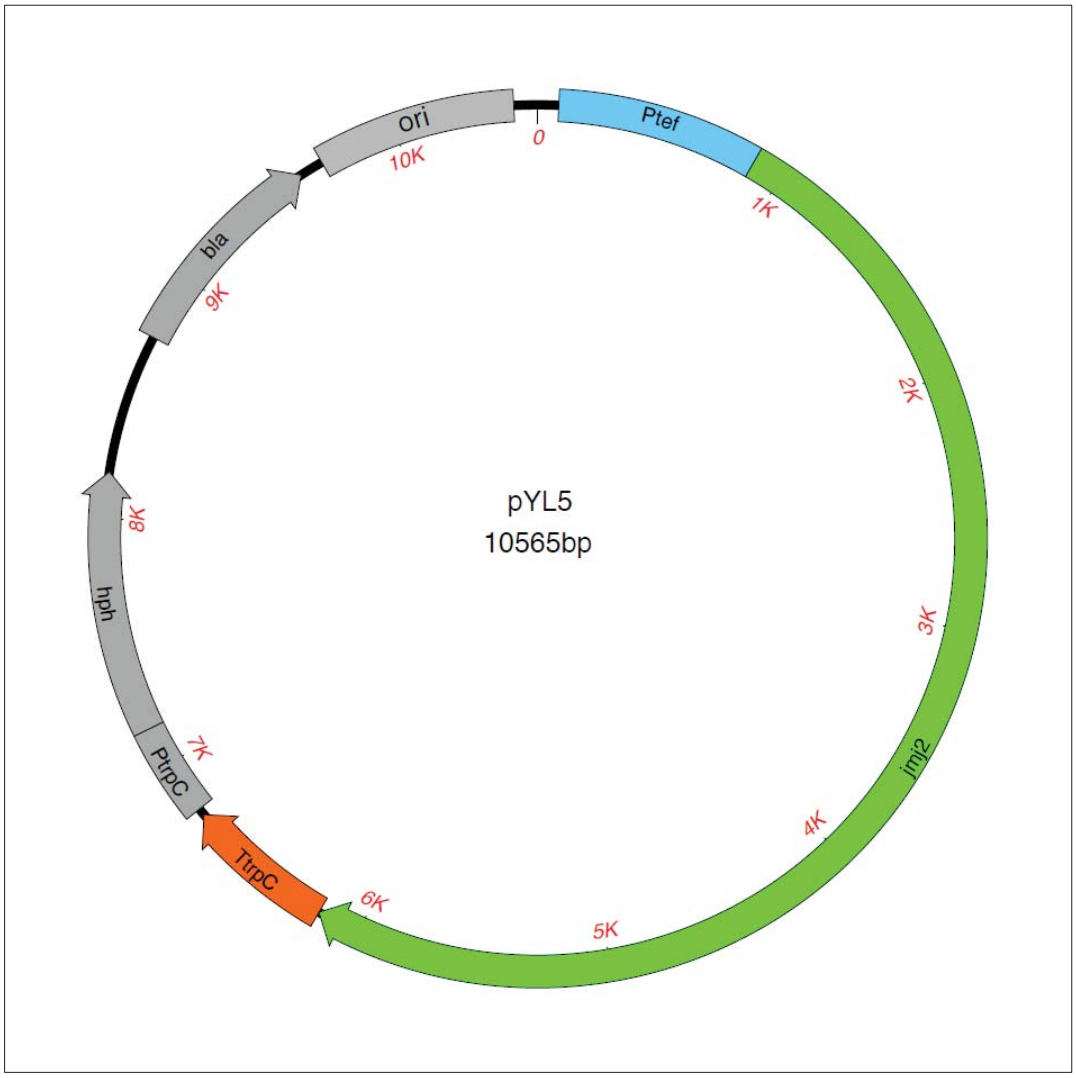

**Appendix 7. Plasmid map of pYL6.**

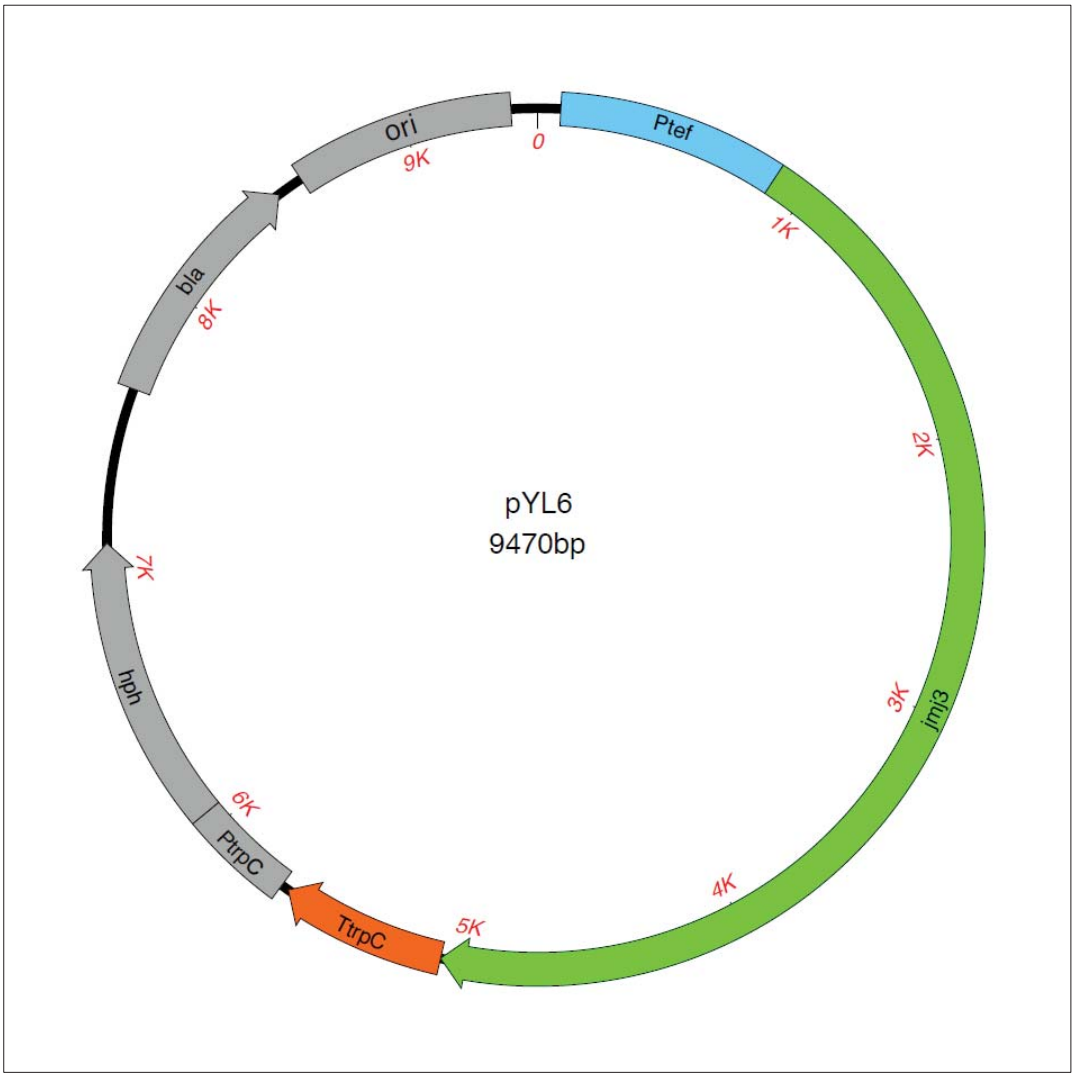

**Appendix 8. Plasmid map of pYL7.**

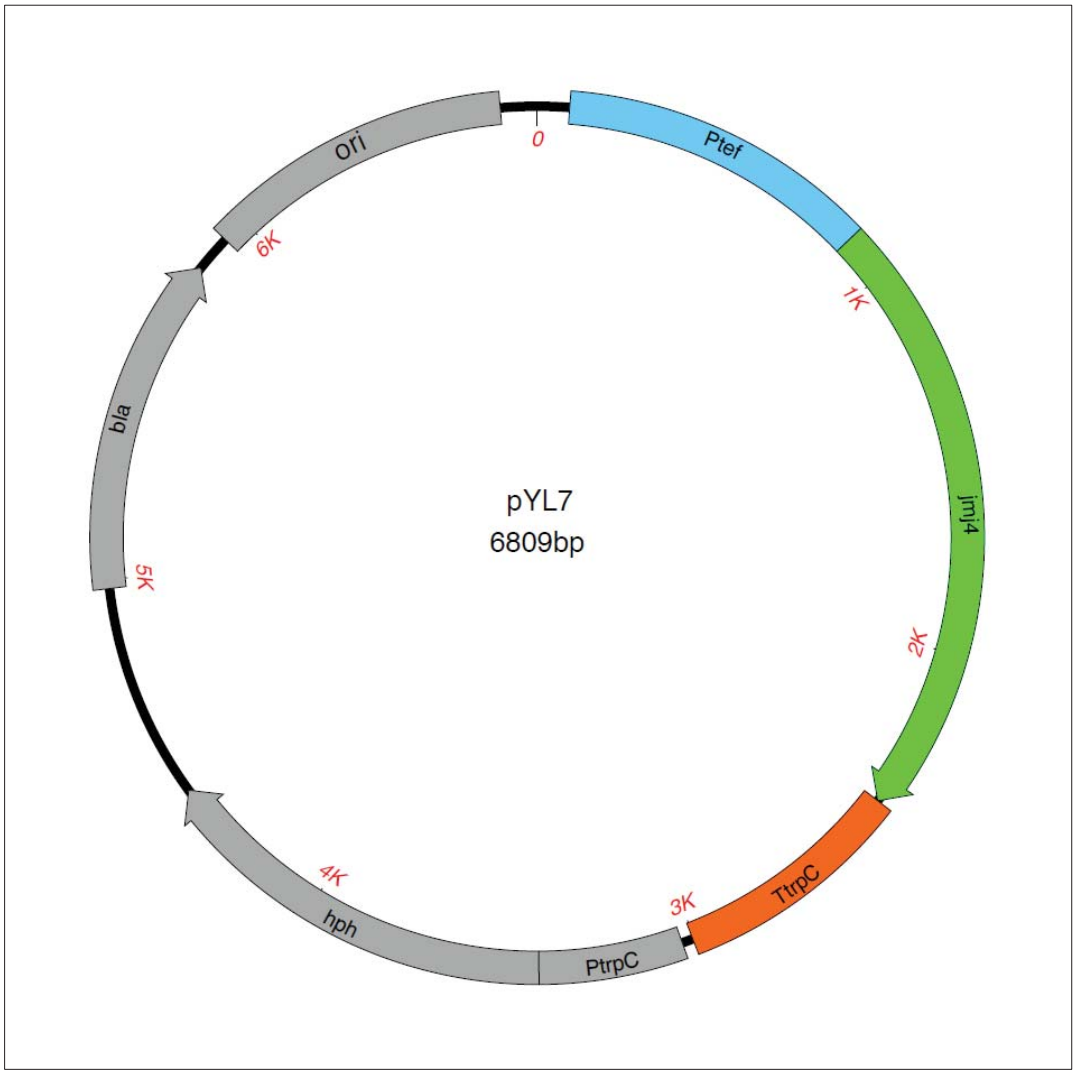

**Appendix 9. Plasmid map of pYL8.**

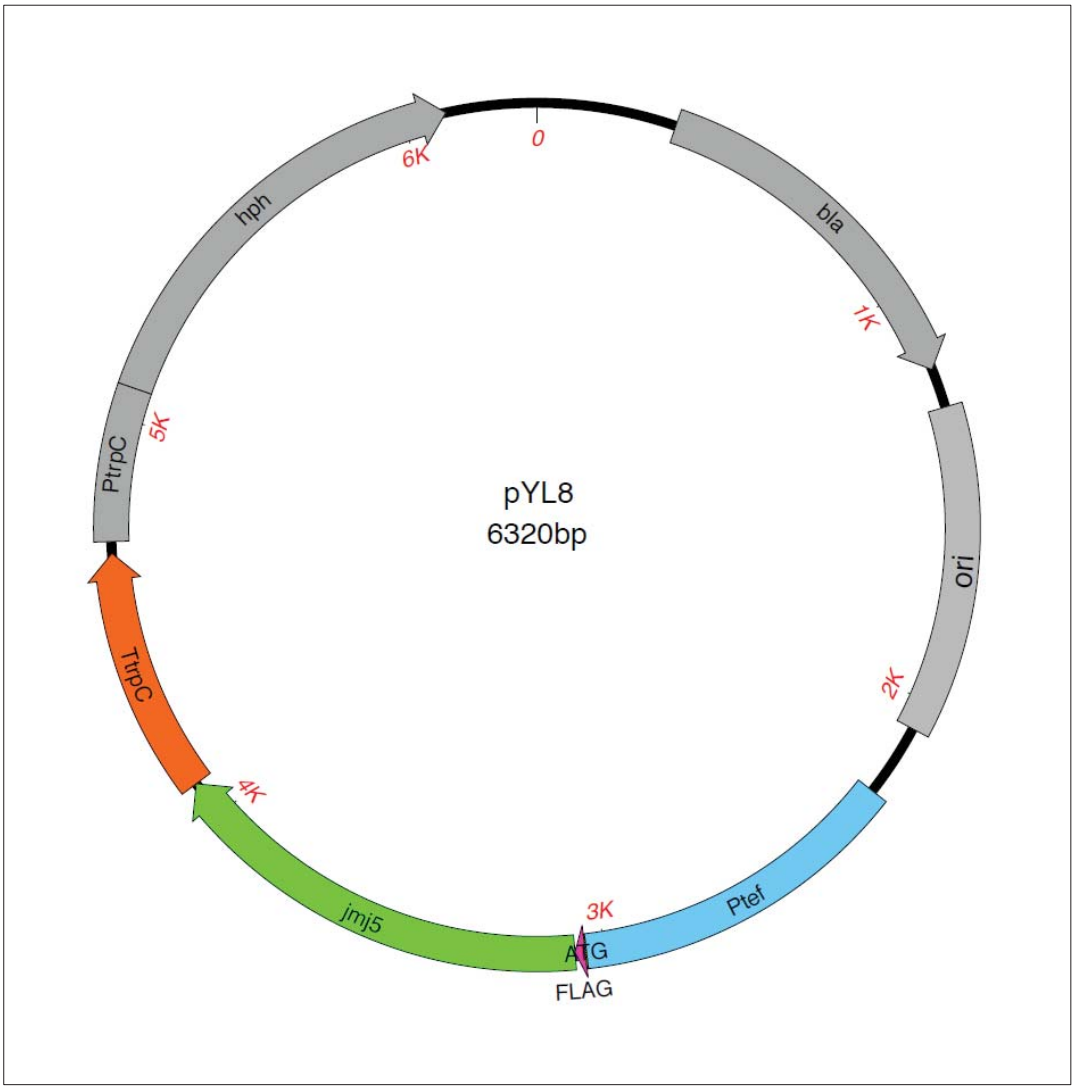

**Appendix 10. Plasmid map of pYL9.**

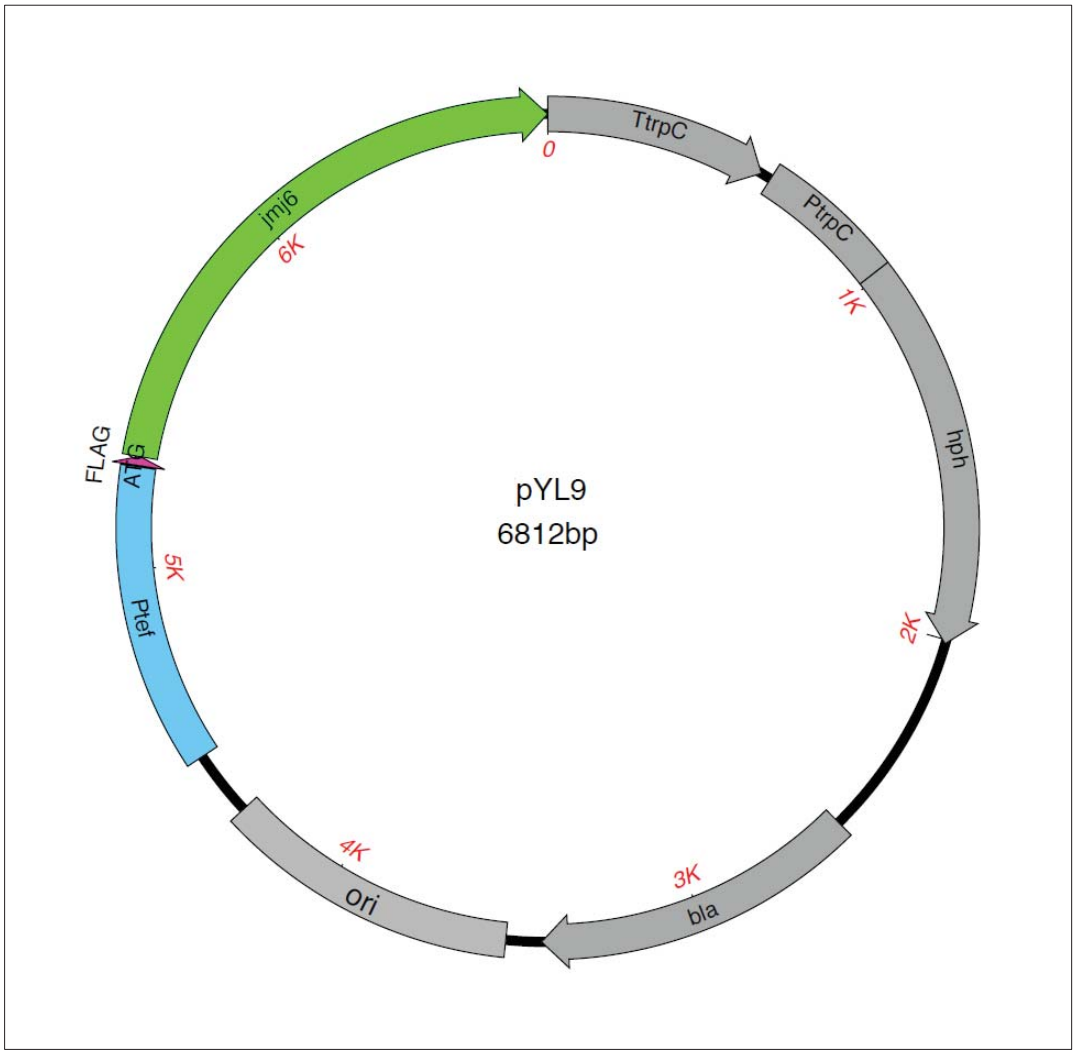

**Appendix 11. Plasmid map of pYL10.**

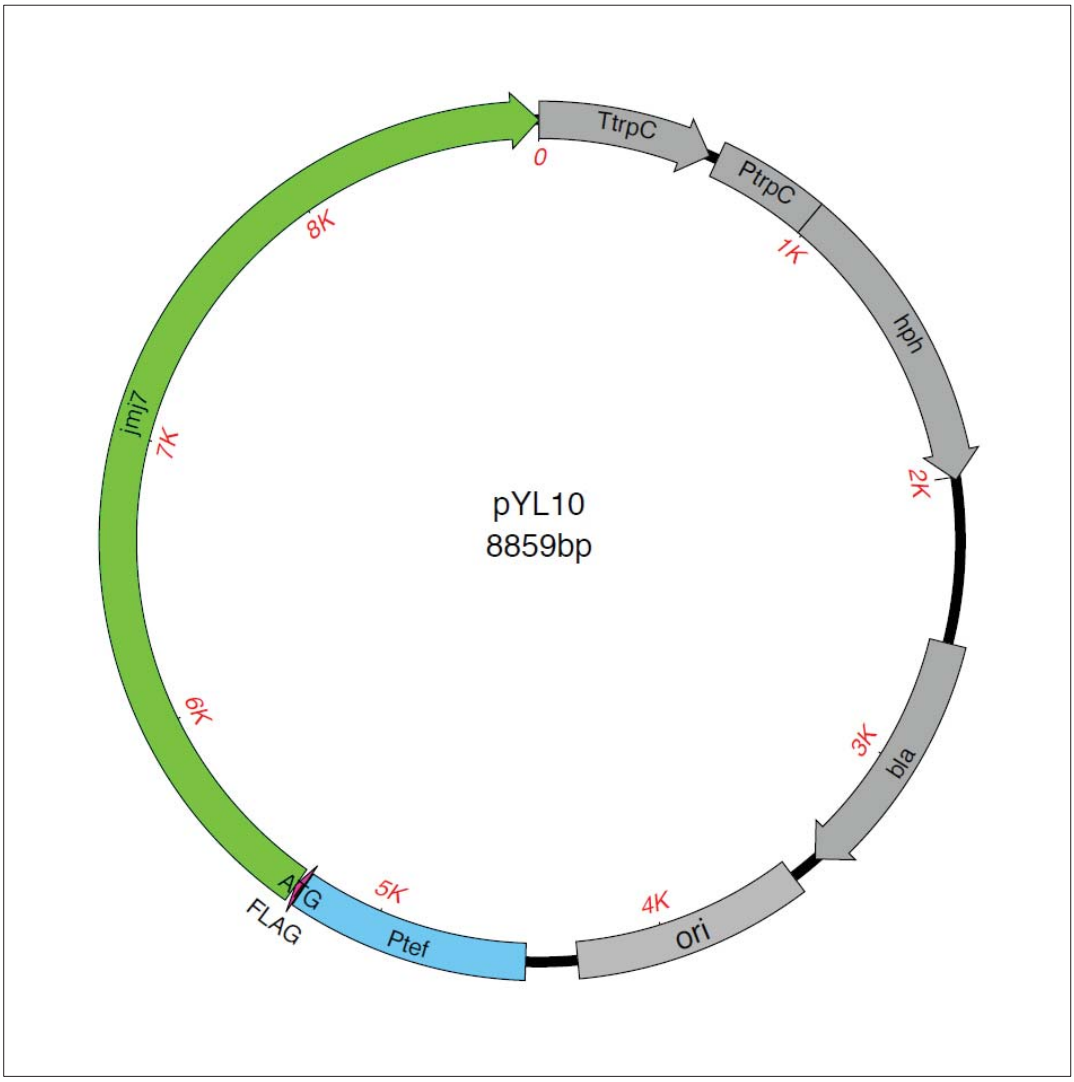

**Appendix 12. Plasmid map of pYL11.**

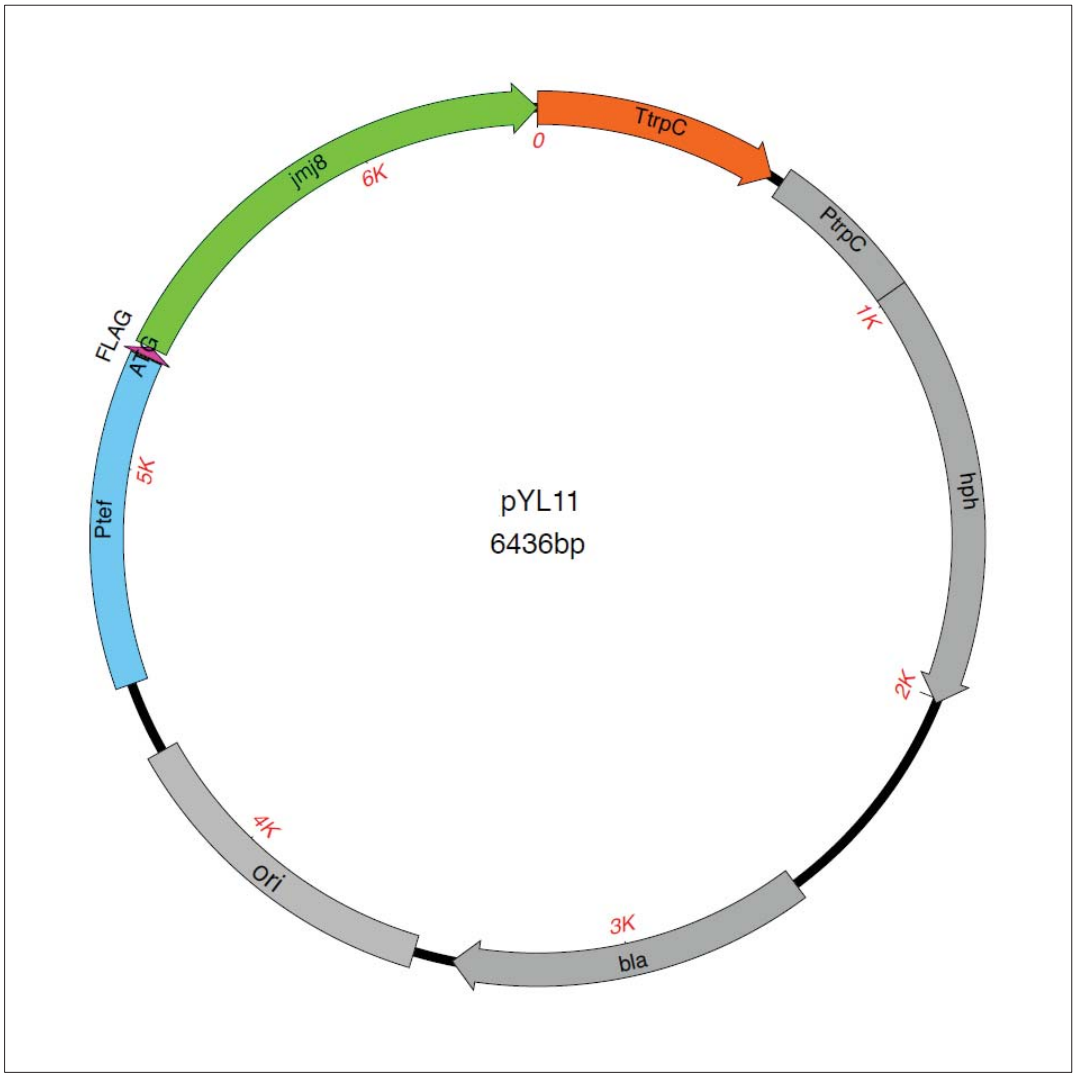

**Appendix 13. Plasmid map of pYL12.**

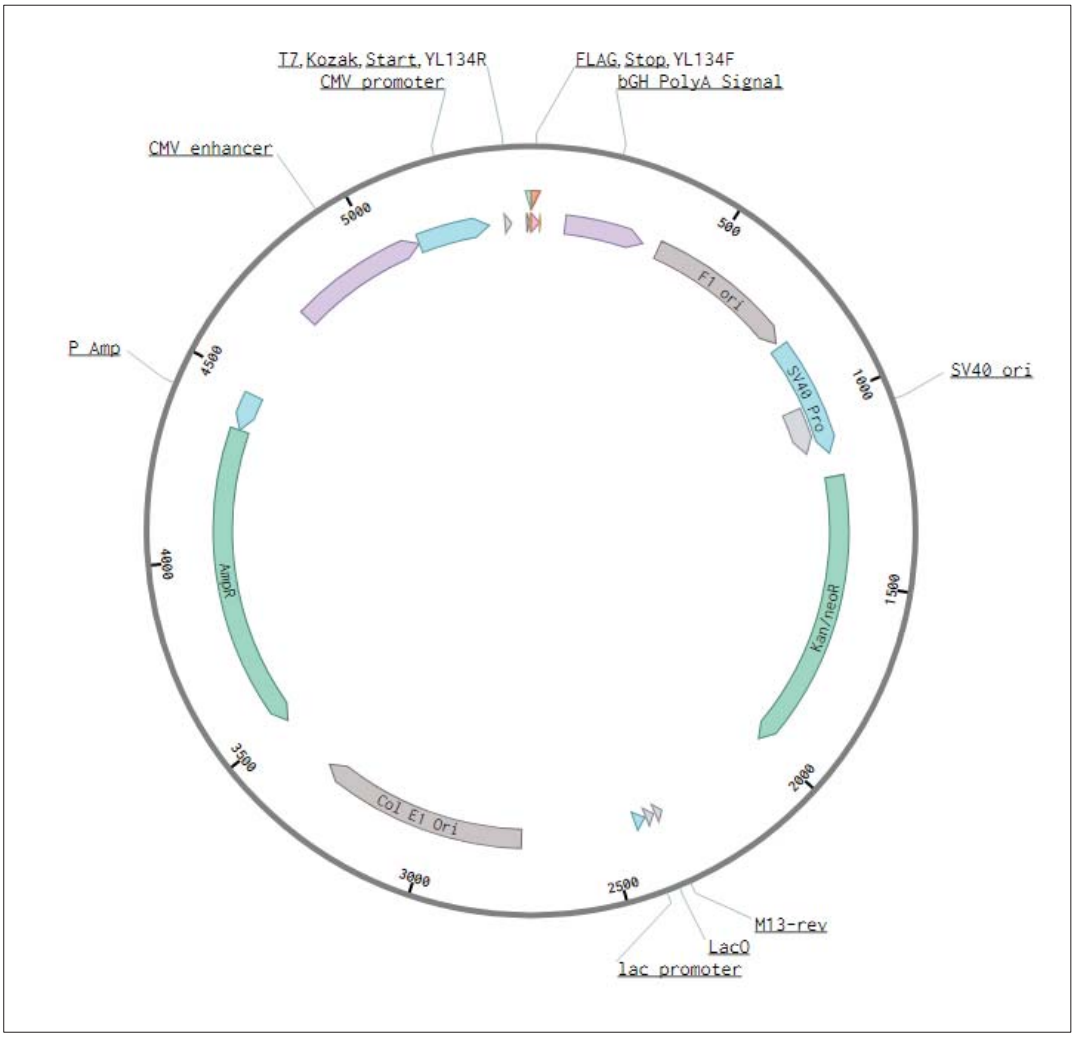

**Appendix 14. Plasmid map of pYL13.**

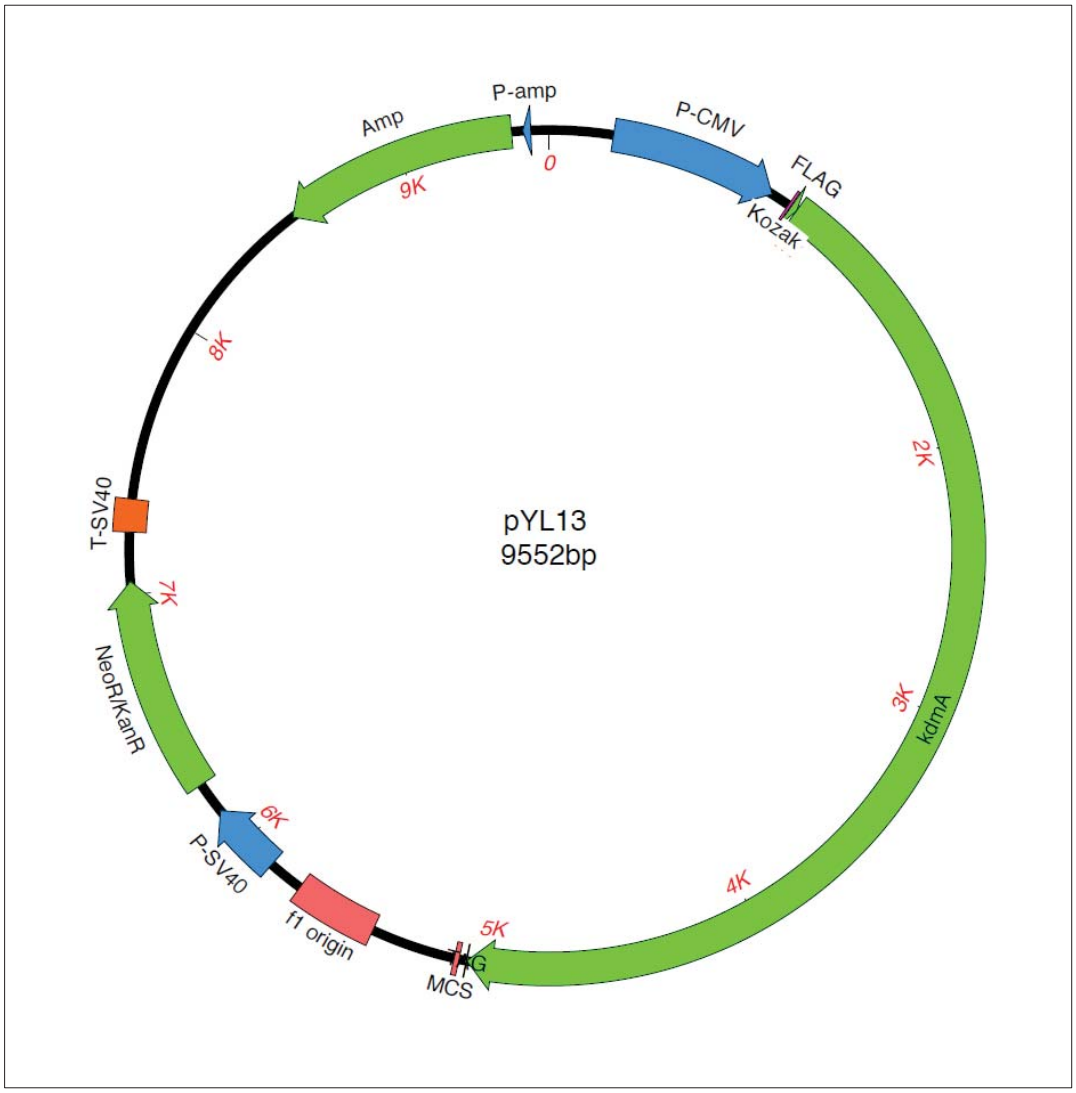

**Appendix 15. Plasmid map of pYL14.**

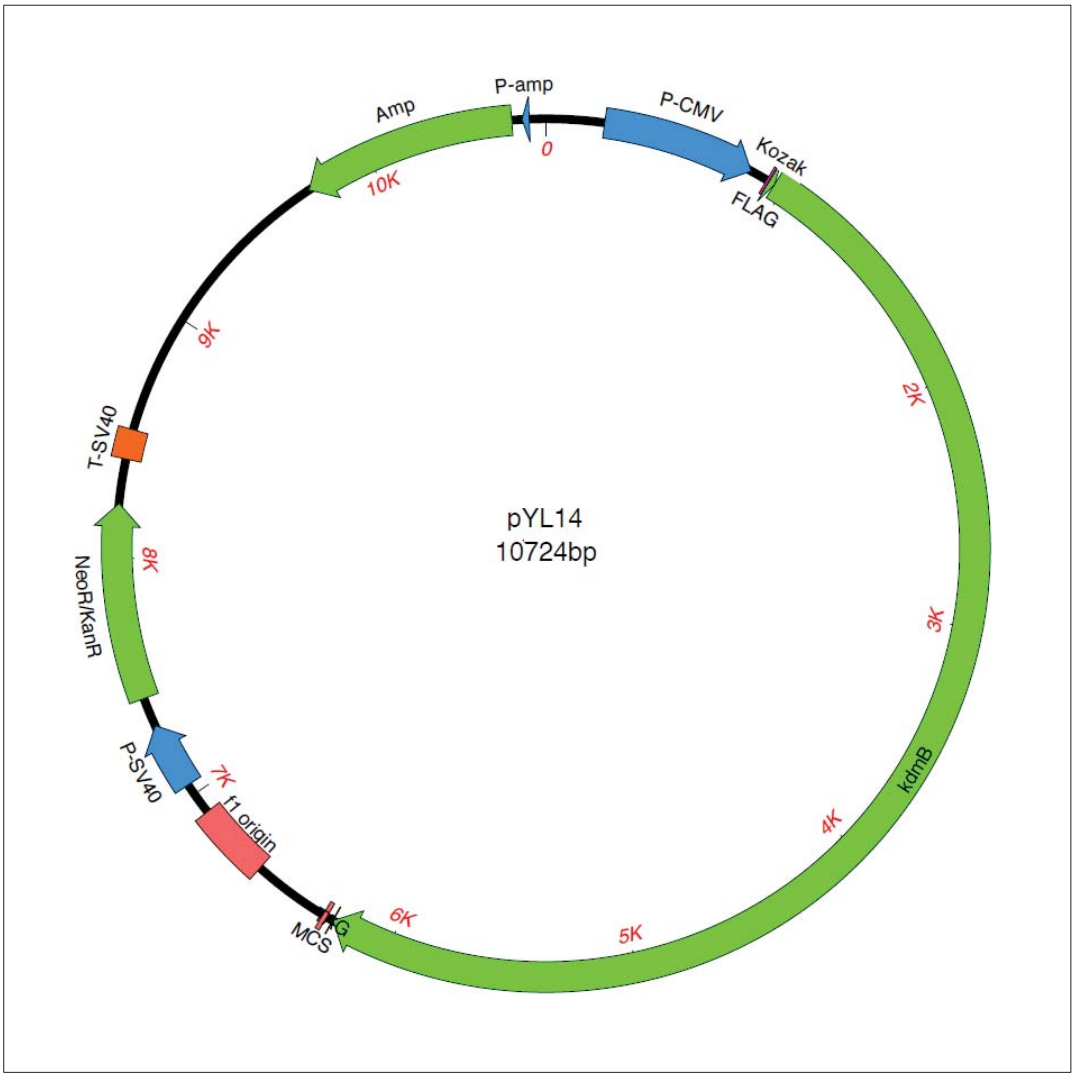

**Appendix 16. Plasmid map of pYL15.**

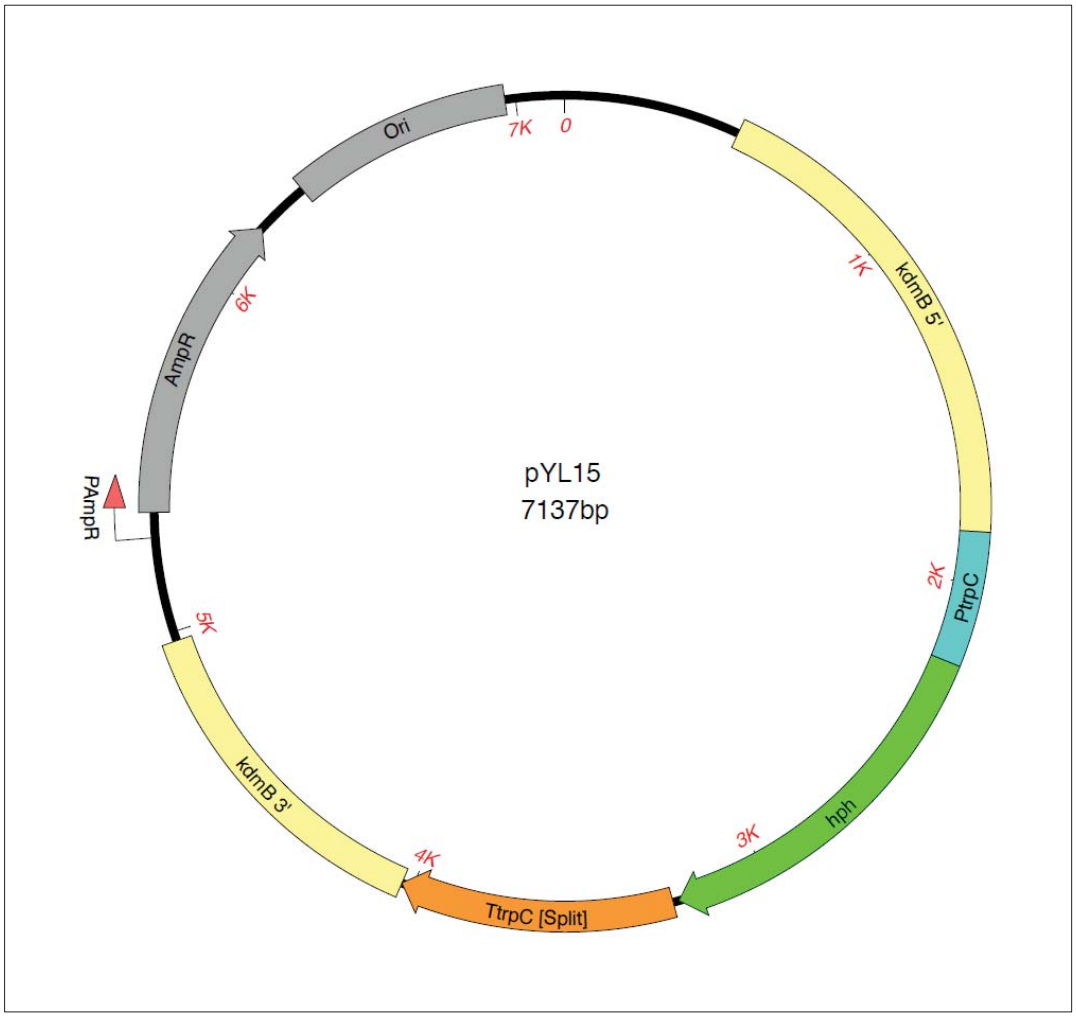

**Appendix 17. Plasmid map of pYL19.**

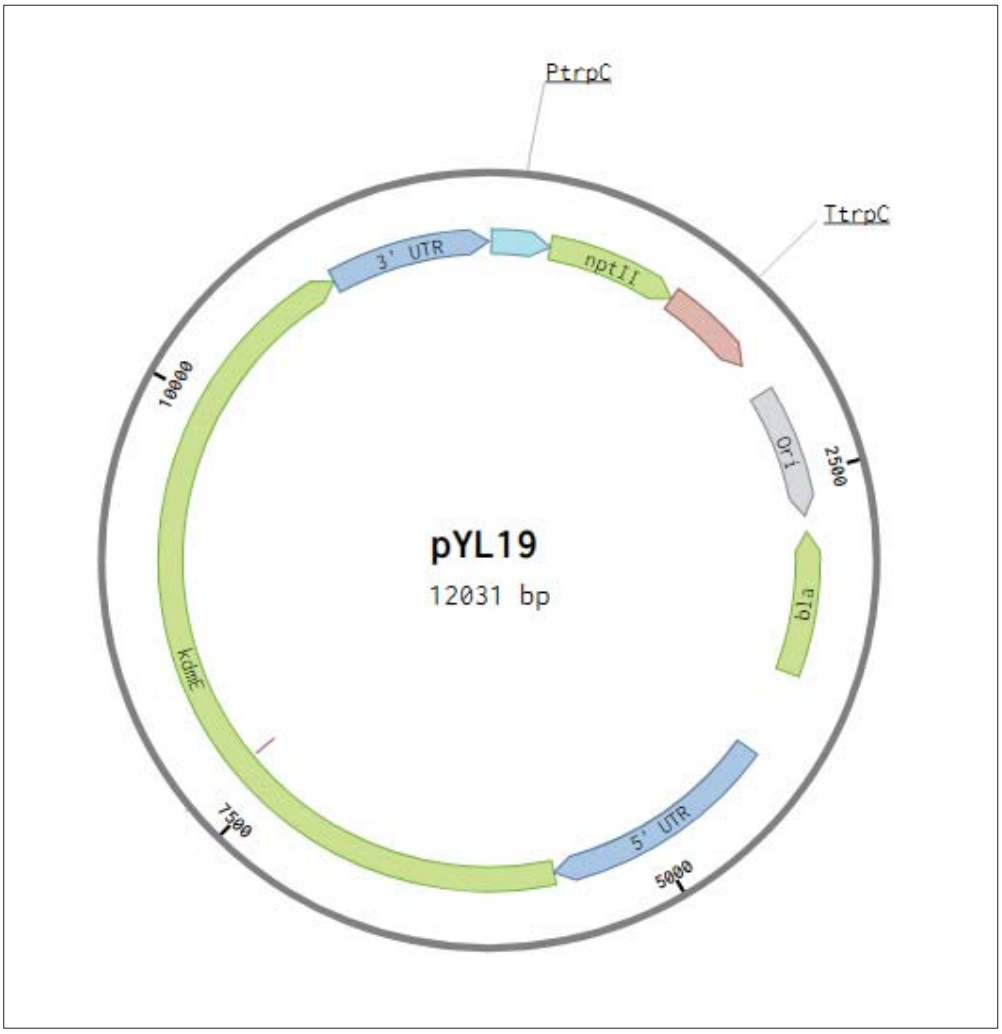

**Appendix 18. Plasmid map of pYL20.**

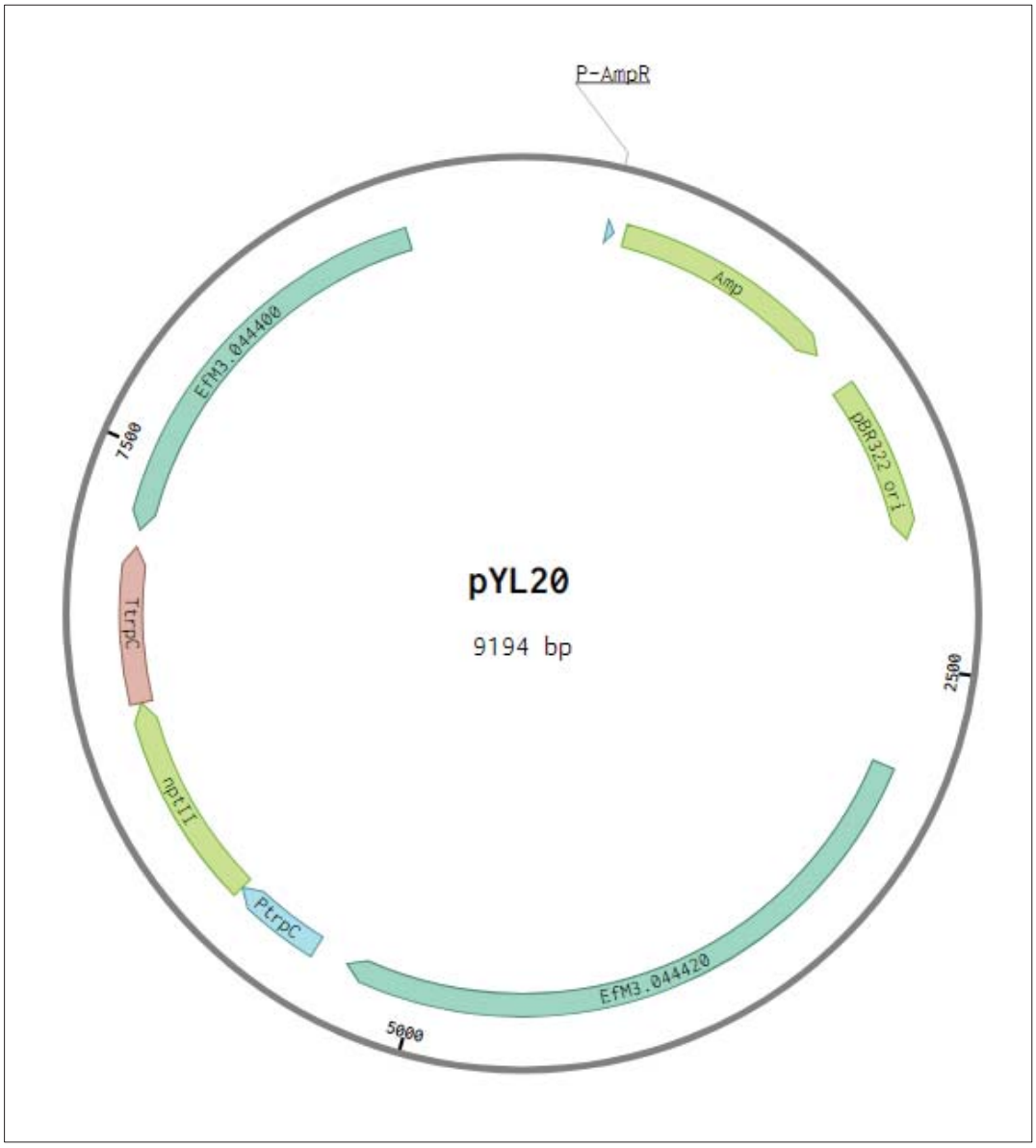

**Appendix 19. Plasmid map of pYL23.**

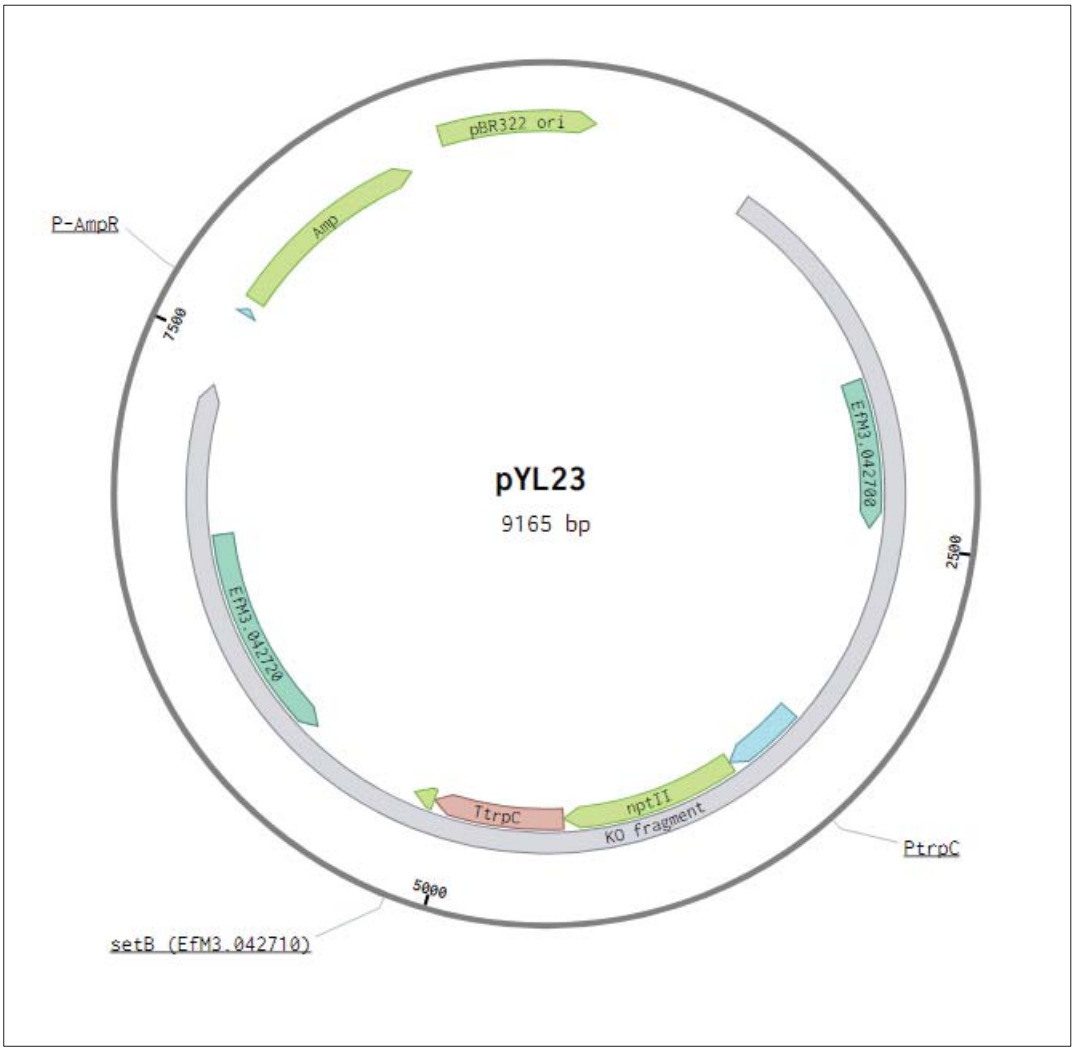

**Appendix 20. Plasmid map of pYL25.**

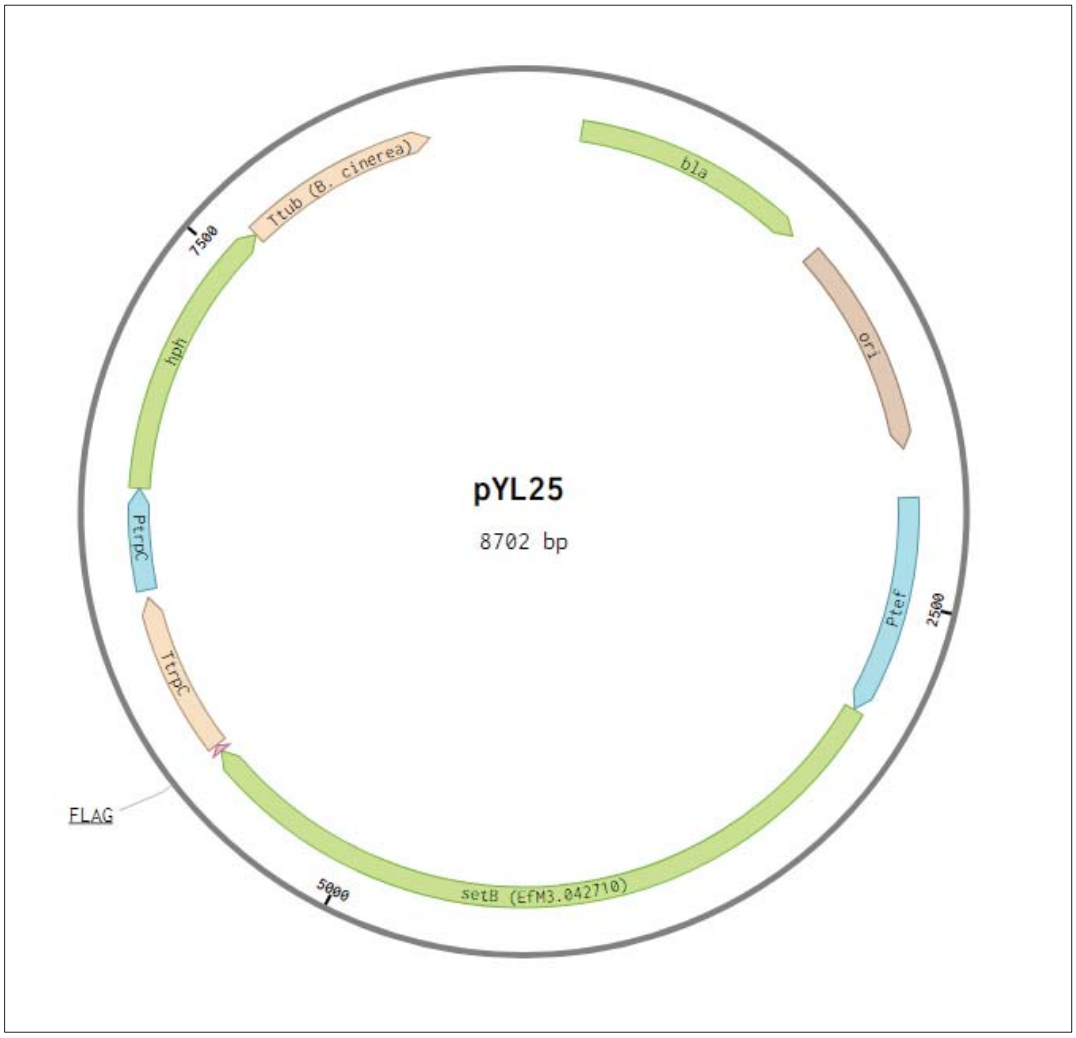

**Appendix 21. Plasmid map of pYL30.**

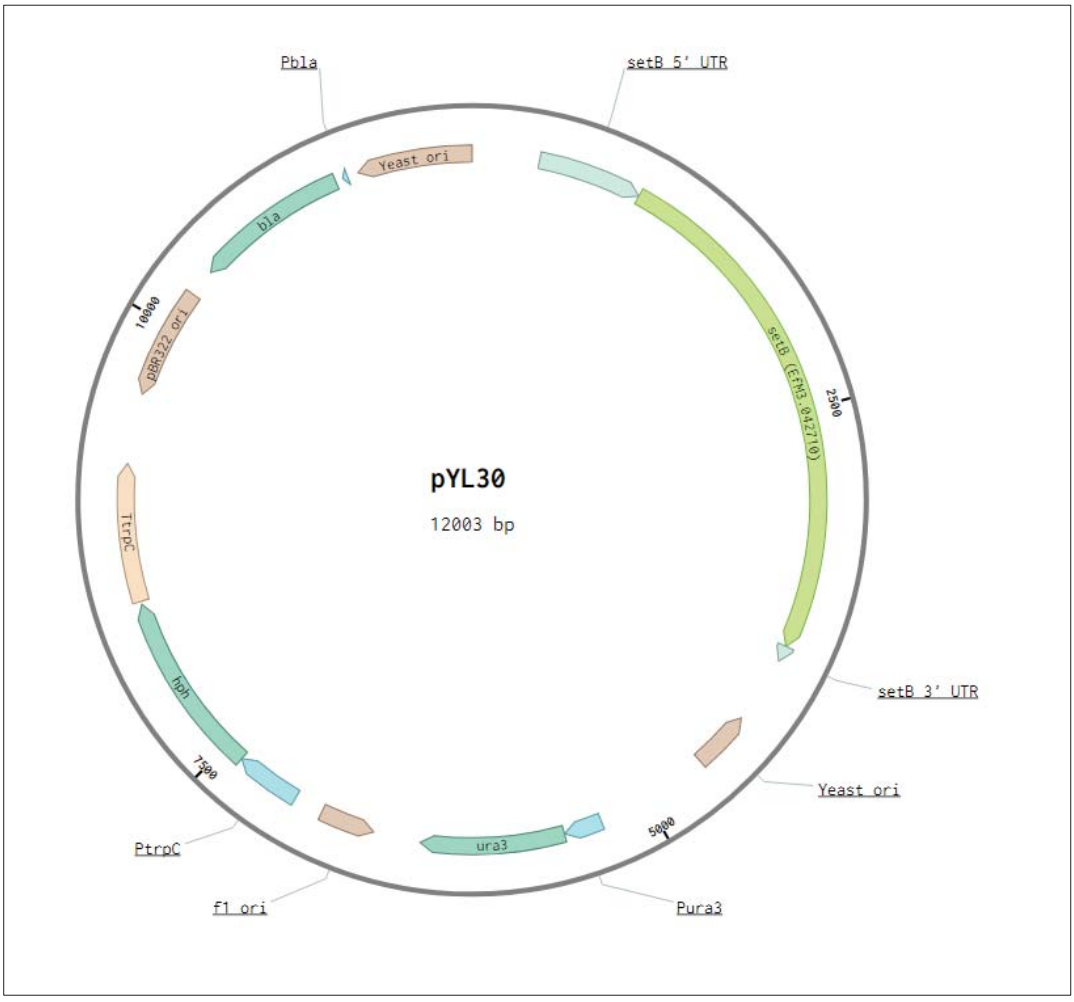

**Appendix 22.** Hits of Jmj1-8 outside fungi. Results of BLAST searches against non-fungal proteins in the UniProtKB protein database and in the non-redundant NCBI protein database (For Jmj3 only).

| **Jmj1** | **Organism** | **Score** | **Coverage** | **E-value** | **Identity** | **Accession** |
|---|---|---|---|---|---|---|
| | *Mus musculus* | 297 | 29% | 2e-67 | 40% | Q3U2K5 |
| | *Homo sapiens* | 238 | 14% | 1e-66 | 52% | Q6B0I6 |
| | *Drosophila melanogaster* | 301 | 24% | 1e-66 | 45% | Q9V6L0 |
| **Jmj2** | **Organism** | **Score** | **Coverage** | **E-value** | **Identity** | **Accession** |
| | *Drosophila melanogaster* | 607 | 66% | 7e-124 | 33% | Q9VMJ7 |
| | *Sus scrofa* | 492 | 66% | 3e-116 | 30% | A1YVX4 |
| | *Mus musculus* | 551 | 64% | 3e-116 | 30% | Q3UXZ9 |
| | *Canis lupus* | 546 | 64% | 2e-115 | 30% | Q38JA7 |
| | *Danio rerio* | 549 | 66% | 2e-115 | 30% | Q6IQX0 |
| **Jmj3 (JmjC domain)** | **Organism** | **Score** | **Coverage** | **E-value** | **Identity** | **Accession** |
| | *Quercus suber* | 738 | 54% | 0.0 | 49% | XP_023925490 |
| | *Naegleria gruberi* | 182 | 41% | 3e-43 | 25% | XP_002683406 |
| | *Dictyostelium purpureum* | 164 | 42% | 3e-37 | 25% | XP_003293704 |
| | *Acytostelium subglobosum* | 164 | 43% | 4e-37 | 24% | XP_012749567 |
| **Jmj4** | **Organism** | **Score** | **Coverage** | **E-value** | **Identity** | **Accession** |
| | *Rattus norvegicus* | 181 | 54% | 1e-50 | 40% | 497B8 |
| | *Arabidopsis thaliana* | 181 | 67% | 2e-50 | 35% | Q8RWR1 |
| | *Salmo salar* | 177 | 54% | 3e-49 | 39% | B5XF11 |
| **Jmj5** | **Organism** | **Score** | **Coverage** | **E-value** | **Identity** | **Accession** |
| | *Arabidopsis thaliana* | 67 | 46% | 4e-11 | 27% | Q8RWR1 |
| | *Salmo salar* | 60.8 | 46% | 4e-09 | 28% | B5XF11 |
| **Jmj6** | **Organism** | **Score** | **Coverage** | **E-value** | **Identity** | **Accession** |
| | *Arabidopsis thaliana* | 273 | 86% | 6e-85 | 35% | Q67XX3 |
| | *Xenopus laevis* | 155 | 48% | 3e-41 | 34% | Q6GND3 |
| **Jmj7** | **Organism** | **Score** | **Coverage** | **E-value** | **Identity** | **Accession** |
| | *Mus musculus* | 178 | 62% | 2e-45 | 26% | Q8BYR1 |
| | *Danio rerio* | 166 | 27% | 4e-44 | 36% | Q08BV2 |
| **Jmj8** | **Organism** | **Score** | **Coverage** | **E-value** | **Identity** | **Accession** |
| | *Homo sapiens* | 169 | 94% | 5e-53 | 35% | P0C870 |
| | *Mus musculus* | 168 | 94% | 1e-52 | 35% | P0C872 |
| | *Dictyostelium discoideum* | 142 | 87% | 2e-42 | 32% | Q54CS7 |

## References


Adhvaryu, K.K., S.A. Morris, B.D. Strahl & E.U. Selker, (2005) Methylation of histone H3 lysine 36 is required for normal development in Neurospora crassa. *Eukaryot Cell* **4**: 1455-1464.

Ajiro, K., (2000) Histone H2B phosphorylation in mammalian apoptotic cells An association with DNA fragmentation. *Journal of Biological Chemistry* **275**: 439-443.

Allis, C.D., S.L. Berger, J. Cote, S. Dent, T. Jenuwien, T. Kouzarides, L. Pillus, D. Reinberg, Y. Shi, R. Shiekhattar, A. Shilatifard, J. Workman & Y. Zhang, (2007) New nomenclature for chromatin-modifying enzymes. *Cell* **131**: 633-636.

An, S., K.J. Yeo, Y.H. Jeon & J.-J. Song, (2011) Crystal structure of the human histone methyltransferase ASH1L catalytic domain and its implications for the regulatory mechanism. *Journal of Biological Chemistry* **286**: 8369-8374.

Annunziato, A., (2008) DNA packaging: nucleosomes and chromatin. *Nature Education* **1**: 26.

Bacetty, A.A., M.E. Snook, A.E. Glenn, J.P. Noe, P. Nagabhyru & C.W. Bacon, (2009) Chemotaxis disruption in Pratylenchus scribneri by tall fescue root extracts and alkaloids. *J Chem Ecol* **35**: 844-850.

Bacon, C.W., (1995) Toxic endophyte-infected tall fescue and range grasses: historic perspectives. *Journal of animal science* **73**: 861-870.

Bannister, A.J. & T. Kouzarides, (2011) Regulation of chromatin by histone modifications. *Cell Res* **21**: 381-395.

Bannister, A.J., P. Zegerman, J.F. Partridge, E.A. Miska, J.O. Thomas, R.C. Allshire & T. Kouzarides, (2001) Selective recognition of methylated lysine 9 on histone H3 by the HP1 chromo domain. *Nature* **410**: 120-124.

Barski, A., S. Cuddapah, K. Cui, T.Y. Roh, D.E. Schones, Z. Wang, G. Wei, I. Chepelev & K. Zhao, (2007) High-resolution profiling of histone methylations in the human genome. *Cell* **129**: 823-837.

Basenko, E.Y., T. Sasaki, L. Ji, C.J. Prybol, R.M. Burckhardt, R.J. Schmitz & Z.A. Lewis, (2015) Genome-wide redistribution of H3K27me3 is linked to genotoxic stress and defective growth. *Proc Natl Acad Sci U S A* **112**: E6339-6348.

Bayram, Ö. & G.H. Braus, (2011) Coordination of secondarymetabolism and development in fungi: the velvet familyof regulatory proteins. *FEMS microbiology reviews* **36**: 1-24.

Beuchle, D., G. Struhl & J. Muller, (2001) Polycomb group proteins and heritable silencing of Drosophila Hox genes. *Development* **128**: 993-1004.

Bok, J.W., Y.M. Chiang, E. Szewczyk, Y. Reyes-Dominguez, A.D. Davidson, J.F. Sanchez, H.C. Lo, K. Watanabe, J. Strauss, B.R. Oakley, C.C. Wang & N.P. Keller, (2009) Chromatin-level regulation of biosynthetic gene clusters. *Nat Chem Biol* **5**: 462-464.

Bok, J.W., D. Hoffmeister, L.A. Maggio-Hall, R. Murillo, J.D. Glasner & N.P. Keller, (2006a) Genomic mining for Aspergillus natural products. *Chemistry & biology* **13**: 31-37.

Bok, J.W. & N.P. Keller, (2004) LaeA, a regulator of secondary metabolism in Aspergillus spp. *Eukaryotic cell* **3**: 527-535.

Bok, J.W., D. Noordermeer, S.P. Kale & N.P. Keller, (2006b) Secondary metabolic gene cluster silencing in Aspergillus nidulans. *Molecular microbiology* **61**: 1636-1645.

Briggs, S.D., M. Bryk, B.D. Strahl, W.L. Cheung, J.K. Davie, S.Y. Dent, F. Winston & C.D. Allis, (2001) Histone H3 lysine 4 methylation is mediated by Set1 and required for cell growth and rDNA silencing in *Saccharomyces cerevisiae*. *Genes Dev* **15**: 3286-3295.

Brownell, J.E., J. Zhou, T. Ranalli, R. Kobayashi, D.G. Edmondson, S.Y. Roth & C.D. Allis, (1996) Tetrahymena histone acetyltransferase A: a homolog to yeast Gcn5p linking histone acetylation to gene activation. *Cell* **84**: 843-851.

Bryk, M., S.D. Briggs, B.D. Strahl, M.J. Curcio, C.D. Allis & F. Winston, (2002) Evidence that Set1, a factor required for methylation of histone H3, regulates rDNA silencing in *S. cerevisiae* by a Sir2-independent mechanism. *Curr Biol* **12**: 165-170.

Bultman, T.L. & A. Leuchtmann, (2008) Biology of the Epichloë–Botanophila interaction: an intriguing association between fungi and insects. *Fungal Biology Reviews* **22**: 131-138.

Campos, E.I. & D. Reinberg, (2009) Histones: annotating chromatin. *Annu Rev Genet* **43**: 559-599.

Canzio, D., E.Y. Chang, S. Shankar, K.M. Kuchenbecker, M.D. Simon, H.D. Madhani, G.J. Narlikar & B. Al-Sady, (2011) Chromodomain-mediated oligomerization of HP1 suggests a nucleosome-bridging mechanism for heterochromatin assembly. *Mol Cell* **41**: 67-81.

Cao, R., L. Wang, H. Wang, L. Xia, H. Erdjument-Bromage, P. Tempst, R.S. Jones & Y. Zhang, (2002) Role of histone H3 lysine 27 methylation in Polycomb-group silencing. *Science* **298**: 1039-1043.

Carvin, C.D. & M.P. Kladde, (2004) Effectors of lysine 4 methylation of histone H3 in *Saccharomyces cerevisiae* are negative regulators of *PHO5* and *GAL1-10*. *J Biol Chem* **279**: 33057-33062.

Charlton, N.D., J.Y. Shoji, S.R. Ghimire, J. Nakashima & K.D. Craven, (2012) Deletion of the fungal gene soft disrupts mutualistic symbiosis between the grass endophyte Epichloe festucae and the host plant. *Eukaryot Cell* **11**: 1463-1471.

Chen, Z., J. Zang, J. Whetstine, X. Hong, F. Davrazou, T.G. Kutateladze, M. Simpson, Q. Mao, C.H. Pan, S. Dai, J. Hagman, K. Hansen, Y. Shi & G. Zhang, (2006) Structural insights into histone demethylation by JMJD2 family members. *Cell* **125**: 691-702.

Cheutin, T., A.J. McNairn, T. Jenuwein, D.M. Gilbert, P.B. Singh & T. Misteli, (2003) Maintenance of stable heterochromatin domains by dynamic HP1 binding. *Science* **299**: 721-725.

Chiara, M., F. Fanelli, G. Mulè, A.F. Logrieco, G. Pesole, J.F. Leslie, D.S. Horner & C. Toomajian, (2015) Genome sequencing of multiple isolates highlights subtelomeric genomic diversity within Fusarium fujikuroi. *Genome biology and evolution* **7**: 3062-3069.

Chujo, T. & B. Scott, (2014) Histone H3K9 and H3K27 methylation regulates fungal alkaloid biosynthesis in a fungal endophyte-plant symbiosis. *Mol Microbiol* **92**: 413-434.

Connolly, L.R., K.M. Smith & M. Freitag, (2013) The *Fusarium graminearum* histone H3 K27 methyltransferase KMT6 regulates development and expression of secondary metabolite gene clusters. *PLoS Genet* **9**: e1003916.

Cuthbert, G.L., S. Daujat, A.W. Snowden, H. Erdjument-Bromage, T. Hagiwara, M. Yamada, R. Schneider, P.D. Gregory, P. Tempst, A.J. Bannister & T. Kouzarides, (2004) Histone deimination antagonizes arginine methylation. *Cell* **118**: 545-553.

Czermin, B., R. Melfi, D. McCabe, V. Seitz, A. Imhof & V. Pirrotta, (2002) Drosophila enhancer of Zeste/ESC complexes have a histone H3 methyltransferase activity that marks chromosomal Polycomb sites. *Cell* **111**: 185-196.

Dhayalan, A., A. Rajavelu, P. Rathert, R. Tamas, R.Z. Jurkowska, S. Ragozin & A. Jeltsch, (2010) The Dnmt3a PWWP domain reads histone 3 lysine 36 trimethylation and guides DNA methylation. *J Biol Chem* **285**: 26114-26120.

Diebold, B.A. & G.M. Bokoch, (2001) Molecular basis for Rac2 regulation of phagocyte NADPH oxidase. *Nature immunology* **2**: 211-215.

Eaton, C.J., M.P. Cox, B. Ambrose, M. Becker, U. Hesse, C.L. Schardl & B. Scott, (2010) Disruption of signaling in a fungal-grass symbiosis leads to pathogenesis. *Plant Physiol* **153**: 1780-1794.

Eaton, C.J., P.Y. Dupont, P. Solomon, W. Clayton, B. Scott & M.P. Cox, (2015) A Core Gene Set Describes the Molecular Basis of Mutualism and Antagonism in Epichloe spp. *Mol Plant Microbe Interact* **28**: 218-231.

Edmunds, J.W., L.C. Mahadevan & A.L. Clayton, (2008) Dynamic histone H3 methylation during gene induction: HYPB/Setd2 mediates all H3K36 trimethylation. *The EMBO journal* **27**: 406-420.

Eissenberg, J.C., T.C. James, D.M. Foster-Hartnett, T. Hartnett, V. Ngan & S. Elgin, (1990) Mutation in a heterochromatin-specific chromosomal protein is associated with suppression of position-effect variegation in Drosophila melanogaster. *Proceedings of the National Academy of Sciences* **87**: 9923-9927.

Fanti, L. & S. Pimpinelli, (2008) HP1: a functionally multifaceted protein. *Curr Opin Genet Dev* **18**: 169-174.

Fingerman, I.M., C.L. Wu, B.D. Wilson & S.D. Briggs, (2005) Global loss of Set1-mediated H3 Lys4 trimethylation is associated with silencing defects in *Saccharomyces cerevisiae*. *J Biol Chem* **280**: 28761-28765.

Fletcher, L.R. & I.C. Harvey, (1981) An association of a Lolium endophyte with ryegrass staggers. *N Z Vet J* **29**: 185-186.

Freitag, M., (2017) Histone Methylation by SET Domain Proteins in Fungi. *Annu Rev Microbiol* **71**: 413-439.

Freitag, M., P.C. Hickey, T.K. Khlafallah, N.D. Read & E.U. Selker, (2004) HP1 is essential for DNA methylation in Neurospora. *Molecular cell* **13**: 427-434.

Gacek-Matthews, A., H. Berger, T. Sasaki, K. Wittstein, C. Gruber, Z.A. Lewis & J. Strauss, (2016) KdmB, a Jumonji histone H3 demethylase, regulates genome-wide H3K4 trimethylation and is required for normal induction of secondary metabolism in *Aspergillus nidulans*. *PLoS Genet* **12**: e1006222.

Gacek-Matthews, A., L.M. Noble, C. Gruber, H. Berger, M. Sulyok, A.T. Marcos, J. Strauss & A. Andrianopoulos, (2015) KdmA, a histone H3 demethylase with bipartite function, differentially regulates primary and secondary metabolism in *Aspergillus nidulans*. *Mol Microbiol* **96**: 839-860.

Galazka, J.M., A.D. Klocko, M. Uesaka, S. Honda, E.U. Selker & M. Freitag, (2016) Neurospora chromosomes are organized by blocks of importin alpha-dependent heterochromatin that are largely independent of H3K9me3. *Genome Res* **26**: 1069-1080.

Gibson, D.G., L. Young, R.-Y. Chuang, J.C. Venter, C.A. Hutchison & H.O. Smith, (2009) Enzymatic assembly of DNA molecules up to several hundred kilobases. *Nature methods* **6**: 343-345.

Goldmark, J.P., T.G. Fazzio, P.W. Estep, G.M. Church & T. Tsukiyama, (2000) The Isw2 chromatin remodeling complex represses early meiotic genes upon recruitment by Ume6p. *Cell* **103**: 423-433.

Gottschling, D.E., O.M. Aparicio, B.L. Billington & V.A. Zakian, (1990) Position effect at *S. cerevisiae* telomeres: reversible repression of Pol II transcription. *Cell* **63**: 751-762.

Goujon, M., H. McWilliam, W. Li, F. Valentin, S. Squizzato, J. Paern & R. Lopez, (2010) A new bioinformatics analysis tools framework at EMBL–EBI. *Nucleic Acids Res* **38**: W695-W699.

Govindaraghavan, M., S.L. Anglin, A.H. Osmani & S.A. Osmani, (2014) The Set1/COMPASS histone H3 methyltransferase helps regulate mitosis with the CDK1 and NIMA mitotic kinases in Aspergillus nidulans. *Genetics* **197**: 1225-1236.

Gu, Q., H.A. Tahir, H. Zhang, H. Huang, T. Ji, X. Sun, L. Wu, H. Wu & X. Gao, (2017) Involvement of FvSet1 in Fumonisin B1 Biosynthesis, Vegetative Growth, Fungal Virulence, and Environmental Stress Responses in Fusarium verticillioides. *Toxins (Basel)* **9**.

Hassa, P.O., S.S. Haenni, M. Elser & M.O. Hottiger, (2006) Nuclear ADP-ribosylation reactions in mammalian cells: where are we today and where are we going? *Microbiology and Molecular Biology Reviews* **70**: 789-829.

Hayakawa, T., Y. Ohtani, N. Hayakawa, K. Shinmyozu, M. Saito, F. Ishikawa & J. Nakayama, (2007) RBP2 is an MRG15 complex component and down-regulates intragenic histone H3 lysine 4 methylation. *Genes Cells* **12**: 811-826.

Honda, S., Z.A. Lewis, M. Huarte, L.Y. Cho, L.L. David, Y. Shi & E.U. Selker, (2010) The DMM complex prevents spreading of DNA methylation from transposons to nearby genes in Neurospora crassa. *Genes Dev* **24**: 443-454.

Horton, J.R., A.K. Upadhyay, H.H. Qi, X. Zhang, Y. Shi & X. Cheng, (2010) Enzymatic and structural insights for substrate specificity of a family of jumonji histone lysine demethylases. *Nat Struct Mol Biol* **17**: 38-43.

Howe, F.S., H. Fischl, S.C. Murray & J. Mellor, (2017) Is H3K4me3 instructive for transcription activation? *BioEssays* **39**: 1-12.

Hsia, D.A., C.G. Tepper, M.R. Pochampalli, E.Y. Hsia, C. Izumiya, S.B. Huerta, M.E. Wright, H.W. Chen, H.J. Kung & Y. Izumiya, (2010) KDM8, a H3K36me2 histone demethylase that acts in the cyclin A1 coding region to regulate cancer cell proliferation. *Proc Natl Acad Sci U S A* **107**: 9671-9676.

Huang, F., M.B. Chandrasekharan, Y.C. Chen, S. Bhaskara, S.W. Hiebert & Z.W. Sun, (2010) The JmjN domain of Jhd2 is important for its protein stability, and the plant homeodomain (PHD) finger mediates its chromatin association independent of H3K4 methylation. *J Biol Chem* **285**: 24548-24561.

Ingvarsdottir, K., C. Edwards, M.G. Lee, J.S. Lee, D.C. Schultz, A. Shilatifard, R. Shiekhattar & S.L. Berger, (2007) Histone H3 K4 demethylation during activation and attenuation of *GAL1* transcription in *Saccharomyces cerevisiae*. *Mol Cell Biol* **27**: 7856-7864.

Itoh, Y., R. Johnson & B. Scott, (1994) Integrative transformation of the mycotoxin-producing fungus, Penicillium paxilli. *Curr Genet* **25**: 508-513.

Jamieson, K., M.R. Rountree, Z.A. Lewis, J.E. Stajich & E.U. Selker, (2013) Regional control of histone H3 lysine 27 methylation in Neurospora. *Proc Natl Acad Sci U S A* **110**: 6027-6032.

Janevska, S. & B. Tudzynski, (2017) Secondary metabolism in Fusarium fujikuroi: strategies to unravel the function of biosynthetic pathways. *Applied Microbiology and Biotechnology*: 1-16.

Johnson, L.J., A.C.M. de Bonth, L.R. Briggs, J.R. Caradus, S.C. Finch, D.J. Fleetwood, L.R. Fletcher, D.E. Hume, R.D. Johnson, A.J. Popay, B.A. Tapper, W.R. Simpson, C.R. Voisey & S.D. Card, (2013a) The exploitation of epichloae endophytes for agricultural benefit. *Fungal Diversity* **60**: 171-188.

Johnson, L.J., A. Koulman, M. Christensen, G.A. Lane, K. Fraser, N. Forester, R.D. Johnson, G.T. Bryan & S. Rasmussen, (2013b) An extracellular siderophore is required to maintain the mutualistic interaction of Epichloe festucae with Lolium perenne. *PLoS Pathog* **9**: e1003332.

Kanoh, J., S. Francesconi, A. Collura, V. Schramke, F. Ishikawa, G. Baldacci & V. Géli, (2003) The Fission Yeast spSet1p is a Histone H3-K4 Methyltransferase that Functions in Telomere Maintenance and DNA Repair in an ATM Kinase Rad3-dependent Pathway. *Journal of Molecular Biology* **326**: 1081-1094.

Keller, C., R. Adaixo, R. Stunnenberg, K.J. Woolcock, S. Hiller & M. Buhler, (2012) HP1(Swi6) mediates the recognition and destruction of heterochromatic RNA transcripts. *Mol Cell* **47**: 215-227.

Keller, N.P., G. Turner & J.W. Bennett, (2005) Fungal secondary metabolism—from biochemistry to genomics. *Nature Reviews Microbiology* **3**.

Keogh, M.-C., S.K. Kurdistani, S.A. Morris, S.H. Ahn, V. Podolny, S.R. Collins, M. Schuldiner, K. Chin, T. Punna & N.J. Thompson, (2005) Cotranscriptional set2 methylation of histone H3 lysine 36 recruits a repressive Rpd3 complex. *Cell* **123**: 593-605.

Kirby, E.J.M., (1961) Host-parasite relations in the choke disease of grasses. *Trans. Brit. mycol. Soc.* **44**: 493-503.

Kizer, K.O., H.P. Phatnani, Y. Shibata, H. Hall, A.L. Greenleaf & B.D. Strahl, (2005) A novel domain in Set2 mediates RNA polymerase II interaction and couples histone H3 K36 methylation with transcript elongation. *Mol Cell Biol* **25**: 3305-3316.

Klein, B.J., L. Piao, Y. Xi, H. Rincon-Arano, S.B. Rothbart, D. Peng, H. Wen, C. Larson, X. Zhang, X. Zheng, M.A. Cortazar, P.V. Pena, A. Mangan, D.L. Bentley, B.D. Strahl, M. Groudine, W. Li, X. Shi & T.G. Kutateladze, (2014) The histone-H3K4-specific demethylase KDM5B binds to its substrate and product through distinct PHD fingers. *Cell Rep* **6**: 325-335.

Klose, R.J., E.M. Kallin & Y. Zhang, (2006a) JmjC-domain-containing proteins and histone demethylation. *Nat Rev Genet* **7**: 715-727.

Klose, R.J., K. Yamane, Y. Bae, D. Zhang, H. Erdjument-Bromage, P. Tempst, J. Wong & Y. Zhang, (2006b) The transcriptional repressor JHDM3A demethylates trimethyl histone H3 lysine 9 and lysine 36. *Nature* **442**: 312-316.

Klose, R.J. & Y. Zhang, (2007) Regulation of histone methylation by demethylimination and demethylation. *Nat Rev Mol Cell Biol* **8**: 307-318.

Kosugi, S., M. Hasebe, M. Tomita & H. Yanagawa, (2009) Systematic identification of cell cycle-dependent yeast nucleocytoplasmic shuttling proteins by prediction of composite motifs. *Proceedings of the National Academy of Sciences* **106**: 10171-10176.

Krogan, N.J., J. Dover, S. Khorrami, J.F. Greenblatt, J. Schneider, M. Johnston & A. Shilatifard, (2002) COMPASS, a histone H3 (lysine 4) methyltransferase required for telomeric silencing of gene expression. *J Biol Chem* **277**: 10753-10755.

Kumar, S., G. Stecher & K. Tamura, (2016) MEGA7: Molecular Evolutionary Genetics Analysis version 7.0 for bigger datasets. *Molecular biology and evolution* **33**: 1870-1874.

Lachner, M., R. Sengupta, G. Schotta & T. Jenuwein, (2004) Trilogies of histone lysine methylation as epigenetic landmarks of the eukaryotic genome. In: Cold Spring Harbor symposia on quantitative biology. Cold Spring Harbor Laboratory Press, pp. 209-218.

Lando, D., D.J. Peet, D.A. Whelan, J.J. Gorman & M.L. Whitelaw, (2002) Asparagine hydroxylation of the HIF transactivation domain: a hypoxic switch. *Science* **295**: 858-861.

Lane, G., B. Tapper, E. Davies, M. Christensen & G. Latch, (1997) Occurrence of extreme alkaloid levels in endophyte-infected perennial ryegrass, tall fescue, and meadow fescue. In: Neotyphodium/Grass Interactions. Springer, pp. 433-436.

Latchs, G. & M. Christensen, (1985) Artificial infection of grasses with endophytes. *Ann Appl Biol* **107**: 17-24.

Letunic, I., T. Doerks & P. Bork, (2014) SMART: recent updates, new developments and status in 2015. *Nucleic Acids Res* **43**: D257-D260.

Lewis, E.B., (1978) A gene complex controlling segmentation in Drosophila. *Nature* **276**: 565-570.

Lewis, Z.A., S. Honda, T.K. Khlafallah, J.K. Jeffress, M. Freitag, F. Mohn, D. Schubeler & E.U. Selker, (2009) Relics of repeat-induced point mutation direct heterochromatin formation in Neurospora crassa. *Genome Res* **19**: 427-437.

Lewis, Z.A. & E.U. Selker, (2010) Chromatin Structure and Modification. In: Cellular and Molecular Biology of Filamentous Fungi. American Society of Microbiology, pp. 113-123.

Li, B., M. Carey & J.L. Workman, (2007) The role of chromatin during transcription. *Cell* **128**: 707-719.

Li, J., D. Moazed & S.P. Gygi, (2002) Association of the histone methyltransferase Set2 with RNA polymerase II plays a role in transcription elongation. *J Biol Chem* **277**: 49383-49388.

Li, L., C. Greer, R.N. Eisenman & J. Secombe, (2010) Essential functions of the histone demethylase lid. *PLoS Genet* **6**: e1001221.

Li, T., X. Chen, X. Zhong, Y. Zhao, X. Liu, S. Zhou, S. Cheng & D.X. Zhou, (2013) Jumonji C domain protein JMJ705-mediated removal of histone H3 lysine 27 trimethylation is involved in defense-related gene activation in rice. *Plant Cell* **25**: 4725-4736.

Li, Y., P. Trojer, C.-F. Xu, P. Cheung, A. Kuo, W.J. Drury, Q. Qiao, T.A. Neubert, R.-M. Xu & O. Gozani, (2009) The target of the NSD family of histone lysine methyltransferases depends on the nature of the substrate. *Journal of Biological Chemistry* **284**: 34283-34295.

Liang, G., R.J. Klose, K.E. Gardner & Y. Zhang, (2007) Yeast Jhd2p is a histone H3 Lys4 trimethyl demethylase. *Nat Struct Mol Biol* **14**: 243-245.

Liang, J., B. Zhang, S. Labadie, D.F. Ortwine, M. Vinogradova, J.R. Kiefer, V.S. Gehling, J.C. Harmange, R. Cummings, T. Lai, J. Liao, X. Zheng, Y. Liu, A. Gustafson, E. Van der Porten, W. Mao, B.M. Liederer, G. Deshmukh, M. Classon, P. Trojer, P.S. Dragovich & L. Murray, (2016) Lead optimization of a pyrazolo[1,5-a]pyrimidin-7(4H)-one scaffold to identify potent, selective and orally bioavailable KDM5 inhibitors suitable for in vivo biological studies. *Bioorg Med Chem Lett* **26**: 4036-4041.

Liu, H., C. Wang, S. Lee, Y. Deng, M. Wither, S. Oh, F. Ning, C. Dege, Q. Zhang, X. Liu, A.M. Johnson, J. Zang, Z. Chen, R. Janknecht, K. Hansen, P. Marrack, C.Y. Li, J.W. Kappler, J. Hagman & G. Zhang, (2017) Clipping of arginine-methylated histone tails by JMJD5 and JMJD7. *Proc Natl Acad Sci U S A* **114**: E7717-E7726.

Liu, Y., N. Liu, Y. Yin, Y. Chen, J. Jiang & Z. Ma, (2015) Histone H3K4 methylation regulates hyphal growth, secondary metabolism and multiple stress responses in *Fusarium graminearum*. *Environ Microbiol* **17**: 4615-4630.

Livak, K.J. & T.D. Schmittgen, (2001) Analysis of relative gene expression data using real-time quantitative PCR and the 2− ΔΔCT method. *methods* **25**: 402-408.

Lomberk, G., L. Wallrath & R. Urrutia, (2006) The heterochromatin protein 1 family. *Genome biology* **7**: 228.

Lu, F., X. Cui, S. Zhang, T. Jenuwein & X. Cao, (2011) Arabidopsis REF6 is a histone H3 lysine 27 demethylase. *Nat Genet* **43**: 715-719.

Lucio-Eterovic, A.K., M.M. Singh, J.E. Gardner, C.S. Veerappan, J.C. Rice & P.B. Carpenter, (2010) Role for the nuclear receptor-binding SET domain protein 1 (NSD1) methyltransferase in coordinating lysine 36 methylation at histone 3 with RNA polymerase II function. *Proceedings of the National Academy of Sciences* **107**: 16952-16957.

Lukito, Y., T. Chujo & B. Scott, (2015) Molecular and cellular analysis of the pH response transcription factor PacC in the fungal symbiont *Epichloe festucae*. *Fungal Genet Biol* **85**: 25-37.

Maes, T., E. Carceller, J. Salas, A. Ortega & C. Buesa, (2015) Advances in the development of histone lysine demethylase inhibitors. *Curr Opin Pharmacol* **23**: 52-60.

Maison, C. & G. Almouzni, (2004) HP1 and the dynamics of heterochromatin maintenance. *Nat Rev Mol Cell Biol* **5**: 296-304.

Malinowski, D. & D. Belesky, (1999) Neotyphodium coenophialum-endophyte infection affects the ability of tall fescue to use sparingly available phosphorus. *Journal of Plant Nutrition* **22**: 835-853.

Margueron, R. & D. Reinberg, (2011) The Polycomb complex PRC2 and its mark in life. *Nature* **469**: 343-349.

Mersman, D.P., H.N. Du, I.M. Fingerman, P.F. South & S.D. Briggs, (2009) Polyubiquitination of the demethylase Jhd2 controls histone methylation and gene expression. *Genes Dev* **23**: 951-962.

Miller, T., N.J. Krogan, J. Dover, H. Erdjument-Bromage, P. Tempst, M. Johnston, J.F. Greenblatt & A. Shilatifard, (2001) COMPASS: a complex of proteins associated with a trithorax-related SET domain protein. *Proc Natl Acad Sci U S A* **98**: 12902-12907.

Mingot, J.M., E.A. Espeso, E. Dıez & M. Peñalva, (2001) Ambient pH signaling regulates nuclear localization of the Aspergillus nidulans PacC transcription factor. *Molecular and Cellular Biology* **21**: 1688-1699.

Mohan, M., H.M. Herz, E.R. Smith, Y. Zhang, J. Jackson, M.P. Washburn, L. Florens, J.C. Eissenberg & A. Shilatifard, (2011) The COMPASS family of H3K4 methylases in Drosophila. *Mol Cell Biol* **31**: 4310-4318.

Morris, S.A., Y. Shibata, K. Noma, Y. Tsukamoto, E. Warren, B. Temple, S.I. Grewal & B.D. Strahl, (2005) Histone H3 K36 methylation is associated with transcription elongation in Schizosaccharomyces pombe. *Eukaryot Cell* **4**: 1446-1454.

Mosammaparast, N. & Y. Shi, (2010) Reversal of histone methylation: biochemical and molecular mechanisms of histone demethylases. *Annu Rev Biochem* **79**: 155-179.

Moshkin, Y.M., T.W. Kan, H. Goodfellow, K. Bezstarosti, R.K. Maeda, M. Pilyugin, F. Karch, S.J. Bray, J.A. Demmers & C.P. Verrijzer, (2009) Histone chaperones ASF1 and NAP1 differentially modulate removal of active histone marks by LID-RPD3 complexes during NOTCH silencing. *Mol Cell* **35**: 782-793.

Müller, J., C.M. Hart, N.J. Francis, M.L. Vargas, A. Sengupta, B. Wild, E.L. Miller, M.B. O'Connor, R.E. Kingston & J.A. Simon, (2002) Histone methyltransferase activity of a Drosophila Polycomb group repressor complex. *Cell* **111**: 197-208.

Murén, E., M. Öyen, G. Barmark & H. Ronne, (2001) Identification of yeast deletion strains that are hypersensitive to brefeldin A or monensin, two drugs that affect intracellular transport. *Yeast* **18**: 163-172.

Nakai, K. & P. Horton, (1999) PSORT: a program for detecting sorting signals in proteins and predicting their subcellular localization. In.: Elsevier Current Trends, pp.

Nakayama, J., J.C. Rice, B.D. Strahl, C.D. Allis & S.I. Grewal, (2001) Role of histone H3 lysine 9 methylation in epigenetic control of heterochromatin assembly. *Science* **292**: 110-113.

Nathan, D., D.E. Sterner & S.L. Berger, (2003) Histone modifications: Now summoning sumoylation. *Proceedings of the National Academy of Sciences* **100**: 13118-13120.

Nelson, C.J., H. Santos-Rosa & T. Kouzarides, (2006) Proline isomerization of histone H3 regulates lysine methylation and gene expression. *Cell* **126**: 905-916.

Nguyen, A.T. & Y. Zhang, (2011) The diverse functions of Dot1 and H3K79 methylation. *Genes & development* **25**: 1345-1358.

Nislow, C., E. Ray & L. Pillus, (1997) SET1, a yeast member of the trithorax family, functions in transcriptional silencing and diverse cellular processes. *Mol Biol Cell* **8**: 2421-2436.

Noma, A., Y. Kirino, Y. Ikeuchi & T. Suzuki, (2006) Biosynthesis of wybutosine, a hyper-modified nucleoside in eukaryotic phenylalanine tRNA. *The EMBO journal* **25**: 2142-2154.

Pai, C.-C., R.S. Deegan, L. Subramanian, C. Gal, S. Sarkar, E.J. Blaikley, C. Walker, L. Hulme, E. Bernhard & S. Codlin, (2014) A histone H3K36 chromatin switch coordinates DNA double-strand break repair pathway choice. *Nature communications* **5**: 4091.

Palmer, J.M., J.W. Bok, S. Lee, T.R. Dagenais, D.R. Andes, D.P. Kontoyiannis & N.P. Keller, (2013) Loss of CclA, required for histone 3 lysine 4 methylation, decreases growth but increases secondary metabolite production in *Aspergillus fumigatus*. *PeerJ* **1**: e4.

Perrin, R.M., N.D. Fedorova, J.W. Bok, R.A. Cramer Jr, J.R. Wortman, H.S. Kim, W.C. Nierman & N.P. Keller, (2007) Transcriptional regulation of chemical diversity in Aspergillus fumigatus by LaeA. *PLoS pathogens* **3**: e50.

Pham, K.T., Y. Inoue, B.V. Vu, H.H. Nguyen, T. Nakayashiki, K. Ikeda & H. Nakayashiki, (2015) MoSET1 (Histone H3K4 Methyltransferase in Magnaporthe oryzae) Regulates Global Gene Expression during Infection-Related Morphogenesis. *PLoS Genet* **11**: e1005385.

Pinskaya, M., S. Gourvennec & A. Morillon, (2009) H3 lysine 4 di- and tri-methylation deposited by cryptic transcription attenuates promoter activation. *EMBO J* **28**: 1697-1707.

Plath, K., J. Fang, S.K. Mlynarczyk-Evans, R. Cao, K.A. Worringer, H. Wang, C. Cecile, A.P. Otte, B. Panning & Y. Zhang, (2003) Role of histone H3 lysine 27 methylation in X inactivation. *Science* **300**: 131-135.

Pokholok, D.K., C.T. Harbison, S. Levine, M. Cole, N.M. Hannett, T.I. Lee, G.W. Bell, K. Walker, P.A. Rolfe, E. Herbolsheimer, J. Zeitlinger, F. Lewitter, D.K. Gifford & R.A. Young, (2005) Genome-wide map of nucleosome acetylation and methylation in yeast. *Cell* **122**: 517-527.

Popay, A. & J. Baltus, (2001) Black beetle damage to perennial ryegrass infected with AR1 endophyte. In: PROCEEDINGS OF THE CONFERENCE-NEW ZEALAND GRASSLAND ASSOCIATION. pp. 267-272.

Popay, A., D. Hume, J. Baltus, G. Latch, B. Tapper, T. Lyons, B. Cooper, C. Pennell, J. Eerens & S. Marshall, (1999) Field performance of perennial ryegrass (Lolium perenne) infected with toxin-free fungal endophytes (Neotyphodium spp.). *Ryegrass endophyte: an essential New Zealand symbiosis. Grassland Research and Practice Series* **7**: 113-122.

Popay, A., D. Hume, R. Mainland & C. Saunders, (1995) Field resistance to Argentine stem weevil (Listronotus bonariensis) in different ryegrass cultivars infected with an endophyte deficient in lolitrem B. *New Zealand Journal of Agricultural Research* **38**: 519-528.

Prestige, R., (1982) An association of Lolium endophyte with ryegrass resistance to Argentine stem weevil. In: Proc. NZ Weed Pest Control Conf. 35th, 1982. pp. 119-122.

Rasmussen, S., G.A. Lane, W. Mace, A.J. Parsons, K. Fraser & H. Xue, (2012) The use of genomics and metabolomics methods to quantify fungal endosymbionts and alkaloids in grasses. *Methods Mol Biol*: 213-226.

Rea, S., F. Eisenhaber, D. O'carroll, B.D. Strahl, Z.-W. Sun, M. Schmid, S. Opravil, K. Mechtler, C.P. Ponting & C.D. Allis, (2000) Regulation of chromatin structure by site-specific histone H3 methyltransferases. *Nature* **406**: 593-599.

Reyes-Dominguez, Y., S. Boedi, M. Sulyok, G. Wiesenberger, N. Stoppacher, R. Krska & J. Strauss, (2012) Heterochromatin influences the secondary metabolite profile in the plant pathogen Fusarium graminearum. *Fungal Genet Biol* **49**: 39-47.

Reyes-Dominguez, Y., J.W. Bok, H. Berger, E.K. Shwab, A. Basheer, A. Gallmetzer, C. Scazzocchio, N. Keller & J. Strauss, (2010) Heterochromatic marks are associated with the repression of secondary metabolism clusters in Aspergillus nidulans. *Mol Microbiol* **76**: 1376-1386.

Robyr, D., Y. Suka, I. Xenarios, S.K. Kurdistani, A. Wang, N. Suka & M. Grunstein, (2002) Microarray deacetylation maps determine genome-wide functions for yeast histone deacetylases. *Cell* **109**: 437-446.

Roguev, A., D. Schaft, A. Shevchenko, W.W. Pijnappel, M. Wilm, R. Aasland & A.F. Stewart, (2001) The Saccharomyces cerevisiae Set1 complex includes an Ash2 homologue and methylates histone 3 lysine 4. *EMBO J* **20**: 7137-7148.

Rowan, D.D., (1993) Lolitrems, peramine and paxilline: mycotoxins of the ryegrass/endophyte interaction. *Agriculture, Ecosystems & Environment* **44**: 103-122.

Roze, L.V., A.E. Arthur, S.Y. Hong, A. Chanda & J.E. Linz, (2007) The initiation and pattern of spread of histone H4 acetylation parallel the order of transcriptional activation of genes in the aflatoxin cluster. *Mol Microbiol* **66**: 713-726.

Ryu, H.-Y. & S.H. Ahn, (2014) Yeast histone H3 lysine 4 demethylase Jhd2 regulates mitotic ribosomal DNA condensation. *BMC Biol* **12**: 75.

Ryu, H.-Y., B.-H. Rhie & S.H. Ahn, (2014) Loss of the Set2 histone methyltransferase increases cellular lifespan in yeast cells. *Biochemical and biophysical research communications* **446**: 113-118.

Saikia, S., D. Takemoto, B.A. Tapper, G.A. Lane, K. Fraser & B. Scott, (2012) Functional analysis of an indole-diterpene gene cluster for lolitrem B biosynthesis in the grass endosymbiont *Epichloë festucae*. *FEBS Letters* **586**: 2563-2569.

Santos-Rosa, H., R. Schneider, A.J. Bannister, J. Sherriff, B.E. Bernstein, N.T. Emre, S.L. Schreiber, J. Mellor & T. Kouzarides, (2002) Active genes are tri-methylated at K4 of histone H3. *Nature* **419**: 407-411.

Santos-Rosa, H., R. Schneider, B.E. Bernstein, N. Karabetsou, A. Morillon, C. Weise, S.L. Schreiber, J. Mellor & T. Kouzarides, (2003) Methylation of histone H3 K4 mediates association of the Isw1p ATPase with chromatin. *Mol Cell* **12**: 1325-1332.

Schardl, C.L., A. Leuchtmann & M.J. Spiering, (2004) Symbioses of grasses with seedborne fungal endophytes. *Annu Rev Plant Biol* **55**: 315-340.

Schardl, C.L., C.A. Young, J.R. Faulkner, S. Florea & J. Pan, (2012) Chemotypic diversity of epichloae, fungal symbionts of grasses. *Fungal Ecology* **5**: 331-344.

Schardl, C.L., C.A. Young, U. Hesse, S.G. Amyotte, K. Andreeva, P.J. Calie, D.J. Fleetwood, D.C. Haws, N. Moore, B. Oeser, D.G. Panaccione, K.K. Schweri, C.R. Voisey, M.L. Farman, J.W. Jaromczyk, B.A. Roe, D.M. O'Sullivan, B. Scott, P. Tudzynski, Z. An, E.G. Arnaoudova, C.T. Bullock, N.D. Charlton, L. Chen, M. Cox, R.D. Dinkins, S. Florea, A.E. Glenn, A. Gordon, U. Guldener, D.R. Harris, W. Hollin, J. Jaromczyk, R.D. Johnson, A.K. Khan, E. Leistner, A. Leuchtmann, C. Li, J. Liu, J. Liu, M. Liu, W. Mace, C. Machado, P. Nagabhyru, J. Pan, J. Schmid, K. Sugawara, U. Steiner, J.E. Takach, E. Tanaka, J.S. Webb, E.V. Wilson, J.L. Wiseman, R. Yoshida & Z. Zeng, (2013) Plant-symbiotic fungi as chemical engineers: multi-genome analysis of the clavicipitaceae reveals dynamics of alkaloid loci. *PLoS Genet* **9**: e1003323.

Schneider, J., A. Wood, J.S. Lee, R. Schuster, J. Dueker, C. Maguire, S.K. Swanson, L. Florens, M.P. Washburn & A. Shilatifard, (2005) Molecular regulation of histone H3 trimethylation by COMPASS and the regulation of gene expression. *Mol Cell* **19**: 849-856.

Schultz, J., F. Milpetz, P. Bork & C.P. Ponting, (1998) SMART, a simple modular architecture research tool: identification of signaling domains. *Proc Natl Acad Sci U S A* **95**: 5857-5864.

Scott, B., Y. Becker, M. Becker & G. Cartwright, (2012) Morphogenesis, Growth, and Development of the Grass Symbiont Epichlöe festucae. **22**: 243-264.

Shao, Z., F. Raible, R. Mollaaghababa, J.R. Guyon, C.-t. Wu, W. Bender & R.E. Kingston, (1999) Stabilization of chromatin structure by PRC1, a Polycomb complex. *Cell* **98**: 37-46.

Shi, X., T. Hong, K.L. Walter, M. Ewalt, E. Michishita, T. Hung, D. Carney, P. Pena, F. Lan, M.R. Kaadige, N. Lacoste, C. Cayrou, F. Davrazou, A. Saha, B.R. Cairns, D.E. Ayer, T.G. Kutateladze, Y. Shi, J. Cote,

K.F. Chua & O. Gozani, (2006) ING2 PHD domain links histone H3 lysine 4 methylation to active gene repression. *Nature* **442**: 96-99.
Shi, Y., F. Lan, C. Matson, P. Mulligan, J.R. Whetstine, P.A. Cole, R.A. Casero & Y. Shi, (2004) Histone demethylation mediated by the nuclear amine oxidase homolog LSD1. *Cell* **119**: 941-953.
Shilatifard, A., (2012) The COMPASS family of histone H3K4 methylases: mechanisms of regulation in development and disease pathogenesis. *Annu Rev Biochem* **81**: 65-95.
Shinohara, Y., M. Kawatani, Y. Futamura, H. Osada & Y. Koyama, (2016) An overproduction of astellolides induced by genetic disruption of chromatin-remodeling factors in *Aspergillus oryzae*. *J Antibiot (Tokyo)* **69**: 4-8.
Shoji, K., K. Hara, M. Kawamoto, T. Kiuchi, S. Kawaoka, S. Sugano, T. Shimada, Y. Suzuki & S. Katsuma, (2014) Silkworm HP1a transcriptionally enhances highly expressed euchromatic genes via association with their transcription start sites. *Nucleic Acids Res* **42**: 11462-11471.
Shwab, E.K., J.W. Bok, M. Tribus, J. Galehr, S. Graessle & N.P. Keller, (2007) Histone deacetylase activity regulates chemical diversity in Aspergillus. *Eukaryot Cell* **6**: 1656-1664.
Sievers, F., A. Wilm, D. Dineen, T.J. Gibson, K. Karplus, W. Li, R. Lopez, H. McWilliam, M. Remmert & J. Söding, (2011) Fast, scalable generation of high-quality protein multiple sequence alignments using Clustal Omega. *Mol Syst Biol* **7**: 539.
Silva, J., W. Mak, I. Zvetkova, R. Appanah, T.B. Nesterova, Z. Webster, A.H. Peters, T. Jenuwein, A.P. Otte & N. Brockdorff, (2003) Establishment of histone h3 methylation on the inactive X chromosome requires transient recruitment of Eed-Enx1 polycomb group complexes. *Developmental cell* **4**: 481-495.
Skaar, J.R., J.K. Pagan & M. Pagano, (2013) Mechanisms and function of substrate recruitment by F-box proteins. *Nature reviews Molecular cell biology* **14**: 369-381.
Smith, B., L. McLeay & P. Embling, (1997) Effect of the mycotoxins penitrem, paxilline and lolitrem B on the electromyographic activity of skeletal and gastrointestinal smooth muscle of sheep. *Res Vet Sci* **62**: 111-116.
South, P.F., K.M. Harmeyer, N.D. Serratore & S.D. Briggs, (2013) H3K4 methyltransferase Set1 is involved in maintenance of ergosterol homeostasis and resistance to Brefeldin A. *Proceedings of the National Academy of Sciences* **110**: E1016-E1025.
Southern, E.M., (1975) Detection of specific sequences among DNA fragments separated by gel electrophoresis. *Journal of molecular biology* **98**: 503IN3509-3508IN5517.
Soyer, J.L., M. El Ghalid, N. Glaser, B. Ollivier, J. Linglin, J. Grandaubert, M.H. Balesdent, L.R. Connolly, M. Freitag, T. Rouxel & I. Fudal, (2014) Epigenetic control of effector gene expression in the plant pathogenic fungus Leptosphaeria maculans. *PLoS Genet* **10**: e1004227.
Spitzer, M., J. Wildenhain, J. Rappsilber & M. Tyers, (2014) BoxPlotR: a web tool for generation of box plots. *Nature methods* **11**: 121-122.
Squazzo, S.L., H. O'Geen, V.M. Komashko, S.R. Krig, V.X. Jin, S.W. Jang, R. Margueron, D. Reinberg, R. Green & P.J. Farnham, (2006) Suz12 binds to silenced regions of the genome in a cell-type-specific manner. *Genome Res* **16**: 890-900.
Strahl, B.D., P.A. Grant, S.D. Briggs, Z.W. Sun, J.R. Bone, J.A. Caldwell, S. Mollah, R.G. Cook, J. Shabanowitz, D.F. Hunt & C.D. Allis, (2002) Set2 Is a Nucleosomal Histone H3-Selective Methyltransferase That Mediates Transcriptional Repression. *Molecular and Cellular Biology* **22**: 1298-1306.
Strahl, B.D., R. Ohba, R.G. Cook & C.D. Allis, (1999) Methylation of histone H3 at lysine 4 is highly conserved and correlates with transcriptionally active nuclei in Tetrahymena. *Proceedings of the National Academy of Sciences* **96**: 14967-14972.
Strauss, J. & Y. Reyes-Dominguez, (2011) Regulation of secondary metabolism by chromatin structure and epigenetic codes. *Fungal Genet Biol* **48**: 62-69.
Studt, L., S. Janevska, B. Arndt, S. Boedi, M. Sulyok, H.U. Humpf, B. Tudzynski & J. Strauss, (2017) Lack of the COMPASS Component Ccl1 Reduces H3K4 Trimethylation Levels and Affects Transcription of Secondary Metabolite Genes in Two Plant-Pathogenic Fusarium Species. *Front Microbiol* **7**: 2144.
Studt, L., S.M. Rosler, I. Burkhardt, B. Arndt, M. Freitag, H.U. Humpf, J.S. Dickschat & B. Tudzynski, (2016) Knock-down of the methyltransferase Kmt6 relieves H3K27me3 and results in induction of cryptic and otherwise silent secondary metabolite gene clusters in Fusarium fujikuroi. *Environ Microbiol* **18**: 4037-4054.

Sun, X.J., J. Wei, X.Y. Wu, M. Hu, L. Wang, H.H. Wang, Q.H. Zhang, S.J. Chen, Q.H. Huang & Z. Chen, (2005) Identification and characterization of a novel human histone H3 lysine 36-specific methyltransferase. *J Biol Chem* **280**: 35261-35271.

Suzuki, T., K.i. Minehata, K. Akagi, N.A. Jenkins & N.G. Copeland, (2006) Tumor suppressor gene identification using retroviral insertional mutagenesis in Blm-deficient mice. *The EMBO journal* **25**: 3422-3431.

Takemoto, D., A. Tanaka & B. Scott, (2006) A p67Phox-like regulator is recruited to control hyphal branching in a fungal-grass mutualistic symbiosis. *Plant Cell* **18**: 2807-2821.

Tamaru, H. & E.U. Selker, (2001) A histone H3 methyltransferase controls DNA methylation in Neurospora crassa. *Nature* **414**: 277-283.

Tamura, K., G. Stecher, D. Peterson, A. Filipski & S. Kumar, (2013) MEGA6: molecular evolutionary genetics analysis version 6.0. *Molecular biology and evolution* **30**: 2725-2729.

Tanaka, A., G.M. Cartwright, S. Saikia, Y. Kayano, D. Takemoto, M. Kato, T. Tsuge & B. Scott, (2013) ProA, a transcriptional regulator of fungal fruiting body development, regulates leaf hyphal network development in the Epichloe festucae-Lolium perenne symbiosis. *Mol Microbiol* **90**: 551-568.

Tanaka, A., M.J. Christensen, D. Takemoto, P. Park & B. Scott, (2006) Reactive oxygen species play a role in regulating a fungus-perennial ryegrass mutualistic interaction. *Plant Cell* **18**: 1052-1066.

Tanaka, A., D. Takemoto, T. Chujo & B. Scott, (2012) Fungal endophytes of grasses. *Curr Opin Plant Biol* **15**: 462-468.

Tanaka, Y., Z.-i. Katagiri, K. Kawahashi, D. Kioussis & S. Kitajima, (2007) Trithorax-group protein ASH1 methylates histone H3 lysine 36. *Gene* **397**: 161-168.

Taunton, J., C.A. Hassig & S.L. Schreiber, (1996) A mammalian histone deacetylase related to the yeast transcriptional regulator Rpd3p. *SCIENCE-NEW YORK THEN WASHINGTON-*: 408-410.

Tsukada, Y., J. Fang, H. Erdjument-Bromage, M.E. Warren, C.H. Borchers, P. Tempst & Y. Zhang, (2006) Histone demethylation by a family of JmjC domain-containing proteins. *Nature* **439**: 811-816.

Tsukada, Y., T. Ishitani & K.I. Nakayama, (2010) KDM7 is a dual demethylase for histone H3 Lys 9 and Lys 27 and functions in brain development. *Genes Dev* **24**: 432-437.

Tu, S., Y.C. Teng, C. Yuan, Y.T. Wu, M.Y. Chan, A.N. Cheng, P.H. Lin, L.J. Juan & M.D. Tsai, (2008) The ARID domain of the H3K4 demethylase RBP2 binds to a DNA CCGCCC motif. *Nat Struct Mol Biol* **15**: 419-421.

Tudzynski, P. & J. Scheffer, (2004) Claviceps purpurea: molecular aspects of a unique pathogenic lifestyle. *Molecular Plant Pathology* **5**: 377-388.

Vakoc, C.R., M.M. Sachdeva, H. Wang & G.A. Blobel, (2006) Profile of histone lysine methylation across transcribed mammalian chromatin. *Molecular and cellular biology* **26**: 9185-9195.

Van Dongen, P.W. & A.N. de Groot, (1995) History of ergot alkaloids from ergotism to ergometrine. *European Journal of Obstetrics & Gynecology and Reproductive Biology* **60**: 109-116.

Wagner, E.J. & P.B. Carpenter, (2012) Understanding the language of Lys36 methylation at histone H3. *Nat Rev Mol Cell Biol* **13**: 115-126.

Wakimoto, B.T., (1998) Beyond the nucleosome: epigenetic aspects of position–effect variegation in Drosophila. *Cell* **93**: 321-324.

Wang, H., L. Wang, H. Erdjument-Bromage, M. Vidal, P. Tempst, R.S. Jones & Y. Zhang, (2004) Role of histone H2A ubiquitination in Polycomb silencing. *nature* **431**: 873-878.

Wang, J., S.T. Jia & S. Jia, (2016) New Insights into the Regulation of Heterochromatin. *Trends Genet* **32**: 284-294.

Wang, J., J. Mager, Y. Chen, E. Schneider, J.C. Cross, A. Nagy & T. Magnuson, (2001) Imprinted X inactivation maintained by a mouse Polycomb group gene. *Nature genetics* **28**: 371-375.

Wang, S.S., B.O. Zhou & J.Q. Zhou, (2011) Histone H3 lysine 4 hypermethylation prevents aberrant nucleosome remodeling at the *PHO5* promoter. *Mol Cell Biol* **31**: 3171-3181.

Wei, Y., C.A. Mizzen, R.G. Cook, M.A. Gorovsky & C.D. Allis, (1998) Phosphorylation of histone H3 at serine 10 is correlated with chromosome condensation during mitosis and meiosis in Tetrahymena. *Proceedings of the National Academy of Sciences* **95**: 7480-7484.

Whetstine, J.R., A. Nottke, F. Lan, M. Huarte, S. Smolikov, Z. Chen, E. Spooner, E. Li, G. Zhang, M. Colaiacovo & Y. Shi, (2006) Reversal of histone lysine trimethylation by the JMJD2 family of histone demethylases. *Cell* **125**: 467-481.

Wilkinson, H.H., M.R. Siegel, J.D. Blankenship, A.C. Mallory, L.P. Bush & C.L. Schardl, (2000) Contribution of fungal loline alkaloids to protection from aphids in a grass-endophyte mutualism. *Molecular Plant-Microbe Interactions* **13**: 1027-1033.

Wysocka, J., T. Swigut, H. Xiao, T.A. Milne, S.Y. Kwon, J. Landry, M. Kauer, A.J. Tackett, B.T. Chait, P. Badenhorst, C. Wu & C.D. Allis, (2006) A PHD finger of NURF couples histone H3 lysine 4 trimethylation with chromatin remodelling. *Nature* **442**: 86-90.

Xie, L., C. Pelz, W. Wang, A. Bashar, O. Varlamova, S. Shadle & S. Impey, (2011) KDM5B regulates embryonic stem cell self-renewal and represses cryptic intragenic transcription. *EMBO J* **30**: 1473-1484.

Yamane, K., C. Toumazou, Y. Tsukada, H. Erdjument-Bromage, P. Tempst, J. Wong & Y. Zhang, (2006) JHDM2A, a JmjC-containing H3K9 demethylase, facilitates transcription activation by androgen receptor. *Cell* **125**: 483-495.

Yuan, W., J. Xie, C. Long, H. Erdjument-Bromage, X. Ding, Y. Zheng, P. Tempst, S. Chen, B. Zhu & D. Reinberg, (2009) Heterogeneous nuclear ribonucleoprotein L Is a subunit of human KMT3a/Set2 complex required for H3 Lys-36 trimethylation activity in vivo. *J Biol Chem* **284**: 15701-15707.

Zhang, X., Y.V. Bernatavichute, S. Cokus, M. Pellegrini & S.E. Jacobsen, (2009) Genome-wide analysis of mono-, di-and trimethylation of histone H3 lysine 4 in Arabidopsis thaliana. *Genome biology* **10**: R62.